THESE

Presentée pour obtenir le grade de

DOCTEUR DE L'UNIVERSITE DE STRASBOURG

Discipline: Sciences de la Terre et de l'Environnement

par

Gabriela TAPIA PADILLA

MODELISATION ET OPTIMISATION DES PROCESSUS DE DEPOLLUTION BIOLOGIQUE DES MATRICES POREUSES CONTAMINEES PAR DES PESTICIDES: VERS UNE NOUVELLE FONCTIONNALITE DES BASSINS D'ORAGE

Soutenue publiquement le 17 décembre 2010 devant la commission d'examen:

GREGOIRE Caroline	IDAE à l'Ecole Nationale de Génie de l'Eau et de l'Environnement de Strasbourg/ Laboratoire d'Hydrologie et de Géochimie de Strasbourg	Directrice de thèse
MOSE Robert	Professeur à l'Institut de Mécanique des Fluides et des Solides de Strasbourg	Codirecteur de thèse
MARTINEZ Luis	Professeur à l'Université Henri Poincaré Nancy I	Rapporteur externe
CAPRI Ettore	Professeur à l'Université Catholique du Sacre Cœur, Piacenza Italie	Rapporteur externe
LEHMANN François	Maître de conférences à l'Université de Strasbourg (Laboratoire d'Hydrologie et de Géochimie de Strasbourg)	Rapporteur interne
TOURNEBIZE Julien	Chercheur au Cemagref Antony (UR HBAN)	Examinateur
WANKO NGNIEN Adrien	Maître de conférences à l'Institut de Mécanique des Fluides et des Solides de Strasbourg	Membre invité

ACKNOWLEDGEMENTS

I would like to thank all the people who contributed in some way to the work described in this thesis. First I would like to thank to my supervisors, Dr. Caroline GREGOIRE and Dr. Robert MOSE, for accepting me into their research groups: the Hydrology and Geochemistry Laboratory of Strasbourg (LHYGES) and the Urban Hydraulics research team (HU/IMFS), based at the National School for Water and Environment Engineering in Strasbourg, France (ENGEES). In particular, I would like to extend my sincere and deep gratitude to Dr. Adrien Wanko, for his guidance and support throughout the course of my study. Without his continued support and interest, this thesis would not have been the same as presented here. I am also grateful to Dr. Luis MARTINEZ, Dr. Ettore CAPRI, Dr. François LEHMANN, and Dr. Julien TOURNEBIZE for being part of the examining committee and thesis jury.

My sincere appreciation also extends to Dr. Antoine-Georges SADOWSKI, Dr. José VAZQUEZ and all the members of the HU group for contributing to a convivial atmosphere at work and providing their assistance at various occasions. Special thanks to my several office-mates through all these years for their company and the coffe breaks: Fabien, Renaud, Georges, Rabih, Matthieu, Nicolas, Jonathan, Damien, Alain, and Noëlle.

A fellowship from the Region d'Alsace is gratefully acknowledged, as well as the funding from the European Commision under the frame of the European LIFE ENVIRONMENT project ARTWET (LIFE 06 ENV/F/000133).

I should give a special mention to my friends for their help and encouragement. I am thankful to the Association Anahuacalli, especially to the dance group members, whose help and humor allowed me to get through this project. Finally, my deeplest gratitude is to my family for their unconditional love and support.

.

TABLE OF CONTENTS

LIST OF FIGURES

LIST OF TABLES

LIST OF ABBREVIATIONS AND DEFINITIONS

MRL	Maximum residue level that is legally permitted in specific food items and animal feed
ADI	Amount of a pesticide, in mg/kg body weight, which can be ingested, on daily basis, during lifetime
Arfd	Acute reference dose
BOD	Biological oxygen demand
MCPA	
AZP	Oorganophosphate insecticide azinphosmethyl
HRT	Hydraulic residence time
W(x,z,t)	Sink/source terms [T^{-1}] –Richards' equation
x	Horizontal spatial coordinate [L]
Z	Vertical spatial coordinate, Elevation head [L]
T	Time [T]
C(h)	Specific water (or moisture) capacity of soil [L^{-1}]
K	Unsaturated hydraulic conductivity [LT^{-1}]
H	Soil water pressure head [L].
f(C,t)	Sink/source terms [$ML^{-3}T^{-1}$]- transport equation
C	Solution concentration [ML^{-3}],
S	Sorbed concentration [$M\ M^{-1}$],
ρ	Soil bulk density [ML^{-3}],
$\vec{q}$	Flow rate per unit area [LT^{-1}], also known as specific discharge or Darcy flux.
D	Dispersion tensor [L^2T^{-1}],
θ	soil volumetric water (or moisture) content [L^3L^{-3}]
H	Henry's Law constant
K_{ow}	Octanol water partition coefficient
K_d	Distribution or partitioning coefficient
K_{OC}	Soil organic carbon sorption coefficient
F_{OC}	Organic carbon fraction of the soil
K_f and n	Empirical constants - Freundlich equation
pH	Potential of Hydrogen (degree of acidity or alkalinity of a substance)
2D	Two-dimensional
Ω	Flow domain
G	Triangular element in a space-discretization of the domain Ω
Ω_D	Dirichlet boundary condition
Ω_N	Neumann boundary condition
∂_G	Boundary of the element G
$E_i\ (\forall i = 1,2,3)$	Edge of the element G
$E \subset \partial G$	Edge E belongs to the boundary of the element G
$G \supset E$	The element G s one of the elements that edge E belongs to.
$\hat{h}$	Transformed pressure head [L]
κ	Universal constant ($\cong$ -0.04 cm^{-1} or $-4m^{-1}$)
$\hat{K}$	Transformed hydraulic conductivity
$\vec{q}_G$	Approximation of $\vec{q}$ over the element G Vector function belonging to the lowest order Raviart-Thomas space

$\vec{n}_{G,E_i}$	Normal unit vector exterior to the edge E_i
$\hat{Th}_{G,E_j}$	Transformed average piezometric charge at the edge E_j of the triangular element G
z_{G,E_j}	Elevation head at the centre of the edge E_j
$\vec{n}_{K,E_j}$	Normal unit vector exterior to the edge E_j,
$\hat{h}_G$	Transformed average piezometric charge at the element G
z_G	Elevation head at the centroid of the element
K_G	Hydraulic conductivity in the element G
$\hat{K}_G$	Transformed hydraulic conductivity in the element G
K_{G,E_j}	Hydraulic conductivity at the edge E_j
$\hat{K}_{G,E_j}$	Transformed hydraulic conductivity at the edge E_j
$\vec{w}_i$	Vector fields basis used as basis functions over each element K
$\delta_{i,j}$	Kronecker symbol $\begin{cases}\delta_{i,j}=1 \quad if \quad i=j \\ \delta_{i,j}=0 \quad if \quad i\neq j\end{cases} \qquad \forall i=1,2,3$
Q_{G,E_j}	Water flux over the edge E_j belonging to the element G [$L^2\ T^{-1}$]
$\hat{B}_{G,i,j}$	Auxiliary variable $\hat{B}_{G,i,j}=\int_G\left(\hat{K}_G^{-1}\vec{w}_j\right)\vec{w}_i$
K_G^A	Dimensionless anisotropy tensor
Ks_G	Saturated hydraulic conductivity [LT^{-1}]
Kr_G	Relative hydraulic conductivity function given by the modified Mualem-van Genuchten expression
a_G	Anisotropy ratio $a_G=\frac{K_z}{K_x}$.
Se	Effective saturation
Sc	Saturation at the cut-off point h_e
h_e	Free parameter in the modified Mualem-van Genuchten model referred as the air entry value [L] [L]
α_v	Free parameter in the modified Mualem-van Genuchten model related to the mean pore size of the soil [L^{-1}],
m_v	Parameter in the modified Mualem-van Genuchten model given by $m_v=1-\frac{1}{n_v}$ [-]
n_v	Free parameter in the van Genuchten model related to the uniformity of the soil pore-size [-],
τ	Empirical parameter in the modified Mualem-van Genuchten expression related to tortuosity [-].
h_a	Real air-entry value of the soil
R_{max}	Maximal pore radius
σ_w	Surface tension at the air-water interface

ρ_w	Density of water
g	Gravity constant
θ_r	Residual water content [L^3L^{-3}]
θ_s	Saturated water content [L^3L^{-3}]
m	Picard iteration level
n	Time level iteration
S_s	Specific storage [L^{-1}],
S_w	Degree of saturation $S_w = \frac{\theta}{\varphi}$
φ	Porosity [L^3L^{-3}]
f(x,y,t)	Source /sink term which represents the volume of water added / removed per unit time to/ from a unit volume of soil [T^{-1}]
Δt	Time step
Δx	Grid size in x direction
Δz	Grid size in z direction
∇	Gradient operator
tol_f	Tolerance for the switching procedure

,

1

Chapter 1 – Introduction

Section 1.1. Introduction: Version française

La présence et le devenir des pesticides comme polluants organiques persistant dans l'environnement, principalement les sols, est une préoccupation permanente des politiques publiques ou privées en charge du contrôle de la qualité environnementale; ceci au vu de nombreux travaux publiés qui ont bénéficié d'une façon ou d'une autre de soutiens financiers. Le devenir des pesticides dans l'environnement prend en compte des processus qui déterminent leur persistance et mobilité, le transport, le transfert et les processus de transformation. Ces processus sont affectés par les propriétés physiques et chimiques des pesticides, les caractéristiques du sol, des conditions locales du climat et de l'humidité, de la population biologique et des pratiques de manutention des utilisateurs. En outre, la variance de la structure chimique des pesticides est un indicateur de leur comportement dans l'environnement, sachant que la dégradation ou transformation d'un pesticide induit un changement de structure et donc de comportement. Face à ce risque avéré de pollution environnementale, la communauté scientifique et les professionnels de l'assainissement redoublent d'ardeur pour une compréhension fine des processus impliqués dans le devenir des pesticides ainsi que pour le développement des procédés concourant à la réduction de la pollution diffuse generée.

Des études récentes ont souligné la capacité des zones humides artificielles à la réduction des pesticides issus du ruissellement des eaux de surface [Gregoire et al., 2009 ; 2010]. La modélisation des processus dominants impliqués dans le devenir des pesticides au sein des massifs poreux constituant les zones humides artificielles est l'objet de ces travaux de recherche.

Tout d'abord, dans une première partie, nous exposons l'état d'avancement de la recherche dans ce domaine. Après un point bibliographique sur les différentes études traitant des capacités des zones humides artificielles à dégrader les pesticides, une revue des généralités sur les processus d'écoulement des eaux, du transport des polluants et les phénomènes de biodégradation a été effectuée. Tout particulièrement, les processus dans une zone humide artificielle.

Cette partie s'achève par l'état de l'art des différents modèles numériques existant pour simuler le couplage entre hydrodynamique en milieux poreux et transport réactif.

Dans une seconde partie, nous abordons le développement d'un nouvel outil numérique de simulation pour comprendre le devenir des pesticides dans une zone humide artificielle. Tous les processus affectant la dynamique des pesticides ne sont pas connus et la description quantitative des processus connus n'est toujours pas possible [Rao et Jessup, 1982]. Ce constat émerge d'une revue bibliographique qui recense et analyse les difficultés rencontrées par les modèles de simulation du devenir des pesticides lors d'essais de vérification. La vérification ou l'usage de ces modèles est généralement difficile du fait des méthodes inadéquates pour la mesure et l'estimation des paramètres d'entrée.

Le modèle développé est fondé sur la méthode de discrétisation des éléments finis mixtes hybrides. Il représente une contribution aux méthodes numériques employées pour la simulation d'écoulement des eaux souterraines et du transport des polluants dans les milieux poreux à saturation variable. La formulation utilisée est basée sur les propriétés de l'espace de Raviart-Thomas, considérant un domaine bidimensionnel divisé en éléments triangulaires. Cette technique a été particulièrement bien adaptée pour la simulation d'écoulement en milieu poreux saturé hétérogène lors des études antérieures. En milieu poreux non saturé, l'hétérogénéité est liée à la fois à l'hétérogénéité des massifs filtrants et à une distribution non uniforme de la teneur en eau dans la zone humide artificielle. L'originalité ici est l'application des éléments finis mixtes hybrides pour un milieu poreux à saturation variable tant pour simuler l'hydrodynamique que pour le transport.

L'équation de Richards qui gouverne l'hydrodynamique du modèle a été modifiée par l'addition d'une variable de transformation de pression. Cette méthode présentée par Pan et Wierenga [1995] est numériquement robuste pour tous les cas en milieux poreux hétérogènes à saturation variable, et avec des conditions aux limites de type Dirichlet ou Neumann. La technique de condensation de la masse proposée par Belfort [2006] été utilisée pour limiter l'apparition d'oscillations, problèmes liés à l'expression discrète du terme exprimant la variation de la masse dans le volume. En outre, l'algorithme de gestion des conditions aux limites proposé par Van Dam et Feddes [2000] pour les scénarios d'infiltration et d'évaporation est repris afin d'éviter l'apparition de résultats sans réalité physique.

Pour l'équation de transport une formulation originale a été utilisée. L'approximation du flux de transport convectif et dispersif est effectuée par un unique vecteur. Il n'est donc pas fait usage de la technique de séparation d'opérateurs qui introduit des biais propres à chaque opérateur.

Afin de contrôler les oscillations non physiques quand la convection est le processus dominant, un outil pour limiter le flux est présenté. L'outil suggéré limitant le flux permet de préserver la précision et la stabilité pour une large gamme des nombres de Peclet.

Différents modèles de cinétiques de biodégradation de pesticide, spécifiquement liés à l'environnement des sols sont implémentés à la suite de l'hydrodynamique et du transport.

La solution numérique s'obtient après résolution du système d'équations linéaires, où les inconnues sont les traces de pression de l'eau pour l'hydrodynamique et les traces de concentration pour le transport. La matrice associée au système d'équations pour l'hydrodynamique est symétrique et définie positive. Par conséquent, elle peut effectivement être résolue par la méthode du gradient conjugué, préconditionné avec une décomposition de Cholesky incomplète en utilisant la procédure Eisenstat [Eisenstat, 1981]. En revanche, la matrice associée au transport est non symétrique du fait du limiteur de flux. Ainsi, la méthode itérative du gradient conjugué, préconditionné avec le procédure de Eisenstat ILU est utilisée pour résoudre ce système algébrique.

La discrétisation en temps joue également un rôle important au cours de la simulation. Une sélection inadéquate du pas de temps peut conduire à une mauvaise approximation de l'hydrodynamique et de transport de polluant. Pour cette raison, l'incrément temporel est automatiquement adapté à chaque itération.

Dans une troisième partie, la vérification du modèle hydrodynamique est effectuée par la comparaison entre les résultats de références issues de la littérature et ceux du modèle développé. Plusieurs problèmes en mono et bidimensionnel sont traités. L'infiltration au sein de sols initialement très secs, induisant de forts gradients de teneur en eau est simulés avec succès. Une comparaison entre les résultats obtenus avec le modèle numérique commercial HYDRUS (dans le cas d'infiltration dans une colonne de sol), des solutions analytiques et le modèle développé a permis de valider l'efficacité du limiteur de flux proposé.

La quatrième partie concerne l'application du modèle numérique aux conditions de terrain via des sites expérimentaux. L'usage des modèles est généralement difficile du fait des méthodes inadéquates pour la mesure et l'estimation des paramètres d'entrée des modèles. En outre, les méthodes de mesures des paramètres d'entrée ne sont parfois pas disponibles. Par ailleurs, leur utilisation à l'échelle de terrain est confrontée à des problèmes majeurs. Nous en dénombrons ici quelques-uns:

- les propriétés physiques, chimiques et biologiques du sol varient spatialement et temporellement.

- le comportement des pesticides est déterminé par une multitude de processus dynamiques qui ont lieu simultanément.
- les modèles mathématiques de transformation biologique sont en général issus des relations développées par la description des cinétiques microbiennes en batch ou cultures continues. La flore microbienne est restreinte à la phase aqueuse qui peut être comparée à un réacteur biologique où différentes substances sont introduites [Soulas et Fournier, 1981]. Cette approche, aussi intéressante soit-elle, trouve sa limitation du fait de la très grande complexité des sols. Alexander et Scow [1989] relèvent que la composition physico-chimique des sols est hautement complexe, la communauté microbienne assez hétérogène et les constituants abiotiques sont couramment réactifs. En conséquence, l'application des modèles cinétiques de biodégradation est sujette à caution. Pour cette raison, nous n'aborderons pas la validation des processus biologiques dans cette partie.

Nous proposons un usage du modèle numérique pour optimiser le fonctionnement hydraulique de sites réels construits dans le cadre du projet européen ARTWET (LIFE 06 ENV/F/000133).

Le premier site est situé à l'interface rural/urbain sur la commune de Rouffach (Alsace, France). C'est un bassin d'orage construit originalement pour la régulation hydraulique. Le bassin d'orage constitue l'ouvrage récepteur des flux ruisselants générés majoritairement sur les parcelles et chemins viticoles. Après un stockage transitoire, les volumes collectés dans le bassin d'orage sont envoyés vers les collecteurs d'assainissement aval, attention deconnecté de la station d'épuration avant d'être rejetés vers le milieu naturel. Des mesures ont montré la présence de produits phytosanitaires en concentration non négligeable dans les eaux superficielles, allant de plusieurs centaines de $\mu g / L$ aux parcelles à quelques $\mu g / L$ dans les rivières de plaine. Par ailleurs, le bassin d'orage présente une potentialité de bio et phyto-remédiation de par l'existence d'une accumulation de sédiments transportés depuis les parcelles et de la colonisation de ce milieu par une végétation. Par conséquent, il devient un élément de traitement potentiel de la charge polluante, qu'il est alors intéressant d'optimiser.

L'optimisation de la conception de bassins d'orage est effectuée par la construction d'une zone humide artificielle d'écoulement horizontal (HFCW dans la terminologie anglosaxonne), dans le but de réduire la concentration et le flux des pesticides dans les eaux qui y transitent. Afin d'optimiser la gestion hydraulique du HFCW, des expériences de traceurs numériques sont effectuées pour simuler plusieurs scénarios. Des charges

hydrauliques réalistes sont simulées et les différents profils de pression sont examinés. Les courbes de percée sont exploitées pour calculer la distribution du temps de séjour de polluant dissous dans le HFCW, ainsi que la capacité de stockage. Les effets induits par une hétérogénéité d'adsorption dans le milieu sont analysés. Nous donnons une expression empirique pour calculer la capacité de stockage. Le bassin ne pouvant traiter que la pollution stockée, nous proposons par le biais de la modélisation des choix opérationnels optimisant les capacités de stockage du bassin. Ainsi une gestion hydraulique du HFCW est suggérée en relation avec les temps de retention et de dégradation des pesticides.

Section 1.2. Introduction: English version

The presence and fate of pesticides, as persistent organic pollutants in the environment, especially in soil, are a permanent concern of public or private policies on environmental quality control. This is confirmed by the existence of several published research works, which have been benefited in one way or another from financial support. Pesticides fate in the environment takes into account the processes that determine their persistence, mobility, transport, transfer and transformation. These processes are affected by physical and chemical properties of the pesticides, soil characteristics, local conditions of climate and humidity, biologic population and user's handling practices. In addition, the variance of the chemical structure of pesticides is an indicator of their behavior in the environment, knowing that the degradation or transformation of a pesticide induces a structural change and therefore a change in its behavior. Face to this proven risk of environmental pollution, the scientific community and sanitation professionals redouble their efforts for a better understanding of the processes governing the fate of pesticides, for the development of processes that contribute to the reduction of this diffuse pollution.

Recent studies have emphasized the ability of constructed wetlands to retain runoff-related pesticide pollution [Gregoire et al., 2009; 2010]. The objective of these research studies is to model the dominant processes that determine the fate of pesticides within the porous medium that constitutes the artificial wetlands.

In the first part of the present work, we outline the progress in this research domain. A literature review was carried out on the different studies dealing with the capacity of artificial wetlands to degrade pesticides, the processes of water flow and transport of pollutants, and the degradation phenomena; particularly, the processes in an artificial wetland. This part is completed by the state of the art of the different existing numerical models to simulate the coupling between hydrodynamics in porous media and reactive transport.

In the second part, we approach the development of a new numerical simulation tool to understand the fate of pesticides in an artificial wetland. Not all the processes affecting the dynamics of pesticides are known and the quantitative description of the known processes is still not possible [Rao and Jessup, 1982]. This finding emerges from a literature review that identifies and analyzes the difficulties encountered by the simulation models of pesticides fate during verification tests. Verification or use of these models is usually difficult, due to the inadequate methods for measuring and estimating the input parameters.

The model developed is based on mixed hybrid finite element method of discretization. It represents a contribution to the numerical methods used to the simulation of groundwater flow and transport of contaminants in variably saturated porous media.

The formulation used is based on Raviart-Thomas' space properties, considering a two-dimensional domain divided into triangular elements. This technique is particularly well adapted to the simulation of heterogeneous flow field. It has been applied in previous works concerned mainly with the flow in heterogeneous saturated porous medium. In unsaturated porous medium, the heterogeneity is due to both the heterogeneous sediment distribution and the non-uniform water content in the constructed wetland. The originality here is to simulate both, flow and solute transport, with the application of the mixed hybrid finite element method for a variably saturated porous medium.

The hydrodynamic model governed by the Richards' equation has been modified by the addition of a variable of pressure transformation. This method presented by Pan and Wierenga [1995] is numerically robust for all the cases in variably saturated, heterogeneous porous media and with Dirichlet or Neumann type boundary conditions. The mass condensation scheme proposed by Belfort [2006] was used in order to avoid oscillation problems related to the discrete expression of the term representing mass variation in the volume. Moreover, the algorithm for the management of boundary conditions proposed by Van Dam and Feddes [2000] and applied to simulate infiltration and evaporation scenarios has been implemented in order to avoid results without physical meaning.

For the transport equation, an original formulation was used. A unique vector approximated the advective-dispersive transport flux. Thus, it does not make use of the operator splitting technique, which introduces into the solution an intrinsic error associated with each operator. In order to control the non-physical oscillations when convection is the dominant process, a flux-limiting tool was introduced. The suggested flux-limiting tool makes it possible to preserve precision and unconditional stability for a large range of Peclet numbers.

Following the hydrodynamic and transport modelling, different pesticide biodegradation kinetic models have been implemented, specifically related to the environment of soils.

The numerical solution is obtained after the resolution of a system of linear equations, where the unknowns are the water pressure traces for the hydrodynamics and traces of concentration for the transport. The matrix associated with the hydrodynamics equations system is symmetric and definite positive. Therefore, it can be effectively solved by the

conjugate gradient method, preconditioned with an incomplete Cholesky decomposition using the Eisenstat procedure [Eisenstat, 1981]. In contrast, the matrix associated with the transport is nonsymmetric. Thus, the conjugate gradient squared iterative method with the Eisenstat ILU preconditioning procedure will be used to solve this algebraic system.

Time discretization also plays an important role during the simulation. An inadequate time step selection may lead to an inaccurate approximation for the hydrodynamics and solute transport calculations. For this reason, the time increment is automatically adjusted at each time level.

In the third part, hydrodynamic model verification was performed by comparison between reference results from the literature and those computed by the model developed. Several problems in one and two dimensions were treated. The infiltration in soils that were initially very dry, led to strong gradients in water content being simulated successfully. Besides, a comparison among the results calculated by the commercial numerical model HYDRUS (in the case of infiltration into a column of soil), analytical solutions and the model developed permitted the validation of the effectiveness of the proposed flux-limiter.

The fourth part is concerned with the application of the numerical model to field conditions via experimental sites. Model use is usually difficult because of inadequate methods for measuring and estimating the input parameters of the models. Furthermore, the methods to measure the input parameters sometimes are not available or their use on field conditions is confronted with many issues. We list a few of them here:

The physical, chemical and biological properties of soil vary spatially and temporally. Pesticides behavior is determined by a multitude of dynamic processes, which take place simultaneously.

Mathematical models of biological transformation result in general from the relations developed by the description of microbial kinetics in batch or continuous cultures. The microbial flora is restricted to the aqueous phase that can be compared to a biological reactor where various substances are introduced [Soulas and Fournier, 1981]. Although it is very interesting, this approach has limitations because of the large complexity of the soils. Alexander and Scow [1989] indicate that the physicochemical composition of the soils is highly complex; the microbial community is heterogeneous enough; and the abiotic constituents are usually reactive. In consequence, the application of the kinetic models of biodegradation is subject to question. For this reason, we will not approach the validation of the biological processes in this part.

We propose the use of the numerical model to optimize the hydraulic functioning of real sites constructed under the frame of the European project ARTWET (LIFE 06 ENV/F/000133).

The first site is located in the rural/urban interface in Rouffach (Alsace, France). It is a stormwater basin, originally constructed for flow regulation purposes.

It receives streaming flows generated mainly over the roads and vineyard parcels. After transitory storage, the volumes collected are sent towards a downstream collector. Then they are conducted to a water treatment station and, finally, they are released to the natural environment. Measurements have shown the presence of pesticides at considerable concentrations upstream and downstream of the station. This station is not, indeed, designed to treat pesticides. The stormwater basin has the potentiality of biodegradation and phytodegradation, derived from the existence of an accumulation of the sediments transported from the parcels and the colonization of this medium by vegetation. Therefore, it becomes an element of potential treatment of the polluting load, which is interesting to optimize.

The optimization of the stormwater basin design is being carried out by the construction of a horizontal-flow constructed wetland (HFCW), which improves its biological potentialities with the aim of reducing pesticide concentration in the in-transit water. In order to optimize the HFCW's hydraulic management, numerical tracer experiments were carried out to simulate several scenarios. Realistic hydraulic loads were simulated and different pressure profiles were examined. Breakthrough curves have been exploited to calculate the solute residence time distribution in the HFCW, as well as the storage capacity. The effects induced by adsorption heterogeneity in the medium were analyzed. An empirical expression to calculate the storage capacity has been constructed. The HFCW can only treat the stored pollution. Thus, we propose operational alternatives to optimize the storage capacity of the HFCW through the application of the model. Hence, a hydraulic management of the HFCW is suggested in relation to the times of retention and pesticide degradation.

Section 1.3. References first chapter

Alexander M., Scow M., 1989. Kinetics of Biodegradation in Soil. *Soil Science Society of America and American Society of Agronomy, 677 S. Segoe Rd., Madison*, WI 53711, USA. Reactions and Movement of Organic Chemicals in Soils, SSSA Special Publication no. 22

Belfort, B., 2006. Modélisation des écoulements en milieux poreux non saturés par la méthode des elements finis mixtes hybrids, Ph.D. Thesis, University Louis Pasteur. Strasbourg, France, 239 pp.

Eisenstat, S.C., 1981. Efficient implementation of a class of preconditioned conjugate gradient methods. SIAMS Journal of Scientific and Statistical Computing 2, 1-4.

Gregoire, C., Elsaesser, D., Huguenot, D., Lange, J., Lebeau, T., Merli, A., Mose, R., Passeport, E., Payraudeau, S., Schütz, T., Schulz, R., Tapia-Padilla, G., Tournebize, J., Trevisan, Marco, Wanko, A., 2009. Mitigation of agricultural nonpoint-source pesticide pollution in artificial wetland ecosystems. Environmental chemistry letters, 7(3): 205-231.

Gregoire, C., Payraudeau, S., Domange, N., 2010. Use and fate of 17 pesticides applied on a vineyard catchment. International Journal of Environmental Analytical Chemistry, 90(3-6): 406-420.

Pan L., Wierenga, P.J., 1995. A transformed pressure head-based approach to solve Richard's equation for variably saturated soils. Water Resour. Res. 31, 925-931.

Rao, P.S.C., Jessup, R.E., 1982. Development and verification of simulation models for describing pesticide dynamics in soils. Ecol. Model. 16, 67-75.

Soulas, G., Fournier, J.C., 1981. Soil aggregates as a natural sampling unit for studying behaviour of microorganisms in the soil: application to pesticide degrading microorganisms, Chemosphere 10, 431-440.

Van Dam, J.C., Feddes, R.A., 2000. Numerical simulation of infiltration, evaporation and shallow groundwater levels with the Richards equation. J. Hydrol. 233, 72-85.

2

Chapter 2 - State of the art

This chapter includes a state-of-the-art review on pesticides and their effects on environment and human health, followed by a short overview of the European Pesticide Legislation. Different methods of pesticide risk reduction were approached from the point of view of management and the development of remediation techniques. The use of constructed wetlands is then proposed. Then, a brief history about the utilization of constructed wetlands in water treatment is given. The next section concerns the application of constructed wetlands for the treatment of pesticide non-point source pollution. A subsequent section contains an extended description of the different processes occurring in constructed wetlands (hydrodynamics, transport, and fate of pesticides). Finally, this chapter presents a literature review on numerical modeling techniques.

Section 2.1. Pesticides, environment and human health

Pesticide is a general term that includes several types of chemicals, such as herbicides, insecticides, fungicides, rodenticides, among others, designed to stop unwanted growth. Over the years, the use of pesticides has greatly increased with the evolution of the intensive agriculture. Based on the World Environmental Databook 2008/2009 [Euromonitor international, 2009], United States was the country with higher total pesticide consumption (370,993 tonnes) in 2007, followed by France (116,754 tonnes). The increase in their pesticide consumption in comparison to 2001 was higher for France (17.18%) than for United States (2.82%). In France, the presence of pesticides in the environment has been confirmed by several studies: in surface water [Garmouma et al., 2001; Irace-Guigand et al., 2004; Comoretto et al., 2007; Pesce et al., 2008, Botta et al., 2009], groundwater [Morvan et al., 2006; Baran et al., 2007, Baran et al., 2008; Gutierrez and Baran, 2009], soil [Duquenne et al., 1996; Mamy et al., 2008a; Schreck et al., 2008], and atmosphere [Chevreuil et al., 1996; Khalil Granier and Chevreuil, 1997; Sanusi et al., 2000; Bedos et al., 2002; Briand et al, 2002; Scheyer et al., 2005, Scheyer et al., 2007]. According to the French Institute for the Environment [IFEN, 2006], in a survey performed in 2004, pesticides residues were detected in 96% of the measurement points of superficial water and 61% of groundwater.

Particular interest is given to water contamination, especially when impacted water bodies are used for drinking water supply or when water discharges are close to a sensitive habitat. Risk assessment and effects on wildlife resulting from pesticide contamination of aquatic ecosystems was the subject of different studies [Belfroid et al., 1998; Cuppen et al., 2000; Van den Brink et al., 2000; Hanson et al., 2002, Yamaguchi et al., 2003; Wendt-Rasch et al., 2004; Altinok et al., 2006; Capkin et al., 2006; Boesten et al., 2007; Houdart et al., 2009; Van den Brink et al., 2009]. Different approaches to estimate the environmental impact of pesticide use have been developed [Van der Werf, 1996; Levitan, 2000; Falconer, 2002; Bues et al., 2004], as well as procedures or indicators for environmental risk assessment of pesticides [Reus et al., 2002; Finizio and Villa, 2002; Sánchez-Bayo et al., 2002; Padovani et al., 2004; De Schampheleire et al., 2007; Mamy et al., 2008b; Centofanti et al., 2008; Sala and Vighi, 2008; Guérit et al, 2008]. As an alternative method for risk assessment, bioassays are early-warning systems that can be effectively used to detect the presence of pesticides [Hansen, 2007].

In some instances, transformation products have similar toxicity than their parent compounds. Thus, there is a need to consider them during the environmental risk-assessment process [Kolpin et al., 1998 and 2000; Andreu and Picó, 2004].

Concern is increasing for the determination whether there is a potential human health risk associated with pesticide exposure. Several studies have examined the relationship between the exposure to pesticides and the risk to develop cancer [O'Leary et al., 2004; De Brito Sá Stoppelli and Cretana, 2005], an increase in genotoxic damage [Bolognesi, 2003], chromosomal aberrations [Carbonell et al., 1995], endocrine disruption [McKinlay et al., 2008], damage in the reproductive system [Petrelli and Mantovani, 2002], depression as a major risk factor for suicide [Parrón et al., 1996], or problems in the central nervous system [Hogberg et al., 2009]. Although positive associations are difficult to establish, convincing connections support the cause-effect hypothesis.

The hazard of a pesticide on humans depends upon the toxicity of the pesticide, the magnitude of the dose received and the length of exposure time. Acute toxicity of a pesticide refers to the effects from a single dose or repeated exposure over a short time. Chronic toxicology refers to the effects of long-term or repeated lower level exposures. Important criteria have been established to help in the preservation of public health, such as the maximum residue level (MRL) that is legally permitted in specific food items and animal feed; as well as the amount of a pesticide, in mg/kg body weight, which can be ingested, on daily basis, during lifetime (refered as ADI), and the concept of the acute reference dose (ARfd). The mean dietary intake should not exceed the ADI over a considerable period of time, while short-term excursions in intakes should not exceed the ArfD [Nasreddine and Parent-Massin, 2002]. Human toxicity is generally estimated based on data on the toxicity of pesticides to rats and other animals. Test animals are examined for a wide variety of toxic effects [Durham and Williams, 1972], such as carcinogenicity, mutagenicity, teratogenicity, liver damage, reproductive disorders, nerve damage, and allergenic sensitization. However, dose-response data in experimental animals can only serve as a guide to the probable human toxicity of a pesticide.

In order to protect human health, the environment and wildlife, different regulatory agencies or organizations have established guidelines or standards values for maximum residue levels in food, soil, atmosphere, and water [WHO, 1997; US EPA, 2002; Hamilton et al., 2003; Adriaens, 2008; Menard et al., 2008].

Section 2.2. European Pesticide Legislation

A harmonized framework for the regulation of plant protection products in the European Community was set up through the adoption of Council Directive 91/414/EEC [Conseil de l'Europe, 1991] concerning the placing of plant protection products on the market. Regulation EC No 396/2005 of the European Parliament and of the Council [European Commission, 2005] has harmonized the highest level of a pesticide residue that is legally tolerated in or on food and feed of plant and animal origin, amending Council Directive 91/414/EEC. In France, the Ministries responsible for consumption, health, agriculture, and ecology have implemented an interministerial plan [PIRRP, 2006] intended to reduce the risk that pesticide use can generate on health, the environment and biodiversity.

The Water Framework Directive (Directive 2000/60/EC) commits European Union member states to achieve a good qualitative and quantitative status of all water bodies by 2015 [European Commission, 2000]. As a response, further monitoring programs were established. Directive 2008/105/EC [European Commission, 2008] sets the environmental quality standards to be accomplished for a list of priority substances, including several pesticides. The registration, evaluation, authorization and restriction of these substances are dealt through the application of the Regulation EC 1907/2006 [European Community Council, 2007]. European Water Framework Directive defines a frame for the management and the protection of waters, organized along large river basins, which are naturally defined by the catchment divides. The French Law on Water and Aquatic Environments of 30 December 2006 [LEMA, 2006] has set up action plans against diffuse pollution to be implemented in sensitive sectors as catchments of drinking-water wells, diffuse erosion areas, and wetlands of particular interest.

The Drinking Water Directive 98/83/EC in the European Union [European Community Council, 1998] established regulatory measures on the quality of water intended for human consumption, fixing a maximum threshold concentration limit of 0.10 μg L^{-1} for each individual pesticide (except for aldrin, dieldrin, heptachlor and heptachlor epoxide) and 0.5 μg L^{-1} for the total pesticides (sum of all individual pesticides detected and quantified in the monitoring procedure).

Section 2.3. Pesticide Risk Reduction

Pesticide risk reduction can be approached from the point of view of management or the development of remediation techniques. The application of both approaches leads to the minimization of the environmental impact caused by pesticide contamination.

2.3.1. Management approach

Pesticide entry into water can be originated from point or non-point sources [Barriuso et al., 1996; Müller et al., 2002; US EPA, 2003]. Agricultural non-point sources of pollution are a major cause of water quality impairment [Dowd et al., 2008]. Farmers, regulators, and other stakeholders face political, budgetary and technical barriers in order to achieve environmental outcomes. Henle et al. [2008] offer an approach of identification and evaluation to reconciliation strategies for the conflicts between agriculture and biodiversity conservation in Europe.

Some of these strategies include the establishment of national programs, which enable the revision of approval schemes in accordance with new knowledge for the minimization of hazards and risks to health and environment from the use of pesticides. These programs can improve controls on the use and distributions of pesticides. In addition, the implementation of pesticides registration programs permits the elimination of undesirable pesticides, or reduction in the levels of harmful active substances, and the registration of safer products.

The utilization of integrated crop and pest management is also suggested in order to encourage the use of low-input or pesticide-free crop farming [European Commission, 2002 and 2009]. In addition, the promotion of codes of good practices for handling, storage, use and disposal of pesticides are recommended, as well as the consideration of possible application of financial instruments. Significant changes in farming practices have been achieved as a result of negotiation between farmers and water suppliers through the establishiment of co-operative agreements [Heinz et al., 2002]. The improvement in the efficiency of the application process is also important, because of the influence in the toxicant distribution [Ebert and Downer, 2006]. An increase in the number of farmers using such approaches reduces the dependence on, and risk due to pesticide use.

Moreover, the establishment of environmental monitoring programs can result in the application of tighter controls and restrictions on product use. Besides, the monitoring and investigation of non-target impacts upon wildlife by pesticides may lead to the identification of responsible pesticides for review and the investigation of use patterns or compliance

actions, such as the installation of unsprayed or buffer zones in the agriculture to reduce the risks to wild life [European Crop Protection Association, 2008].

The collection of information on suspected adverse reactions from the use of pesticides will also improve health monitoring. Furthermore, a review of trends in a transparent monitoring system provides a clear understanding of what and where pesticides are used. It permits the identification of priorities and the development of suitable indicators. It may also provide statistical evidence to test the significance of site and chemical factors and their interactions concerning to pesticide environmental contamination and site vulnerability [Worral et al., 2002; Loague and Corwin, 2005].

2.3.2. Remediation techniques

Carter [2000] presents a list of methods developed to reduce pesticide entry into water (Table 1). These methods can be considered as physical, engineering and educational solutions.

Adsorption is a physical process effective for pesticide removal [Carrizosa et al., 2000; Aslan and Türkman, 2004; De Wilde et al., 2009]. El Bakouri et al. [2009] propose the use of natural organic substances to prevent the mobility of pesticides from agricultural soil to groundwater resources. A removal efficiency of more than 90% was obtained in an application for chlorinated pesticides included in European Water Framework Directive. Other methods include the possibility of using geotextiles for the retention of pesticides in agricultural watersheds. In a study performed by Boutron et al. [2009], pesticide adsorption on geotextile fibres was larger than for sediments, but it was lower than for dead leaves.

Another potential decontamination technique is the biobed. The main function of the biobed is to reduce environmental pesticide concentration due to the strong adsorption of the pesticide on the organic components and rapid degradation by the active microbiological component. The use of biobeds has been proposed to retain spilled pesticides especially during filling or cleaning of agricultural spraying equipment [von Wirén-Lehr et al., 2001; Torstensson, 2000; Spliid et al., 2006]. A modified biobed system technique based on biological reactors has proved to be efficient for the cleaning of water contaminated with persistent pesticides and it was suggested for reducing point-source contamination at farm level [Vischetti et al., 2004].

Table 1. Methods to reduce pesticide entry into water [Carter, 2000]

Entry Route	Methods to reduce pesticide entry into water
DIFFUSE	
Drainflow and interflow	Restrict flow when peak losses are anticipated to increase time for degradation and sorption (which may result in localized waterlogging)
	Manage soil structure e.g. create fine tilth to increase sorption and water retention (which may reduce infiltration, increase runoff, cause poor drainage and cause increased root disease pressures, etc.)
	Incorporate additives to soil surface e.g. organic material or stabilizers
	Restricted application areas e.g. protection zones
	Reduce drain intensity
	Optimization of application rates
	Target timing of applications to avoid potential loss periods
Surface flow	Buffer zones with various surface treatments e.g. grass strips
	Contour cultivations
	Manage soil surface e.g. reservoir tillage, minimal tillage
Base seepage	No specific measures
Leaching	Restricted application areas
	Restrict application to products with appropriate properties to minimize leaching manage soil structure e.g. create fine tilth to increase sorption and retention incorporate additives to soil surface e.g. organic material or stabilizers
Precipitation	No specific measure
Spray drift	No-spray zones e.g. LERAPS
	Manage vegetation adjacent to water e.g. hedges, interception plants
	low drift application technology
	Education of operator to choose optimal conditions
POINT	
Tank filling	Container modifications e.g. anti-glug necks, pack size, returnable packs
	Add container rinsate to the tank mix
	Engineering solutions e.g. tank full alarm, direct injection
	Remove operations from drained impermeable areas
	Biobeds
	Interception areas drained to waste collection site
	Education of operator
Spillages	Remove operations from drained impermeable areas
	Biobeds
	Interception areas drained to waste collection site
	Use of sorbent pads/ material and materials to intercept spills or clean up
	Use of licensed hazardous waste contractors
	Immediate incineration of empty containers if permitted or storage under cover before return or disposal
	Education of operator
Faulty equipment	Regular maintenance and servicing of sprayer
	Sprayer testing
Washing and waste disposal	Biobeds
	Other on farm treatment systems e.g. Sentinel system
	Authorized waste disposal
	Dispose of tank sump contents appropriately
Sumps, soakaways and drainage	Requirement for licensing
	Diversion from direct discharge to water
Direct entry including overspray	Avoidance
	Education of operator
Consented discharges	Requirement for licensing and compliance with Environmental Quality Standards

Moreover, the use of several microorganisms including bacteria and fungi for biosorption has been studied for the degradation of some pesticides [Ju et al., 1997; Benoit et al., 1998; Esposito et al., 1998; Lièvremont et al., 1998; Cullington and Walker, 1999; Khadrani et al., 1999; Hong et al., 2000; Tixier et al., 2002; Aksu, 2005; Castillo et al., 2006; Barragán-Huerta et al., 2007; Ghosh et al., 2009].

Bioremediation is the use of living organisms, primarily microorganisms, to degrade the environmental contaminants into less toxic forms [Vidali, 2001]. Supplying nutrients, carbon sources or electron donors to these microorganisms, the rate of natural microbial degradation of contaminants is enhanced [Frazar, 2000]. With the aim to examine the bioremediation's efficacy under more realistic conditions, studies in open soil microcosms were performed for atrazine-contaminated soils [Lima et al., 2009].

Futhermore, bioturbation refers to the biological reworking of soils and sediments by inhabiting organisms such as plant roots and burrowing animals. Soil bioturbation by earthworms may change the distribution and degradation of pesticides [Monard et al., 2008].

Phytoremediation is another technology that can be applied to remediate pesticide-contaminated sites [Arthur et al., 2000]. Phytoremediation is defined by Susarla et al. [2002] as an emerging technology that uses plants and then the associated rhizosphere microorganisms to remove, transform, or contain toxic chemicals located in soils, sediments, groundwater, surface water and even the atmosphere. Phytoremediation as a tool for contaminant mitigation is not a new concept [Salt et al., 1998; Dietz and Schnoor, 2001, Pivetz, 2001; Trapp and Ulrich, 2001; Singh and Jain, 2003; Pilon-Smits, 2005; Ahalya and Ramachandra, 2006]. The mechanisms of phytoremediation include the following processes (Figure 1)

- Phytoextraction (also called phytoaccumulation) is the process used by plants to accumulate contaminants into the roots and leaves.
- Phytostimulation (also called rhizodegradation) – The soil in the root zone, also called rhizosphere soil usually consists of 10-100 times greater number of indigenous microorganisms than in bulk soil. Degradation of some pesticides due to microbial activity in this soil has been found to be effective [Singh et al., 2004; Sun et al., 2004; Plangklang and Reungsang, 2008]. Microbial activity can be improved using the technique of bioaugmentation, which involves the addition of microorganisms that are capable of degrading pesticide [Dams et al., 2007].
- Phytodegradation. Breakdown of pollutants via enzymatic activities, usually inside tissues.

- Phytovolatilization. In this process, plants take up water containing the pollutant and release the contaminant into the atmosphere through their leaves.
- Phytostabilization – isolation and containment of contaminants within soil through the prevention of erosion and leaching. This process effectively reduces the bioavailability of the harmful contaminants.
- Hydraulic Control. In this process, trees indirectly remediate by controlling groundwater movement.

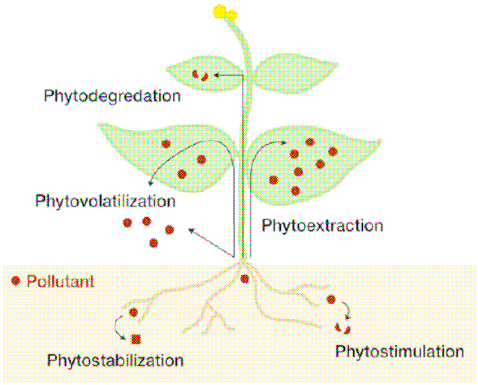

Fig. 1. Phytoremediation mechanisms [Pilon-Smits, 2005]

Past research indicates significant differences in the tolerance of plants to pesticides present in soil and water, and that some plants are more effective than others for pesticide remediation proposes. Karthikeyan et al. [2004] present a review on the potential remediation of soil and water contaminated with pesticide, using nontarget plants such as trees, shrubs, and grasses.

Phytoremediation of herbicides using conventional plants has been well studied. Investigations have demonstrated herbicide degradation by wetland riparian soils [Entry et al., 1995; Entry and Emmingham, 1996] and prairie grasses [Belden et al., 2004]. But, recent investigations propose the use of transgenic plants with improved potential of degradation of pesticides [Eapen et al., 2007; Kawahigashi, 2009; Macek et al., 2000].

According to Schnoor et al. [1995] phytoremediation is best suited to sites with shallow contamination (< 5 m depth) and those containing moderately hydrophobic pollutants (log K_{ow} = 0.5-3), short-chain aliphatic chemicals, or excess nutrients. Because of their root lengths, phytoremediation is usually limited to a depth of ten feet for groundwater remediation, and for soil or sediment remediation to the top three feet of the soil [Frazar, 2000]. Selection of the appropriate plants is then essential and the plants must be resistant to the pollutant to be removed.

In a study performed in The Netherlands, the creation of a 3-m buffer zone adjacent to a ditch decreased drift deposition in the ditch by a minimum of 95%, and only four of the 17 pesticides investigated posed a minor risk to aquatic organisms. With a 6-m buffer zone no drift deposition in the ditch could be measured [de Snoo and de Wit, 1998]. Another investigation also resulted in a very high reduction of the spray drift and the ecotoxicological risk for aquatic ecosystem, due to the presence of vegetative buffer strips and a tree row in a vineyard situated near Piacenza (Northen Italy) for protecting the water body in the middle of the agricultural field [Vischetti et al 2008]. Besides, an experiment carried out on the low plains of the Veneto Region (Italy) tested the performance of buffer strips to reduce concentration of herbicides (terbuthylazine, alarchlor, nicosulfuron, pendimethalin, linuron) in subsurface water. A grass strip 5m wide and 1 m wide row of trees achieved abatement in concentration between 60 and 90%, depending on the chemical and time elapsed since application. Even if the buffer showed good degradation potential, it was not sufficient to satisfy the EU limit for environmental and drinking water. The authors mention as a possible reason for this the insufficient buffer width [Borin et al., 2004]. Dabrowski et al. [2005] stated that emergent aquatic vegetation may be as effective in reducing spray deposition in surface waters as increasing buffer zone width.

The ability of aquatic plants to accumulate pesticide and their influence on the fate of pesticides had been demonstrated in several studies [Karen et al., 1998; Hand et al., 2001].

Previous studies have also supported the benefits of aquatic vegetation within drainage ditches for mitigation of pesticides [Bouldin et al., 2004; Herzon and Helenius, 2008]. In natural ditches, sorption is critically influenced by bottom substratum nature but also by hydrodyamic conditions such as water flow and height [Margoum et al., 2006]. In a study carried out by Moore et al. [2001b], one hour following a simulated storm runoff event, mean percentage concentrations of the herbicide atrazine and the insecticide lambda-cyhalothrin associated with plant material were 61% and 87% of the total measured, respectively. In another study Cooper et al. [2004] found that approximately 99% of the measured pyrethroid insecticide esfenvalerate was associated with ditch vegetation three hours following initiation of the simulated storm runoff. Therefore, it was demonstrated that plants serve as an important site for pesticide sorption during runoff events.

Burrows and Edwards [2002] proposed the use of integrated soil microcosm as terrestrial model ecosystems to assess simultaneously the overall effects of a single pesticide, on a range of representative soil organisms, ecosystem processes, and environmental fate.

Bennet [2005] confirmed the importance of vegetated buffers zones. His study suggests that vegetated wetlands have the potential to contribute to aqueous-phase pesticide risk mitigation. Sherrard et al. [2004] conducted four experiments using constructed wetland mesocosms to determine if chlorothalonil and chlorpyrifos in simulated runoff could be efficiently decreased, resulting in a potential decline in mortality in receiving aquatic system organisms. The study demonstrated the feasibility of constructed wetlands to retain runoff-related pesticide pollution.

Reichenberger et al. [2007] presented a review on mitigation strategies to reduce pesticide inputs into water bodies. The effectiveness of the strategies with respect to their practicability was evaluated. Some of these strategies were grassed buffer strips located at lower edges of fields, riparian buffer strips, constructed wetlands, subsurface drains, pesticide application rate reduction, product substitution and shift of the application date. In his conclusion he stated: "constructed wetlands are promising tools for mitigating pesticides via runoff/erosion and drift into surface waters, but their effectiveness still has to be demonstrated for weakly and moderately sorbing compounds". Based on this knowledge, the present work is focused on constructed wetlands to reduce pesticide non-point source pollution. A detailed description and examples of application are given in the following sections.

Section 2.4. Wetlands treatment history

Over the last decades, the interest in the optimization of the biological, physical, and chemical processes that occur in natural wetland systems as an option for water treatment has significantly increased [Mitsch, 1995; Bavor et al., 1995; Mitchell et al., 1995; Gopal and Mitsch, 1995; Shutes, 2001]. Constructed wetlands are engineered, man-made ecosystems that have been designed to utilize the natural processes involving wetland vegetation, soils, and their associated microbial assemblages to assist in water treating [Žáková, 1996; Haber, 1999; Vymazal, 1996a, 1996b, 2002, 2005 and 2009; Youngchul et al., 2006; Babatunde et al., 2008]. Constructed wetlands are being considered as a sustainable and promising option, whose performance, cost and resources utilization can complement or replace conventional water treatment [Griffith, 1992; Tack et al., 2007; Arias and Brown, 2009; Zhang et al., 2009].

Kadlec and Knight [1996] gave a good historical account of the use of natural and constructed wetlands. Constructed wetlands were primarily used to treat municipal or domestic waters. Research studies on the use of constructed wetland for wastewater treatment

began in Europe in the 1950's and in the United States in the 1960's. However, they can be used to treat different kinds of wastewaters: municipal wastewater, especially in small communities [Brix, 1994a; US EPA 2000, Kivaisi, 2001; Zhou et al., 2009]; urban stormwater runoff [Shutes et al., 1997; Koob et al., 1999; Birch et al., 2004; Revitt et al., 2004]; farm dairy, swine or agricultural wastewater [Cronk, 1996; Nguyen, 2000; Hunt and Poach, 2001; Borin et al., 2001b; Dunne et al., 2005]; aquaculture wastewater [Lin et al., 2002 and 2005; Schulz et al., 2003a; Sindilariu et al., 2009]; landfill leachate [Bulc, 2006; Nivala et al., 2007; Yalcuk and Ugurlu, 2009]; mine drainage [Tarutis Jr. et al., 1999; Brenner, 2001; Sheoran and Sheoran, 2006]; and other effluents such as waste waters from food processing industries [Vrhovšek et al.,1996] or textile industries [Davies et al., 2005; Bulc and Ojstršek, 2008]. The use of constructed wetlands effluents in the perspective of reclamation and water reuse has been the subject of different studies [Greenway and Simpson, 1996; House et al., 1999; Greenway, 2005; Ghermandi et al., 2007; Rousseau et al., 2008]. Another function of constructed wetlands is to retain surface water, which helps to decrease floods and pollution associated with floods [Sim et al., 2008].

Vymazal and Kröpfelová [2008] presented a list of examples of the use of constructed wetlands for the treatment of different types of pollution. The abilities of constructed wetlands to improve water quality are widely recognized, and their efficiency reducing suspended solids, biological oxygen demand (BOD), nitrogen, phosphorus, trace metal, toxic organic compounds, pathogens and other pollutants has been reported in several studies [Gersberg et al., 1983; Yang et al., 1995; Magmedov et al., 1996; Polprasert et al., 1996; Drizo et al., 1997; Ottová et al., 1997; Scholes et al., 1998; Nairn and Mitsch, 2000; Luederitz et al., 2001; Jing et al., 2001; Ye et al., 2001; Lim et al., 2003; Karathanasis et al., 2003; Huett et al., 2005; Vymazal, 2007; Vymazal and Kröpfelová, 2009, Khan et al., 2009; Kröpfelová et al., 2009; Tang et al., 2009]. However, evaluating potential effects in wildlife should be an integral part of the planning stage for treatment wetlands [Lemly and Ohlendorf, 2002].

Numerous international conferences have been convened to present findings on wetlands research. An annotated chronology of some of these conferences from the year 1976 to 2007 was presented by Kadlec and Wallace, [Kadlec and Wallace, 2008: Table 1.2, p12] . Recent conferences to be included in this chronology include the 11th International Conference on Wetland Systems for Water Pollution Control, held in Indore, India in 2008 and the 3rd International Symposium on Wetland Pollutant Dynamics and Control (WETPOL 2009) held in Barcelona, Spain in 2009.

Constructed wetlands consist of four main compartiments: plants, sediment and soil, microbial biomass and aqueous phase loaded with the chemicals, and typically include beds filled with poorly drained graded medium and aquatic plants [Imfeld et al., 2009]. Constructed wetlands for water treatment can be classified, according to their basic design into subsurface-flow and surface flow. Water flows above the substrate in surface wetlands, whereas in subsurface-flow wetlands water flows (horizontally or vertically) through the matrix and out of the system.

Research has shown that constructed or restored wetlands may help to control non-point sources of pollution. Nutrients, pesticides, and sediments are the main detrimental non-point source constituents [Kao et al., 2001b].

Nutrient enrichment is the primary contributor to hypoxia, which is the condition in which dissolved oxygen is below the level necessary to sustain most animal life.

Therefore, the creation and restoration of wetlands have been proposed as a solution to this problem [Mitsch et al., 2005; Mitsch and Day Jr., 2006; Kovacic et al., 2006]. In order to preserve and restore wetlands, Crumpton [2001] demonstrated the need for a landscape approach. It was shown that wetlands could improve water quality at the watershed scale if they are sited and designed to intercept a significant portion of the subsurface water moving through a watershed.

MacDonald et al. [1998] proposed a methodology to estimate the environmental benefits associated with the use of constructed wetlands to control agricultural non-point source pollution. Nutrient reduction differs depending on factors such as nutrient concentration, seasonality, hydraulic loading, water-residence time, soil type, plant species, and water chemistry [Moreno et al., 2007]. The ability of constructed or restored wetlands to remove nutrients and organic loads from water coming from the farming areas has been well demonstrated [Romero et al., 1999; Kovacic et al., 2000; Borin et al., 2001a, 2001b; Koskiaho et al., 2003; Jordan et al., 2003; Fink and Mistch, 2004; Braskerud, 2002a; O'Geen et al., 2007; Borin and Tocchetto, 2007; Blankenberg et al., 2008]. Phosphorus is given special attention, because it is often the limiting nutrient for algal growth in freshwater ecosystems [Correll, 1999; Braskerud, 2002b; Liikanen et al., 2004; Braskerud et al., 2005; Scholz et al., 2007; Tang et al., 2008]. Moreover, the creation of permanently flooded wetlands using run-off from irrigated fields was suggested as an efficient tool to restore or improve salinized soils [Moreno-Mateos et al., 2008 and 2010]. However, research concerning the treatment of pesticides in constructed wetlands is more limited, due in part to the fact that these organic compounds and their transformation products are difficult to analyze [Runes, 2003].

Section 2.5. Constructed wetlands and pesticides

Analytical results presented by several authors have demonstrated, with different grades of success, the capability of constructed and natural wetlands to remove agricultural pesticide runoff-related non-point source pollution from surface water [Kao et al., 2001a; Runes et al., 2001a; Runes et al., 2001b; Moore et al., 2002; Schulz et al., 2003b, Schulz et al., 2003c; Schulz, 2004; Moore et al., 2007; Borges et al., 2009]. The potential of constructed wetlands to reduce the environmental risk originated from spray drift-related pesticide pollution has also been highlighted [Schulz et al., 2003d].

In order to decrease the risk to aquatic receiving systems is necessary to decrease exposure [Moore et al., 2002]. This can be achieved by decreasing concentration, frequency of exposure, duration, or altering the form of exposure (bioavailable vs bound).

Different remediation pathways such as rhizo-microbial degradation, soil and sediment interactions, and macrophyte-specific pesticide uptake have been investigated as a single component of the dynamic process occurring in constructed wetlands for the removal of non-point source pesticide contamination.

One reason for the effectiveness of constructed wetlands lies in the presence of aquatic plants. The larger aquatic plants growing in wetlands are often called macrophytes [Brix 1994b and 1997]. The importance of macrophytes in pesticide mitigation has been proved by several investigations contrasting vegetated and nonvegetated wetland systems [Schulz et al., 2003c; Milam et al., 2004; Bouldin et al., 2005; Moore et al., 2006]. However, in a study comparing four types of macrophytes and nonvegetated systems, no statistically significant difference was noted in the efficiency to remove permethrin in water. The authors [Moore et al., 2009a] mention the relative short pesticide residence time (4-h) as a possible cause for seeing no significant difference between vegetated and unvegetated mesocosms. Even with longer ditch residence time (nearly 8-h) no significant differences were found [Moore et al., 2008]. But plant samples following a 12-h experiment indicate vegetation's potential role in cleaning water impacted by pesticide runoff, suggesting the need to examinate increased hydraulic retention times and mixed plant communites for more effective permethrin remediation.

McKinlay and Kasperek [1999] tested in the laboratory four species of macrophyte (Common Club-rush, Bulrush, Yellow Iris and Common Reed). A vertical subsurface flow test system was built for each of the macrophyte species in a glasshouse. Results showed the ability to decontaminate water polluted with the herbicide, atrazine.

The capacity of macrophytes to remove pesticides was also confirmed by a comparison of five aquatic macrophytes to assess their capacity to remove two fungicides (dimethomorph and pyrimethanil), commonly detected in the Champagne area in France. Among these macrophytes, duckweeds (Lemna minor and Spirodela polyrhiza) resulted as the best species for the removal of the selected fungicides [Dosnon-Olette et al, 2009].

Another comparison of the remediation attributes of vegetatives species was performed between Juncus effesus and Ludwigia peploides, common to agricultural drainages in the Mississippi Delta, USA. Their remediation capacity was assessed using atrazine and lambda-cyhalothrin. While greater atrazine uptake was measured in Juncus effessus, greater lambda-cyhalothrin uptake occurred in Ludwigia peploides [Bouldin et al., 2006]. An investigation performed by Olette et al. [2008] demonstrated the uptake capacity of selected aquatic plants (Lemna minor, Elodea Canadensis and Cobomba aquatica) on three pesticides: copper sulphate (fungicide), flazasulfuron (herbicide) and dimethomorph (fungicide). Removal percentages of the pesticide loads for all species tested ranged from 2.5 % to 50% during four days of incubation.

Macrophytes provide an increased surface area for sorption as well as for microbial activity. According to Luckeydoo et al. [2002], the vital role of vegetation in processing water passing through wetlands is accomplished through biomass nutrient storage, sedimentation, and by providing unique microhabitats for beneficial microorganisms. Macrophytes serve as filters by allowing contaminants to flow into plants and stems, which are then sorbed to macrophyte biofilms [Kadlec and Knight, 1996]. Field data shows that plants accelerate pesticide dissipation from aquatic systems by increasing sedimentation, biofilm contact and photolysis [Rose et al., 2008]. In constructed wetlands for phytoremediation, a variety of emergent, submerged, and floating aquatic species are used [Pilon-Smits, 2005]. Brisson and Chazarenc [2009] provide an approach that could help better guide macrophyte species selection for constructed wetland. ITRC [2009] presents a database of different plants used in the remediation of pesticides.

Cheng et al. [2002] presented results showing that pesticides, parathion and omethoate, were completely removed from water in a constructed wetland after a four-month period of application. However, it was observed a low removal of herbicides, 36% for MCPA and no significant removal efficiency for dicamba. A multifunctionality of constructed wetlands in tropical and subtropical areas was also evidenced. The wetland area can be used for earning high yields of biomass as a source of renewable energy supply. Pesticide removal efficiency was also confirmed in constructed wetlands on cotton farms. Results demonstrate

that macrophytes and algae can reduce the persistence of pesticides in on-farm water and provide some data for modeling [Rose et al., 2006].

Pesticides residues, especially those that are N-based appear to be effectively broken down and rendered inactive in constructed wetlands, even after short retention times. Braskerud and Haarstad [2003] reported a > 65% reduction in the detection of 13 agricultural pesticides (including MCPA, Mecoprop, Dicamba and Propachlor) in a small constructed wetland, less than 0.04% of catchment area with an average hydraulic loading >0.8 meters per day. Further research by Stearman et al. [2003], in a 2-year study of 14 planted and clear water constructed wetland, reported 82% and 77% removal of the pesticides metalachlor and simazine, respectively, in runoff water from a container nursery. In clear ponds the removal rates were less effective (63% and 64%). They also concluded that SSF wetlands were the best performing design for pesticide removal.

However, it should be considered that the potential of wetlands to reduce toxicants can also lead to unwanted long-term accumulation of chemicals, as documented for natural wetland areas [Donald et al., 1999].

The capacity of constructed wetlands to retain pesticides is achieved through the process of sorption to either plant or sediment material. Numerous studies attempted to quantify insecticide retention in wetlands by monitoring input and output measurements. In South Africa, Schulz and Peall [2001] investigated the retention of the organophosfate insecticides azinphosmethyl (AZP) and chlorpyrifos and the organochlorine insecticide endosulfan introduced during a heavy rainfall event followed by edge-of-field runoff from a 400-ha fruit orchards area into a 0.44 ha wetland. The constructed wetland is located along one of the tributaries shortly before its entry into the Lourens River. A toxicological evaluation employing midge larvae (Chironomus species) bioassays in situ at the wetland inlet and outlet revealed an 89% reduction in toxicity below the wetland during runoff. A retention rate between 77 and 93% of water-diluted AZP was found. Chlorpyriphos and endosulfan were undetectable in the outlet water samples, suggesting a retention rate of almost 100%. Retention was also assessed for aqueous-phase AZP input following drift during application in orchards. The reduction of AZP load was 54.1± 3.8% and the bioassays revealed a significant reduction of toxicity [Schulz et al., 2001]. In a further study demonstrated retention of approximately 55 and 25% of chlorpyrifos by sediments and plants, respectively, in wetland mesocosms (59-73 m in length) in Oxford, Mississippi, as well as a more than 90% reduction in concentrations and in situ toxicity of chlorpyrifos in the wetland in South Africa [Moore et al., 2002].

Aqueous and sediment bioassays with freshwater test organisms had been used to examine the use of constructed wetlands to mitigate the ecological impacts of pesticide contamination from agricultural fields into receiving aquatic systems [Smith, Jr. et al., 2007].

Concerning the effectiveness of constructed wetlands and the determination of appropriate wetland design parameters for pesticide mitigation, Moore et al. [2000 and 2001a] presented results from monitoring transport and fate into constructed wetland for atrazine and metolachlor associated runoff mitigation. When dealing specifically with herbicides, many factors must be considered during the design process, for example: intended threshold concentration of the wetland, size necessary for effective mitigation, potential impacts to the wetland itself and effects to aquatic receiving systems. Economical and ecological benefits and risks must be thoroughly considered before implementing constructed wetlands as sole best management practices in agricultural systems [Moore et al., 2000].

The use of a constructed wetland system in the Mississippi Delta, USA (180m x 30m) was evaluated for the mitigation of lamba-cyhalothrin and cyfluthrin concentration associated with a simulated storm runoff event [Moore et al., 2009b]. Based on conservative effects concentrations for invertebrates and regression analysis of maximum observated wetland aqueous concentrations, new design specification was proposed (215 m x 30m). The results of this experiment could be used to model future design specificiations for constructed wetland mitigation of pyrethroid insecticides.

2.5.1. Design parameters

In addition to a hydrologic analysis, chemical half-life and hydraulic retention time are key parameters in designing constructed wetlands for non-point source pollution control.

2.5.1.1. Hydrologic analysis

There is evidence about the strong influence that hydrology may have on the environmental fate of pesticides. In a laboratory assessment of fluometuron degradation in soil from a constructed wetland, fluometuron was degraded rapidly under saturated conditions, but was very persistent under flooded conditions [Weaver et al., 2004]. Wetland performance has been observed to be seasonally variable, controlled by hydrological inputs [Dunne et al., 2005]. Changes in concentrations of pesticides in groundwater have been observed to be much slower than in streams, and responses of groundwater to changing use

can be delayed for years or decades in some systems [U.S. Geological Survey, 1999]. Continuous hydrologic modeling provides a rich source of information that can be manipulated to evaluate annual and monthly water balances, flood frequency distributions and other indicators [Konyha et al., 1995].

2.5.1.2. Chemical Half-life

The half-life is a measure of the persistence of a pesticide in soil. Chemical half-lives are first order disappearance coefficients. They represent the time required for a pesticide to degrade in soil to one-half its original amount. Pesticides can be categorized as non-persistent (half life is less than 30 days); moderately persistent (half-life between 30 to 100 days); or persistant (if taking longer than 100 days to degrade to half of the orginal concentration) [Poissant et al., 2008]. Experimental studies in wetlands can be conducted to provide half-lives for specific chemicals and wetland characteristics.

2.5.1.3. Hydraulic retention time

The hydraulic residence time (HRT) is the basis for hydraulic design. It represents the average time required for a parcel of water to pass through a wetland. An optimal hydraulic residence time will allow pesticide fixation in the soil, so pesticide concentration can be reduced according to the various degradation processes.

Section 2.6. Processes

The unsaturated zone is, by definition, a multiphase system with at least two fluid phases present: air and water. Interest in the unsaturated zone is related to the growing concern about the adverse effects on the quality of the subsurface environnement caused from agricultural, industrial, and municipal activities. To prevent continued contamination of receiving environments and to develop more effective cleaning methods, it is necessary to have reliable mathematical models. The first step for modelling is the conceptual understanding of the physical problem. Once the concepts are formulated, the physical system is translated into a mathematical framework resulting in equations that describe the process [Mercer and Faust, 1980].

2.6.1. Hydrodynamics

Richards' equation represents the movement of water in a variably saturated, rigid, isothermal porous media with incompressible water and a continuous air phase. An important assumption in deriving the Richards' equation [Richards, 1931] is to assume that the air present in the unsaturated zone has infinite mobility. In other words, the air-phase pressure is assumed constant and equal to the atmospheric pressure, and air moves without interfering with water and/or contaminant. This assumption is reasonable in most cases because the mobility of the air phase is much larger than that of the water, due to the viscosity difference between the two fluids. Tegnander [2001] has found that in order to obtain equivalence between the fractional flow model and the Richards' model, the mobility ratio should at least be 100. Other assumptions in deriving Richards' equation are constant water density and negligible porosity changes. Including the air as a separate phase gives the fractional flow approach [Vauclin, 1989].

Constructed wetland hydrodynamics modelling has been conducted in Curienne (France). The hydraulic residence time distributions of the subsurface horizontal flow constructed wetland were estimated [Chazarenc et al., 2003]. A simulation was also performed for a subsurface flow wetland using the commercial computational fluid dynamic (CFD) code and the hydraulic residence time distribution was obtained. Their results indicated that the hydraulic performance of the wetland was predominantly affected by the wetland configuration [Fan et al., 2008].

2.6.2. Transport

The pesticide transport is described by a classical advection-dispersion equation with the presence of sink/source term, which takes into account the pesticide degradation. Advective transport occurs when dissolved chemicals are moving with the water flow. Dispersion refers to the spreading and mixing caused in part by molecular diffusion and microscopic variation in velocities within individual pores [Anderson, 1979]. Molecular diffusion occurs as species move from higher to lower concentrations. Mechanical dispersion is caused by flow and presence of a pore system and is in the direction of groundwater flow. Thus, this component is directly related to the advection properties of the system and it is the predominant transport mechanism at high velocities [Khalifa, 2003]. The combined effect of molecular diffusion and mechanical dispersion is referred as hydrodynamic dispersion.

2.6.3. Pesticides fate in the environment

The fate of pesticides in the environment is influenced by many factors that determine their persistence and mobility [Gavrilescu, 2005]. An understanding of the fate processes can help to prevent soil and water contamination. Fate processes can be beneficial if they move to the target area or destroy its potentially harmful residues. But, inappropriate or poorly planned use of pesticides can result in an environmental damage or injury of nontarget plants and animals.

2.6.3.1. Sorption

Sorption is defined as the transfer of a solute between a fluid and a solid phase. Sorption includes both adsorption and absorption. Physical adsorption refers to the attraction caused by the surface tension of a solid that causes molecules to be held at the surface of the solid. Chemical adsorption involves actual chemical bonding at the solid's surface. Absorption is a process in which the molecules or atoms of one phase penetrate those of another phase [Reddy and DeLaune, 2008].

Due to the different physical and chemical properties of both the sorbate and the sorbent, there are several possible sorption mechanisms such as functional groups, acid-base character, polarity and polarizability, charge distribution, water solubility, hydrophobicity, configuration and conformation [Hapeman, 2003].

Sorption occurs when a pesticide molecule comes in contact with soil constituents establishing a pseudo-equilibrium with these constituents [Cáceres et al., 2010]. Pesticides can also be released from soil and affect the environment, this process is called desorption.

Dordio et al. [2007] state that "the efficiency of constructed wetlands systems in the removal of pollutants can be significantly enhanced by using a support matrix with a greater capacity to retain contaminants by sorption phenomena, ionic exchange or other physico-chemical processes".

2.6.3.1.1. <u>Adsorption</u>

Some of the factors affecting adsorption include the type of pesticide, and properties of the soil such as moisture, pH, organic matter type and content, clay mineralogy, cation exchange capacities, and Eh [Schwab et al., 2006]. In general adsorption of pesticides in soils

is more closely related to the organic matter content than any other single property [Spark and Swift, 2002; Coquet, 2002].

Sorption isotherms are used to quantify the amount of chemical sorbed onto the solid phase. The most common sorption isotherm used for pesticides is represented by the Freundlich equation: $S = K_f C^{1/n}$. Where S is the sorbed concentration; C is the solution concentration, and K_f and $1/n$ are empirical constants. If n=1, a linear equation results: $S = K_d C$. Where K_d is better known as distribution or partitioning coefficient and it represents the ratio of the concentration of the solute between the solid matrix and the solution phase. When organic carbon is assumed to be the dominant sorbent in soil, the soil organic carbon sorption coefficient K_{OC} is used. K_{OC} is calculated by dividing a measured K_d in a specific soil by the organic carbon fraction F_{OC} of the soil: $K_{OC} = \frac{K_d}{F_{OC}}$.

K_{OC} values are usually seen as an universal constant used to measure the relative potential mobility of pesticides in soils, however there is evidence that it is not [Wauchope et al., 2002]. For example, when soils of very low organic matter content are studied, K_{OC} can vary more than K_d.

Adsorption is one of the key factors to determine the mobility and availability for bio- and chemical degradation. K_{OC} describes the tendency of a pesticide to bind to soil particles. The binding forces and the types of mechanisms operating in the adsorption processes of pesticides onto the soil humic substances include ionic, hydrogen and covalent bonding, charge-transfer or electron donor ± acceptor mechanisms, van der Waal forces, ligand exchange, and hydrophobic bonding or partitioning. Two or more mechanisms may occur simultaneously depending on the nature of the functional group and the acidity of the system [Gevao et al., 2000]. Adsorption coefficient values greater than 1000 indicate a pesticide that is very strongly attached to soil, values less than 300-500 indicate the pesticide tend to move with water [Gavrilescu, 2005].

In a constructed wetland located within Stanislaus County, California, sedimentation of pesticide-laden particles was the main mechanism for pyrethroid removal, which was influenced by hydraulic residence time and vegetation density. Decreases in sediment concentration of pyrethroids suggested that the wetlands were efficient at trapping particles with adsorbed pyrethroids after the tailwater passed through the sediment basin [Budd et al., 2009].

2.6.3.1.2 **Absorption**

Plants, animals, humans or microorganisms can absorb pesticides. Once absorbed, pesticides may be broken down or stored inside the organism. Pesticides residues may be release back into the environment when the animal dies or as the plant decays.

Uptake of pesticides into plant foliage varies with plants and chemicals. It can be influenced by adjuvants and environmental conditions [Wang and Liu, 2007]. The lipophilic nature of pesticides is a determining factor affecting their uptake into plants. It can be characterized by the octanol water partition coefficient (K_{OW}). Cheng et al. [2009] results suggest that the effect of plant growth on contaminant removal in constructed wetlands was different specifically in plants and contaminants.

2.6.3.2. Runoff

Runoff is the movement of pesticides in water over a sloping surface. The pesticides are either mixed in the water or bound to eroding soil. Runoff can occur when water is added to a field faster than it can be absorbed into the soil.

A pesticide molecule can exist either in the dissolved phase or associated with a particle or colloid. The transport will be governed by water flow for the dissolved phase and by the movement of the particle for the associated phase. The amount of pesticide runoff depends on the slope, soil texture, moisture and erodibility, the amount and timing of a rain-event (irrigation or rainfall) and the type of pesticide used. Pesticides with solubilities greater than 30 ppm are more likely to move with water.

Runoff is one of the most important pesticide entry pathways in surface waters. In a study under field conditions, runoff by rainfall of the pesticides acetochlor, atrazine, chlorpyrifos, and propisochlor during a five-month period at normal weather conditions caused losses that were primarily dependent on rainfall volume and intensity [Konda and Pásztor, 2001].

2.6.3.3. Leaching

Leaching is the movement of pesticides in water through the soil. The factors influencing the pesticide leaching into groundwater include characteristics of the soil and pesticide, and their interaction with water from a rain-event such as irrigation or rainfall.

Leaching of a pesticide through the soil profile is strongly influenced by preferential flow. Preferential flow is the process in which water and solute rapidly move through soil macropores, bypassing much of the soil matrix. Several factors such as size, geometry, and distribution of macropores affect preferential flow. Pesticide leaching below the root zone has been demonstrated in sandy and loamy soil [Flury, 1996].

2.6.3.4. Volatilization

Volatilization (or vapour drift) is the process of solids or liquids converting into gas, which can move with air currents away from the initial application site.

The potential for a pesticide to volatilize, or become a gas, is expressed terms of the Henry's Law constant:

$$H = \frac{\text{vapor pressure}}{\text{solubility}}$$

A high value for the constant H indicates a tendency for the pesticide to volatilize.

Volatilization is dependant on several factors including temperature, humidity, air movement, soil characteristics, and the mode of pesticide applications. Several investigations have been conducted in the field using a pesticide volatilization-modeling tool [Ferrari et al., 2003; Bedos et al., 2009]. Pesticides volatilize most readily from sandy and wet soils. Volatilization is also increased by hot, dry or windy weather. Even though changes in ambient temperature and/or the effect of micrometeorological conditions had been often neglected when predicting pesticide volatilization from fields [Yates et al., 2002].

2.6.3.5. Wind transfer

Pesticides can be carried in the wind during application. They can also be transported on small particulates such as soil or on larger objects like leaves that are caught up by wind.

Spray-drift occurs when the wind is strong enough to pick up and carry fine spray droplets. Granular and powder pesticide formulations will also drift. Some factors affecting spray-drift are the dropet size, wind speed, temperature and humidity. Gil and Sinfort [2005] presented a bibliographic review about the importance of spray drift on emission of pesticides and air quality.

In an agricultural area in the Western Cape, South Africa, it was found that wind was an important factor to explain most of the organophosphate pesticide azinphos methyl transfer to adjacent nontarget areas, after spraying events [Reinecke and Reinecke, 2007].

Results from Dabrowski et al. [2006] suggest that spray –drift-derived azinphos-methyl concentrations are more effectively mitigated by aquatic macrophytes than those of runoff.

A review of bibliography on the occurrence of pesticides in the atmosphere (in Europe) and the subsequent deposition gave as result a classification of pesticides according to their deposition pattern [Dubus et al., 2000]. It shows that wet deposition has been particulary monitored as dry deposition contributes to only a minor extent to the total deposition.

2.6.3.6. Soil erosion

Soil erosion occurs when a soil surface is worn away by water or wind. Pesticides adsorbed to soil particles will also be picked up and carried by the wind or water.

Small constructed wetlands are found to be more efficient as sedimentation basins for eroded soil material than expected from calculation based on detention time. Braskerud [2001] results show that macrophytes stimulate sediment retention by decreasing the resuspension of constructed wetland sediment. Braskerud [2003] found that clay retention was higher than predicted, suggesting that the increase in the settling velocity is the result of clay and fine silt having transported and settled as aggregates. Sveistrup et al. [2008] supports this hypothesis. However, the round shape of the aggregates in the wetlands shows that they have undergone erosion on the way from the agricultural site to the wetland, where sedimentation takes place. Therefore, it is suggested to construct wetlands as close to the source of erosion as possible, to minimize the risk of breakdown of aggregates.

2.6.3.7. Chemical degradation

Chemical degradation is the breakdown of pesticides by chemical reactions, such as photolysis, hydrolysis, oxidation and reduction [Bavcon et al., 2003]. The rate and type of chemical reactions that occur are influenced by the binding of pesticides to the soil, soil temperatures, pH levels and moisture.

Since natural water pH oscille between 5 and 9, hydrolysis is a process of less importance in superficial water, even if it can be an important via of pesticide degradation in groundwaters, where photodegradation seldom takes place.

2.6.3.8. Phytodegradation

Phytodegradation is defined as a breakdown of pollutants by plant enzymes or enzyme cofactors [Susarla et al., 2002]. Typical constructed wetland plants such as common reed (Phragmites australis) have shown the capability to degradate organic compounds.

2.6.3.9. Microbial degradation

Microbial degradation is the breakdown of chemicals by microorganisms such as fungi and bacteria [Nawab et al., 2003]. It tends to increase when temperature is warm, soil pH is favorable, soil moisture and oxygen are adequate and soil fertility is good. Soulas and Lagacherie [2001] described the main microbial processes, which contribute to the transformation of pesticides in the soil and their mathematical expressions. Heterogeneity in the special distribution of the degradation miicrofora was found as a probably significant source of uncertainty in the predictive capacity of modelling.

Lin et al. [2008] studied the effect of salinity on the degradation of atrazine in subsurface flow constructed wetland. Salinity impacted on the growth of bacteria, resulting in a switch of the microbial community.

2.6.3.10. Photodegradation

Photodegradation is the breakdown of a compound caused by the adsorption of ultraviolet, visible or infrared radiation (light). All pesticides are susceptible to photodegradation to some extent. The rate of breakdown is influenced by the intensity and spectrum of sunlight, length of exposure, and the properties of the pesticide.

Burrows et al. [2002] presented a review of the mechanisms of photodegradation of pesticides. Photodegradation studies were classified in four categories:

- direct photodegradation (photoreactivity under both solar and ultraviolet irradiation),
- photosensitized degradation, based on the absorption of light by a molecule it can involve redox processes such as the photo-Fenton reaction [Paterlini and Nogueira, 2005],
- photocatalized degradation, cyclic photoprocesses in the pesticide photodegrade, but spontaneous regeneration of the catalyst occurs to allow the sequence to continue indefinitely until all the substrate is destroyed [Hincapié et al., 2005; Phanikrishna Sharma et al., 2008]
- and degradation by reaction with hydroxyl radical.

Lányi and Dinya [2005] outlined the photodegradation pattern of some N-containing herbicides that belong to the groups of triazines (atrazine, cyanazine, terbuthylazine, terbutryn) and ureas (choloroxuron, methabenzthiazuron, diuron, fenuron), as well as thiolcarbamates (butylate, cycloate, EPTC, molinate, vernolat).

Recent research [Araña et al., 2008] studied the degradation of two commercial pesticides (Ronstar and Folimat) and two fungicides (pyrimethanil and triadimenol) treated by means of TiO_2-photocatalysis and wetland reactors. The photocatalytic methods were very efficient at the degradation and toxicity reduction of pyrimethanil, triadimenol and Folimat. The toxicity of Ronstar was reduced by 78% but the component oxadiazon was not degraded. Best results regarding toxicity reduction were achieved by combining photocatalytic and biological methods and the continuous dosage of the sample.

Section 2.7. Pesticide dynamics modelling

According to Rao and Jessup [1982], a model to simulate pesticide dynamics in a soil profile must include at least the following three key processes: water and solute transport, adsorption-desorption, and degradation.

Siimes and Kämäri [2003] carried out an inventory, where there were identified 82 solute transport and pesticide models available. A detailed description of these models was provided, in addition to a comparative analysis. Compiled databases such as CAMASE [1996], REM [2006], or papers such as Vink et al. [1997], Vanclooster et al. [2000], FOCUS [1995, 1997, 2000], Jones and Russell [2001], Dubus et al. [2002], Garratt et al. [2002], Mouvet [2004], Köhne et al. [2009], provide not only description, but information concerning the application and validation of pesticide fate models, as well as a comparison of capacity and performance among them. Vanclooster et al. [2000], and the papers referred to therein, gave a detailed description of different models to simulate pesticide leaching.

Parametrization and testing of sophisticated mathematical models and the corresponding computer simulation programs had been applied to pesticides and had been the subject for several publications: CREAMS [Knisel, 1980]; HYDRUS 2D [Pang et al., 2000; Gärdenäs et al 2006; Toscano et al., 2009]; PRZM / PRZM-2 / PRZM-3 [Trevisan et al., 2000a; Farenhorst et al., 2009; Luo and Zhang, 2010], VARLEACH [Trevisan et al., 2000b], PELMO [Klein et al., 2000; Ferrari et al., 2005], GLEAMS [Leonard et al., 1987; Cryer and Havens, 1999; Rekolainen et al., 2000], CRACK-NP [Armstrong et al., 2000], OPUS [Smith, 1995], PEARL [Leistra et al, 2001], PESTLA [Boesten and Gottesburen, 2000], RZWQM

[RZWQM Development Team, 1998; Cameira et al., 2000; Malone et al., 2003; Bayless et al., 2008], MACRO [Jarvis, 1995; Jarvis 1997; Jarvis et al., 2000], LEACHM/LEACHP, [Dust et al., 2000; Spurlock et al., 2006; Klier et al., 2008], SIMULAT [Aden and Diekkrüger, 2000], and PESTFADE [Clemente et al., 1998]. Some models employ the fugacity concept and require information on chemical properties, for example CHEMFRANCE [Devillers and Bintein, 1995; Bintein and Devillers, 1996a and 1996b], CLFUG [Ares et al., 1998]. Fugacity is a property of a substance that describes its tendency to abandon a phase.

As an extension of the HYDRUS-2D variably saturated water flow and solute transport software package, the multicomponent reactive transport model CW2D was developed to describe the biochemical transformation and degradation processes in subsurface flow constructed wetlands [Langergraber 2003; Langergraber and Šimunek, 2005; Langergraber 2008; Langergraber et al., 2009].

Dubus et al. [2003] carried out a review of the different sources of uncertainty in pesticides fate modelling. Many field data would be necessary to validate the precision of the predictions of these models. According to Aubertot et al. [2005], only a few data about flow and solute transport in heterogeneous artificial wetland systems are available. The lack of good modelling practice can induce user subjectivity in the estimation of model parameters, which have an impact in the modelling results [Francaviglia et al., 2000]. Therefore, it is difficult to find a model that gives at the same time complete satisfaction to the users on the approximation of the hydrodynamics and on the transport and the degradation of the substrate. On this subject, certain authors think that the implementation of an important biochemical process may very well override the disadvantage of a simple water flow concept [Van der Zee and Boesten, 1991; Gottesbüren et al., 1994, in Vink et al., 1997]. Holvoet et al. [2004] don’t share this affirmation. According to this author, the first stage in pesticide fate modelling is the development of a reliable hydrodynamic model. For this reason, we have chosen to optimize the calculation of the hydrodynamics by the mixed hybrid finite element method (described in detail in chapter 3) and to implement rigorously the transport and the biological processes, in order to conserve the physical and biological senses of the phenomena, while avoiding a very great complexity. Simple models having a minimum of variable of entry may provide sufficiently accurate description of the pesticide dynamics in an agricultural ecosystem [Rao and Jessup, 1982].

Section 2.8. References second chapter

Aden, K., Diekkrüger, B., 2000. Modeling pesticide dynamics of four different sites using the model system SIMULAT. Agricultural Water Management, 44(1-3): 337-355.

Adriaens, P., Limnotech, 2008. Annex D. Decision Framework for management of contaminated soils. In Dyke, P.H., Disposal Technology Options Study. Final Report. The Africa Stockpiles Programme. WWF International

Ahalya, N., Ramachandra, T.V., 2006. Phytoremediation : Processes and mechanisms. Journal of Ecobiology, 18(1): 33-38.

Aksu, Z., 2005. Application of biosorption for the removal of organic pollutant: a review. Process Biochemistry, 40(3-4): 997-1026.

Altinok, I., Capkin, E., Karahan, S., Boran, M., 2006. Effects of water quality and fish size on toxicity of methiocarb, a carbamate pesticide, to rainbow trout. Environmental Toxicology and Pharmacology, 22(1): 20-26.

Anderson, M.P., 1979. Using models to simulate the movement of contaminants through groundwater flow systems. CRC Critical Reviews in Environmental Control, 9(2): 97-156.

Andreu, V., Picó, Y., 2004. Determination of pesticides and their degradation products in soil : critical review and comparison of methods. Trends in Analytical Chemistry, 23(10-11): 772-789.

Araña, J., Garriga I Cabo, C., Fernández Rodríguez, C., Herrera Melián, J.A., Ortega Méndez, J.A., Doña Rodríguez, J.M., Pérez Peña, J., 2008. Combining Ti-O_2-photocatalysis and wetland reactors for the efficient treatment of pesticides. Chemosphere, 71(4):788-794.

Ares, J., Miglierina, A.M., Sánchez, R., Rosell, R., 1998. CLFUG: A GIS-scaleable model of pesticide fate in soil-groundwater system based on clearance and fugacity paradigms. Environmental Modeling and Assessment, 3 (1-2):95-105.

Arias, M.E., Brown, M.T., 2009. Feasibility of using constructed treatment wetlands for municipal wastewater treatment in the Bogotá Savannah, Colombia. Ecological Engineering, 35(7): 1070-1078.

Armstrong, A.C., Matthews, A.M., Portwood, A.M., Leeds-Harrison, P.B., Jarvis, N.J., 2000. CRACK-NP: a pesticide leaching model for cracking clay soils. Agricultural Water Management, 44(1-3): 183-199.

Arthur, E.L., Perkovich, B.S., Anderson, T.A., Coats, J.R., 2000. Degradation of an Atrazine and Metolachlor herbicide mixture in pesticide-contaminated soils from two agrochemical dealerships in Iowa. Water, Air, and Soil Pollution, 119(1-4): 75-90.

Aslan, Ş., Türkman, A., Simultaneous biological removal of endosulfan ($\alpha+\beta$) and nitrates from drinking waters using wheat straw as substrate. Environment International, 30(4): 449-455.

Aubertot, J.N., Barbier, J.M., Carpentier, A., Gril, J.J., Guichard, L., Lucas, P., Savary, S., Savini, I., Voltz, M. (eds.), 2005. Reducing the use of pesticides and limiting their environmental impact. Executive Summary of the Expert Report. (Pesticides, agriculture et environnement. Réduire l'utilisation des pesticides et limiter leurs impacts environnementaux. Expertise scientifique collective, synthèse du rapport, INRA et CEMAGREF). France, 64 p.

Babatunde, A.O., Zhao, Y.Q.,O'Neill, M., O'Sullivan, B., 2008. Constructed wetlands for environmental pollution control: A review of developments, research and practice in Ireland. Environment International, 34(1):116-126.

Baran, N., Mouvet, C., Négrel, Ph., 2007. Hydrodynamic and geochemical constraints on pesticide concentrations in the groundwater of an agricultural catchment (Brévilles, France). Environmental Pollution, 148(3): 729-738.

Baran, N., Lepiller, M., Mouvet, C., 2008. Agrucultural diffuse pollution in a chalk aquifer (Trois Fontaines, France) : influence of pesticide properties and hydrodynamic constraints. Journal of Hydrology, 358(1-2): 56-69.

Barragán-Huerta, B.E., Costa-Pérez, C., Peralta-Cruz, J., Barrera-Cortés, J., Esparza-García, F., Rodríguez-Vázquez, R., 2007. Biodegradation of organochlorine pesticides by bacteria grown in microniches of the porous structure of green bean coffee. International Biodeterioration and Biodegradation, 59(3): 239-244.

Barriuso, E., Calvet, R., Schiavon, M., Soulas, G. 1996. Les pesticides et les polluants organiques des sols. Transformations et dissipation. Etudes et Gestion des Sols 3(4): 279-296.

Bavcon, M., Trebše, P., Zupančič-Kralj, L., 2003. Investigations of the determination and transformations of diazinon and malathion under environmental conditions using gas chromatography coupled with a flame ionisation detector. Chemosphere, 50(5): 595-601.

Bavor, H.J., Roser, D.J., Adcock, P.W., 1995. Challenges for the development of advanced constructed wetlands technology. Water Science and Technology, 32(3): 13-20.

Bayless, R.E., Capel, P.D., Barbash, J.E., Webb, R.M.T., Hancock, T.L.C., Lampe, D.C., 2008. Simulated fate and transport of metolachlor in the unsaturated zone, Maryland, USA. Journal of Environmental Quality, 37(3):1064-1072.

Bedos, C., Cellier, P., Calvet, R., Barriuso, E., 2002. Occurrence of pesticides in the atmosphere in France. Agronomie, 22(1): 35-49.

Bedos, C., Génermont, S., Le Cadre, E., Garcia, L., Barriuso, E., Cellier, P., 2009. Modelling pesticide volatilization after soil application using the mechanistic model Volt'Air. Atmospheric Environment 43(22-23): 3630-3639.

Belden, J.B., Phillips, T.A, Coats, J.R., 2004. Effect of prairie grass on the dissipation, movement, and bioavailability of selected herbicides in prepared soil columns. Environmental Toxicology and Chemistry, 23(1): 125-132.

Belfroid, A.C., van Drunen, M., Beek, M.A., Schrap, S.M., van Gestel, C.A.M., van Hattum, B., 1998. Relative risks of transformation products of pesticides for aquatic ecosystems. Science of the Total Environment, 222(3): 167-183.

Bennett, E.R. 2005. Fate and effects of insecticides in vegetated agricultural drainage ditches and constructed wetlands: a valuable approach in risk mitigation. Dissertation. (Natural Sciences) – University of Koblenz-Landau, Germany. 189 pp.

Benoit, P., Barriuso, E., Calvet, R., 1998. Biosorption characterization of herbicides, 2,4-D and atrazine, and two chlorophenols on fungal mycelium. Chemosphere, 37(7): 1271-1282.

Bintein, S., Devillers, J., 1996a. Evaluating the environmental fate of lindane in France. Chemosphere, 32(12): 2427-2440.

Bintein, S., Devillers, J., 1996b. Evaluating the environmental fate of atrazine in France. Chemosphere, 32(12): 2441-2456.

Birch, G.F., Matthai, C., Fazeli, M.S., Suh, J.Y., 2004. Efficiency of a constructed wetland in removing contaminants from stormwater. Wetlands, 24(2): 459-466.

Blankenberg, A.-G.B., Haarstad, K., Søvik, A.-K., 2008. Nitrogen retention in constructed wetland filters treating diffuse agriculture pollution. Desalination, 226(1-3): 114-120.

Boesten, J.J.T.I., Gottesbüren, B., 2000. Testing PESTLA using two modelers for bentazone and ethoprophos in a sandy soil. Agricultural Water Management, 44(1-3): 283-305.

Boesten, J.J.T.I., Köpp, H., Adriaanse, P.I., Brock, T.C.M., Forbes, V.E., 2007. Conceptual model for improving the link between exposure and effects in the aquatic risk assessment of pesticides. Ecotoxicology and Environmental Safety, 66(3): 291-308.

Bolognesi, C., 2003. Genotoxicity of pesticides: a review of human biomonitoring studies. Mutation Research/ Reviews in Mutation Research; 543(3): 251-272.

Borges, A.C., Calijuri, M.C., Matos, A.T., Queiroz, M.E.L.R., 2009. Horizontal subsurface flow constructed wetlands for mitigation of ametryn-contaminated water. Water SA, 35(4): 441-445.

Borin, M., Tocchetto, D., 2007. Five year water and nitrogen balance for a constructed surface flow wetland treating agricultural drainage waters. Science of the Total Environment, 380(1-3): 38-47.

Borin, M., Bonaiti, G., Giardini, L., 2001a. Controlled drainage and wetlands to reduce agricultural pollution: A lysimetric study. Journal of Environmental Quality, 30(4): 1330-1340.

Borin, M., Bonaiti, G., Santamaria, G., Giardini, L., 2001b. A constructed surface flow wetland for treating agricultural waste waters. Water Science and Technology, 44(11-12): 523-530.

Borin, M., Bigon, E., Zanin, G., Fava, L., 2004. Performance of a narrow buffer strip in abating agricultural pollutants in the shallow subsurface water flux. Environmental Pollution, 131(2): 313-321.

Botta, F., Lavison, G., Couturier, G., Alliot, F., Moreau-Guigon, E., Fauchon, N., Guery, B., Chevreuil, M., 2009. Transfer of glyphosate and its degradate AMPA to surface waters through urban sewerage systems. Chemosphere, 77(1): 133-139.

Bouldin, J.L., Milam, C.D., Farris, J.L., Moore, M.T., Smith, Jr., S., Cooper, C.M., 2004. Evaluating toxicity of Asana XL ® (esfenvalerate) amendments in agricultural ditch mesocosms. Chemosphere, 56(7): 677-683.

Bouldin, J.L., Farris, J.L., Moore, M.T., Smith, Jr., S., Stephens, W.W., Cooper, C.M., 2005. Evaluated fate and effects of atrazine and lambda-cyhalothrin in vegetated and unvegetated microcosms. Environmental Toxicology, 20(5): 487-498.

Bouldin, J.L., Farris, J.L., Moore, M.T., Smith, Jr., S., Cooper, C.M., 2006. Hydroponic uptake of atrazine and lambda-cyhalothrin in Juncus effesus and Ludwigia peploides. Chemosphere, 65(6): 1049-1057.

Boutron, O., Gouy, V., Touze-Foltz, N., Benoit, P., Chovelon, J.M., Margoum, C., 2009. Geotextile fibres retention properties to prevent surface water nonpoint contamination by pesticides in agricultural areas. Geotextiles and Geomembranes, 27(4): 254-261.

Braskerud, B.C., 2001. The influence of vegetation on sedimentation and resuspension of soil particles in small constructed wetlands. Journal of Environmental Quality, 30(4): 1447-1457.

Braskerud, B.C., 2002a. Factors affecting nitrogen retention in small constructed wetlands treating agricultural non-point source pollution. Ecological Engineering, 18(3): 351-370.

Braskerud, B.C., 2002b. Factors affecting phosphorus retention in small constructed wetlands treating agricultural non-point source pollution. Ecological Engineering, 19(1): 41-61.

Braskerud, B.C., 2003. Clay particle retention in small constructed wetlands. Water Research, 37(16): 3793-3802.

Braskerud, B.C., Tonderski, K.S., Wedding, B., Bakke, R., Blankenberg, A.G., Ulén, B., Koshiaho, J., 2005. Can constructed wetlands reduce the diffuse phosphorus loads to eutrophic water in cold temperate regions? Journal of Environmental Quality, 34(6): 2145-2155.

Braskerud, B.C., Haarstad, K., 2003. Screening the retention of thirteen pesticides in a small constructed wetland. Water Science and Technology, 48(5): 267-274.

Brenner, F.J., 2001. Use of constructed wetlands for acid mine drainage abatement and stream restoration. Water Science and Technology, 44(11-12): 449-454.

Briand, O., Seux, R., Millet, M., Clément, M., 2002. Influence de la pluviométrie sur la contamination de l'atmosphère et des eaux de pluie par les pesticides. Journal of Water Science, 15(4): 767-787.

Brisson, J., Chazarenc, F., 2009. Maximizing pollutant removal in constructed wetlands : Should we pay more attention to macrophyte species selection ?. Science of the Total Environment, 407(13): 3923-2930.

Brix, H., 1994a. Use of constructed wetlands in water pollution control : historical development, present status, and future perspectives. Water Science and Technology, 30(8): 209-223.

Brix, H., 1994b. Functions of macrophytes in constructed wetlands. Water Science and Technology, 29(4): 71-78.

Brix, H., 1997. Do macrophytes play a role in constructed treatment wetlands?. Water Science and Technology, 35(5): 11-17

Budd, R., O'Green, A., Goh, K.S., Bondarenko, S., Gan, J., 2009. Efficacy of constructed wetlands in pesticide removal from tailwaters in the Central Valley, California. Environmental Science and Technology, 43(8): 2925-2930.

Bues, R., Bussières, P., Dadomo, M., Dumas, Y., Garcia-Pomar, M.I., Lyannaz, J.P., 2004. Assessing the environmental impacts of pesticides used on processing tomato crops. Agriculture, Ecosystems and Environment, 102(2): 155-162.

Bulc, T.G., 2006. Long term performance of a constructed wetland for landfill leachate treatment. Ecological Engineering, 26(4): 365-374.

Bulc, T.G., Ojstršek, A., 2008. The use of constructed wetland for dye-rich textile wastewater treatment. Journal of Hazardous Materials, 155(1-2): 76-82.

Burrows, L.A., Edwards, C.A., 2002. The use of integrated soil microcosms to predict effects of pesticides on soil ecosystems. European Journal of Soil Biology, 38(3-4): 245-249.

Burrows, H.D., Canle L, M., Santaballa, J.A., Steenken, S., 2002. Reaction pathways and mechanisms of photodegradation of pesticides. Journal of Photochemistry and Photobiology B: Biology, 67(2): 71-108.

Cáceres, T., Megharaj, M., Venkateswarlu, K., Sethunathan, N., Naidu, R., 2010. Fenamiphos and related organophosphorus pesticides: Environmental fate and toxicology, pp. 117-162. In D.M. Withacre (ed.), Reviews of Environmental Contamination and Toxicology Continuation of Residue Reviews. Reviews of Evironmental Contamination and Toxicology 205.

CAMASE. 1996. Register of agro-ecosystems models. In Plentinger MC, Penning de Vries FWT, (ed.). CAMASE: Concerted action for the development and testing of quantitative methods for research on agricultural system and the environment. DLO Research Institute for Agrobiology and Soil Fertility, Wageningen, the Netherlands. 420 pp.

Cameira, M.R., Ahuja, L., Fernando, R.M., Pereira, L.S., 2000. Evaluating field measured soil hydraulic properties in water transport simulations using the RZWQM. Journal of Hydrology, 236(1-2): 78-90.

Capkin, E., Altinok, I., Karahan, S., 2006. Water quality and fish size affect toxicity of endosulfan, an organochlorine pesticide, to rainbow trout. Chemosphere, 64(10): 1793-1800.

Carbonell, E., Valbuena, A., Xamena, N., Creus, A., Marcos, R., 1995. Temporary variations in chromosomal aberrations in a group of agricultural workers exposed to pesticides. Mutation research/ Genetic Toxicology, 344(3-4): 127-134.

Carrizosa, M.J., Calderón, M.J., Hermosín, M.C., Cornejo, J., 2000. Organosmectites as sorbent and carrier of the herbicide bentazone. Science of the Total Environment, 247(2-3): 285-293.

Carter, A., 2000. How pesticides get into water –and proposed reduction measures. Pesticide Outlook (now renamed Outlooks on pest management), 11(4): 149-156.

Castillo, M.A., Felis, N., Aragón, P., Cuesta, G., Sabater, C., 2006. Biodegradation of the herbicide diuron by streptomycetes isolated from soil. International Biodeterioration and Biodegradation, 58(3-4): 196-202.

Centofanti, T., Hollis, J.M., Blenkinsop, S., Fowler, H.J., Truckell, I., Dubus, I.G., Reichenberger, S., 2008. Development of agro-environmental scenarios to support pesticide risk assessment in Europe. Science of the Total Environment, 407(1): 574-588.

Chazarenc, F., Merlin, G., Gonthier, Y., 2003. Hydrodynamics of horizontal subsurface flow constructed wetlands. Ecological Engineering, 21(2-3):165-173.

Cheng, S., Vidakovic-Cifrek, Z., Grosse, W., Karrenbrock, F., 2002. Xenobiotics removal from polluted water by a multifunctional constructed wetland. Chemosphere, 48(4): 415-418.

Cheng X.-Y., Liang, M.-Q., Chen, W.-Y., Liu, X.-C., Chen, Z.-H., 2009. Growth and contaminant removal effect of several plants in constructed wetlands. Journal of Integrative Plant Biology, 51(3): 325-335

Chevreuil, M., Garmouma, M., Teil, M.J., Chesterikoff, A., 1996. Occurrence of organochlorines (PCBs, pesticides) and herbicides (triazines, phenylureas) in the atmosphere and in the fallout from urban and rural stations of the Paris area. Science of the Total Environment, 182(1-3): 25-37.

Clemente, R.S., Prasher, S.O., Salehi, F., 1998. Performance testing and validation of PESTFADE. Agricultural Water Management, 37(3): 205-224.

Comoretto, L., Arfib, B., Chiron, S., 2007. Pesticides in the Rhône river delta (France): Basic data for a field-based exposure assessment. Science of the Total Environment 380(1-3):124-132.

Conseil de l'europe, 1991. Council Directive 91/414/CEE of 15 July 1991 concerning the placing of plant protection products on the market. Official Journal of the European Union, L230, 19/08/1991, pp. 1-32.

Cooper, C.M., Moore, M.T., Bennett, E.R., Smith, Jr., S., Farris, J.L., Milam, C.D., Shields, Jr., F.D., 2004. Innovative uses of vegetated drainage ditches for reducing agricultural runoff. Water Science and Technology, 49(3): 117-123.

Coquet, Y., 2002. Variation of pesticide sorption isotherm in soil at the catchment scale. Pest Management Science: 59(1): 69-78.

Correll, D.L., 1999. Phosphorus: a rate limiting nutrient in surface waters. Poultry Science, 78(5): 674-682.

Cronk, J.K., 1996. Constructed wetlands to treat wastewater from dairy and swine operations: a review. Agriculture, Ecosystems and Environment, 58(2-3): 97-114.

Crumpton, W.G., 2001. Using wetlands for water quality improvement in agricultural watersheds; the importance of a watershed scale approach. Water Science and Technology, 44(11-12): 559-564.

Cryer, S.A., Havens, P.L., 1999. Regional sensitivity analysis using a fractional factorial method for the USDA model GLEAMS. Environmental Modelling and Software, 14(6): 613-624.

Cullington, J.E., Walker, A., 1999. Rapid biodegradation of diuron and other phenylurea herbicides by a soil bacterium. Soil Biology and Biochemistry, 31(5): 677-686.

Cuppen, J.G.M., Van den Brink, P.J., Camps, E., Uil, K.F., Brock, T.C.M., 2000. Impact of the fungicide carbendazim in freshwater microcosms. I. Water quality, breakdown of particulate organic matter and responses of macroinvertebrates. Aquatic Toxicology, 48(2-3): 233-250.

Dabrowski, J.M., Bollen, A., Bennett, E.R., Schulz, R., 2005. Pesticide interception by emergent aquatic macrophytes: Potential to mitigate spray-drift input in agricultural streams. Agriculture, Ecosystems and Environment, 111(1-4): 340-348.

Dabrowski, J.M., Bennett, E.R., Bollen, A., Schulz, R., 2006. Mitigation of azinphos-methyl in a vegetated stream: comparison of runoff-and spray drift. Chemosphere, 62(2): 204-212.

Dams, R.I., Paton, G.I., Killham, K., 2007. Rhizoremediation of pentachlorophenol by Sphingobium chlorophenolicum ATCC 39723. Chemosphere, 68(5): 864-870.

Davies, L.C., Carias, C.C., Novais, J.M., Martins-Dias, S., 2005. Phytoremediation of textile effluents containing azo dye by using Phragmites australis in a vertical flow intermittent feeding constructed wetland. Ecological Engineering, 25(5): 594-605.

De Brito Sá Stoppelli, I.M., Crestana, S., 2005. Pesticide exposure and cancer among rural workers from Bariri, São Paulo State, Brazil. Environment International, 31(5): 731-738.

De Schampheleire, M., Spanoghe, P., Brusselman, E., Sonck, S., 2007. Risk assessment of pesticide spray drift damage in Belgium. Crop Protection, 26(4): 602-611.

De Snoo, G.R., de Wit, P.J., 1998. Buffer zones for reducing pesticide drift to ditches and risks to aquatic organisms. Ecotoxicology and Environmental Safety, 41(1): 112-118.

De Wilde, T., Spanoghe, P., Ryckeboer, J., Jaeken, P., Springael, D., 2009. Sorption characteristics of pesticides on matrix substrates used in biopurification systems. Chemosphere, 75(1): 100-108.

Devillers, J., Bintein, S., 1995. CHEMFRANCE : A regional level III fugacity model applied to France. Chemosphere, 30(3): 457-476.

Dietz, A.C., Schnoor, J.L., 2001. Advances in phytoremediation. Environmental Health Perspectives Supplements, 109(1): 163-168.

Donald, D.B., Syrgiannis, J., Hunter, F., Weiss, G., 1999. Agricultural pesticides threaten the ecological integrity of northen prairie wetlands. Science of the Total Environment, 231(2-3): 173-181.

Dordio, A.V., Teimão, J., Ramalho, I., Palace Carvalho, A.J., Estêvão Candeias, A.J., 2007. Selection of a support matrix for the removal of some phenoxyacetic compounds in constructed wetlands systems. Science of the Total Environment, 380(1-3) : 237-246.

Dosnon-Olette, R., Couderchet, M., Eullaffroy, P., 2009. Phytoremediation of fungicides by aquatic macrophytes : Toxicity and removal rate. Ecotoxicology and Environmental Safety, 72(8): 2096-2101.

Dowd, B.M., Press, D., Los Huertos, M., 2008. Agricultural nonpoint source water pollution policy: The case of California's Central Coast. Agriculture, Ecosystems & Environment, 128(3): 151-161.

Drizo, A., Frost, C.A., Smith, K.A., Grace, J., 1997. Phosphate and ammonium removal by constructed wetlands with horizontal subsurface flow, using shale as a substrate. Water Science and Technology, 35(5): 95-102.

Dubus, I.G. Hollis, J.M., Brown, C.D., 2000. Pesticides in rainfall in Europe. Environmental Pollution, 110(2): 331-344.

Dubus, I.G., Beulke, S., Brown, C.D., 2002. Review - Calibration of pesticide leaching models: critical review and guidance for reporting. Pest Management Science, 58(8) : 745-758.

Dubus, I.G., Brown, C.D., Beulke, S., 2003. Sources of uncertainty in pesticide fate modelling. The Science of the Total Environment, 317(1-3): 53-72.

Dunne, E.J., Culleton, N., O'Donovan, G., Harrington, R., Olsen, A.E., 2005. An integrated constructed wetland to treat contaminants and nutrients from diary farmyard dirty water. Ecological Engineering, 24(3): 219-232.

Duquenne, P., Parekh, N.R., Catroux, G., Fournier, J.C., 1996. Effect of inoculant density, formulation, dispersion and soil nutrient amendment on the removal of carbofuran residues from contaminated soil. Soil Biology and Biochemistry, 28(12): 1805-1811.

Durham, W.F., Williams, C.H., 1972. Mutagenic, Teratogenic, and Carcinogenic Properties of Pesticides. Annual Review of Entomology, 17: 123-148.

Dust, M., Baran, N., Errera, G., Hutson, J.L., Mouvet, C., 2000. Simulation of water and solute transport in field soils with the LEACHP model. Agricultural Water Management, 44(1-3): 225-245.

Eapen, S., Singh, S., D'Souza, S.F., 2007. Advances in development of transgenic plants for remediation of xenobiotic pollutants. Biotechnology Advances, 25(5): 442-451.

Ebert, T.A., Downer, R.A., 2006. A different look at experiments on pesticide distribution. Crop protection, 25(4): 299-309

El Bakouri, H., Morillo, J., Usero, J., Ouassini, A., 2009. Natural attenuation of pesticide water contamination by using ecological adsorbents: Application for chlorinated pesticides included in European Water Framework Directive. Journal of Hydrology, 364(1-2): 175-181;

Entry, J.A., and W.H. Emmingham. 1996. Influence of vegetation on microbial degradation of atrazine and 2,4-dichlorophenoxyacetic acid in riparian soils. Canadien Journal of Soil Science, 76(1):101-106.

Entry, J.A., Donnelly, P.A., Emminham, W.H., 1995. Atrazine and 2,4,-D mineralization in relation to microbial biomass in soils of young-, second-, and old-growth riparian forest. Applied Soil Ecology, 2(2): 77-84.

Esposito, E., Paulillo, S.M., Manfio, G.P., 1998. Biodegradation of the herbicide diuron in soil by indigenous actinomycetes. Chemosphere, 37(3): 541-548.

Euromonitor international. 2009. World Environmental Databook 2008/2009. 2nd editon. Section 3. World Environmental Trends. Pesticide Consumption. Table 3.81 pp. 117

European Commission, 2002. Integrated Crop Management Systems in the EU, Amended Final Report for European Commission DG Environment, Submitted by Agra CEAS Consulting Ltd. Job No 1882/BDB/May 2002. 141 pp.

European Commission, 2009. Development of guidance for establishing Integrated Pest Management (IMP) principles. Final Report for European Commission DG Environment. Submitted by BiPRO GmbH. Project Number 07.0307/2008/504015/ETU/B3. 111 pp.

European Commission, 2000. Directive 2000/60/EC of the European Parliament and of the Council of 23 October 2000 establishing a framework for Community action in the field of water policy. Official Journal of the European Communities L 327, 22/12/2000, pp .1-72

European Commission, 2005. Regulation (EC) No 396/2005 of the European Parliament and of the Council of 23 February 2005 on maximum residue levels of pesticides in or on food and feed of plant and animal origin and amending Council Directive 91/414/EEC. Official Journal of the European Union, L70 , 16/03/2005, pp. 1-16.

European Commission, 2008. Directive 2008/105/EC of the European Parliament and of the Council of 16 December 2008 on environmental quality standards in the field of water policy, amending and subsequently repealing Council Directives 82/176/EEC, 83/513/EEC, 84/156/EEC, 86/280/EEC and amending Directive 2000/60/EC of the European Parliament and of the Council. Official Journal of the European Union, L 348, 24/12/2008, pp. 84-97.

European Community Council, 1998. Council Directive 98/83/EC of 3 November 1998 on the quality of water intended for human consumption. Official Journal of the European Communities, Volume 41, L 330, 5/12/1998, pp. 32-54.

European Community Council, 2007. Regulation (EC) No 1907/2006 of the European Parliament and of the Council of 18 December 2006 concerning the Registration, Evaluation, Authorization and restriction of Chemicals (REACH), establishing a European Chemicals Agency, amending Directive 1999/45/EC and repealing Council Regulation (EEC) No 793/93 and Commission Regulation (EC) No 1488/94 as well as Council Directive 76/769/EEC and Commission Directives 91/155/EEC, 93/67/EEC, 93/105/EC and 2000/21/EC. Official Journal of the European Union L 396 of 30 December 2006.

European Crop Protection Association, 2008. Impact assessment on the proposed changes for authorization and use of pesticides. Report for the European Crop Protection Association. Submitted by Agra CEAS Consulting Ltd. Job No 2373/CC/November 2008. 42 pp.

Falconer, K., 2002. Pesticide environmental indicators and environmental policy. Journal of Environmental Management, 65(3): 285-300.

Fan, L., Reti, H., Wang, W., Lu, Z., Yang, Z., 2008. Application of computational fluid dynamic to model the hydraulic performance of subsurface flow wetlands. Journal of Environmental Sciences, 20(12): 1415-1422.

Farenhorst, A., McQueen, D.A.R., Saiyed, I., Hilderbrand, C., Li, S., Lobb, D.A., Messing, P., Schumacher, T.E., Papiernik, S.K., Lindstrom, M.J., 2009. Variations in soil properties and herbicide sorption coefficients with depth in relation to PRZM (pesticide root zone model) calculations. Geoderma, 150(3-4): 267-277.

Ferrari, F., Trevisan, M., Capri, E., 2003. Predicting and measuring environmental concentration of pesticides in air after soil application. Journal of Environmental Quality, 32(5):1623-1633.

Ferrari, F., Klein, M., Capri, E., Trevisan, M., 2005. Prediction of pesticide volatization with PELMO 3.31. Chemosphere, 60(5): 705-713.

Finizio, A., Villa, S., 2002. Environmental risk assessment for pesticides: A tool for decision making. Environmental Impact Assessment Review, 22(3): 235-248.

Fink, D.F., Mitsch, W.J., 2004. Seasonal and storm event nutrient removal by a created wetland in an agricultural watershed. Ecological Engineering, 23(4-5): 313-325.

Flury, M., 1996. Experimental evidence of transport of pesticides through field soils – A review. Journal of Environmental Quality, 25(1) : 25-45

FOCUS, 1995. Leaching models and EU registration. Doc 4952/VI/95, 124 pp.

FOCUS, 1997. Soil persistence models and EU registration. 77 pp.

FOCUS, 2000. FOCUS Groundwater scenarios in the EU review of active substances. Report of the FOCUS Groundwater Scenarios Workgroup, EC Document Reference SANCO/321/2000 rev.2, 202pp.

Francaviglia, R., Capri, E., Klein, M., Hosang, J., Aden, K., Trevisan, M., Errera, G., 2000. Comparing and evaluating pesticide leaching models: results for the Tor Mancina data set (Italy). Agricultural Water Management 44(1-3): 135-151.

Frazar, C., 2000. The bioremediation and phytoremediation of pesticide-contaminated sites. National Network of Environmentla Studies (NNEMS) Fellow, Washington DC.

Gärdenäs, A.I., Šimunek, J., Jarvis, N., van Genuchten, M.Th., 2006. Two-dimensional modelling of preferential water flow and pesticide transport from a tile-drained field. Journal of Hydrology, 329(3-4): 647-660.

Garmouma, M., Blanchoud, H., Teil, M.J., Blanchard, M., Chevreuil, M., 2001. Triazines in the Marne and the Seine Rivers (France): Longitudinal Evolution and Flows. Water, Air, and Soil Pollution, 132(1-2):1-17

Garratt, J.A., Capri, E., Trevisan, M., Errera, G., Wilkins, R.M., 2002. Parameterisation, evaluation and comparison of pesticide leaching models to data from a Bologna field site, Italy. Pest Management Science, 59(1): 3-20.

Gavrilescu, M., 2005. Review - Fate of pesticides in the environment and its bioremediation. Engineering in Life Sciences, 5(6): 497-526.

Gersberg, R.M., Elkins, B.V., Goldman, C.R., 1983. Nitrogen removal in artificial wetlands. Water Research, 17(9): 1009-1014.

Gevao, B., Semple, K.T., Jones, K.C., 2000. Bound pesticide residues in soils: a review. Environmental Pollution, 108(1): 3-14.

Ghermandi, A., Bixio, D., Thoeye, C., 2007. The role of free water surface constructed wetlands as polishing step in municipal wastewater reclamation and reuse. Science of the Total Environment, 380(1-3): 247-258.

Ghosh, S., Das, S.K., Guha, A.K., Sanyal, A.K., 2009. Adsorption behavior of lindane on Rhizopus oryzae biomass: Physico-chemical studies. Journal of Hazardous Materials, 172(1): 485-490.

Gil, Y., Sinfort, C., 2005. Emission of pesticides to the air during sprayer application : A bibliographic review. Atmospheric Environment, 39(28): 5183-5193.

Gopal, B., Mitsch, W.J., 1995. The role of vegetation in creating and restoring wetlands – An international perspective. Ecological Engineering, 5(1): 1-3.

Gottesbüren, B., Pestemer, W., Beulke, S., 1994. Characteristics and effects of the time course of the sorption behavior of herbicides in soil (in German). Zeitschrift für Pflanzenkrankheiten und Pflanzenschutz, Sonderheft. XIV: 661-670.

Greenway, M., 2005. The role of constructed wetlands in secondary effluent treatment and water reuse in subtropical and arid Australia. Ecological Engineering, 25(5): 501-509.

Greenway, M., Simpson, J.S., 1996. Artificial wetlands for wastewater treatment, water reuse and wildlife in Queensland, Australia. Water Science and Technology , 33(10-11): 221-229.

Griffith, K.L., 1992. Constructed wetlands: a growing opportunity for the construction industry. Master of Science Thesis. Department of Civil Engineering, Massachusetts Institute of Technology. 97 pp.

Guérit, I., Bocquené, G., James, A., Thybaud, E., Minier, C., 2008. Environmental risk assessment: A critical approach of the European TGD in an in situ application. Ecotoxicology and Environmental Safety, 71(1): 291-300.

Gutierrez, A., Baran, N., 2009. Long-term transfer of diffuse pollution at catchment scale: Respective roles of soil, and the unsaturated and saturated zones (Brévilles, France). Journal of Hydrology, 369(3-4): 381-391.

Haber, R., 1999. Constructed wetlands: a chance to solve wastewater problems in developing countries. Water Science and Technology, 40(3): 11-17.

Hamilton, D.J., Ambrus, A., Dieterle, R.M., Felsot, A.S., Harris, C.A., Holland, P.T., Katayama,A., Kurihara, N., Linders, J., Unsworth, J., Wong, S.S., 2003. Regulatory limits for pesticide residues in water (IUPAC Technical Report). Pure and Applied Chemistry, 75(8): 1123-1155.

Hand, L.H., Kuet, S.F., Lane, M.C.G., Maund, S.J., Warinton, J.S., Hill, I.R., 2001. Influences of aquatic plants on the fate of the pyrethroid insecticide Lambda-cyhalothrin in aquatic environments. Environmental Toxicology and Chemistry, 20(8): 1740-1745.

Hansen, P.-D., 2007. Risk assessment of emerging contaminants in aquatic systems. Trends in Analytical Chemistry, 26(11): 1095-1099.

Hanson, M.L., Sibley, P.K., Mabury, S.A., Solomon, K.R., Muir, D.C.G., 2002. Trichloroacetic acid (TCA) and trifluoroacetic acid (TFA) mixture toxicity to the macrophytes Myriophyllum spicatum and Myriophyllum sibiricum in aquatic microcosms. Science of the Total Environment, 285(1-3): 247-259.

Hapeman, C.J., McConnell, L.L., Rice, C.P., Sadeghi, A.M., Schmidt, W.F., McCarty, G.W., Starr, J.L., Rice, P.J., Angier, J.T., Harman-Fetcho, J.A., 2003. Current United States Department of Agriculture – Agricultural Research Service research on understanding agrochemical fate and transport to prevent and mitigate adverse environmental impacts. Pest Management Science, 69(6-7): 681-690.

Heinz, I., Andrews, K., Brouwer, F., Zabel, T., 2002. Voluntary arrangements to cope with diffuse pollution from agriculture and their role in European water policy. Water Science and Technology, 46(6-7): 27-34.

Henle, K., Alard, D., Clitherow, J. Cobb, P., Firbank, L., Kull, T., McCracken, D., Moritz, R.F.A., Niemela, J., Rebane, M., Wascher, D., Watt, A., Young, J., 2008. Identifying and managing the conflicts between agriculture and biodiversity conservation in Europe – A review. Agriculture, Ecosystems and Environment, 124(1-2): 60-71.

Herzon, I., Helenius, J., 2008. Agricultural drainage ditches, their biological importance and functioning. Biological Conservation, 141(5): 1171-1183.

Hincapié, M., Maldonado, M.I., Oller, I., Gernjak, W., Sánchez-Pérez, Ballesteros, M.M., Malato, S., 2005. Solar photocatalytic degradation and detoxification of EU priority substances. Catalysis Today, 101(3-4): 203-210.

Hogberg, H.T., Kinsner-Ovaskainen, A., Hartung, T., Coecke, S., Bal-Price, A.K., 2009. Gene expression as a sensitive endpoint to evaluate cell differentiation and maturation of the developing central nervous system in primary cultures of rat cerebellar granule cells (CGCs) exposed to pesticides. Toxicology and Applied Pharmacology, 235(3): 268-286.

Holvoet, K., van Griensven, A., Seuntjens, P., Vanrolleghem, P.A. 2004. Hydrodynamic modelling with Soil and Water Assessment Tool (SWAT) for predicting dynamic behaviour of pesticides. In: Young Researches 2004. Lens, P. and Stuetz R. (eds). Water and Environment Management Series, IWA Publishing, London, pp. 211-218.

Hong, H.-B., Hwang, S.-H., Chang, Y.-S., 2000. Biosorption of 1,2,3,4-tetrachlorodibenzo-p-dioxin and polychlorinated dibenzofurans by Bacillus pumilus. Water Research, 34(1): 349-353.

Houdart, M., Tixier, P., Lassoudière, A., Saudubray, F., 2009. Assessing pesticide pollution risk : from field to watershed. Agronomy for Sustainable Development, 29(2): 321-327.

House, C.H., Bergmann, B.A., Stomp, A.M., Frederick, D.J., 1999. Combining constructed wetlands and aquatic and soil filters for reclamation and reuse of water. Ecological Engineering, 12(1-2): 27-38.

Huett, D.O., Morris, S.G., Smith, G., Hunt, N., 2005. Nitrogen and phosphorus removal from plant nursery runoff in vegetated and unvegetated subsurface flow wetlands. Water Research, 39(14): 3259-3272.

Hunt, P.G., Poach, M.E., 2001. State of the art for animal wastewater treatment in constructed wetlands. Water Science and Technology, 44(11-12): 19-25.

Imfeld, G., Braeckevelt, M., Kuschk, P., Richnow, H.H., 2009. Monitoring and assessing processes of organic chemicals removal in constructed wetlands. Chemosphere, 74(3): 349-362.

IFEN, 2006. L'environnement en France, édition 2006. Institut Français de l'environnement. Orléans, France, www.ifen.fr/publications/dernieres.htm

Irace-Guigand, S., Aaron, J.J., Scribe, P., Barcelo, D., 2004. A comparison of the environmental impact of pesticide multiresidues and their occurrence in river waters surveyed by liquid chromatography coupled in tandem with UV diode array detection and mass spectrometry. Chemosphere, 55(7): 973-981.

ITRC (Interstate Technology & Regulatory Council). 2009. Phytotechnology Technical and Regulatory Guidance and Decision Trees, Revised. PHYTO-3. Washington, D.C.: Interstate Technology & Regulatory Council, Phytotechnologies Team, Tech Reg Update. Available at www.itrcweb.org

Jarvis, N.J., 1995. Simulation of soil water dynamics and herbicide persistence in a silt loam soil using the MACRO model. Ecological Modelling, 81(1-3): 97-109.

Jarvis, N.J., 1997. MACRO-DB: a decision-support tool for assessing pesticide fate and mobility in soils. Environmental Modelling and Software, 12(2-3): 251-265.

Jarvis, N.J., Brown, C.D., Granitza, E., 2000. Sources of error in model predictions of pesticide leaching: a case study using the MACRO model. Agricultural Water Management, 44(1-3): 247-262.

Jing, S.-R., Lin, Y.-F., Lee, D.-Y., Wang, T.-W., 2001. Nutrient removal from polluted river water by using constructed wetlands. Bioresource Technology, 76(2): 131-135.

Jones, R.L., Russell, M.H., (ed.). 2001. FIFRA Environmental model validation task force. Final report, American Crop Protection Association, Washington. 768 p. Available at www.femvtf.com

Jordan, T.E., Whigham, D.F., Hofmockel, K.H., Pittek, M.A., 2003. Nutrient and sediment removal by a restored wetland receiving agricultural runoff. Journal of Environmental Quality, 32(4): 1534-1547.

Ju, Y.-H., Chen, T.-C., Liu, J.C., 1997. A study on the biosorption of lindane. Colloids and Surfaces B: Biointerfaces, 9(3-4): 187-196.

Kadlec, R.H., Knight, R.L., 1996. Treatment Wetlands. Boca Raton, Florida, USA: Lewis-CRC Press. 893 pp.

Kadlec, R.H., Wallace, S.D., 2008. Treatment Wetlands (2nd edition). CRC Press, Boca Raton, 952 p.

Kao, C.M., Wang, J.Y., Wu, M.J., 2001a. Evaluation of atrazine removal processes in a wetland. Water Science and Technology, 44(11-12): 539-544.

Kao, C.M., Wang, J.Y., Lee, H.Y., Wen, C.K., 2001b. Application of a constructed wetland for non-point source pollution control. Water Science and Technology, 44(11-12): 585-590.

Karathanasis, A.D., Potter, C.L., Coyne, M.S., 2003. Vegetation effects on fecal bacteria, BOD, and suspended solid removal in constructed wetlands treating domestic wastewater. Ecological Engineering, 20(2): 157-169.

Karen, D.J., Joab, B.M., Wallin, J.M., Johnson, K.A., 1998. Partitioning of chlorpyrifos between water and an aquatic macrophyte (Elodea densa). Chemosphere, 37(8): 1579-1586.

Karthikeyan, R., Davis, L.C., Erickson, L.E., Al-Khatib, K., Kulakow, P.A., Barnes, P.L., Hutchinson, S.L., Nurzhanova, A.A., 2004. Potential for plant-based remediation of pesticide-contaminated soil and water using nontarget plants such as trees, shrubs, and grasses. Critical reviews in plant sciences, 23(1): 91-101.

Kawahigashi, H., 2009. Transgenic plants for phytoremediation of herbicides. Current Opinion in Biotechnology, 20(2): 225-230.

Khadrani, A., Seigle-Murandi, F., Steiman, R., Vroumsia, T., 1999. Degradation of three phenylurea herbicides (chlortoluron, isoproturon and diuron) by micromycetes isolated from soil. Chemosphere, 38(13): 3041-3050.

Khalifa, M.E., 2003. Some analytical solutions for the advection-dispersion equation. Applied Mathematics and Computation, 139(2-3): 299-310.

Khalil Granier, L., Chevreuil, M., 1997. Behaviour and spatial and temporal variations of polychlorinated biphenyls and lindane in the urban atmosphere of the Paris area, France. Atmospheric Environment, 31(22): 3787-3802.

Khan, S., Ahmad, I., Shah, M.T., Rehman, S., Khaliq, A., 2009. Use of constructed wetland for the removal of heavy metals from industrial wastewater. Journal of Environmental Management, 90(11): 3451-3457.

Kivaisi, A., 2001. The potential of constructed wetlands for wastewater treatment and reuse in developing countries: a review. Ecological Engineering, 16(4): 545-560.

Klein, M., Hosang, J. Schäfer, H., Erzgräber, B., Resseler, H., 2000. Comparing and evaluating pesticide leaching models Results of simulations with PELMO. Agricultural Water Management 44(1-3): 263-281.

Klier, C., Grundmann, S., Gayler, S., Priesack, E., 2008. Modelling the environmental fate of the herbicide glyphosate in soil lysimeters. Water, Air, and Soil Pollution: Focus, 8(2): 187-207.

Knisel, W.G., 1980. CREAMS: A field scale model for chemicals, runoff, and erosion from agricultural management systems. U.S. Department of Agriculture, Conservation Research Report No. 26, 640 pp.

Köhne, J.M., Köhne, S., Šimůnek, J., 2009. A review of model applications for structured soils: b) Pesticide transport. Journal of Contaminant Hydrology, 104(1-4): 36-60.

Kolpin, D.W., Thurman, E.M., Linhart, S.M, 1998. The environmental occurrence of herbicides: The importance of degradates in ground water. Archives of Environmental Contamination and Toxicity, 35(3): 385-390.

Kolpin, D.W., Thurman, E.M., Linhart, S.M., 2000. Finding minimal herbicide concentrations in groundwater? Try looking for their degradates. Science of the Total Environment, 248(2-3): 115-122.

Konda, L.N., Pásztor, Z., 2001. Environmental distribution of acetochlor, atrazine, clorpyrifos, and propisochlor under field conditions. Journal of Agricultural and Food Chemistry, 49(8): 3859-3863.

Konyha, K.D., Shaw, D.T., Weiler, K.W., 1995. Hydrologic design of a wetland: advantages of continuous modeling. Ecological Engineering, 4(2): 99-116.

Koob, T., Barber, M.E., Hathhorn, W.E., 1999. Hydrologic design consideration of constructed wetlands for urban stormwater runoff. JAWRA Journal of the American Water Resources Association, 35(2):323-331.

Koskiaho, J., Ekholm, P., Räty, M., Riihimäki, J., Puustinen, M., 2003. Retaining agricultural nutrients in constructed wetlands –experiences under boreal conditions. Ecological Engineering, 20(1): 89-103.

Kovacic, D.A., David, M.B., Gentry, L.E., Starks, K.M., Cooke, R.A., 2000. Effectiveness of constructed wetlands in reducing nitrogen and phosphorus export from agricultural tile drainage. Journal of Environmental Quality, 29(4): 1262-1274.

Kovacic, D.A., Twait, R.M., Wallace, M.P., Bowling, J.M., 2006. Use of created wetlands to improve water quality in the Midwet- Lake Bloomington case study. Ecological engineering, 28(3): 258-270.

Kröpfelová, L., Vymazal, J., Švehla, J., Štíchová, J., 2009. Removal of trace elements in three horizontal sub-surface flow constructed wetlands in the Czech Republic. Environmental Pollution, 157(4): 1186-1194.

Langergraber, G., 2003. Simulation of subsurface flow constructed wetlands—results and further research needs. Water Science and Technology, 48(5): 157–166.

Langergraber, G., Šimunek, J., 2005. Modeling variably saturated water flow and multicomponent reactive transport in constructed wetlands. Vadoze Zone Journal, 4(4): 924-938.

Langergraber, G., 2008. Modelling of processes in subsurface flow constructed wetlands: A review. Vadose Zone Journal 7(2): 830-842.

Langergraber, G., Giraldi, D., Mena, J., Meyer, D., Peña, M., Toscano, A., Brovelli, A., Korkusuz, E.A., 2009. Recent developments in numerical modelling of subsurface flow constructed wetlands. Science of the Total Environment, 407(13): 3931-3943.

Lángy, K., Dinya, Z., 2005. Photodegradation study for assessing the environmental fate of some triazine-, urea- and thiolcarbamate- type herbicides. Microchemical Journal, 80(1): 79-87.

Leistra, M., van der Linden, A.M.A., Boesten, J.J.T.I., Tiktak, A., van den Berg, F., 2001. PEARL model for pesticide behaviour and emissions in soil-plant systems. Description of processes. Alterra report 13, RIVM report 711401009, Alterra, Wageningen, 107 pp.

LEMA, 2006. Loi sur l'Eau et les Milieux Aquatiques, Loi n°2006-1772 du 30 décembre 2006, Journal Officiel de la République Français, 31 décembre 2006.

Lemly, A.D., Ohlendorf; H.M., 2002. Regulatory implications of using constructed wetlands to treat selenium-laden wastewater. Ecotoxicology and Environmental Safety, 52(1): 46-56.

Leonard, R.A., Knisel, W.G., Still, D.A., 1987. GLEAMS: Groundwater loading effects of agricultural management systems. Transactions of the ASAE 30(5): 1403-1418.

Levitan, L., 2000. "How to", and "why":: assessing the enviro-social impacts of pesticides. Crop Protection, 19(8-10): 629-636.

Lièvremont, D., Seigle-murandi, F., Benoit-guyod, J.-L., 1998. Removal of PCNB from aqueous solution by a fungal adsorption process. Water Research, 32(12): 3601-3606.

Liikanen, A., Puustinen, M., Koskiaho, J., Väisänen, T., Martikainen, P., Hartikainen, H., 2004. Phosphorus removal in a wetland constructed on former arable land. Journal of Environmental Quality, 33(3): 1124-1132.

Lim, P.E., Tay, M.G., Mak, K.Y., Mohamed, N., 2003. The effect of heavy metals on nitrogen and oxygen demand removal in constructed wetlands. The Science of the Total Environment, 301(1-3): 13-21.

Lima, D., Viana, P., André, S., Chelinho, S., Costa, C., Ribeiro, R., Sousa, J.P., Fialho, A.M., Viegas, C.A., 2009. Evaluating a bioremediation tool for atrazine contaminated soils in open soil microcosms: The effectiveness of bioaugmentation and biostimulation approaches. Chemosphere, 74(2): 187-192.

Lin, Y.-F., Jing, S.-R., Lee, D.-Y., Wang, T.-W., 2002. Nutrient removal from aquaculture wastewater using a constructed wetlands system. Aquaculture, 209(1-4):169-184.

Lin, Y.-F., Jing, S.-R., Lee, D.-Y., Chang, Y.-F., Chen, Y.-M., Shih, K.-C., 2005. Performance of a constructed wetland treating intensive shrimp aquaculture wastewater under high hydraulic loading rate. Environmental Pollution, 134(3): 411-421.

Lin, T., Wen, Y., Jiang, L., Li, J., Yang, S., Zhou, Q., 2008. Study of atrazine degradation in subsurface flow constructed wetland under different salinity. Chemosphere, 72(1): 122-128.

Loague, K., Corwin, D.L., 2005. Groundwater vulnerability to pesticides: An overview of approaches and methods of evaluation. J.H. Lehr (ed.) In: Encyclopedia of Water (Volume 5). John Wiley and Sons, Inc. New York, NY., pp: 594-599.

Luckeydoo, L.M., Fausey, N.R., Brown, L.C., and Davis, C.B. 2002. Early development of vascular vegetation of constructed wetlands in northwest Ohio receiving agricultural waters. Agriculture, Ecosystems and Environment, 88(1): 89-94.

Luederitz, V., Eckert, E., Lange-Weber, M., Lange, A., Gersberg, R.M., 2001. Nutrient removal efficiency and resource economics of vertical flow and horizontal flow constructed wetlands. Ecological Engineering, 18(2): 157-171.

Luo, Y., Zhang, M., 2010. Spatially distributed pesticide exposure assessment in the Central Valley, California, USA. Environmental Pollution, 158(5): 1629-1637.

MacDonald, H.F., Bergstrom, J.C., Houston, J.E., 1998. A proposed methodology for measuring incremental environmental benefits from using constructed wetlands to control agricultural non-point source pollution. Journal of Environmental Management, 54(4): 259-267.

Macek, T., Macková, M., Káš, J., 2000. Exploitation of plants for the removal of organics in environmental remediation. Biotechnology advances, 18(1): 23-34.

Magmedov, V.G., Zakharchenko, M.A., Yakovleva, L.I., Ince, M.E., 1996. The use of constructed wetlands for the treatment of run-off and drainage waters: the UK and Ukraine experience. Water Science and Technology, 33(4-5): 315-323.

Malone, R.W., Logsdon, S., Shipitalo, M.J., Weatherington-Rice, J., Ahuja, L., Ma, L., 2003. Tillage effect on macroporosity and herbicide transport in percolate. Geoderma, 116(1-2): 191-215.

Mamy L., Gabrielle, B., Barriuso, E., 2008a. Measurement and modelling of glyphosate fate compared with that of herbicides replaced as a result of the introduction of glyphosate-resistant oilseed rape. Pest Management Science, 64(3): 262-275.

Mamy L., Barriuso, E., Gabrielle, B., 2008. Evaluer les risques environnementaux des pesticides. Innovations Agronomiques, 3 : 121-143.

Margoum, C., Malessard, C., Gouy, V., 2006. Investigation of various physicochemical and environmental parameter influence on pesticide sorption to ditch bed substratum by means of experimental design. Chemosphere, 63(11): 1835-1841.

McKinlay, R., Plant, J.A., Bell, J.N.B., Voulvoulis, N., 2008. Endocrine disrupting pesticides: Implications for risk assessment. Environment International, 34(2): 168-183.

McKinlay, R.G., Kasperek, K., 1999. Observations on decontamination of herbicide-polluted water by marsh plant systems. Water Research, 33(2): 505-511.

Menard, C., Heraud, F., Nougadere, A., Volatier, J.L., Leblanc, J.C., 2008. Relevance of integrating agricultural practices in pesticide dietary intake indicator. Food and Chemical Toxicology, 46(10): 3240-3253.

Mercer, J.W., Faust, C.R., 1980. Ground-water modeling : mathematical models. Ground water, 18(3): 212-227.

Milam, C.D., Bouldin, J.L., Farris, J.L., Schulz, R., Moore, M.T., Bennett, E.R., Cooper, C.M., Smith Jr, S., 2004. Evaluating acute toxicity of methyl parathion application in constructed wetland mesocosms. Environmental Toxicology, 19(5): 471-479.

Mitchell, D.S., Chick, A.J., Raisin, G.W., 1995. The use of wetlands for water pollution control in Australia: an ecological perspective. Water Science and Technology, 32(3): 365-373.

Mitsch, W.J., 1995. Restoration and creation of wetlands –providing the science and engineering basis and measuring success. Ecological Engineering, 4(2): 61-64.

Mitsch, W.J., Day, Jr., J.W., 2006. Restoration of wetlands in the Mississipi – Ohio – Missouri (MOM) River Basin: Experience and needed research. Ecological Engineering, 26(1): 55-69.

Mitsch, W.J., Day, J.W., Zhang, L., Lane, R.R., 2005. Nitrate-nitrogen retention in wetlands in the Mississippi River Basin. Ecological Engineering, 24(4): 267-278.

Monard, C., Martin-Laurent, F., Vecchiato, C., Francez, A.J., Vandenkoornhuyse, P., Binet, F., 2008. Combined effect of bioaugmentation and bioturbation on atrazine degradation in soil. Soil Hydrology and Biochemistry, 40(9): 2253-2259.

Moore, M.T., Rodgers Jr., J.H., Cooper, C.M., Smith Jr., S., 2000. Constructed wetlands for mitigation of atrazine-associated agricultural runoff. Environmental Pollution 110(3):393-399.

Moore, M.T., Rodgers Jr., J.H., Smith Jr., S., Cooper, C.M., 2001a. Mitigation of metolachlor-associated agricultural runoff using constructed wetlands in Mississippi, USA. Agriculture, Ecosystems and Environment, 84(2): 169-176.

Moore, M.T., Bennett, E.R., Cooper, C.M., Smith, Jr., S., Shields, Jr., F.D., Milam, C.D., Farris, J.L., 2001b. Transport and fate of atrazine and lamba-cyhalothrin in agricultural drainage ditch in the Mississippi Delta, USA. Agriculture, Ecosystems and Environment, 87(3): 309-314.

Moore, M.T., Schulz, R., Cooper, C.M., Smith Jr., S., Rodgers Jr., J.H., 2002. Mitigation of chlorpyrifos runoff using constructed wetlands. Chemosphere, 46(6):827-835.

Moore, M.T., Bennett, E.R., Cooper, C.M., Smith Jr., S., Farris, J.L., Drouillard, K.G., Schulz, R., 2006. Influence of vegetation in mitigation of methyl parathion runoff. Environmental Pollution, 142(2): 288-294.

Moore, M.T., Cooper, C.M., Smith Jr., S., Cullum, R.F., Knight, S.S., Locke, M.A., Bennett, E.R., 2007. Diazinon mitigation in constructed wetlands: influence of vegetation. Water, Air, and Soil Pollution, 184(1-4): 313-321.

Moore, M.T., Denton, D.L., Cooper, C.M., Wrysinski, J., Miller, J.L., Reece, K., Crane, D., Robins, P., 2008. Mitigation assessment of vegetated drainage ditches for collecting irrigation runoff in California. Journal of Environmental Quality, 37(2): 486-493.

Moore, M.T., Kröger, R., Cooper, C.M., Smith Jr., S., 2009a. Ability to four emergent macrophytes to remediate permethrin in mesocosm experiments. Archives of Environmental Contamination and Toxicology, 57(2): 282-288.

Moore, M.T., Cooper, C.M., Smith Jr., S., Cullum, R.F., Knight, S.S., Locke, M.A., Bennett, E.R., 2009b. Mitigation of two pyrethroid insecticides in a Mississippi Delta constructed wetland. Environmental Pollution, 157(1): 250-256.

Moreno, D., Pedrocchi, C., Comín, F.A., García, M., Cabezas, A., 2007. Creating wetlands for the improvement of water quality and landscape restoration in semi-arid zones degraded by intensive agricultural use. Ecological Engineering, 30(2): 103-111.

Moreno-Mateos, D., Comín, F.A., Pedrocchi, C., Rodríguez-Ochoa, R., 2008. Effects of wetland construction on nutrient, SOM and salt content in semi-arid zones degraded by intensive agricultural use. Applied Soil Ecology, 40(1): 57-66.

Moreno-Mateos, D., Pedrocchi, C., Comín, F.A., 2010. Effects of wetland construction on water quality in a semi-arid catchment degradated by intensive agriculture use. Ecological Engineering, 36(5): 631-639.

Morvan, X., Mouvet, C., Baran, N., Gutierrez, A., 2006. Pesticides in the groundwater of a spring draining a sandy aquifer: Temporal variability of concentrations and fluxes. Journal of Contaminant Hydrology, 87(3-4): 176-190.

Mouvet, C., Albrechtsen, H.J., Baran, N., Chen, T., Clausen, L., Darsy, C., Desbionne, S., Douguet, J.-M., Dubus, I.G., Esposito, A., Fialkiewicz, W., Gutierrez, A., Haverkamp, R., Herbst, M., Howles, D., Jarvis, N.J., Jørgensen, P.R., Larsbo, M., Meiwirth, K., Mermoud, A., Morvan, X., Normand, B., O'Connor, M., Ritsema, C., Roessle, S., Roulier, S., Soutter, M., Stenemo, F., Thiéry, D., Trevisan, M., Vachaud, G., Vereecken, H., Vischetti, C., 2004. PEGASE. Pesticides in European Groundwaters: detailed study of representative Aquifers and Simulation of possible Evolution scenarios. Dubus, I.G., Mouvet, C. (Eds.). Final Report of the European Project #EVK1-CT1990-00028. BRGM/RP-52897-FR, 358 p. 196 fig., 57 tabl., 1 app. Available at http://www.brgm.fr/Pegase

Müller, K., Bach, M., Hartmann, H., Spiteller, M., Frede, H.G. 2002. Point- and Nonpoint-Source Pesticide Contamination in the Zwester Ohm Catchment, Germany. Journal of Environmental Quality, 31(1-5) : 309- 318.

Nair, R.W., Mitsch, W.J., 1999. Phosphorus removal in created wetland ponds receiving river overflow. Ecological Engineering, 14(1-2): 107-126.

Nasreddine, L., Parent-Massin, D., 2002. Review article - Food contamination by metals and pesticides in the European Union. Should we worry?. Toxicology Letters, 127(1-3): 29-41.

Nawab, A., Aleem, A., Malik, A., 2003. Determination of organochlorine pesticides in agricultural soil with special reference to γ-HCH degradation by Pseudomonas strains. Bioresource Technology, 88(1): 41-46.

Nguyen, L.M., 2000. Organic matter composition, microbial biomass and microbial activity in gravel-bed constructed wetlands treating farm dairy wastewaters. Ecological engineering, 16(2): 199-221.

Nivala, J., Hoos, M.B., Cross, C., Wallace, S., Parkin, G., 2007. Treatment of landfill leachate using an aerated, horizontal subsurface-flow constructed wetland. Science of the Total Environment, 380(1-3): 19-27.

O'Geen, A.T., Maynard, J.J., Dahlgren, R.A., 2007. Efficacy of constructed wetlands to mitigate non-point source pollution from irrigation tailwaters in the San Joaquin Valley, California, USA. Water Science and Technology, 55(3): 55-61.

O'Leary, E.S., Vena, J.E., Freudenheim, J.L., Brasure, J., 2004. Pesticide exposure and risk of breast cancer : a nested case-control study of residentially stable women living on Long Island. Environmental Research, 94(2): 134-144.

Olette, R., Couderchet, M., Biagianti, S., Eullaffroy, P. 2008. Toxicity and removal of pesticides by selected aquatic plants. Chemosphere 70(8): 1414-1421.

Ottová, V., Balcarová, J., Vymazal, J., 1997. Microbial characteristics of constructed wetlands. Water Science and Technology, 35(5): 117-123.

Padovani, L., Trevisan, M., Capri, E., 2004. A calculation procedure to assess potential environmental risk of pesticides at the farm level. Ecological Indicators, 4(2): 111-123.

Pang, L., Close, M.E., Watt, J.P.C., Vincent, K.W., 2000. Simulation of picloram, atrazine, and simazine leaching through two New Zealand soils and into groundwater using HYDRUS-2D. Journal of Contaminant Hydrology, 44(1): 19-46.

Parrón, T., Hernández, A.F., Villanueva, E., 1996. Increased risk of suicide with exposure to pesticides in an intensive agricultural area. A 12- year retrospective study. Forensic Science International, 79(1): 53-63.

Paterlini, W.C., Nogueira, R.F.P., 2005. Multivariate analysis of photo-Fenton degradation of the herbicides tebuthiuron, diuron and 2,4-D. Chemosphere, 58(8): 1107-1116.

Pesce, S., Fajon, C., Bardot, C., Bonnemoy, F., Portelli, C., Bohatier, J., 2008. Longitudinal changes in microbial planktonic communities of a French river in relation to pesticide and nutrient inputs. Aquatic Toxicology, 86(3):352-360.

Petrelli, G., Mantovani, A., 2002. Environmental risk factors and male fertility and reproduction. Contraception, 65(4): 297-300.

Phanikrishna Sharma, M.V., Durga Kumari, V., Subrahmanyam, M., 2008. TiO_2 supported over SBA-15: An efficient photocatalyst for the pesticide degradation using solar light. Chemosphere, 73(9): 1562-1569.

Pilon-Smits, E., 2005. Phytoremediation. Annual Review of Plant Biology, 56: 15-39.

PIRRP, 2006. Communiqué de presse: Plan interministériel de réduction des risques liés aux pesticides 2006-2009. 28 juin, 2006. Paris, France

Pivetz, B.E., 2001. Phytoremediation of contaminated soil and ground water at hazardous waste sites. EPA Groundwater Issue. Report number EPA/540/S-01/500. U.S. Environmental Protection Agency, 36 pp.

Plangklang, P., Reungsang, A., 2008. Effects of rhizosphere remediation and bioaugmentation on carbofuran removal from soil. World Journal of Microbiology and Biotechnology, 24(7): 983-989.

Poissant, L., Beauvais, C., Lafrance, P., Deblois, C., 2008. Pesticides in fluvial wetlands catchments under intensive agriculture activities. Science of the total environment, 404(1): 182-195.

Polprasert, C., Dan, N.P., Thayalakumaran, N., 1996. Application of constructed wetlands to treat some toxic wastewaters under tropical conditions. Water Science and Technology, 34(11): 165-171.

Rao, P.S.C., Jessup, R.E., 1982. Development and verification of simulation models for describing pesticide dynamics in soils. Ecological Modelling, 16(1): 67-75.

Reddy, K.R., DeLaune, R.D., 2008. Biogeochemistry of wetlands: science and applications. CRC Press, Taylor & Francis Group. Boca Raton, FL, USA, 800 pp.

Reichenberger, S., Bach, M., Skitschak, A., Frede, H.G., 2007. Mitigation strategies to reduce pesticide inputs into ground- and surface water and their effectiveness; A review. Science of the Total Environment, 384(1-3): 1-35.

Reinecke, S.A., Reinecke, A.J., 2007. The impact of organophosphate pesticides in orchards on earthworms in the Western Cape, South Africa. Ecotoxicology and Environmental Safety, 66(2):244-251

Rekolainen, S., Gouy, V., Francaviglia, R., Eklo, O.-M., Bärlund, I., 2000. Simulation of soil water, bromide and pesticide behaviour in soil with the GLEAMS model. Agricultural Water Management, 44(1): 201-224.

REM, 2006. Register of Ecological Models. A meta-database for existing mathematical models in ecology. University of Kassel and National Research Center for Environment and Health (GSF).http://ecobas.org/www-server/index.html, visited on September 23, 2009.

Reus, J., Leendertse, P., Bockstaller, C., Fomsgaard, I., Gutsche, V., Lewis, K., Nilsson, C., Pussemier, L., Trevisan, M., van der Werf, H., Alfarroba, F., Blümel, S., Isart, J., McGrath, D., Seppälä, T., 2002. Comparison and evaluation of eight pesticide environmental risk indicators developed in Europe and recommendations for future use. Agriculture, Ecosystems and Environment, 90(2): 177-187.

Revitt, D.M., Shutes, R.B.E., Jones, R.H., Forshaw, M., Winter, B., 2004. The performances of vegetative treatment systems for highway runoff during dry and wet conditions. Science of the Total Environment, 334-335: 261-270.

Richards, L.A., 1931. Capillary conduction of liquids through porous mediums. Physics, 1(5): 318-333.

Romero, J.A., Comín, F.A., García, C., 1999. Restored wetlands as filters to remove nitrogen. Chemosphere, 39(2): 323-332.

Rose, M.T., Crossan, A.N., Kennedy, I.R., 2008. The effect of vegetation on pesticide dissipation from ponded treatment wetlands: Quantification using a simple model. Chemosphere, 72(7):999-1005.

Rose, M.T., Sanchez-Bayo, F., Crossan, A.N., Kennedy, I.R., 2006. Pesticide removal from cotton farm tailwater by a pilot-scale ponded wetland. Chemosphere, 63(11): 1849-1858.

Rousseau, D.P.L., Lesage, E., Story, A., Vanrolleghem, P.A., De Pauw, N., 2008. Constructed wetlands for water reclamation. Desalination, 218(1-3): 181-189.

Runes, H.B., Jenkins, J.J., Bottomley, P.J., 2001a. Atrazine degradation by bioaugmented sediment from constructed wetlands. Applied Microbiology and Biotechnology, 57(3): 427-432.

Runes, H.B., Bottomley, P.J., Lerch, R.N., Jenkins, J.J., 2001b. Atrazine remediation in wetland microcosms. Environmental Toxicology and Chemistry, 20(5): 1059-1066.

Runes, H.B., Jenkins, J.J., Moore, J.A., Bottomley, P.J., Wilson, B.D., 2003. Treatment of atrazine in nursery irrigation runoff by a constructed wetland. Water Research, 37(3): 539-550.

RZWQM Development Team: Hanson, J.D., Ahuja, L.R, Shaffer, M.D., Rojas, K.W., DeCoursey, D.G., Farahani, H., Johnson, K., 1998. RZWQM: Simulating the effects of management of water quality and crop production. Agricultural systems, 57(2): 161-195.

Sala, S., Vighi, M., 2008. GIS-based procedure for site-specific risk assessment of pesticides for aquatic ecosystems. Ecotoxicology and Environmental Safety, 69(1): 1-12.

Salt, D.E., Smith, R.D., Raskin, I., 1998. Phytoremediation. Annual Review of Plant Physiology and Plant Molecular Biology, 49: 643-668.

Sánchez-Bayo, F., Baskaran, S., Kennedy, I.R., 2002. Ecological relative risk (EcoRR): another approach for risk assessment of pesticides in agriculture. Agriculture, Ecosystems and Environment, 91(1-3): 37-57.

Sanusi, A., Millet, M., Mirabel, P., Wortham, H., 2000. Comparison of atmospheric pesticide concentrations measured at three sampling sites: local, regional and long-range transport. Science of the Total Environment, 263(1-3): 263-277.

Scheyer, A., Morville, S., Mirabel, P., Millet, M., 2007. Variability of atmospheric pesticide concentrations between urban and rural areas during intensive pesticide application. Atmospheric Environment, 41(17): 3604-3618.

Scheyer, A., Graeff, C., Morville, S., Mirabel, P., Millet, M., 2005. Anaylisis of some organochlorine pesticides in an urban atmosphere (Strasbourg, east of France). Chemosphere, 58(11):1517-1524.

Schnoor, J.L., Light, L.A., McCutcheon, S.C., Wolfe, N.L., Carreia, L.H., 1995. Phytoremediation of organic and nutrient contaminants. Environmental Science and Technology, 29(7): 318A-323A.

Scholes, L., Shutes, R.B.E., Revitt, D.M., Forshaw, M., Purchase, D., 1998. The treatment of metals in urban runoff by constructed wetlands. The Science of the Total Environment, 214(1-3): 211-219.

Scholz, M., Sadowski, A.J., Harrington, R., Carroll, P., 2007. Integrated Constructed Wetlands assessment and design for phosphate removal. Biosystems Engineering, 97(3): 415-423.

Schreck, E., Geret, F., Gontier, L., Treilhou, M., 2008. Development and validation of a rapid multiresidue method for pesticide determination using gas chromatography-mass spectrometry: A realistic case in vineyard soils. Talanta, 77(1): 298-303.

Schulz, R., Peall, S.K.C., 2001. Effectiveness of a constructed wetland for retention of nonpoint-source pesticide pollution in the Lourens River Catchment, South Africa. Environmental Science and Technology, 35(2): 422-426.

Schulz, R., Peall, S.K.C., Hugo, C., Krause, V., 2001. Concentration load and toxicity of spraydrift-borne azinphos-methyl at the inlet and outlet of a constructed wetland. Ecological Engineering, 18(2): 239-245.

Schulz, C., Gelbrecht, J., Rennert, B., 2003a. Treatment of rainbow trout farm effluents in constructed wetland with emergent plants and subsurface horizontal water flow. Aquaculture, 217(1-4): 207-221.

Schulz, R., Moore, M.T., Bennett, E.R., Farris, J.L., Smith Jr., S., Cooper, C.M., 2003b. Methyl parathion toxicity in vegetated and nonvegetated wetland mesocosms. Environmental Toxicology and Chemistry, 22(6): 1262-1268.

Schulz, R., Moore, M.T., Bennett, E.R., Milam, C.D., Bouldin, J.L., Farris, J.L., Smith Jr., S., Cooper, C.M., 2003c. Acute toxicity of methyl-parathion in wetland mesocosms: assessing the influence of aquatic plants using laboratory testing with Hyalella azteca. Archives of Environmental Contamination and Toxicology, 45(3): 331-336.

Schulz, R., Hahn, C., Bennett, E.R., Dabrowski, J.M., Thiere, G., Peall, S.K.C., 2003d. Fate and Effects of Azinphos-methyl in a flow-through wetland in South Africa. Environmental Science and Technology, 37(10): 2139-2144.

Schulz, R. 2004. Field studies on exposure, effects and risk mitigation of aquatic nonpoint-source insecticide pollution. Journal of Environmental Quality, 33(2):419-448.

Schwab, A.P., Splichal, P.A., Banks,M.K., 2006. Adsorption of atrazine and alachlor to aquifer material and soil. Water, Air and Soil Pollution, 177(1-4): 119-134.

Sheoran, A.S., Sheoran, V., 2006. Heavy metal removal mechanism of acid mine drainage in wetlands: A critical review. Minerals Engineering, 19(2): 105-116.

Sherrard, R.M., Bearr, J.S., Murray-Gulde, C.L., Rodgers Jr., J.H., Shah, Y.T., 2004. Feasibility of construced wetlands for removing chlorothalonil and chlorpyrifos from aqueous mixtures. Environmental Pollution, 127(3): 385-394.

Shutes, R.B.E., Revitt, D.M., Mungur, A.S., Scholes, L.N.L., 1997. The design of wetland systems for the treatment of urban run off. Water Science and Technology, 35(5): 19-25.

Shutes, R.B.E., 2001. Artificial wetlands and water quality improvement. Environment International, 26(5-6): 441-447.

Siimes, K., Kämäri, J. 2003. A review of available pesticide leaching models: Selection of models for simulation of herbicide fate in Finnish sugar beet cultivation. Boreal Environment Research, 8(1):31-51.

Sim, C.H., Yussoff, M.K., Shutes, B., Ho, S.C., Mansor, M., 2008. Nutrient removal in a pilot and full scale constructed wetland, Putrajaya city, Malaysia. Journal of Environmental Management, 88(2): 307-317.

Sindilariu, P.-D., Brinker, A., Reiter, R., 2009. Factors influencing the efficiency of constructed wetlands used for the treatment of intensive trout farm effluent. Ecological Engineering, 35(5): 711-722.

Singh, O.V., Jain, R.K., 2003. Phytoremediation of toxic aromatic pollutants from soil. Applied Microbiology and Biotechnology, 63(2): 128-135.

Singh, N., Megharaj, M., Kookana, R.S., Naidu, R., Sethunathan, N., 2004. Atrazine and simazine degradation in Pennisetum rizosphere. Chemosphere, 56(3): 257-263.

Smith, R.E., 1995. Opus simulation of a wheat/sugarbeet plot near Neuenkirchen, Germany. Ecological Modelling, 81(1-3): 121-132.

Smith Jr, S., Lizotte Jr, R.E., Moore, M.T. 2007. Toxicity Assessment of Diazinon in a Constructed Wetland Using Hyalella Azteca. Bulletin of Environmental Contamination and Toxicology, 79(1): 58-61.

Soulas, G., Lagacherie, B., 2001. Modelling of microbial degradation of pesticides in soils. Biology and Fertility of Soils, 33(6): 551-557.

Spark, K.M., Swift, R.S., 2002. Effect of soil composition and dissolved organic matter on pesticide sorption. Science of the Total Environment, 298(1-3): 147-161.

Spliid, N.H., Helweg, A., Heinrichson, K., 2006. Leaching and degradation of 21 pesticides in a full-scale model biobed. Chemosphere, 65(11): 2223-2232.

Spurlock, F., Clayton, M., Troiano, J., 2006. Modeling herbicide movement to ground water in irrigated sandy soils of the San Joaquin Valley, California. Water, Air and Soil Pollution, 176(1-4): 93-111.

Stearman, G.K., George, D.B., Carlson, K., Lansford, S., 2003. Pesticide removal from container nursery runoff in constructed wetland cells. Journal of Environmental Quality, 32(4):1458-1556.

Sun, H., Xu, J., Yang, S., Liu, G., Dai, S., 2004. Plant uptake of aldicarb from contaminated soils and its enhanced degradation in the rhizosphere. Chemosphere, 54(4): 569-574.

Susarla, S., Medina, V.F., McCutcheon, S.C., 2002. Phytoremediation: An ecological solution to organic chemical contamination. Ecological Engineering, 18(5): 647-658.

Sveistrup, T.E., Marcelino, V., Braskerud, B.C., 2008. Aggregates explain the high clay retention of small constructed wetlands : a micromorphological study. Boreal Environment Research, 13(3): 275-284.

Tack, F.M.G., De Pauw, N., Du Laing, G. Rousseau, D., 2007. Contaminants in natural and constructed wetlands : Pollutant dynamics and control. Science of the Total Environment, 380(1-3): 1-2.

Tang, X., Eke, P.E., Scholz, M., Huang, S., 2009. Processes impacting on benzene removal in vertical-flow constructed wetlands. Bioresource Technology, 100(1): 227-234.

Tang, X.Q., Huang, S.L., Scholz, M, FCIWEM, 2008. Comparison of phosphorus removal between vertical subsurface flow constructed wetlands with different substrates. Water and Environment Journal, 23(3): 180-188.

Tarutis Jr., W.J., Stark, L.R., Williams, F.M., 1999. Sizing and performance estimation of coal mine drainage wetlands. Ecological Engineering, 12(3-4): 353-372.

Tegnander, C., 2001. Models for ground water flow: A numerical comparison between Richards' model and the fractional flow model. Transport in porous media, 43(2): 213-224.

Tixier, C., Sancelme, M., Aït-Aïsa, S., Widehem, P., Bonnemoy, F., Cuer, A., Truffaut, N., Veschambre, H., 2002. Biotransformation of phenylurea herbicides by a soil bacterial strain, Arthrobacter sp. N2: structure, ecotoxicity and fate of diuron metabolite with soil fungi. Chemosphere, 46(4): 519-526.

Torstensson, L., 2000. Experiences of biobeds in practical use in Sweden. Pesticide Outlook, 11(5): 206-211.

Toscano, A., Langergraber, G., Consoli, S., Cirelli, G.L., 2009. Modelling pollutant removal in a pilot-scale two-stage subsurface flow constructed wetlands. Ecological Engineering, 35(2): 281-289.

Trapp, S., Ulrich, K., 2001. Aspect of phytoremediation of organic pollutants. Journal of Soils and Sediments, 1(1): 37-43.

Trevisan, M., Errera, G., Goerlitz, G., Remy, B., Sweeney, P., 2000a. Modelling ethoprophos and bentazone fate in a sandy humic soil with primary pesticide fate model PRZM-2. Agricultural Water Management, 44(1-3): 317-335.

Trevisan, M., Errera, G., Vischetti, C., Walker, A., 2000b. Modelling pesticide leaching in a sandy soil with the VARLEACH model. Agricultural Water Management, 44(1-3): 357-369.

US EPA, 2000. Manual constructed wetlands treatment of municipal wastewaters. U.S. Environmental Protection Agency, EPA/625/R-99/010. 165 pp. <http://www.epa.gov/owow/wetlands/pdf/Design_Manual2000.pdf>.

US EPA, 2002. Code of Federal Regulations Title 40: Protection of Environment. Part 63—National Emission Standards for Hazardous Air Pollutants for Source Categories. Subpart MMM—National Emission Standards for Hazardous Air Pollutants for Pesticide Active Ingredient Production. U.S. Environmental Protection Agency, Federal Register: September 20, 2002, 67(183): 59336-59356 [FR DOC# 02-23260]

US EPA, 2003. National management measures to control nonpoint source pollution from agriculture. U.S. Environmental Protection Agency, Document No. EPA 841-B-03-004.

U.S. Geological Survey, 1999. The Quality of Our Nation's Waters – Nutrients and Pesticides: U.S. Geological Survey Circular 1225, 82p.

Van den Brink, P.J., Hattink, J., Bransen, F., Van Donk, E., Brock, T.C.M., 2000. Impact of the fungicide carbendazim in freshwater microcosms. II. Zooplankton, primary producers and final conclusions. Aquatic Toxicology, 48(2-3): 251-264.

Van den Brink, P.J., Crum, S.J.H., Gylstra, R., Bransen, F., Cuppen, J.G.M., Brock, T.C.M., 2009. Effects of a herbicide-insecticide mixture in freshwater microcosms: Risk assessment and ecological effect chain. Environmental Pollution, 157(1): 237-249.

Van der Werf, H.M.G., 1996. Assessing the impact of pesticides on the environment. Agriculture, Ecosystems and Environment, 60(2-3): 81-96.

Van der Zee, S.E.A.T.M., Boesten, J.J.T.I., 1991. Effects of soil heterogeneity on pesticide leaching to groundwater. Water Resources Research, 27(12): 3051-3063.

Vanclooster, M., Boesten, J.J.T.I., Trevisan, M., Brown, C.D., Capri, E., Eklo, O.M., Gottesbüren, B., Gouy, V., van der Linden, A.M.A., 2000. A European test of pesticide-leaching models: methodology and major recommendations. Agricultural Water Management, 44(1-3): 1-19.

Vauclin, M., 1989. Flow of water and air in soils: Theoretical and experimental aspects. pp 53-91. In H.J. Morel-Seytoux (ed.). Unsaturated flow in hydrologic modelling, theory and practice. Kluwer Academic, Dordrecht, Netherlands.

Vidali, M. 2001. Bioremediation. An overview. Pure and Applied Chemistry, 73(7): 1163-1172.

Vink, J.P.M., Gottesburen, B., Diekkruger, B., van der Zee, S.E.A.T.M., 1997. Simulation and model comparison of unsaturated movement of pesticides from a large clay lysimeter. Ecological Modelling, 105(1): 113-127.

Vischetti, C., Cardinali, A., Monaci, E., Nicelli, M., Ferrari, F., Trevisan, M., Capri, E., 2008. Measures to reduce pesticide spray drift in a small aquatic ecosystem in vineyard estate. Science of the Total Environment, 389(2-3): 497-502.

Vischetti, C., Capri, E., Trevisan, M., Casucci, C., Perucci, P., 2004. Biomassbed: a biological system to reduce pesticide point contamination at farm level. Chemosphere, 55(6): 823-828.

Von Wirén-Lehr, S., Castillo, M.d.P., Torstensson, L., Scheunert, I., 2001. Degradation of isoproturon in biobeds. Biology and Fertility of Soils, 33(6): 535-540.

Vrhovšek, D., Kukanja, V., Bulc, T., 1996. Constructed wetland (CW) for industrial waste water treatment. Water Research, 30(10): 2287-2292.

Vymazal, J., 1996a. Subsurface horizontal-flow constructed wetlands for wastewater treatment – The Czech experience. Wetlands Ecology and Management, 4(3): 199-206.

Vymazal, J., 1996b. Constructed wetlands for wastewater treatment in the Czech Republic the first 5 years experience. Water Science and Technology, 34(11): 159-164.

Vymazal, J., 2002. The use of sub-surface constructed wetlands for wastewater treatment in the Czech Republic: 10 years experience. Ecological Engineering, 18(5): 633-646.

Vymazal, J., 2005. Constructed wetlands for wastewater treatment. Ecological Engineering, 25(5): 475-477.

Vymazal, J. 2007. Removal of nutrients in various types of constructed wetlands. Science of the Total Environment, 380(1-3): 48-65.

Vymazal, J. 2009. The use constructed wetlands with horizontal sub-surface flow for various types of wastewater. Ecological Engineering. 35(1): 1-17.

Vymazal, J., Kröpfelová, L., 2008. Wastewater treatment in constructed wetlands with horizontal sub-surface flow. Serie Environmental Pollution 14. Springer, Dordrecht, The Netherlands. 566 pp.

Vymazal, J., Kröpfelová, L., 2009. Removal of organics in constructed wetlands with horizontal sub-surface flow: A review of the field experience. Science of the Total Environment, 407(13): 3911-3922.

Wang, C.J., Liu, Z.Q., 2007. Foliar uptake of pesticides – Present status and future challenge. Pesticide Biochemistry and Physiology, 87(1): 1-8.

Wauchope, R.D., Yeh, S., Linders, J.B.H.J., Kloskowski, R., Tanaka, K., Rubin, B., Katayama, A., Kördel, W., Gerstl, Z., Lane, M., Unsworth, J.B., 2002. Review - Pesticide soil sorption parameters: theory, measurement, uses, limitations and reliability. Pest Management Science, 58(5): 419-445.

Weaver, M.A., Zablotowicz, R.M., Locke, M.A., 2004. Laboratory assessment of atrazine and fluometuron in soils from a constructed wetland. Chemosphere, 57(8): 853-862.

Wendt-Rasch, L., Van den Brink, P.J., Crum, S.J.H., Woin, P., 2004. The effects of a pesticide mixture on aquatic ecosystems differing in trophic status: responses of the macrophyte Myriophyllum spicatum and the periphytic algal community. Ecotoxicology and Environmental Safety, 57(3): 383-398.

WHO, 1997. Guidelines for predicting dietary intake of pesticides residues (revised). Prepared by the Global Environment Monitoring System – Food Contamination Monitoring and Assessment Programme (GEMS / Food) in collaboration with the Codex Committee on Pesticide Residues WHO/FSF/FOS/97.7. World Health Organization, Accessible sur www.who.int

Worral, F., Besien, T., Kolpin, D.W., 2002. Groundwater vulnerability: interactions of chemical and site properties. Science of the Total Environment, 299(1-3): 131-143.

Yalcuk, A., Ugurlu, A., 2009. Comparison of horizontal and vertical constructed wetland systems for landfill leachate treatment. Bioresource Technology, 100(9): 2521-2526.

Yamaguchi, N., Gazzard, D., Scholey, G., Macdonald, D.W., 2003. Concentrations and hazard assessment of PCBs, organochlorine pesticides and mercury in fish species from the upper Thames: River pollution and its potential effects on top predators. Chemosphere, 50(3): 265-273.

Yang, Y., Xu, Z., Hu, K., Wang, J., Wang, G., 1995. Removal efficiency of the constructed wetland wastewater treatment system at Bainikeng, Shenzhen. Water Science and Technology, 32(3): 31-40.

Yates, S.R., Wang, D., Papiernik, S.K., Gan, J., 2002. Predicting pesticide volatilization from soils. Environmetrics, 13(5-6): 569-578.

Ye, Z.H., Whiting, S.N., Qian, J.H., Lytle, C.M., Lin, Z.-Q., Terry, N., 2001. Trace element removal from coal ash leachate by a 10-year-old constructed wetland. Journal of Environmental Quality, 30(5): 1710-1719.

Youngchul, K., Gilson, H., Jin-Woo, L., Je-Chul, P., Dong-Sup, K., Min-Gi, K., In-Soung, C., 2006. Experiences with constructed wetland systems in Korea. Journal of Ocean University of China, 5(4): 345-350.

Žáková, Z., 1996. Constructed wetlands in the Czech Republic – survey of the research and practical use. Water Science and Technology, 33(4-5): 303-308.

Zhang, D., Gersgberg, R.M., Tan Soon Keat, 2009. Constructed wetlands in China. Ecological Engineering, 35(10): 1367-1378.

Zhou, J.B., Jiang, M.M., Chen, B., Chen, G.Q., 2009. Emergy evaluations for constructed wetland and conventional wastewater treatments. Communications in nonlinear science and numerical simulation, 14(4): 1781-1789.

3

Chapter 3 – Model development

This chapter describes in detail the governing equations, and the development of the model to simulate the hydrodynamics, transport and fate of pesticides. In the first section, an explanation about the use of the mixed hybrid finite element method is given, which is followed by a definition of the space discretization and boundary conditions applied. The next section, describes the different techniques that were used in the hydrodynamic modelling, such as the transformation of the primary variable. A mixed-hybrid formulation for the approximation of flux and average pressure was obtained based on the continuity and mass conservation equations. For a better convergence behavior, it was applied a technique that switches between the mixed-form and the pressure-head based form of the Richards' equation. Special attention was given to the top boundary conditions dealing with ponding or evaporation problems. In order to avoid oscillation problems related to the discrete expression of the term representing mass variation in the volume, a mass condensation scheme was used. Afterward, a new global approach to solve the transport equation was presented. This method uses a MHFEM approximation for both advection and dispersion terms. It includes a flux limiting tool to control oscillation for advection dominant problem. Concentration and solute transport flux approximation equations are introduced, as well as the equations for residence time distribution estimation. The subsequent section contains a schematique representation of several models that have been proposed for the kinetics of biodegradation in soil. Then, a brief description of the techniques used to solve the resulting systems of equations and the convergence criteria are presented, followed by the procedure used for temporal discretization and ajuste of the temporal increments at each time level. Finally, a short explanation about the modelling code structure, the pre- and post processing of results is provided.

Section 3.1. Mixed Hybrid Finite Elements

In order to find approximate solutions for problems of unsaturated water flow or contaminant transport in soil, when there are no analytic solutions describing the result, different numerical methods can be used. Time and space discretization of the Richards equation usually is performed using a finite difference method [Romano et al., 1998; van Dam and Feddes, 2000; Brunone et al., 2003], a finite element method [Ju and Kung, 1997; Prasad et al., 2001; Qi et al., 2008], a finite volume method [Manzini and Ferraris, 2004] or a mixed finite element method [Chavent and Roberts, 1991; Bergamaschi et Putti, 1999]. Some studies to establish a comparison between methods include Farthing et al. [2003], Rees et al. [2004], Belfort and Lehmann [2005]. The use of any of these methods leads to a nonlinear system of algebraic equations. These equations are most often linearized and solved using the Newton-Raphson or Picard iteration methods.

The formulation and solution of unsaturated flow problems often require the use of indirect methods of analysis, based on approximations or numerical thecniques. However, based on different assumptions, several analytical approximations to the solutions of Richards's equation have been obtained [Tracy, 1995, 2006, 2007; Parlange et al., 1999; Hogarth and Parlange, 2000]. Vanderborght et al., [2005] gives an overview of analytical solutions that can be found for simple initial and boundary conditions and to define benchmark scenarios to check the accuracy of numerical solutions of the flow and transport equations.

Analytical solutions for the transport equation are also available [van Genuchten and Alves, 1982; Liu et al., 1998, Leij and Dane, 1990; Leij et al., 1991; Wexler, 1992; Tartakovsky, 2000; Kumar et al., 2009; Kumar et al., 2010]. Freijer et al. [1998] presented analytical solutions to describe leaching and degradation of pesticides in soil columns.

Lagrangian methods were also developed to solve the transport equation. Under this approach, the solute concentrations are not associated with fixed points or volumes, but with moving "parcels" of water associated with a mass of contaminant. This category includes random walk [Salamon et al., 2006] and finite cell methods [Sun, 1999]. Another alternative are the Eulerian-Lagrangian methods, which is less restrictive in space and time discretization. The most popular are the method of characteristics [Zheng, 1993] and those based upon the localized adjoint method [Binning and Celia, 2002; Younes, 2005].

Finite-differece methods approximate the first derivatives (both in space and time) in the partial differential equations as differences between values of variables at adjacent nodes,

with respect to the interval between those adjacent nodes. This method is relatively simple, but it needs uniform rectilinear grids.

Finite volume methods have the ability to handle irregularly-shaped boundaries more accurately than finite difference methods. In the finite volume method the domain is divided into control volumes. The primary variable is approximated only as the average values within the control volumes. The partial differential equations are integrated over each control volume.

When finite-element method is used, the domain of the problem is divided into a set of elements. Therefore, it is able to handle complex geometries. The corners or vertices of these elements are nodes, where point values of the dependent variable are calculated. The calculation of the dependant variable within the element is performed associating a simple equation, called basis function, to each node that is part of an element. An equivalent integral formulation of the partial differential equation is then evaluated.

The term mixed method is used in problems where two or more physical variables are involved. In mixed finite element methods both stress and displacement fields are approximated as primary variables. For fluid dynamics, the Raviart-Thomas mixed finite element method of lowest order allows us to compute an approximation of pressure head and velocity field simultaneously (with the same order of convergence). The mixed finite element method is more robust, but it presents numerical difficulties related to the size and form of the linear system of equations to solve. In order to obtain a positive definite matrix, hybridization is applied. The hybridization technique is applicable when the computational domain can be represented as a union of a finite number of smaller subdomains. In the mixed hybrid formulation the pressure and velocity are calculated by solving an equivalent symmetric positive definite linear system. This technique provides more information since pressure on the edges is computed as well.

The numerical tool used to solve flow and solute transport equations in the present work is the mixed hybrid finite element method (MHFEM). This technique is particularly well adapted to the simulation of heterogeneous flow field [Mosé et al, 1994; Younes et al., 1999; Nayagum, 2001]. It has been applied in previous works concerning mainly to the flow in heterogeneous saturated porous medium. In unsaturated porous medium, the heterogeneity is due to both the heterogeneous sediment distribution and the non-uniform water content in the storm basin. The originality here is to simulate both, flow and solute transport, with the application of MHFEM for a variably saturated porous medium.

Section 3.2. Space discretization and boundary conditions

A two-dimensional (2D) flow domain Ω is defined, and it is space-discretized into triangular elements G. Boundary conditions to be applied at domain boundaries are of Dirichlet (Ω_D), or Neumann (Ω_N) types (including free-drainage type).

The boundary of each element G is denoted as ∂_G. Since the elements are triangles, it is composed of three edges denominated E_i ($\forall i = 1,2,3$).

Section 3.3. 2D Hydrodynamic modelling

Richards' equation is obtained by combining Buckingham-Darcy's Law (equation 3.1) with the Continuity Equation.

$$\vec{q} = -K\nabla(h + z) \tag{3.1}$$

Where:

- $\vec{q}$ denotes the discharge per unit area [LT^{-1}],
- K is the unsaturated hydraulic conductivity [LT^{-1}],
- h is the pressure head [L],
- z is the elevation head [L] (elevation above some datum). The vertical coordinate is defined positive upward.

Pressure head is negative in the unsaturated zone. At the water table, the pressure head is zero and equals the atmospheric pressure. Below the water table (saturated zone), pressure head is positive and increases with depth.

3.3.1. Variable transformation

Some researches have attributed convergence difficulty to the presence of sharp wetting fronts [Diersch and Perrochet 1999; Williams and Miller, 1999]. To smear the wetting front and to improve the convergence, the pressure head variable h is transformed into a new dependent variable $\hat{h}$ [Pan and Wierenga, 1995].

$$\hat{h} = \begin{cases} \dfrac{h}{1+\kappa h} & h < he \\ h & h \geq he \end{cases} \tag{3.2}$$

Where: κ is a constant ($-0.05 < \kappa < -0.01$ cm^{-1}) independent of both the $K(h)$ and $C(h)$ relationship [Pan and Wierenga, 1995].

$\hat{h}$ is transformed pressure head [L].

Then equation (3.1) can be rewriting as

$$\vec{q} = -K\frac{\partial h}{\partial \hat{h}} \cdot \frac{\partial \hat{h}}{\partial h}\nabla(h+z) = -K\frac{\partial h}{\partial \hat{h}} \cdot \nabla\hat{h} - K\nabla z \tag{3.3}$$

Using the inverse equation of the transformed variable:

$$h = \begin{cases} \dfrac{\hat{h}}{1-\kappa\hat{h}} & \hat{h} < he \\ \hat{h} & \hat{h} \geq he \end{cases} \tag{3.4}$$

A transformed hydraulic conductivity is defined as $\hat{K}$:

$$\hat{K} = K\frac{\partial h}{\partial \hat{h}} = \begin{cases} \dfrac{K}{\left[1-\kappa\hat{h}\right]^2} & h < he \\ K & h \geq he \end{cases} \tag{3.5}$$

Or in terms of the variable h, it can be expressed as:

$$\hat{K} = \begin{cases} K[1+\kappa h]^2 & h < he \\ K & h \geq he \end{cases} \tag{3.6}$$

Thus equation (3.3) can be represented as:

$$\vec{q} = -\hat{K}\nabla\hat{h} - K\nabla z \tag{3.7}$$

3.3.2. Darcy flux approximation over an element

The hydraulic conductivity tensor K is assumed invertible. Then, integrating over the element G, using the base function $\vec{u}_G$, equation (3.7) can be expressed as

$$\int_G \vec{u}_G \left(\hat{K}^{-1} \vec{q} \right) = -\int_G \vec{u}_G \nabla \hat{h} - \int_G \vec{u}_G \hat{K}^{-1} K \nabla z \qquad (3.8)$$

An approximation can be obtained under the application of the product rule of divergence:

$$\int_G \vec{u}_G \left(\hat{K}^{-1} \vec{q} \right) = -\int_G \left[\nabla \left(\hat{h} \vec{u}_G \right) - \hat{h} \nabla \vec{u}_G \right] - \int_G \hat{K}^{-1} K \left[\nabla \left(z \vec{u}_G \right) - z \nabla \vec{u}_G \right] \qquad (3.9)$$

Applying the divergence-Gauss theorem and considering K constant over the element

$$\int_G \vec{u}_G \left(\hat{K}^{-1} \vec{q} \right) = \int_G \hat{h} \nabla \vec{u}_G - \int_{\partial G} \hat{h} \vec{u}_G \vec{n}_{\partial G} + \hat{K}_G^{-1} K_G \int_G z \nabla \vec{u}_G - \hat{K}_G^{-1} K_G \int_{\partial G} z \vec{u}_G \vec{n}_{\partial G} \qquad (3.10)$$

Where ∂G is the frontier of the element G, which is composed of three edges E_j $(\forall j = 1,2,3)$

Based on the mixed hybrid formulation presented by Arnold and Brezzi [1985] and Chavent and Jaffé [1986], the average piezometric charge by edge was chosen as the unknown of the system. The Darcy flux $\vec{q}$ is approximated over each element by a vector $\vec{q}_G$ belonging to the lowest order Raviart-Thomas space [Raviart and Thomas, 1977].

On each element the vector function $\vec{q}_G$ has the following properties: $\nabla \vec{q}_G$ is constant over the element G, $\vec{q}_G \vec{n}_{G,E_i}$ is constant over the edge E_i of the triangle, $\forall i = 1,2,3$, where $\vec{n}_{G,E_i}$ is the normal unit vector exterior to the edge E_i. $\vec{q}_G$ is perfectly determined by knowing the flux through the edges [Chavent and Roberts, 1989].

Given the replacement of $\vec{q}$, h, z, and K^{-1} by their approximations over the element G:

$$\int_G \left(\hat{K}_G^{-1} \vec{q}_G \right) \vec{u}_G = \int_G \hat{h}_G \nabla \vec{u}_G - \int_{i \subset \partial G} T\hat{h}_{G,E_i} \vec{u}_G \vec{n}_{G,E_i} + \hat{K}_G^{-1} K_G \int_G z_G \nabla \vec{u}_G - \hat{K}_G^{-1} K_G \int_{i \subset \partial G} z_{G,E_i} \vec{u}_G \vec{n}_{G,E_i} \qquad \forall i = 1,2,3 \quad (3.11)$$

Where:

- $T\hat{h}_{G,E_i}$ is the approximation of the mean of transformed pressure head at the edge E_i of the triangular element G [L],
- $\vec{n}_{G,E_i}$ is the normal unit vector exterior to the edge E_i,
- $\vec{u}_G$ is a base function,
- z_{G,E_i} is the elevation head at the centre of the edge E_i [L],
- z_G is the elevation head at the centroid of the element G [L],
- $\hat{h}_G$ is the approximation of the mean of transformed pressure head at the element G [L],
- $\vec{q}_G$ is the approximation of the velocity field $\vec{q}$ over the element [LT^{-1}],
- K_G is the approximation of the mean hydraulic conductivity in the element G [LT^{-1}],
- $\hat{K}_G$ is the approximation of the mean transformed hydraulic conductivity in the element G [LT^{-1}],
- K_{G,E_i} is the approximation of the mean hydraulic conductivity at the edge E_i [LT^{-1}],
- $\hat{K}_{G,E_i}$ is the approximation of the mean transformed hydraulic conductivity at the edge E_i [LT^{-1}].

Moreover, with the MHFEM, the normal component of $\vec{q}_G$ is continuous from G to the adjacent element G' and $\vec{q}_G$ is calculated with the help of the vector fields basis $\vec{w}_i$, used as basis functions over each element G. These vector fields are defined by $\int_{E_i} \vec{w}_j \cdot \vec{n}_{G,E_i} = \delta_{i,j}$, where $\delta_{i,j}$ is the Kronecker symbol: $\begin{cases} \delta_{i,j} = 1 & \text{if} \quad i = j \\ \delta_{i,j} = 0 & \text{if} \quad i \neq j \end{cases}, \quad \forall i = 1,2,3.$

Figure 2 summarizes the notation used and describe the mixed hybrid finite element method. Appendix I presents the details about function basis and the development of elements using mapping from the simple geometry of a reference element to the geometry of the real element.

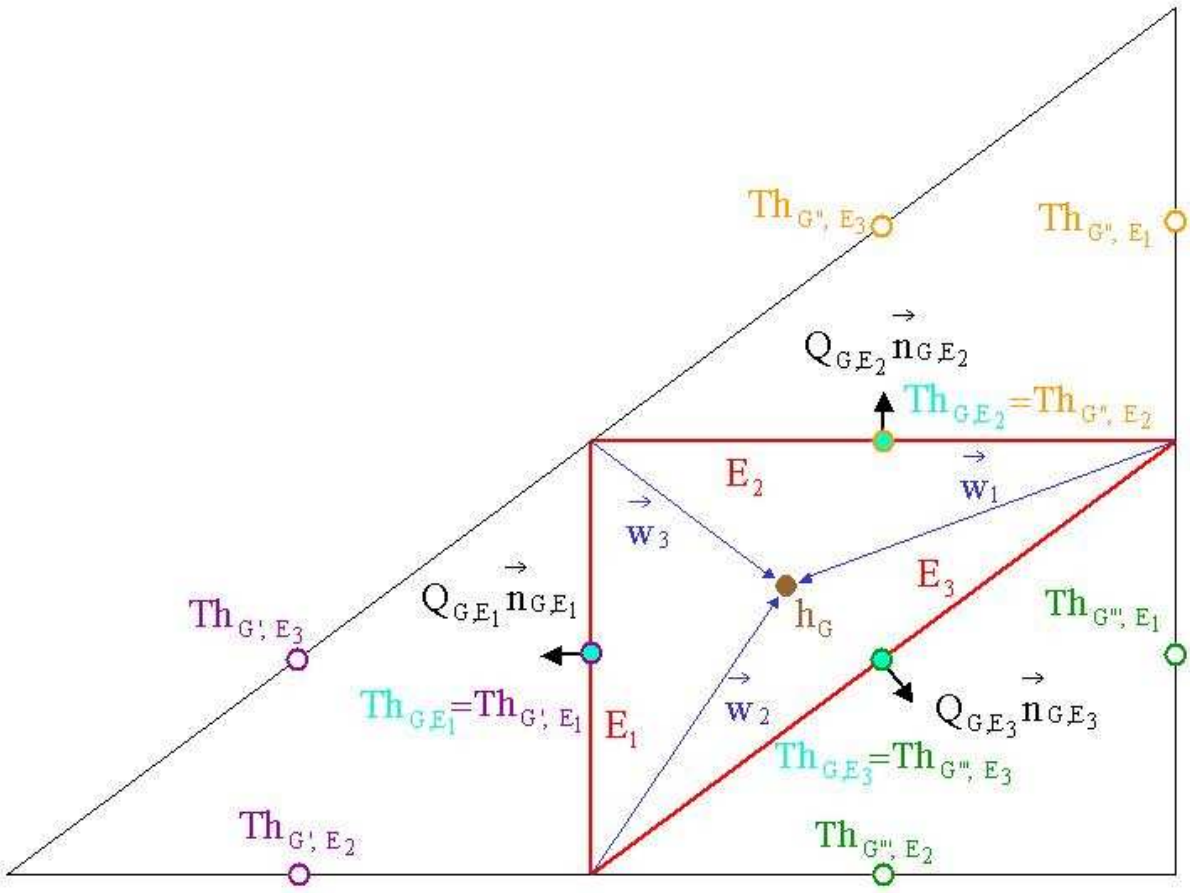

Fig. 2. Schematic representation of the mixed hybrid finite element method

Therefore, with the use of these basis functions equation 3.12 can be represented as:

$$\int_G \left(\hat{K}_G^{-1} \vec{q}_G \right) \vec{w}_i = \int_G \hat{h}_G \nabla \vec{w}_i - \int_{i \subset \partial G} T\hat{h}_{G,E_i} \vec{w}_i \vec{n}_{G,E_i} + \hat{K}_G^{-1} K_G \int_G z_G \nabla \vec{w}_i - \hat{K}_G^{-1} K_G \int_{i \subset \partial G} z_{G,E_i} \vec{w}_i \vec{n}_{G,E_i} \qquad \forall i = 1,2,3 \quad (3.12)$$

So that, these functions correspond to a vector $\vec{q}_G$ having a unitary flux through the edge E_i, and null flux through the other edges:

$$\vec{q}_G = \sum_{j=1}^{3} Q_{G,E_j} \vec{w}_j \qquad (3.13)$$

with Q_{G,E_j} the water flux over the edge E_j belonging to the element G [$L^2\ T^{-1}$].

Consequently, with the use of expression 3.13 and reordering terms in equation 3.12, we get:

$$\sum_{j=1}^{3} Q_{G,E_j} \int_G \left(\hat{K}_G^{-1} \vec{w}_j \right) \vec{w}_i = \hat{h}_G \int_G \nabla \vec{w}_i - T\hat{h}_{G,E_i} \int_{i \subset \partial G} \vec{w}_i \vec{n}_{G,E_i} + \hat{K}_G^{-1} K_G z_G \int_G \nabla \vec{w}_i - \hat{K}_G^{-1} K_G z_{G,E_i} \int_{i \subset \partial G} \vec{w}_i \vec{n}_{G,E_i} \qquad \forall i = 1,2,3 \quad (3.14)$$

Based on the divergence-Gauss theorem:

$$\int_G \nabla \vec{w}_i = \int_{\partial G} \vec{w}_i \vec{n}_{G,E_i} = 1 \qquad (3.15)$$

And defining an auxiliary variable

$$\hat{B}_{G,i,j} = \int_G \left(\hat{K}_G^{-1} \vec{w}_j \right) \vec{w}_i \qquad (3.16)$$

Equation (3.14) can be represented as:

$$\sum_{j=1}^{3} Q_{G,E_j} \hat{B}_{G,i,j} = \hat{h}_G - T\hat{h}_{G,E_i} + \hat{K}_G^{-1} K_G z_G - \hat{K}_G^{-1} K_G z_{G,E_i} \qquad \forall i = 1,2,3 \quad (3.17)$$

Or in a matrix form:

$$Q_{G,E}\hat{B}_G = \hat{h}_G DIV_G^T + \hat{K}_G^{-1}K_G z_G DIV_G^T - \hat{Th}_{G,E} - \hat{K}_G^{-1}K_G z_{G,E} \tag{3.18}$$

Where:

$$Q_{G,E} = \begin{bmatrix} Q_{G,E_1} \\ Q_{G,E_2} \\ Q_{G,E_3} \end{bmatrix}, \qquad DIV_G^T = \begin{bmatrix} 1 \\ 1 \\ 1 \end{bmatrix}, \qquad \hat{Th}_{G,E} = \begin{bmatrix} \hat{Th}_{G,E_1} \\ \hat{Th}_{G,E_2} \\ \hat{Th}_{G,E_3} \end{bmatrix},$$

$$z_{G,E} = \begin{bmatrix} z_{G,E_1} \\ z_{G,E_2} \\ z_{G,E_3} \end{bmatrix}, \qquad \hat{B}_G = \begin{bmatrix} \hat{B}_{G,1,1} & \hat{B}_{G,1,2} & \hat{B}_{G,1,3} \\ \hat{B}_{G,2,1} & \hat{B}_{G,2,2} & \hat{B}_{G,2,3} \\ \hat{B}_{G,3,1} & \hat{B}_{G,3,2} & \hat{B}_{G,3,3} \end{bmatrix}$$

Since $\hat{B}_G$ is an invertible matrix, an auxiliary variably $\hat{\alpha}_{G,E_i} = \sum_{j=1}^{3} \hat{B}_{G,i,j}^{-1}$ can be defined

$$\begin{aligned} Q_{G,E_i} = \hat{\alpha}_{G,E_i}\hat{h}_G + \sum_{j=1}^{3} \hat{B}_{G,i,j}^{-1}\hat{K}_G^{-1}K_G z_G \\ - \sum_{j=1}^{3} \hat{B}_{G,i,j}^{-1}\hat{Th}_{G,E_j} - \sum_{j=1}^{3} \hat{B}_{G,i,j}^{-1}\hat{K}_G^{-1}K_G z_{G,E_j} \end{aligned} \qquad \forall i = 1,2,3 \tag{3.19}$$

3.3.3. Continuity of fluxes and pressure

The continuity of fluxes between two adjacent elements is given by

$$Q_{G,E_i} + Q_{G',E_i} = 0 \tag{3.20}$$

where E_i is the common edge between two elements, G and G'. This equation is valid for all the interior edges E_i ($\forall i = 1,2,3$) of the domain Ω.

The continuity of pressure is represented by

$$Th_{G,E_i} = Th_{G',E_i} \tag{3.21}$$

3.3.4. Boundary conditions

Boundary conditions to be applied at domain boundaries are of Dirichlet (Ω_D), or Neumann (Ω_N) types (including the case of unit hydraulic gradient boundary condition).

3.3.4.1. Dirichlet boundary conditions

The variable of water pressure at the edge is prescribed at the boundary as a constant value. This boundary condition is represented by the term I_{G,E_i}, which is defined by

$$\hat{I}_{G,E_i} = \sum_{E_j \subset \partial\Omega_D} \hat{B}^{-1}_{G,i,j}\left(T\hat{h}_{G,E_j} + \hat{K}_G^{-1} K_G z_{G,E_j}\right) \qquad \forall i = 1,2,3 \quad (3.22)$$

Therefore equation 3.19 can be rewritten as

$$Q_{G,E_i} = \hat{\alpha}_{G,E_i}\hat{h}_G + \sum_{j=1}^{3}\hat{B}^{-1}_{G,i,j}\hat{K}_G^{-1}K_G z_G - \sum_{E_j \not\subset \partial\Omega_D}\hat{B}^{-1}_{G,i,j}T\hat{h}_{G,E_j} - \sum_{E_j \not\subset \partial\Omega_D}\hat{B}^{-1}_{G,i,j}\hat{K}_G^{-1}K_G z_{G,E_j} - \hat{I}_{G,E_i} \qquad \forall i = 1,2,3 \quad (3.23)$$

3.3.4.2. Neumann boundary conditions

Neumann boundary conditions are used when a prescribed flow across the bounding edges is known. This constant flux boundary condition can be represented by the equality

$$Q_{G,E_i} = Q_{N_{G,E_i}} \qquad \forall E_i \subset \partial\Omega_N \quad (3.24)$$

Where:
$$Q_{N_{G,E_i}} = \hat{\alpha}_{G,E_i}\hat{h}_G + \sum_{j=1}^{3}\hat{B}^{-1}_{G,i,j}\hat{K}_G^{-1}K_G z_G - \sum_{E_j \not\subset \partial\Omega_D}\hat{B}^{-1}_{G,i,j}T\hat{h}_{G,E_j} - \sum_{E_j \not\subset \partial\Omega_D}\hat{B}^{-1}_{G,i,j}\hat{K}_G^{-1}K_G z_{G,E_j} - \hat{I}_{G,E_i} \qquad \forall E_i \subset \partial\Omega_N \quad (3.25)$$

3.3.4.3. Unit hydraulic gradient boundary condition

Or for the assumption of a flux equal to the hydraulic conductivity for any particular pressure head at given time, also known as unit hydraulic gradient boundary condition

$$Q_{N_{G,E_i}} = K_{G E_i} \quad (3.26)$$

3.3.5. Matrix form of the continuity of flux

$$\hat{D}\hat{h} + \hat{D}\hat{L} - \hat{R}T\hat{h} - \hat{R}\hat{J} - \hat{I} - \hat{V} = 0 \tag{3.27}$$

Where:

$$\hat{D} = \left[\hat{D}_{E,G}\right]_{nf,nm} \qquad \hat{D}_{E,G} = \begin{cases} \hat{\alpha}_{G,E} & \text{if} \quad E \subset \partial G \\ 0 & \text{if} \quad E \not\subset \partial G \end{cases}$$

$$\hat{R} = \left[\hat{R}_{E,E'}\right]_{nf,nf} \qquad \hat{R}_{E,E'} = \sum_{G \supset (E \text{ and } E')} \hat{B}^{-1}_{G,E,E'} \qquad \forall E \not\subset \partial\Omega_D,\ \forall E' \not\subset \partial\Omega_D$$

$$\hat{V} = \left[\hat{V}_E\right]_{nf} \qquad \hat{V}_E = \begin{cases} Q_{N\,G,E} & \forall E \subset \partial\Omega_N \\ 0 & \forall E \not\subset \partial\Omega_N \end{cases}$$

$$\hat{I} = \left[\hat{I}_E\right]_{nf} \qquad \hat{I}_E = \sum_{G \supset E} I_{G,E} \qquad \forall E \not\subset \partial\Omega_D$$

$$\hat{J} = \left[\hat{J}_E\right]_{nf} \qquad \hat{J}_E = \hat{K}_G^{-1} K_G z_{G,E} \qquad \forall E \not\subset \partial\Omega_D$$

$$\hat{L} = \left[\hat{L}_G\right]_{nm} \qquad \hat{L}_G = \hat{K}_G^{-1} K_G z_G \qquad \forall G \subset \Omega$$

$$\hat{h} = \left[\hat{h}_G\right]_{nm} \qquad \hat{h}_G = \hat{h}_G \qquad \forall G \subset \Omega$$

$$T\hat{h} = \left[T\hat{h}_E\right]_{nf} \qquad T\hat{h}_E = T\hat{h}_{G,E} \qquad \forall E \not\subset \partial\Omega_D$$

nm	is the number of elements in Ω.
nf	is the number of edges over the domain Ω where the pressure has not been imposed.
$\sum_{G \supset (E \text{ and } E')}$	is the sum over the elements G containing the set of internal edges E and E'
$\sum_{G \supset E}$	is the sum over the elements G containing the edge E.

3.3.6. Soil properties

Spatial variability of soil properties has to be considered in order to provide reliable simulation results. Presented below is a detailed description of these properties.

3.3.6.1. Hydraulic conductivity

In a heterogeneous soil (e.g. layered soil), the hydraulic conductivity varies with respect to location. The estimation of the conductivity can be represented by the relationship $K = KsKrK^A$.

Where: Ks is the saturated hydraulic conductivity [LT^{-1}],

K^A is a dimensionless anisotropy tensor,

Kr is the relative hydraulic conductivity function.

The anisotropy tensor has an array of 4 coefficients written in the form of a square matrix: $K^A = \begin{bmatrix} K_{xx} & K_{xz} \\ K_{zx} & K_{zz} \end{bmatrix}$. Under the assumption that the principal directions of the hydraulic conductivity tensor coincide with the coordinate axis x and z, then all the coefficients of the tensor reduce to zero except the diagonal ones: $K^A = \begin{bmatrix} K_x & 0 \\ 0 & K_z \end{bmatrix}$. The relationship between the components of this tensor is defined by an anisotropy ratio $a = \frac{K_z}{K_x}$. If the two components are identical ($a = 1$), the medium is said to be isotropic. In isotropic case, the tensor is equal to the identity tensor $K^A = I = \begin{bmatrix} 1 & 0 \\ 0 & 1 \end{bmatrix}$. Values of $a \neq 1$ indicate anisotropy ($K_x \neq K_z$) due to a pore structure with a preferred orientation in the plane.

The relative hydraulic conductivity function is dimensionless and it is given by the modified Mualem-van Genuchten expression [Ippisch et al., 2006]:

$$Kr = \begin{cases} Se^{\tau}\left[\dfrac{1-\left(1-(SeSc)^{1/m_V}\right)^{m_V}}{1-\left(1-Sc^{1/m_V}\right)^{m_V}}\right]^2 & Se < 1 \\ 1 & Se \geq 1 \end{cases} \qquad (3.28)$$

Where: Se is the effective saturation, which is given by the function

$$Se = \begin{cases} \frac{1}{Sc}\left[1+\left|\alpha_v h\right|^{n_v}\right]^{-m_v} & h < h_e \\ 1 & h \geq h_e \end{cases}$$

Sc is the saturation at the cut-off point h_e in the classical van Genuchten model

$$Sc = \left[1+\left|\alpha_v h_e\right|^{n_v}\right]^{-m_v}$$

α_v is a free parameter related to the mean pore size of the soil [L^{-1}],

n_v is a free parameter related to the uniformity of the soil pore-size [-],

τ is an empirical parameter for tortuosity [-].

h_e is a free parameter, referred as the air entry value [L]

m_v is a parameter in the modified Mualem-van Genuchten expression given by $m_v = 1 - \frac{1}{n_v}$ [-]

Estimations of h_e can be derived from the maximal pore size in the soil or from inverse modelling with h_e as free parameter. The introduction of an air-entry value h_e in the van Genuchten model or the use of a different model with air-entry value is obligatory if $n_v < 2$ or $\alpha_v h_a > 1$.

Where: h_a is the real air-entry value of the soil, $h_a = 2\sigma_w / \rho_w g R_{max}$

R_{max} is the maximal pore radius,

σ_w is the surface tension at the air-water interface,

ρ_w is the density of water at the reference temperature

g is the gravity constant.

In the development of the model, the estimation of average hydraulic conductivity in the element K_G is carried out by using the values of pressure, Th, at the edges belonging to this element. The maximum value obtained from these three hydraulic conductivity values at the edges is considered as the average in the element.

3.3.6.2. Effective Saturation

The dimensionless value Se, referred as effective saturation, was defined by van Genuchten [1980] as a normalized water content:

$$Se = \frac{\theta - \theta_r}{\theta_s - \theta_r} \tag{3.29}$$

Where: θ is the volumetric water content [L^3L^{-3}],

θ_r is the residual water content [L^3L^{-3}], defined as the water content for which the gradient $\frac{d\theta}{dh}$ becomes zero,

θ_s is the saturated water content [L^3L^{-3}].

3.3.6.3. Water content

Volumetric water content (also referred as moisture content), is the quantity of water contained in the soil. It can be expressed in terms of volumetric saturation, defined mathematically as $\theta = \frac{\text{water volume}}{\text{total volume}}$.

Where total volume = soil volume + water volume + void space.

From the effective saturation expression, the volumetric water content is given by

$$\theta = Se(\theta_s - \theta_r) + \theta_r \tag{3.30}$$

The volumetric water content will be equal to porosity in a saturated porous medium, and less than porosity for unsaturated soils.

3.3.6.4. Total Porosity

Total porosity is ratio of the pore volume to the total volume of a representative sample of the medium. Assuming that the soil system is composed of three phases: solid liquid (water) and gas (air).

$$\varphi = \frac{V_l + V_g}{V_s + V_l + V_g} \tag{3.31}$$

Where: φ is total porosity

V_s is the volume of the solid phase

V_l is the volume of the liquid phase

V_g is the olume of the gaseous phase

3.3.6.5. Effective Porosity

Effective porosity n_e is generally defined as the portion of the soil or rock through which chemicals move, or that portion of the media that contributes to flow [Fetter, 1993].

$$n_e = \frac{q}{v} \tag{3.32}$$

Where: q is the specific discharge

v is the mean velocity of a conservative tracer (seepage velocity).

Estimation of effective porosity is best obtained by laboratory or field tracer test, but often they are relatively expensive and time consuming [Stephens et al., 1998]

3.3.6.6. Specific water capacity

The specific water (or moisture) capacity is defined as the slope of the soil moisture characteristic curve at given pressure head: $C(h)=\frac{d\theta}{dh}$, where h is the pressure head and θ is the volumetric water content. Therefore, specific water capacity can be expressed as

$$C(h) = \frac{d\left(Se\left[\theta_s - \theta_r\right] + \theta_r\right)}{dh} = \begin{cases} \dfrac{\alpha_v m_v n_v \left(\theta_s - \theta_r\right) \left|\alpha_v h\right|^{n_v - 1}}{Sc\left[1 + \left(\alpha_v h\right)^{n_v}\right]^{m_v + 1}} & h < h_e \\ 0 & h \geq h_e \end{cases} \tag{3.33}$$

3.3.7. Mass conservation

When using the standard pressure based form of the Richards' equation [Hillel, 1980], the equation of mass conservation is given by equation 3.34, which is valid in each element of discretization G.

$$\int_G C\frac{\partial h}{\partial t} + \int_G S_w S_s \frac{\partial h}{\partial t} + \int_G \nabla \vec{q} = \int_G f(x,z,t) \qquad \forall G \text{ over a domain } \Omega \text{ for } t \subset]0,T[\qquad (3.34)$$

Where:

- $C(h)$ is the specific water (or moisture) capacity [L^{-1}],
- h is the pressure head [L],
- S_s is the specific storage [L^{-1}]. It represents the volume of water released per unit volume of porous medium per unit decrease in the hydraulic head.
- S_w is the degree of saturation, which can be represented by the ratio of the volumetric water content θ and the porosity φ, $S_w = \frac{\theta}{\varphi}$,
- $f(x,z,t)$ is the source /sink term which represents the volume of water added / removed per unit time to/ from a unit volume of soil [$L^3L^{-3}T^{-1}$],
- $\vec{q}$ is flow rate per unit area [LT^{-1}],
- x is the spatial coordinates [L],
- z is the vertical spatial coordinate [L],
- t is time [T].

Applying the chain rule to equation 3.34,

$$\int_G C\frac{\partial h}{\partial \hat{h}}\frac{\partial \hat{h}}{\partial t} + \int_G S_s \frac{\theta}{\varphi}\frac{\partial h}{\partial \hat{h}}\frac{\partial \hat{h}}{\partial t} + \int_G \nabla \vec{q} = \int_G f(x,y,t) \qquad \forall G \text{ over a domain } \Omega \text{ for } t \subset]0,T[\qquad (3.35)$$

with the use of the substitution variables $\hat{C}$ and $\hat{\theta}$,

$$\hat{C} = C\frac{\partial h}{\partial \hat{h}} = \begin{cases} C[1+\kappa h]^2 & h < he \\ C & h \geq he \end{cases} \qquad (3.36)$$

$$\hat{\theta} = \theta \frac{\partial h}{\partial \hat{h}} = \begin{cases} \theta[1 + \kappa h]^2 & h < he \\ \theta & h \geq he \end{cases} \tag{3.37}$$

and the approximation of variables over the element, the following expresion is obtained:

$$\hat{C}_G \frac{\partial \hat{h}_G}{\partial t}|G| + \frac{\hat{\theta}_G}{\varphi_G} S_{sG} \frac{\partial \hat{h}_G}{\partial t}|G| + \nabla \vec{q}_G |G| = F_G \qquad \begin{array}{c} \forall G \text{ over a domain } \Omega \\ \text{for } t \subset]0, T[\end{array} \tag{3.38}$$

with $F_G = \int_G f(x, y, t) = |G| f_G$, and $|G|$ is the area of the element G.

Recalling that based on Raviart-Thomas properties, the chosen approximations $\hat{h}_G$ and $\vec{q}_G$ satisfy: $\hat{h}_G$ and $\nabla \vec{q}_G = \frac{1}{|G|} \sum_{E_i \subset \partial G} Q_{G,E_i}$ are constant over the element G.

$$|G| \hat{C}_G \frac{\partial \hat{h}_G}{\partial t} + |G| \frac{\hat{\theta}_G}{\varphi_G} S_{sG} \frac{\partial \hat{h}_G}{\partial t} + \sum_{i=1}^{3} Q_{G,E_i} = |G| f_G \qquad \begin{array}{c} \forall G \text{ over a domain } \Omega \\ \text{for } t \subset]0, T[\end{array} \tag{3.39}$$

Balance equation when using the standard pressure based form of the Richards' equation

Stability problems and mass balance errors can be more pronounced for sharp wetting fronts in soils with very dry initial conditions and at material interfaces for layered soil profiles. The standard pressure based form of the Richards' equation can lead to large mass balance errors; while the mixed form [Richards, 1931] has improved properties with respect to accurate mass conservative solutions (equation 3.40), but it can have convergence difficulties for dry initial conditions.

$$\int_G \frac{\partial \theta}{\partial t} + \int_G S_w S_s \frac{\partial h}{\partial t} + \int_G \nabla \vec{q} = \int_G f(x, z, t) \qquad \begin{array}{c} \forall G \text{ over a domain } \Omega \\ \text{for } t \subset]0, T[\end{array} \tag{3.40}$$

Using the approximations over the element this equation leads to:

$$|G| \frac{\partial \theta_G}{\partial t} + |G| \frac{\hat{\theta}_G}{\varphi_G} S_{sG} \frac{\partial \hat{h}_G}{\partial t} + \sum_{i=1}^{3} Q_{G,E_i} = |G| f_G \qquad \begin{array}{c} \forall G \text{ over a domain } \Omega \\ \text{for } t \subset]0, T[\end{array} \tag{3.41}$$

Balance equation when using the mixed form of the Richards' equation

3.3.8. Time discretization

The resulting mass balance equation can be time discretizated using different discretization schemes. Shahraiyni and Ashtiani [2009] performed a comparison of implicit finite difference schemes for water flow in unsaturated soils. Their conclusion was that fully implicit was a better scheme than Crank-Nicolson and Runge-Kutta schemes for numerical solution of h-based Richards equation. However, h based algorithms usually require small time steps in order to maintain stability and minimize truncation errors for problems that involve steep wetting fronts into initially dry soils.

h-based formulation and a backward Euler time discretization has shown to produce mass balance errors in several cases. The reason for poor mass balance has been explained by the manner in which the time derivative $\partial\theta/\partial t$ is approximated as $C\partial h/\partial t$. Even if these terms are mathematically equivalent in the continuous partial differential equation, their discrete analogues are not equivalent. This inequality is aggravated by the highly nonlinear nature of C.

Solutions with poor mass balance and associated poor accuracy can be improved by the numerical approach proposed by Celia et al. [1990]. This method is based on a fully implicit (backward Euler) time approximation applied to the mixed form of the Richards' equation.

Kirkland et al. [1992] found that the use of a Crank-Nicholson scheme on the closely related mixed form of Richard's equation fails to reduce truncation error, producing potential instabilities. Thus, he also recommended the use of the fully implicit formulation.

Therefore, the numerical scheme that we use is fully implicit, resulting in the following equations for the h-based and the mixed form of the Richards equation, respectively:

$$\left(\hat{C}_G^{n+1}+\frac{\hat{\theta}_G^{n+1}}{\varphi_G}S_{sG}^{n+1}\right)\left(\hat{h}_G^{n+1}-\hat{h}_G^{n}\right)=\frac{\Delta t^n}{|G|}\left(|G|f_G^{n+1}-\sum_{i=1}^{3}Q_{G,E_i}^{n+1}\right) \tag{3.42}$$

$$\theta_G^{n+1}-\theta_G^{n}+\frac{\hat{\theta}_G^{n+1}}{\varphi_G}S_{sG}^{n+1}\left(\hat{h}_G^{n+1}-\hat{h}_G^{n}\right)=\frac{\Delta t^n}{|G|}\left(|G|f_G^{n+1}-\sum_{i=1}^{3}Q_{G,E_i}^{n+1}\right) \tag{3.43}$$

The superindex n represents that the variables are defined at nth time step, which is defined by $\Delta t^n = t^{n+1} - t^n$.

3.3.9. Linearization

Richards' equation is nonlinear in nature, since K and C are functions of the dependent variable. The Picard iterative process of linearization is based on the theorem of existence and uniqueness of a solution to a certain initial value problem. It consists of constructing a sequence of functions, which will get closer to the desired solution. This method is frequently used because of its ease of implementation, and because it preserves symmetry of the final system of matrix equations.

If the primary variable is pressure head then equation 3.42 is linearized

$$\left(\hat{C}_G^{n+1,m} + \frac{\hat{\theta}_G^{n+1,m}}{\varphi_G} S_{sG}^{n+1,m}\right)\left(\hat{h}_G^{n+1,m+1} - \hat{h}_G^{n}\right) = \frac{\Delta t^n}{|G|}\left(|G| f_G^{n+1,m+1} - \sum_{i=1}^{3} Q_{G,E_i}^{n+1,m+1}\right) \tag{3.44}$$

When the mixed form of the Richards equation is used, equation 3.43 is linearized

$$\theta_G^{n+1,m+1} - \theta_G^{n} + \frac{\hat{\theta}_G^{n+1,m}}{\varphi_G} S_{sG}^{n+1,m}\left(\hat{h}_G^{n+1,m+1} - \hat{h}_G^{n}\right) = \frac{\Delta t^n}{|G|}\left(|G| f_G^{n+1,m+1} - \sum_{i=1}^{3} Q_{G,E_i}^{n+1,m+1}\right) \tag{3.45}$$

Where m is defined as the iteration index.

Celia's approach [Celia et al., 1990] eliminates the mass balance problem by directly approximating the temporal term $\partial\theta/\partial t$ with its algebraic analog [Clement, 1994]. The key of the method is the expansion of $\theta_G^{n+1,m+1}$ in a truncated Taylor serie with respect to h. Neglecting all terms higher than linear, Celia's function can be representated as:

$$\theta_G^{n+1,m+1} = \theta_G^{n+1,m} + \left.\frac{\partial\theta_G}{\partial h_G}\right|^{n+1,m}\left(h_G^{n+1,m+1} - h_G^{n+1,m}\right)$$

$$\theta_G^{n+1,m+1} = \theta_G^{n+1,m} + C_G^{n+1,m}\left(h_G^{n+1,m+1} - h_G^{n+1,m}\right)$$

Or using the transformed variables

$$\theta_G^{n+1,m+1} = \theta_G^{n+1,m} + \hat{C}_G^{n+1,m}\left(\hat{h}_G^{n+1,m+1} - \hat{h}_G^{n+1,m}\right) \tag{3.46}$$

The substitution of this term in equation 3.45 gives

$$\theta_G^{n+1,m} - \theta_G^n + \hat{C}_G^{n+1,m}\left(\hat{h}_G^{n+1,m+1} - \hat{h}_G^{n+1,m}\right) + \frac{\hat{\theta}_G^{n+1,m}}{\varphi_G} S_{sG}^{n+1,m}\left(\hat{h}_G^{n+1,m+1} - \hat{h}_G^n\right) = \frac{\Delta t^n}{|G|}\left(|G| f_G^{n+1,m+1} - \sum_{i=1}^{3} Q_{G,E_i}^{n+1,m+1}\right) \tag{3.47}$$

The flux term is deduced from the expression already obtained in terms of traces of pressure:

$$\begin{aligned}\sum_{i=1}^{3} Q_{G,E_i}^{n+1,m+1} = & \sum_{i=1}^{3}\sum_{j=1}^{3} \hat{B}_{G,i,j}^{-1,n+1,m} \hat{h}_G^{n+1,m+1} \\ & + \sum_{i=1}^{3}\sum_{j=1}^{3} \hat{B}_{G,i,j}^{-1,n+1,m} \hat{K}_G^{-1,n+1,m} K_G^{n+1,m} z_G \\ & - \sum_{i=1}^{3} \sum_{E_j \not\subset \partial\Omega_D} \hat{B}_{G,i,j}^{-1,n+1,m} T \hat{h}_{G,E_j}^{n+1,m+1} \\ & - \sum_{i=1}^{3} \sum_{E_j \not\subset \partial\Omega_D} \hat{B}_{G,i,j}^{-1,n+1,m} \hat{K}_G^{-1,n+1,m} K_G^{n+1,m} z_{G,E_j} - \sum_{i=1}^{3} I_{G,E_i}\end{aligned} \qquad \forall i = 1,2,3 \tag{3.48}$$

3.3.10. Switching technique

The primary variable switching technique has proved to be an effective solution strategy for unsaturated flow problems [Diersch and Perrochet, 1999; Hao et al., 2005]. It is unconditionally mass conservative. Better convergence behavior is achieved using this technique, compared to both the mixed-form and pressure-head based form of the Richards equation.

The primary variable is switched at each iteration, using the following criterion: if $\frac{\theta_G^{n+1,m}}{\varphi_G} > \mathrm{tol}_f$ then pressure head is used as primary variable, if not then a mixed-form of the Richards equation is used. The tolerance for this switching procedure, tol_f, is predefined by the user ($0 \le \mathrm{tol}_f \le 1$).

3.3.11. Average pressure calculation

An expression of average pressure for each element is obtained by multiplying the linearized equation by the term $\left(\hat{C}_G^{n+1,m} + \frac{\hat{\theta}_G^{n+1,m}}{\varphi_G} S_{sG}^{n+1,m}\right)$

$$\begin{aligned}
\hat{h}_G^{n+1,m+1} = & \frac{\frac{\Delta t^n}{|G|} \sum_{i=1}^{3} \sum_{E_j \not\subset \partial\Omega_D} \hat{B}_{G,i,j}^{-1,n+1,m} T\hat{h}_{G,E_j}^{n+1,m+1}}{\hat{C}_G^{n+1,m} + \frac{\hat{\theta}_G^{n+1,m}}{\varphi_G} S_{sG}^{n+1,m} + \frac{\Delta t^n}{|G|} \hat{\alpha}_G^{n+1,m}} \\
& + \frac{\frac{\Delta t^n}{|G|} \sum_{i=1}^{3} \sum_{E_j \not\subset \partial\Omega_D} \hat{B}_{G,i,j}^{-1,n+1,m} \hat{K}_G^{-1,n+1,m} K_G^{n+1,m} z_{G,E_j}}{\hat{C}_G^{n+1,m} + \frac{\hat{\theta}_G^{n+1,m}}{\varphi_G} S_{sG}^{n+1,m} + \frac{\Delta t^n}{|G|} \hat{\alpha}_G^{n+1,m}} \\
& + \frac{\frac{\Delta t^n}{|G|} \left(\sum_{i=1}^{3} I_{G,E_i} + |G| f_G^{n+1,m+1} - \sum_{i=1}^{3} \sum_{j=1}^{3} \hat{B}_{G,i,j}^{-1,n+1,m} \hat{K}_G^{-1,n+1,m} K_G^{n+1,m} z_G \right)}{\hat{C}_G^{n+1,m} + \frac{\hat{\theta}_G^{n+1,m}}{\varphi_G} S_{sG}^{n+1,m} + \frac{\Delta t^n}{|G|} \hat{\alpha}_G^{n+1,m}} + \hat{h}_{0G}^{n+1,m+1}
\end{aligned} \tag{3.49}$$

where:

$$\hat{\alpha}_G^{n+1,m} = \sum_{i=1}^{3} \hat{\alpha}_{G,E_i}^{n+1,m}$$

$$\hat{h}_{0G}^{n+1,m+1} = \begin{cases} \left(\frac{\hat{C}_G^{n+1,m} + \frac{\hat{\theta}_G^{n+1,m}}{\varphi_G} S_{sG}^{n+1,m}}{\hat{C}_G^{n+1,m} + \frac{\hat{\theta}_G^{n+1,m}}{\varphi_G} S_{sG}^{n+1,m} + \frac{\Delta t^n \hat{\alpha}_G^{n+1,m}}{|G|}} \right) \hat{h}_G^n & \text{if} \quad \frac{\theta_G^{n+1,m}}{\varphi_G} > \text{tol}_f \\ \frac{\hat{C}_G^{n+1,m} \hat{h}_G^{n+1,m} - \left(\theta_G^{n+1,m} - \theta_G^n\right) + \frac{\hat{\theta}_G^{n+1,m}}{\varphi_G} S_{sG}^{n+1,m} \hat{h}_G^n}{\hat{C}_G^{n+1,m} + \frac{\hat{\theta}_G^{n+1,m}}{\varphi_G} S_{sG}^{n+1,m} + \frac{\Delta t^n}{|G|} \hat{\alpha}_G^{n+1,m}} & \text{if} \quad \frac{\theta_G^{n+1,m}}{\varphi_G} \le \text{tol}_f \end{cases}$$

3.3.12. Matrix form of the average pressure

$$\hat{h}^{n+1,m+1} - \hat{N}T\hat{h}^{n+1,m+1} - \hat{N}\hat{J}^{n+1,m} - \hat{P}\hat{F}^{n+1,m+1} + \hat{\beta}\hat{L}^{n+1,m} - \hat{H} - \hat{U} = 0 \qquad (3.50)$$

Where:

$$\beta_G = \frac{\frac{\Delta t^n}{|G|}\hat{\alpha}_G^{n+1,m}}{\hat{C}_G^{n+1,m} + \frac{\hat{\theta}_G^{n+1,m}}{\varphi_G} S_{sG}^{n+1,m} + \frac{\Delta t^n}{|G|}\hat{\alpha}_G^{n+1,m}}$$

$$\hat{N} = \left[\hat{N}_{G,E}\right]_{nm,nf} \qquad \hat{N}_{G,E} = \begin{cases} \dfrac{\beta_G \hat{\alpha}_{G,E}^{n+1,m}}{\hat{\alpha}_G^{n+1,m}} & \text{if} \quad E \subset \partial G \\ 0 & \text{if} \quad E \not\subset \partial G \end{cases}$$

$$\hat{P} = \left[\hat{P}_{G,G'}\right]_{nm,nm} \qquad \hat{P}_{G,G'} = \begin{cases} \dfrac{\beta_G}{\hat{\alpha}_G^{n+1,m}} & \text{if} \quad G = G' \\ 0 & \text{if} \quad G \neq G' \end{cases}$$

$$\hat{\beta} = \left[\hat{\beta}_{G,G'}\right]_{nm,nm} \qquad \hat{\beta}_{G,G'} = \begin{cases} \beta_G & \text{if} \quad G = G' \\ 0 & \text{if} \quad G \neq G' \end{cases}$$

$$\hat{H} = \left[\hat{H}_G\right]_{nm} \qquad \hat{H}_G = \sum_{E \subset (\partial G \cap \partial \Omega_D)} \frac{\beta_G \hat{\alpha}_{G,E}^{n+1,m} \left(Th_{G,E} + \hat{K}_G^{-1} K_G z_{G,E}\right)}{\hat{\alpha}_G^{n+1,m}}$$

$$\hat{U} = \left[\hat{U}_G\right]_{nm} \qquad \hat{U}_G = \begin{cases} (1-\beta_G)\hat{h}_G^n & \text{if} \quad \dfrac{\theta_G^{n+1,m}}{\varphi_G} > tol_f \\ \dfrac{\hat{C}_G^{n+1,m}\hat{h}_G^{n+1,m} - \left(\theta_G^{n+1,m} - \theta_G^n\right) + \frac{\hat{\theta}_G^{n+1,m}}{\varphi_G} S_{sG}^{n+1,m}\hat{h}_G^n}{\hat{C}_G^{n+1,m} + \frac{\hat{\theta}_G^{n+1,m}}{\varphi_G} S_{sG}^{n+1,m} + \frac{\Delta t^n \hat{\alpha}_G^{n+1,m}}{|G|}} & \text{if} \quad \dfrac{\theta_G^{n+1,m}}{\varphi_G} \leq tol_f \end{cases}$$

$$\hat{F} = \left[\hat{F}_G\right]_{nm} \qquad \hat{F}_G = |G| f_G \qquad G \subset \Omega$$

3.3.13. Hydrodynamics system of equations using standard MHFEM

A system of linear equations representing the standard mixed hybrid formulation for the Richard's equation can be obtained by coupling equations 3.27 and 3.50.

$$\begin{aligned}\left(\hat{R}^{n+1,m} - \hat{D}^{n+1,m}N\right)T\hat{h}^{n+1,m+1} &= \hat{D}^{n+1,m}\hat{U} - \hat{D}^{n+1,m}\hat{\beta}\hat{L}^{n+1,m} + \hat{D}^{n+1,m}\hat{N}\hat{J}^{n+1,m} \\ &+ \hat{D}^{n+1,m}\hat{P}\hat{F}^{n+1,m+1} + \hat{D}^{n+1,m}\hat{H} + \hat{D}^{n+1,m}\hat{L}^{n+1,m} - \hat{R}^{n+1,m}\hat{J}^{n+1,m} - \hat{I}^{n+1,m} - \hat{V}\end{aligned} \tag{3.51}$$

This system of equations can be rewritten as:

$$[M]_{nf,nf}\left\{T\hat{h}^{n+1,m+1}\right\}_{nf} = \{Y\}_{nf} \tag{3.52}$$

With $T\hat{h}^{n+1,m+1}$ as the unknown of the system. The hybridization consists in introducing the trace of pressure on the boundaries of each cell, ensuring the continuity of flux across these interior edges.

The diagonal coefficients of the matrix [M] are defined as:

$$\hat{M}_{E,E} = \sum_{G \supset E}\left[\hat{B}^{-1}_{G,E,E} - \frac{\frac{\Delta t^n}{|G|}\left(\hat{\alpha}^{n+1,m}_{G,E}\right)^2}{\hat{C}^{n+1,m}_G + \frac{\hat{\theta}^{n+1,m}_G}{\varphi_G}S_{sG}^{n+1,m} + \frac{\Delta t^n}{|G|}\hat{\alpha}^{n+1,m}_G}\right] \qquad \forall E \not\subset \partial\Omega_D$$

and the non diagonal coefficients:

$$\hat{M}_{E,E'} = \sum_{G \supset \left(E \text{ and } E'\right)}\left[\hat{B}^{-1}_{G,E,E'} - \frac{\frac{\Delta t^n}{|G|}\hat{\alpha}^{n+1,m}_{G,E}\hat{\alpha}^{n+1,m}_{G,E'}}{\hat{C}^{n+1,m}_G + \frac{\hat{\theta}^{n+1,m}_G}{\varphi_G}S_{sG}^{n+1,m} + \frac{\Delta t^n}{|G|}\hat{\alpha}^{n+1,m}_G}\right] \qquad \begin{matrix}\forall E \not\subset \partial\Omega_D, \\ \forall E' \not\subset \partial\Omega_D\end{matrix}$$

Unphysical oscillation problems might be presented when using this formulation. These difficulties had been related to the time-dependent terms in the mass matrix [M], since they appear not only in the diagonal coefficients of the matrix.

3.3.14. Mass condensation scheme (Mass lumping)

A common measure to eliminate unphysical oscillations in the numerical solution is the employment of mass lumping techniques. A mass condensation scheme was used here, as described by Belfort [2006]. An expression of flux at each edge Q_{G,E_i} is defined in terms of stationary and transitory flow regimes, see Younes et al. [2006] for details.

Using pressure-head based form of the Richards equation ($T\theta_{G,E_i}^{n+1,m} / \varphi_G > tol_f$):

$$Q_{G,E_i} = \overline{Q}_{G,E_i} + \frac{|G|}{3} f_G - \frac{|G|}{3}\left(TC_{G,E_i} + S_{sG} \frac{T\theta_{G,E_i}}{\varphi_G} \right) \frac{\partial Th_{G,E_i}}{\partial t} \qquad \forall i = 1,2,3 \quad (3.53)$$

Using the mixed form of the Richards equation ($T\theta_{G,E_i}^{n+1,m} / \varphi_G \leq tol_f$):

$$Q_{G,E_i} = \overline{Q}_{G,E_i} + \frac{|G|}{3} f_G - \frac{|G|}{3}\left(\frac{\partial T\theta_{G,E_i}}{\partial t} + S_{sG} \frac{T\theta_{G,E_i}}{\varphi_G} \frac{\partial Th_{G,E_i}}{\partial t} \right) \qquad \forall i = 1,2,3 \quad (3.54)$$

where $\overline{Q}_{G,E_i}$ is the flux corresponding to the stationary problem without the sink/source term over the element G (of area $|G|$) and Th_{G,E_i}, TC_{G,E_i}, $T\theta_{G,E_i}$ represents traces of pression, specific water capacity and water content, respectively, over the edge E_i.

In order to calculate $\overline{Q}_{G,E_i}$, the average pressure over the element $\hat{h}_G$ is obtained as a function of traces of pressure (from equation 3.39 and 3.25), when $\frac{\partial \hat{h}}{\partial t}$=0 (stationary problem) and without the sink /source term over the element G.

$$\hat{h}_G = \frac{\sum_{E_j \not\subset \partial\Omega_D} \hat{\alpha}_{G,E_j} T\hat{h}_{G,E_j} + \sum_{E_j \subset \partial\Omega_D} \hat{\alpha}_{G,E_j} T\hat{h}_{G,E_j}}{\hat{\alpha}_G} + \frac{\sum_{j=1}^{3} \hat{\alpha}_{G,E_j} \hat{K}_G^{-1} K_G z_{G,E_j}}{\hat{\alpha}_G} - \hat{K}_G^{-1} K_G z_G \qquad \forall j = 1,2,3 \quad (3.55)$$

The term $\overline{Q}_{G,E_i}$ can be then obtained as follows:

$$\overline{Q}_{G,E_i} = \hat{\alpha}_{G,E_i} \frac{\sum_{E_j \not\subset \partial\Omega_D} \hat{\alpha}_{G,E_j} T\hat{h}_{G,E_j} + \sum_{E_j \subset \partial\Omega_D} \hat{\alpha}_{G,E_j} T\hat{h}_{G,E_j}}{\hat{\alpha}_G} + \hat{\alpha}_{G,E_i} \frac{\sum_{j=1}^{3} \hat{\alpha}_{G,E_j} \hat{K}_G^{-1} K_G z_{G,E_j}}{\hat{\alpha}_G} - \sum_{E_j \not\subset \partial\Omega_D} \hat{B}_{G,i,j}^{-1} T\hat{h}_{G,E_j} - \sum_{E_j \not\subset \partial\Omega_D} \hat{B}_{G,i,j}^{-1} \hat{K}_G^{-1} K_G z_{G,E_j} - I_{G,E_i} \quad \forall i = 1,2,3 \tag{3.56}$$

Transitory flow regime terms are described by the following approximations

$$S_{sG} \frac{T\theta_{G,E_i}}{\varphi_G} \frac{\partial Th_{G,E_i}}{\partial t} = S_{sG} \frac{T\theta_{G,E_i}}{\varphi_G} \frac{\partial Th_{G,E_i}}{\partial T\hat{h}_{G,E_i}} \frac{\partial T\hat{h}_{G,E_i}}{\partial t} = S_{sG} \frac{T\hat{\theta}_{G,E_i}}{\varphi_G} \frac{\partial T\hat{h}_{G,E_i}}{\partial t} \tag{3.57}$$

$$TC_{G,E_i} \frac{\partial Th_{G,E_i}}{\partial t} = TC_{G,E_i} \frac{\partial Th_{G,E_i}}{\partial T\hat{h}_{G,E_i}} \frac{\partial T\hat{h}_{G,E_i}}{\partial t} = T\hat{C}_{G,E_i} \frac{\partial T\hat{h}_{G,E_i}}{\partial t} \tag{3.58}$$

$$\frac{\partial T\hat{h}_{G,E_i}}{\partial t} = \frac{T\hat{h}_{G,E_i}^{n+1,m+1} - T\hat{h}_{G,E_i}^{n}}{\Delta t} \tag{3.59}$$

$$\frac{\partial T\theta_{G,E_i}}{\partial t} = \frac{T\theta_{G,E_i}^{n+1,m+1} - T\theta_{G,E_i}^{n}}{\Delta t} = \frac{T\theta_{G,E_i}^{n+1,m} + TC_{G,E_i}^{n+1,m}\left(Th_{G,E_i}^{n+1,m+1} - Th_{G,E_i}^{n+1,m}\right) - T\theta_{G,E_i}^{n}}{\Delta t} = \frac{T\theta_{G,E_i}^{n+1,m} + T\hat{C}_{G,E_i}^{n+1,m}\left(T\hat{h}_{G,E_i}^{n+1,m+1} - T\hat{h}_{G,E_i}^{n+1,m}\right) - T\theta_{G,E_i}^{n}}{\Delta t} \tag{3.60}$$

Therefore, the flux at each edge can be representated by

$$Q_{G,E_i}^{n+1,m+1} = \left(\frac{\sum_{E_j \not\subset \partial\Omega_D} \hat{\alpha}_{G,E_i}^{n+1,m} \hat{\alpha}_{G,E_j}^{n+1,m}}{\hat{\alpha}_G^{n+1,m}} - \sum_{E_j \not\subset \partial\Omega_D} \hat{B}_{G,i,j}^{-1,n+1,m} \right) Th_{G,E_j}^{n+1,m+1} + \frac{|G|}{3} f_G$$
$$- \frac{|G|}{3\Delta t} \left(T\hat{C}_{G,E_i}^{n+1,m} + S_{sG}^{n+1,m} \frac{T\hat{\theta}_{G,E_i}^{n+1,m}}{\varphi_G} \right) \hat{Th}_{G,E_i}^{n+1,m+1} + Y_{0_{G,E_i}} + Y_{1_{G,E_i}} + Y_{2_{G,E_i}} \quad (3.61)$$

Where:

$$Y_{0_{G,E_i}} = \left(\frac{\sum_{E_j \subset \partial\Omega_D} \hat{\alpha}_{G,E_i}^{n+1,m} \hat{\alpha}_{G,E_j}^{n+1,m}}{\hat{\alpha}_G^{n+1,m}} - \sum_{E_j \subset \partial\Omega_D} \hat{B}_{G,i,j}^{-1,n+1,m} \right) \hat{Th}_{G,E_{jD}}$$

$$Y_{1_{G,E_i}} = \left(\frac{\sum_{j=1}^{3} \hat{\alpha}_{G,E_i}^{n+1,m} \hat{\alpha}_{G,E_j}^{n+1,m}}{\hat{\alpha}_G^{n+1,m}} - \sum_{j=1}^{3} \hat{B}_{G,i,j}^{-1,n+1,m} \right) \hat{K}_G^{-1,n+1,m} K_G^{n+1,m} z_{G,E_j}$$

$$Y_{2_{G,E_i}} = \begin{cases} \frac{|G|}{3\Delta t} \left(T\hat{C}_{G,E_i}^{n+1,m} + S_{sG}^{n+1,m} \frac{T\hat{\theta}_{G,E_i}^{n+1,m}}{\varphi_G} \right) \hat{Th}_{G,E_i}^{n} & \text{if} \quad \frac{T\theta_{G,E_i}^{n+1}}{\varphi_G} > tol_f \\ -\frac{|G|}{3\Delta t} \left(T\theta_{G,E_i}^{n+1,m} - T\theta_{G,E_i}^{n} - S_{sG}^{n+1,m} \frac{T\hat{\theta}_{G,E_i}^{n+1,m}}{\varphi_G} \hat{Th}_{G,E_i}^{n} - T\hat{C}_{G,E_i}^{n+1,m} \hat{Th}_{G,E_i}^{n+1,m} \right) & \text{if} \quad \frac{T\theta_{G,E_i}^{n+1}}{\varphi_G} \leq tol_f \end{cases}$$

3.3.15. Hydrodynamics system of equations using mass condensation scheme

Incorporating the flux continuity and boundary conditions, the following system of linear equations representing the hydrodynamics is obtained:

$$\hat{M}\hat{Th}^{n+1,m+1} = \hat{V} - \hat{Y}_1 - \hat{Y}_2 \tag{3.62}$$

Where:

$$\hat{M}=\left[\hat{M}_{E,E'}\right]_{nf,nf} \quad \hat{M}_{E,E} = \sum_{G\supset E}\left[\frac{(\hat{\alpha}_{G,E})^2}{\hat{\alpha}_G} - \hat{B}^{-1}_{G,E,E} - \frac{|G|}{3\Delta t}\left(T\hat{C}^{n+1,m}_{G,E} + S_{sG}^{n+1,m}\frac{T\hat{\theta}^{n+1,m}_{G,E}}{\varphi_G}\right)\right] \quad \forall E \not\subset \partial\Omega_D,$$

$$\hat{M}_{E,E'} = \sum_{G\supset(E \text{ and } E')}\left[\frac{\hat{\alpha}_{G,E}\hat{\alpha}_{G,E'}}{\hat{\alpha}_G} - \hat{B}^{-1}_{G,E,E'}\right] \quad \forall E' \not\subset \partial\Omega_D$$

$$\hat{Y}_1 = \left[\hat{Y}_{1E}\right]_{nf} \qquad \hat{Y}_{1E} = \sum_{G\supset E}\left(Y_{0G,E} + Y_{1G,E} + \frac{|G|}{3}f_G\right) \quad \forall E \not\subset \partial\Omega_D$$

$$\hat{Y}_2 = \left[\hat{Y}_{2E}\right]_{nf} \qquad \hat{Y}_{2E} = \sum_{G\supset E} Y_{2G,E} \quad \forall E \not\subset \partial\Omega_D$$

As it can be seen, the terms issues from the mass discretizaton appears only in the diagonal coefficients of the matrix [M], avoiding with this oscillation problems.

This system of equations can be rewritten in terms of the increment in iteration $\Delta\hat{Th}^{n+1,m}_{G,E} = Th^{n+1,m+1}_{G,E} - Th^{n+1,m}_{G,E}$, as the modified Picard iteration technique proposed by Celia et al. [1990]. Only the definition of the residue will change, giving as result a matrix system in the form:

.

$$\left[\hat{M}\right]_{nf,nf}\left\{\Delta Th^{n+1,m}\right\}_{nf} = \left\{\hat{X}\right\}_{nf} \tag{3.63}$$

With $$\hat{X} = V - \hat{Y}_1 + \hat{X}_1 + \hat{X}_2 - \hat{X}_3 Th^{n+1,m}$$

$$\hat{X}_1 = \left[\hat{X}_{1E}\right]_{nf} \qquad \hat{X}_{1E} = \sum_{G \supset E} \frac{|G|}{3\Delta t} S_{sG}^{n+1,m} \frac{T\hat{\theta}_{G,E}^{n+1,m}}{\varphi_G} \left(T\hat{h}_{G,E}^{n+1,m} - T\hat{h}_{G,E}^{n}\right) \qquad \forall E \not\subset \partial\Omega_D$$

$$\hat{X}_2 = \left[\hat{X}_{2E}\right]_{nf} \qquad \hat{X}_{2_E} = \sum_{G \supset E} \begin{cases} \frac{|G|}{3\Delta t} T\hat{C}_{G,E}^{n+1,m} \left(T\hat{h}_{G,E}^{n+1,m} - T\hat{h}_{G,E}^{n}\right) & \text{if} \quad \frac{T\theta_{G,E}^{n+1}}{n_G} > tol_f \\ \frac{|G|}{3\Delta t} \left(T\theta_{G,E}^{n+1,m} - T\theta_{G,E}^{n}\right) & \text{if} \quad \frac{T\theta_{G,E}^{n+1}}{n_G} \le tol_f \end{cases} \qquad \forall E \not\subset \partial\Omega_D$$

$$\hat{X}_3 = \left[\hat{X}_{3E,E'}\right]_{nf,nf} \qquad \hat{X}_{3E,E'} = \sum_{G \supset (E \text{ and } E')} \left[\frac{\hat{\alpha}_{G,E}\hat{\alpha}_{G,E'}}{\hat{\alpha}_G} - \hat{B}_{G,E,E'}^{-1}\right] \qquad \begin{matrix} \forall E \not\subset \partial\Omega_D \\ \forall E' \not\subset \partial\Omega_D \end{matrix}$$

In the present work the Picard linearization scheme was kept to solve the system of equations in terms of traces of pressure.

3.3.16. Top boundary conditions (Evaporation / Infiltration)

Van Dam and Feddes [2000] developed a procedure for 1D models that gives special attention to the top boundary condition, which is important for simulations with ponded water layers or with fluctuating water levels close to the soil surface. This procedure switches from head to flux controlled boundary condition and vice versa (Figure3). Depending on the case, h_{sur} the soil surface pressure head [L], or q_{sur} the soil surface flux [LT^{-}] is prescribed.

The first criterion determines if the soil column is saturated. If it is saturated a second criterion determines wheater at the end of the time step, the soil column will be still saturated or it becomes unsaturated. The inflow Q_{in} into the soil column [L] is calculated considering the fluxes positive when they are directed upward. Q_{in} includes the flux [LT^{-1}] at soil profile bottom q_{bot}, the potential flux at the soil surface q_{top}, root water extraction q_{root}, and the total lateral flux to drains or ditches q_{drain} during the time step. If Q_{in} is positive, more water enters than leaves the profile. The soil profile remains saturated and a head condition is applied. If Q_{in} is negative, the soil profile becomes unsaturated and a flux condition is used.

When the soil column is unsaturated, a comparison between Q_{in} and V_{air} (the total air volume in the soil profile at the start of the time step [L]) determines whether the soil column will remain unsaturated or becomes saturated during the time step.

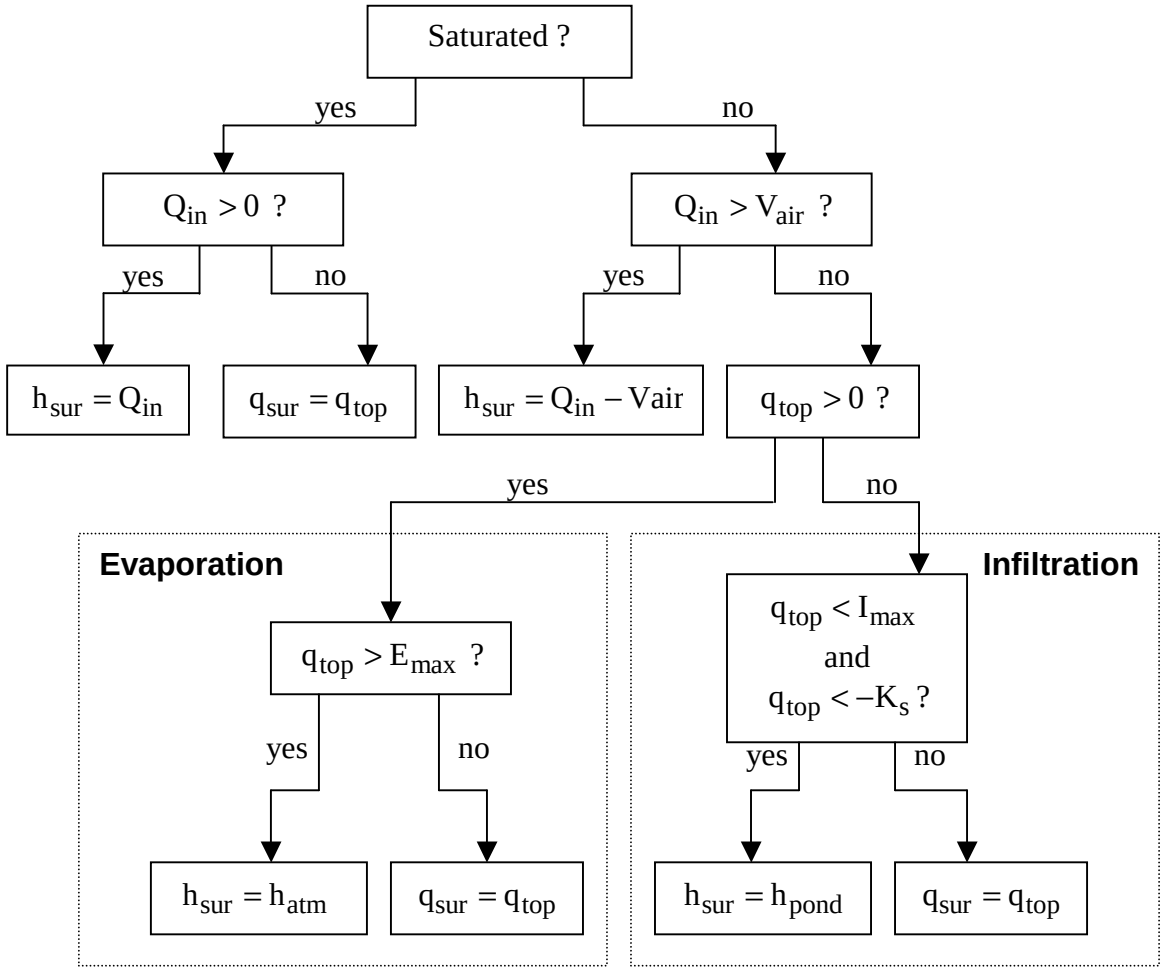

Fig. 3. Procedure to select head or flux top boundary condition [Van Dam and Feddes, 2000]

If the soil becomes saturated a head condition is used. If the soil remains unsaturated, the procedure distingueshes between evaporation and infiltration. The evaporation is limited to E_{max}, a maximum soil evaporation [LT^{-1}], which is in relationship with h_{atm}, the soil water pressure head in equilibrium with the air humidity [L]: $h_{atm} = 13.3x10^5 \ln(e_{act} / e_{sat})$. e_{act} and e_{sat} are the actual and saturated vapour pressure, respectively [kPa]. $h_{atm} \approx -2.75x10^5$ cm [Kroes and van Dam, 2003]. In the case of infiltration, if the potential flux q_{top} exceeds I_{max} (the maximum infiltration flux at the soil surface [LT^{-1}]) and K_{sat} (the top soil saturaturated hydraulic conductivity [LT^{-1}]), a head boundary condition is prescribed as h_{pond}, the height of water ponding on the soil surface at t^j [L].

This procedure was adapted to be used in a 2D domain and using the mixed hybrid formulation of flux.

3.3.17. Mass balance error

Following the approach of Celia et al., [1990], a mass balance measure MB is defined in order to test the ability of the model to conserve mass. The accuracy of the numerical scheme is evaluated by computing a global mass balance error ε_{MB}:

$$MB = \left| \frac{\text{total additional mass in the domain}}{\text{total net flux into the domain}} \right| \tag{3.64}$$

$$\varepsilon_{MB} = 1 - MB \tag{3.65}$$

Where:

Total additional mass in the domain = $\sum_{n=1}^{nt} \sum_{G=1}^{nm} Mass_G$

Total net flux into the domain= $\sum_{n=1}^{nt} \sum_{G=1}^{nm} Flux_G$

nt is the total number of time steps and

nm is the total number of elements in the domain.

With

$$Mass_G = \begin{cases} \frac{|G|}{\Delta t^n}\left(\hat{C}_G^{n+1,m} + \frac{\hat{\theta}_G^{n+1,m}}{\varphi_G} S_{sG}^{n+1,m}\right)\left(\hat{h}_G^{n+1,m+1} - \hat{h}_G^{n}\right) & \text{if} \quad \frac{\theta_{G,E_i}^{n+1,m}}{\varphi_G} > tol_f \\ \frac{|G|}{\Delta t^n}\left(\theta_G^{n+1,m+1} - \theta_G^{n}\right) + \frac{|G|}{\Delta t^n}\frac{\hat{\theta}_G^{n+1,m}}{\varphi_G} S_{sG}^{n+1,m}\left(\hat{h}_G^{n+1,m+1} - \hat{h}_G^{n}\right) & \text{if} \quad \frac{\theta_{G,E_i}^{n+1,m}}{\varphi_G} \le tol_f \end{cases}$$

$$Flux_G = \alpha_G^{n+1,m}\left(\hat{h}_G^{n+1,m+1} + \hat{K}_G^{-1,n+1,m} K_G^{n+1,m} z_G\right) - \sum_{i=1}^{3} \alpha_{G,E_i}^{n+1,m}\left(Th_{G,E_i}^{n+1,m+1} + \hat{K}_G^{-1,n+1,m} K_G^{n+1,m} z_{G,E_i}\right) - |G| f_G^{n+1}$$

Additionally, a mass balance ratio can be computed for each time step MB^n, with their corresponding error $\varepsilon_{MB}{}^n = 1 - MB^n$.

$$MB^n = \left| \frac{\sum_{G=1}^{nm} Mass_G}{\sum_{G=1}^{nm} Flux_G} \right|^n \qquad \varepsilon_{MB}{}^n = 1 - MB^n \tag{3.66}$$

Locally, mass balance error can be computed as:

$$E_{1G} = \left| \frac{\Delta t^n}{|G|} \sum_{i=1}^{3} Q_{G,E_i}^{n+1,m+1} - f_G \Delta t^n + \sum_{i=1}^{3} E_{1G_i} \right| \tag{3.67}$$

With
$$E_{lG_i} = \begin{cases} \frac{1}{3}\left(T\hat{C}_{G,E_i}^{n+1,m} + S_{sG}^{n+1,m} \frac{T\hat{\theta}_{G,E_i}^{n+1,m}}{\varphi_G} \right)\left(T\hat{h}_{G,E_i}^{n+1,m+1} - T\hat{h}_{G,E_i}^{n} \right) & \text{if} \quad \frac{T\theta_{G,E_i}^{n+1}}{\varphi_G} > tol_f \\ \frac{1}{3}\left(T\theta_{G,E_i}^{n+1,m+1} - T\theta_{G,E_i}^{n} + S_{sG}^{n+1,m} \frac{T\hat{\theta}_{G,E_i}^{n+1,m}}{\varphi_G} \left(T\hat{h}_{G,E_i}^{n+1,m+1} - T\hat{h}_{G,E_i}^{n} \right) \right) & \text{if} \quad \frac{T\theta_{G,E_i}^{n+1}}{\varphi_G} \le tol_f \end{cases}$$

$$E_{2G} = \left| \frac{\Delta t^n}{|G|} \left(Mass_G + Flux_G \right) \right| \tag{3.68}$$

A low mass balance error is a necessary but not a sufficient condition to ensure accuracy to the solution. Mass balance error can decrease even if the solutions do not converge [Tocci and Kelley, 1997, Kosugi, 2008].

Kosugi [2008] concluded that is important to check the mass balance and solution convergence at each time step when using the discretization scheme of Celia et al., [1990] to simulate unsaturated water flow.

3.3.18. Maximal convergence errors for pressure head and water content

Maximal convergence errors for pressure Δh_{max} and water content $\Delta\theta_{max}$ are calculated at the end of each time step as follows:

$$\Delta h_{max} = \max\left(\left| h_G^{n+1,m+1} - h_G^{n+1,m} \right| \right) \tag{3.69}$$

$$\Delta\theta_{max} = \max\left(\left| \theta_G^{n+1,m+1} - \theta_G^{n+1,m} \right| \right) \tag{3.70}$$

where max is the generator of the maximal value in the entire spatial domain.

3.3.19. Discrepancy between average pressure and arithmetic mean of edge pressures

$\Delta h_{d\,max}$ represents a measure of disagreement or discrepancy between the average pressure calculated in the element using the mixed hybrid formulation (equation 3.49) and the arithmetic mean of the three edge pressures belonging to this element.

$$\Delta h_{d\,max} = \max\left(\left| h_G^{n+1,m+1} - \frac{1}{3} \sum_{i=1}^{3} Th_{G,E_i}^{n+1,m+1} \right| \right) \tag{3.71}$$

where max is the generator of the maximal value in the entire spatial domain.

3.3.20. Numerical solution and convergence criteria

This method will lead to a system of linear equations, where the unknowns are the water pressure traces (Th). The number of unknowns is equal to the number of edges to which the pressure has not been imposed. The matrix associated with the hydrodynamics equations system is symmetric and definite positive. Therefore, it can be effectively solved by the conjugate gradient method, preconditioned with an incomplete Cholesky decomposition using the Eisenstat procedure [Eisenstat, 1981]. The iteration process for the hydrodydamics when using the mass condensation scheme is stopped when the following conditions are met:

- The difference between the calculated values of edge pressure head between two successive iteration levels is smaller than an absolute iteration convergence tolerance predetermined by the user. More accurate solution can be obtained with smaller values of tolerance, but computational time increases. Values in the range of 0.001 cm to 1 cm are often used [Shahraiyni and Ashtiani, 2009].

$$\left| \mathrm{Th}_{G,E_i}^{n+1,m+1} - \mathrm{Th}_{G,E_i}^{n+1,m} \right| \leq \mathrm{tol}_a \tag{3.72}$$

- The iteration convergence test, which involves both absolute and relative error, is satisfied. Values adopted for the relative tolerance generally are in the range of 10^{-2} to 10^{-5} depending upon the desired accuracy [Kavetski et al., 2001]. This mixed criterion will serve to reduce the number of iterations, in particular when the pressure head changes significantly but not the water content.

$$\left| \mathrm{Th}_{G,E_i}^{n+1,m+1} - \mathrm{Th}_{G,E_i}^{n+1,m} \right| - \mathrm{tol}_r \left| \mathrm{Th}_{G,E_i}^{n+1,m+1} \right| - \mathrm{tol}_a < 0 \tag{3.73}$$

- The difference between the calculated values of water content between two sucessive iteration levels is smaller than a tolerance predetermined by the user. Huang, [1996] suggests a value of 0.0001 for this tolerance criterion, which is interesting for cases where water content changes dramatically with small changes in the pressure head.

$$\left| \mathrm{T}\theta_{G,E_i}^{n+1,m+1} - \mathrm{T}\theta_{G,E_i}^{n+1,m} \right| \leq \mathrm{tol}_c \tag{3.74}$$

For the standard MHFEM formulation, the iteration process is stopped when the relative residual norm is smaller than a relative tolerance predetermined by the user.

$$\frac{\left\| \mathrm{Th}^{n,m+1} - \mathrm{Th}^{n,m} \right\|}{\left\| \mathrm{Th}^{n,m+1} \right\|} = \frac{\sqrt{\sum_{i=1}^{nf} \left(\mathrm{Th}_i^{n,m+1} - \mathrm{Th}_i^{n,m} \right)^2}}{\sqrt{\sum_{i=1}^{nf} \left(\mathrm{Th}_i^{n,m+1} \right)^2}} \leq \mathrm{tol}_r \tag{3.75}$$

3.3.21. Hydrodynamics modelling outline

Numerical method	Mixed hybrid finite element method
Variable Transformation	The pressure head variable h is transformed into the dependent variable $\hat{h}$ [Pan and Wierenga, 1995]
Continuity	Flux and Pressure head
Boundary conditions	Dirichlet and Neumann conditions. Special attention is given to the top boundary conditions: infiltration/evaporation [Van Dam and Feddes, 2000].
Mass conservation	h-based and mixed form of the Richards equation (using Celia et al, [1990] approach).
Switching technique	If the ratio water content / saturation water is bigger or equal to the tolerance specified by the user, then pressure head is used as primary variable, if not then a mixed-form of the Richards equation is used.
Temporal discretization	Fully implicit (backward Euler) method
Linearization	Picard iterative process
Hydraulic conductivity	Modified Mualem-van Genuchten expression [Ippisch et al., 2006]
Oscillation control	Mass lumping: mass condensation scheme [Younes et al., 2006]
Iteration convergence criteria	MHFEM using mass condensation scheme: - Test involving only absolute edge pressure error - Test involving both absolute and relative edge pressure errors - Test involving edge water content error Standard MHFEM -Test involving only relative edge pressure error
Simulation Results	Profiles in time and space: -Pressure head [L] and water content [$L^3 L^{-3}$]. Average approximations by edge and elements. - Darcy Flux approximation over the elements [L T]. Components of the vector. -Water flux over the edges [L^2 T] Computation of errors Mass balance error using the mixed hybrid formulation: -Global mass balance error computed based on the additional mass measured with respect to the initial mass in the system. -Maximum mass balance error computed locally for each element and each time step Maximal convergence errors: -Pressure and water content errors computed as the difference of iterative solutions at the end of each time step. Discrepancy between average pressure and arithmetic mean of edge pressures Cumulative infiltration/evaporation Maximum and minimum adimensional numbers (Co, Pe, Fn)

Section 3.4. 2D Transport modelling

The pesticide transport is described by a classical advection-dispersion equation with the presence of sink/source term, which takes into account the pesticide degradation.

$$\frac{\partial(\theta C)}{\partial t}+\frac{\partial(\rho S)}{\partial t}=\nabla(\theta D\nabla C)-\nabla\left(\vec{q}\,C\right)+f(C,t) \qquad (4.1)$$

Where:

$f(C,t)$	is the net rate of reaction (sink/source terms)	$[ML^{-3}T^{-1}]$,
C	is solution concentration	$[ML^{-3}]$,
S	is the concentration of the species adsorbed on the solid (mass of solute/ mass of solid)	$[M\,M^{-1}]$,
ρ	is soil bulk density	$[ML^{-3}]$,
t	is time	$[T]$,
$\vec{q}$	is flow rate per unit area	$[LT^{-1}]$,
D	is the dispersion tensor	$[L^2T^{-1}]$,
θ	is soil volumetric water content	$[L^3L^{-3}]$.

The first term on the right side of the equation represents the change in concentration due to hydrodynamic dispersion. The second term represents the advective transport. The third term represents the effects of mixing with a source fluid that has a different concentration and all the chemical and biological reactions that cause mass transfer between the liquid and solid phases or conversion of dissolved chemical species.

3.4.1. New approach to solve transport equation

Several flow and transport approximation models in partially or completely saturated porous media have faced a difficulty when the advection is dominant. Hereby, unstable oscillations are raised. Many researchers have then exploited the operator splitting technique (OST) for solving this problem [Herrera and Valocchi, 2006].

The MHFEM has been used by several authors to solve just the dispersion term of the transport equation, whereas a discontinuous finite element method was applied for the advection term, followed by a slope limiting tool to reduce possible oscillations [Siegel et al.,

1997; Ackerer et al., 1999; Oltean and Buès, 2001; Hoteit et al., 2002; Mazzia et al., 2002; Hoteit et al., 2004]. According to Carrayrou et al. [2004], each method used in OST introduces an intrinsic error into the solution.

A new formulation to solve the transport equation is here introduced. A global approach that includes both, advection and dispersion, terms (with the MHFEM approximation) is used:

$$\vec{q}_{\text{advection,dispersion}} = -\theta D \nabla C + \vec{q} C \tag{4.2}$$

New formulation to solve the transport equation using a global approach

An invertible matrix represents the dispersion tensor D, so we can write:

$$\theta^{-1} D^{-1} \vec{q}_{\text{advection,dispersion}} = -\nabla C + \theta^{-1} D^{-1} \vec{q} C \tag{4.3}$$

This equation is valid for each element of the flow domain Ω. Therefore it can be approximated with the use of integral equations and base functions $\vec{u}_G$.

$$\int_G \theta^{-1} D^{-1} \vec{q}_{\text{advection,dispersion}} \vec{u}_G = -\int_G (\nabla C) \vec{u}_G + \int_G \theta^{-1} D^{-1} \vec{q} C \vec{u}_G \tag{4.4}$$

According to the product rule of divergence

$$\int_G (\nabla C) \vec{u}_G = \int_G \nabla \left(C \vec{u}_G \right) - \int_G C \left(\nabla \vec{u}_G \right) \tag{4.5}$$

Based on the Gauss-Divergence Theorem, the continuity on concentration C, and taking in account that the frontier of the element G is composed by three edges E_i:

$$\int_G \nabla \left(C \vec{u}_G \right) = \int_{\partial G} C \vec{u}_G \vec{n}_{\partial G} = \int_{i \subset \partial G} TC_{G,E_i} \vec{n}_{G,E_i} \vec{u}_G \tag{4.6}$$

Where TC_{G,E_i} is the average concentration at the edge E_i of the triangular element G

Substituting the equation (4.6) in equation (4.5) we get:

$$\int_G \theta^{-1} D^{-1} \vec{q}_{\text{advection,dispersion}} \vec{u}_G = -\sum_{i \subset \partial G} TC_{G,E_i} \vec{n}_{G,E_i} \vec{u}_G + \int_G C\left(\nabla \vec{u}_G\right) + \int_G \theta^{-1} D^{-1} \vec{q} C \vec{u}_G \tag{4.7}$$

The advective and dispersive flux $\vec{q}_{\text{advection,dispersion}}$ is approximated over each element by a unique vector $\vec{q}_{\text{adv-disp}_G}$ belonging to the lowest order Raviart-Thomas space.

Therefore, $\nabla \vec{q}_{\text{adv-disp}_G}$ is constant over the element G, and $\vec{q}_{\text{adv-disp}_G} \vec{n}_{G,E_i}$ is constant over the edge E_i, $\forall i = 1,2,3$. $\vec{q}_{\text{adv-disp}_G}$ can be perfectly determined by knowing the transport flux through the edges:

$$\vec{q}_{\text{adv-disp}_G} = \sum_{j=1}^{3} Q_{\text{adv-disp}_{G,E_j}} \vec{w}_j \tag{4.8}$$

with $Q_{\text{adv-disp}G,Ej}$ the advective-dispersive flux over the edge Ej belonging to the element G.

Using the approximations over each element, and the base vectors $\vec{w}_i$ defined by $\int_i \vec{w}_j \cdot \vec{n}_{G_i} = \delta_{ij}$, where δ_{ij} is the Kronecker symbol, equation (4.7) can be then rewritten as:

$$\int_G \theta_G^{-1} D_G^{-1} \vec{q}_{\text{adv-disp}_G} \vec{w}_i = -\sum_{i \subset \partial G} TC_{G,E_i} \vec{n}_{G,E_i} \vec{w}_i + \int_G C_G\left(\nabla \vec{w}_i\right) + \int_G \theta_G^{-1} D_G^{-1} \vec{q}_G C_G \vec{w}_i \quad \forall i = 1,2,3 \tag{4.9}$$

Applying the approximations of flux through the edges from equation (4.8)

$$\int_G \theta_G^{-1} D_G^{-1} \left(\sum_{j=1}^{3} Q_{\text{adv-disp}_{G,E_j}} \vec{w}_j\right) \vec{w}_i = -\sum_{i \subset \partial G} TC_{G,E_i} \vec{n}_{G,E_i} \vec{w}_i + \int_G C_G\left(\nabla \vec{w}_i\right) + \int_G C_G \theta_G^{-1} D_G^{-1} \left(\sum_{j=1}^{3} Q_{G,E_j} \vec{w}_j\right) \vec{w}_i \quad \forall i = 1,2,3 \tag{4.10}$$

Rearranging terms:

$$\sum_{j=1}^{3} Q_{adv-disp_{G,E_j}} \int_G \left(\theta_G^{-1} D_G^{-1} \vec{w}_j \right) \vec{w}_i = -TC_{G,E_i} \int_{i \subset \partial G} \vec{n}_{G,E_i} \vec{w}_i + C_G \int_G \left(\nabla \vec{w}_i \right) + C_G \sum_{j=1}^{3} Q_{G,E_j} \int_G \left(\theta_G^{-1} D_G^{-1} \vec{w}_j \right) \vec{w}_i \qquad \forall i = 1,2,3 \quad (4.11)$$

Under the application of the divergence theorem $\int_G \nabla \vec{w}_i = \int_{\partial G} \vec{w}_i \vec{n}_{G,E_i} = 1$

$$\sum_{j=1}^{3} Q_{adv-disp_{G,E_j}} \int_G \left(\theta_G^{-1} D_G \theta_G^{-1} \vec{w}_j \right) \vec{w}_i = -TC_{G,E_i} + C_G + C_G \sum_{j=1}^{3} Q_{G,E_j} \int_G \left(\theta_G^{-1} D_G^{-1} \vec{w}_j \right) \vec{w}_i \qquad \forall i = 1,2,3 \quad (4.12)$$

3.4.2. Advective-dispersive flux

The formulation for the advective-dispersive flux is then given by:

$$Q_{adv-disp_{G,E_i}} = -\sum_{j=1}^{3} B_{G,i,j}^{-1} TC_{G,E_j} + C_G \gamma_{G,E_i} \qquad \forall i = 1,2,3 \quad (4.13)$$

Where:

C_G is the average concentration at the element G.

TC_{G,E_j} is the average concentration at the edge E_j.

γ_{G,E_i} is an auxiliary variable defined as $\gamma_{G,E_i} = \sum_{j=1}^{3} B_{G,i,j}^{-1} + Q_{G,E_i}$

B_G is a symmetric and invertible 3 x 3 matrix, defined by

$$B_G = \left| B_{G,i,j} \right|_{3,3} \qquad B_{G,i,j} = \int_G \left(\theta_G^{-1} D_G^{-1} \vec{w}_j \right) \vec{w}_i \quad (4.14)$$

The coefficients of the hydrodynamic dispersion tensor are defined as [Bear, 1979]:

$$\theta D_{i,j} = (\alpha_L - \alpha_T)\frac{q_i q_j}{|q|} + (\theta\tau Dm + \alpha_T |q|)\delta_{i,j} \qquad (4.15)$$

With:

α_L	the longitudinal dispersivity of the porous medium [L],
α_T	the transversal dispersivity of the porous medium [L],
q_i , q_j	the components of Darcy flux q [LT^{-1}],
θ	the soil volumetric water content [L^3L^{-3}],
Dm	the molecular diffusion coefficient [L^2 T^{-1}],
τ	is the tortuosity factor [-],
$\delta_{i,j}$	the Kronecker's symbol [-].

See Appendix II for detailed information about the computation of the vector components of the flux approximation.

3.4.3. Continuity equation

The continuity equation is provided for all the interior edges E_i ($\forall i = 1,2,3$) of the domain Ω. The edge E_i is common to the frontiers of the elements G and G'.

$$Q_{adv-disp_{G,E_i}} + Q_{adv-disp_{G',E_i}} = 0 \qquad (4.16)$$

3.4.4. Boundary conditions

Neumann boundary condition, is defined by

$$Q_{G,E_i} = Q_{adv-disp_{N_{G,E_i}}} \qquad \forall E_i \subset \partial\Omega_N \quad (4.17)$$

Where $Q_{adv-disp_{N_{G,E_i}}}$ is the imposed value of flux.

For Dirichlet boundary conditions, the term I_{G,E_i} is defined by

$$I_{G,E_i} = \sum_{E_j \subset \partial\Omega_D} \hat{B}^{-1}_{G,i,j} TC_{G,E_j} \qquad \forall i = 1,2,3 \quad (4.18)$$

3.4.5. Matrix form of the continuity equation

$$DC - RTC - V - I = 0 \tag{4.19}$$

Where:

$D = \left[D_{E,G} \right]_{nft,nm}$ $\quad D_{E,G} = \begin{cases} \gamma_{G,E} & \text{if } E \subset \partial G \\ 0 & \text{if } E \not\subset \partial G \end{cases}$

$R = \left[R_{E,E'} \right]_{nft,nft}$ $\quad R_{E,E'} = \sum_{G \supset (E \text{ and } E')} B^{-1}_{G,E,E'}$ $\quad \forall E \not\subset \partial\Omega_D,\ \forall E' \not\subset \partial\Omega_D$

$V = \left[V_E \right]_{nft}$ $\quad V_{G,E} = \begin{cases} Q_{adv-disp_N G,E} & \forall \quad E \subset \partial\Omega_N \\ 0 & \forall \quad E \not\subset \partial\Omega_N \end{cases}$

$I = \left[I_E \right]_{nft}$ $\quad I_E = \sum_{G \supset E} I_{G,E}$ $\quad \forall E \not\subset \partial\Omega_D$

$C = \left[C_G \right]_{nm}$ $\quad C_G = C_G$ $\quad \forall G \subset \Omega$

$TC = \left[TC \right]_{nft}$ $\quad TC_E = TC_{G,E}$ $\quad \forall E \not\subset \partial\Omega_D$

Nft — Is the number of edges over the domain Ω where the concentration has not been imposed.

3.4.6. Advection-diffusion equation

Recalling the advection-diffusion equation, and integrating over the element G, using a test function v_G = constant over G :

$$\int_G \frac{\partial(\theta C)}{\partial t} v_G + \int_G \frac{\partial(\rho S)}{\partial t} v_G + \int_G \left(\nabla \vec{q}_{\text{advection, dispersion}} \right) v_G = \int_G f(x, y, t) v_G \qquad \forall G \text{ over a domain } \Omega \text{ for } t \subset]0, T[\tag{4.20}$$

Assuming $v_G = 1$, an analogous equation using the approximations over the element can be obtained. It can be expressed in terms of R, the retardation factor (dimensionless), which is given by $R = 1 + \frac{\rho}{\theta}\frac{S}{C}$.

3.4.7. Time discretization

Time discretization was carried out applying a fully implicit (backward Euler) method.

$$\left(\frac{\theta_G^{n+1} R_G^{n+1} C_G^{n+1} - \theta_G^n R_G^n C_G^n}{\Delta t}\right)|G| + \nabla \vec{q}_{adv-disp_G}^{\,n+1}|G| = \int_G f\left(x, y, t^{n+1}\right) \qquad (4.21)$$

3.4.8. Linear-sorption reaction

Considering a linear-sorption reaction, the concentration of solute sorbed to the porous medium is directly proportional to the concentration of the solute in the pore fluid. The ratio of the concentration of the solute between the solid matrix and the solution phase is representated by the isotherm linear adsorption coefficient [L^3M^{-1}], $k_{dG} = \frac{S_G}{C_G}$.

$$\left(\frac{\left(\theta_G^{n+1} + k_{dG}^{n+1}\rho_G^{n+1}\right)C_G^{n+1} - \left(\theta_G^n + k_{dG}^n \rho_G^n\right)C_G^n}{\Delta t}\right)|G| + \nabla \vec{q}_{adv-disp_G}^{\,n+1}|G| - F_G^{n+1} = 0 \qquad (4.22)$$

with $F_G^{n+1} = \int_G f\left(C_G^{n+1}, t^{n+1}\right)$.

3.4.9. Average concentration in the element

Recalling that based on Raviart-Thomas properties $\nabla \vec{q}_{adv-disp_G}$ is constant over the element G:

$$\nabla \vec{q}_{adv-disp_G}^{\,n+1} = \frac{1}{|G|}\sum_{i=1}^{3} Q_{adv-disp_{G,E_i}}^{n+1} = \frac{1}{|G|}\left[C_G^{n+1}\sum_{i=1}^{3}\gamma_{G,E_i} - \sum_{i=1}^{3}\sum_{j=1}^{3} B_{G,i,j}^{-1} TC_{G,E_i}^{n+1}\right] \qquad (4.23)$$

Substituting equation (4.23) in (4.22), an expression to estimate the average concentration in the element G is obtained:

$$C_G^{n+1} = \frac{\left(\theta_G^n + k_{dG}^n \rho_G^n\right) C_G^n + \frac{\Delta t}{|G|}\left(\sum_{i=1}^{3}\sum_{j=1}^{3} B_{G,i,j}^{-1} TC_{G,E_j}^{n+1} + F_G^{n+1}\right)}{\theta_G^{n+1} + k_{dG}^{n+1}\rho_G^{n+1} + \frac{\Delta t}{|G|}\sum_{i=1}^{3}\gamma_{G,E_i}} \tag{4.24}$$

Using the auxiliary variables $\gamma_G = \sum_{i=1}^{3}\gamma_{G,E_i}$ and $\beta_G = \frac{\frac{\Delta t}{|G|}\gamma_G}{\theta_G^{n+1} + k_{dG}^{n+1}\rho_G^{n+1} + \frac{\Delta t}{|G|}\gamma_G}$, the expression of average concentration in the element was rewritten:

$$C_G^{n+1} = \left(\frac{\theta_G^n + k_{dG}^n \rho_G^n}{\theta_G^{n+1} + k_{dG}^{n+1}\rho_G^{n+1}}\right)(1-\beta_G) C_G^n + \frac{\beta_G \sum_{i=1}^{3}\sum_{j=1}^{3} B_{G,i,j}^{-1} TC_{G,E_j}^{n+1}}{\gamma_G} + \frac{\beta_G F_G^{n+1}}{\gamma_G} \tag{4.25}$$

3.4.10. Matrix form of the average concentration

$$C^{n+1} = MC^n + NTC^{n+1} + GF^{n+1} + H \tag{4.26}$$

Where:

$$N = \left[N_{G,E}\right]_{nm,nft} \qquad N_{G,E} = \begin{cases} \frac{\beta_G \alpha_{G,E}}{\gamma_G} & \text{if} \quad E \subset \partial G \\ 0 & \text{if} \quad E \not\subset \partial G \end{cases}$$

$$M = \left[M_{G,G'}\right]_{nm,nm} \qquad M_{G,G'} = \begin{cases} \left(\frac{\theta_G^n + k_{dG}^n \rho}{\theta_G^{n+1} + k_{dG}^{n+1}\rho}\right)(1-\beta_G) & \text{if} \quad G = G' \\ 0 & \text{if} \quad G \neq G' \end{cases}$$

$$G = \left[G_{G,G'}\right]_{nm,nm} \qquad G_{G,G'} = \begin{cases} \frac{\beta_G}{\gamma_G} & \text{if} \quad G = G' \\ 0 & \text{if} \quad G \neq G' \end{cases}$$

$$H = \left[H_G\right]_{nm} \qquad H_G = \sum_{E \subset (\partial G \cap \partial \Omega_D)} \frac{\beta_G \alpha_{G,E}}{\gamma_G} TC_{G,E}$$

3.4.11. Mixed hybrid formulation for the transport equation

$$(R - DN)TC^{n+1} = DMC^{n} + DGF^{n+1} + DH - V - I \tag{4.27}$$

3.4.12. Oscillation control for advection dominant problem- a new flux limiter

The difficulties originated when advection is the dominant process are controlled by a flux limiting tool, which is specific to this mixed approach.

The equation (4.13) expressing the flux by edge is the result of a second order discretization since it is centered on the mesh. Introducing a constant η, we decrease the order of the discretization scheme for the term of advection, in function of the direction of the flux through the edge. The new flux expression by edge is given below. Besides, it will allow obtaining a stable discretization scheme for different η constants.

If $Q_{G,E_i} < 0$

$$\begin{aligned} Q_{adv-disp_{G,E_i}} = &-\sum_{j=1}^{3} B^{-1}_{G,i,j} TC_{G,E_j} + C_G \sum_{j=1}^{3} B^{-1}_{G,i,j} \\ &+ \frac{1}{2}\left[(1-\eta) Q_{G,E_i} C_G + (1+\eta) Q_{G,E_i} TC_{G,E_i}\right] \end{aligned} \tag{4.28a}$$

If $Q_{G,E_i} \geq 0$

$$\begin{aligned} Q_{adv-disp_{G,E_i}} = &-\sum_{j=1}^{3} B^{-1}_{G,i,j} TC_{G,E_j} + C_G \sum_{j=1}^{3} B^{-1}_{G,i,j} \\ &+ \frac{1}{2}\left[(1+\eta) Q_{G,E_i} C_G + (1-\eta) Q_{G,E_i} TC_{G,E_i}\right] \end{aligned} \tag{4.28b}$$

All the equations involving a flux expression need to replace this term according to equation (4.28).

Defining the auxiliary variables $\omega_{G,i}$ $\zeta_{G,i}$ $\alpha_{G,i}$ and γ_G

$$Q_{adv-disp_{G,E_i}} = -\sum_{j=1}^{3} B^{-1}_{G,i,j} TC_{G,E_j} + C_G(\gamma_{G,i}) + \zeta_{G,i} Q_{G,E_i} TC_{G,E_i} \qquad \forall i = 1,2,3 \tag{4.29}$$

Where: $\omega_{G,i} = \begin{cases} \frac{1}{2}(1-\eta) & \text{if} \quad Q_{G,E_i} < 0 \\ \frac{1}{2}(1+\eta) & \text{if} \quad Q_{G,E_i} \geq 0 \end{cases}$ $\zeta_{G,i} = \begin{cases} \frac{1}{2}(1+\eta) & \text{if} \quad Q_{G,E_i} < 0 \\ \frac{1}{2}(1-\eta) & \text{if} \quad Q_{G,E_i} \geq 0 \end{cases}$

$$\alpha_{G_i} = \sum_{j=1}^{3} B^{-1}_{G,i,j} \qquad \gamma_{G,i} = \alpha_{G,i} + \omega_{G,i} Q_{G,i}$$

Recalling that based on Raviart-Thomas properties $\nabla \vec{q}_{adv-disp_G}$ is constant over the element

$$\nabla \vec{q}^{\,n+1}_{adv-disp_G} = -\frac{1}{|G|}\sum_{i=1}^{3}\sum_{j=1}^{3} B^{-1}_{G,i,j} TC^{n+1}_{G,E_j} + \frac{1}{|G|} C^{n+1}_G \sum_{i=1}^{3} \gamma_{G,E_i} + \frac{1}{|G|}\sum_{i=1}^{3} \zeta_{K,i} Q_{G,E_i} TC^{n+1}_{G,E_i} \tag{4.30}$$

The average concentration over the element can be expressed as:

$$C^{n+1}_G = \frac{\left(\theta^n_G + k^n_{dG}\rho^n_G\right)C^n_G}{\theta^{n+1}_G + k^{n+1}_{dG}\rho^{n+1}_G + \lambda_G} + \frac{\lambda_G \sum_{i=1}^{3}\sum_{j=1}^{3} B^{-1}_{G,i,j} TC^{n+1}_{G,E_j}}{\gamma_G\left(\theta^{n+1}_G + k^{n+1}_{dG}\rho^{n+1}_G + \lambda_G\right)} - \frac{\lambda_G \sum_{i=1}^{3} \zeta_{G,i} Q_{G,E_i} TC^{n+1}_{G,E_i}}{\gamma_G\left(\theta^{n+1}_G + k^{n+1}_{dG}\rho^{n+1}_G + \lambda_G\right)} + \frac{\lambda_G F^{n+1}_G}{\gamma_G\left(\theta^{n+1}_G + k^{n+1}_{dG}\rho^{n+1}_G + \lambda_G\right)} \tag{4.31}$$

Or defining the auxiliary variable $\beta_G = \frac{\lambda_G}{\theta^{n+1}_G + k^{n+1}_{dG}\rho^{n+1}_G + \lambda_G}$, this equation can be rewritten as:

$$C^{n+1}_G = \left(\frac{\theta^n_G + k^n_{dG}\rho^n_G}{\theta^{n+1}_G + k^{n+1}_{dG}\rho^{n+1}_G}\right)(1-\beta_G)C^n_G + \frac{\beta_G \sum_{i=1}^{3}\sum_{j=1}^{3} B^{-1}_{G,i,j} TC^{n+1}_{G,E_j}}{\gamma_G} - \beta_G \frac{\sum_{i=1}^{3} \zeta_{G,i} Q_{G,E_i} TC^{n+1}_{G,E_i}}{\gamma_G} + \frac{\beta_G F^{n+1}_G}{\gamma_G} \tag{4.32}$$

3.4.13. Matrix form of the average concentration using the flux limiting tool

$$C^{n+1} = MC^{n} + NTC^{n+1} + GF^{n+1} + H \tag{4.33}$$

Where:

$$N = \left[N_{G,E} \right]_{nm,nft} \qquad N_{G,E} = \begin{cases} \dfrac{\beta_G \left(\alpha_{G,E} - \zeta_{G,E} Q_E \right)}{\gamma_G} & \text{if} \quad E \subset \partial G \\ 0 & \text{if} \quad E \not\subset \partial G \end{cases}$$

$$M = \left[M_{G,G'} \right]_{nm,nm} \qquad M_{G,G'} = \begin{cases} \left(\dfrac{\theta_G^{n} + k_{dG}^{n} \rho}{\theta_G^{n+1} + k_{dG}^{n+1} \rho} \right) \left(1 - \beta_G \right) & \text{if} \quad G = G' \\ 0 & \text{if} \quad G \neq G' \end{cases}$$

$$G = \left[G_{G,G'} \right]_{nm,nm} \qquad G_{G,G'} = \begin{cases} \dfrac{\beta_G}{\gamma_G} & \text{if} \quad G = G' \\ 0 & \text{if} \quad G \neq G' \end{cases}$$

$$H = \left[H_G \right]_{nm} \qquad H_G = \sum_{E \subset (\partial G \cap \partial \Omega_D)} \frac{\beta_G \left(\alpha_{G,E} - \zeta_{G,E} Q_{G,E} \right)}{\gamma_G} TC_{G,E}$$

3.4.14. Matrix form of the continuity equation using the flux limiting tool

Applying the continuity of flux and the boundary conditions equation 4.19 can be rewritten as

$$DC - RTC - V - I = 0 \tag{4.34}$$

Where:

$$D = \left[D_{E,G} \right]_{nft,nm} \qquad D_{E,G} = \begin{cases} \gamma_{G,E} & \text{if} \quad E \subset \partial G \\ 0 & \text{if} \quad E \not\subset \partial G \end{cases}$$

$$R = \left[R_{E,E'} \right]_{nft,nft} \qquad R_{E,E'} = \begin{cases} \sum\limits_{G \supset E \text{ and } E'} B^{-1}_{G,E,E'} - \zeta_{G,E'} Q_{G,E'} & \text{if} \quad E = E' \\ \sum\limits_{G \supset E \text{ and } E'} B^{-1}_{G,E,E'} & \text{if} \quad E \neq E' \end{cases}$$

Where the Neumann boundary condition is representated by the term:

$$Q_{adv-disp_{N_{G,E_i}}} = -\sum_{j=1}^{3} B^{-1}_{G,i,j} TC_{G,E_j} + C_G \gamma_{G,i} + \zeta_{G,i} Q_{G,E_i} TC_{G,E_i} \qquad \forall i \subset \partial \Omega_N \tag{4.35}$$

3.4.15. Residence Time Distribution

A distribution of times that parcels of water spend in a constructed wetland is known as a residence time distribution [Werner and Kadlec, 2000]. RTD is obtained as a breakthrough curve of a non-reactive tracer, and it is represented by an exit age distribution E(t). The function E(t) has units [T^{-1}]

$$E(t) = \frac{C(t)}{\int_0^\infty C(t)dt} \tag{4.36}$$

Where C(t) is the concentration of a tracer measured at the overflow at time t.
The cumulative residence time distribution function, F(t), is obtained integrating E(t)

$$F(t) = \int_0^t E(t)dt \tag{4.37}$$

Tracer techniques consisting in a conservative transport of a solute are then a valuable tool in the verification of the flow model, as it was performed in constructed wetlands by Ojeda et al. [2008] and Ronkanen and Kløve [2008].

Holland et al., [2004] investigated hydrologic factors affecting RTD characteristics. Their results indicate that flow rates did not have a significant effect on RTD characteristics, while water level can have a direct impact on the RTD of a wetland, suggesting that more than RTD may be necessary for analyzing a wetland subject to changing water levels.

The mean residence time is given by the first moment of the age distribution

$$\bar{t} = \int_0^\infty tE(t)dt \tag{4.38}$$

3.4.16. Numerical solution and convergence criterion

For the transport, the unknowns are traces of concentration. The number of unknows is equal to the number of edges to which traces of concentration has not been imposed. In contrast to the hydrodynamics, the matrix associated with the transport is nonsymmetric. Thus, the conjugate gradient squared iterative method with the Eisenstat ILU preconditioning procedure will be used to solve this algebraic system.

The iteration process for the transport is stopped when the relative residual norm of concentration is smaller than a tolerance predetermined by the user

$$\frac{\left\| TC^{n+1,m+1} - TC^{n+1,m} \right\|}{\left\| TC^{n+1,m+1} \right\|} = \frac{\sqrt{\sum_{i=1}^{nf} \left(TC_{G,E_i}^{n+1,m+1} - TC_{G,E_i}^{n+1,m} \right)^2}}{\sqrt{\sum_{i=1}^{nf} \left(TC_{G,E_i}^{n+1,m+1} \right)^2}} \leq \tau_T \qquad (4.39)$$

Where: nf is the number of edges in the flow domain Ω,

Th is a vector that contains trace pressures at the different edges over Ω,

TC is a vector that contains trace concentrations at the different edges over Ω,

n represents a temporal index,

m is an iteration index,

τ_T is the tolerance criterion for the transport.

3.4.17. Maximal convergence errors for concentration

Maximal convergence errors for concentration ΔC_{max} are calculated at the end of each time step as follows:

$$\Delta C_{max} = \max\left(\left| C_G^{n+1,m+1} - C_G^{n+1,m} \right| \right) \qquad (4.40)$$

3.4.18. Transport modelling outline

Transport Equation	Classical advection-dispersion equation with the presence of sink/ source term, which takes into account the pesticide degradation
Numerical method	A new formulation to solve the transport equation is introduced. A global approach that includes both, advection and dispersion terms (approximated with the mixed hybrid finite element method) is used.
Continuity	Advective-dispersive Flux and Concentration
Boundary conditions	Dirichlet and Neumann conditions.
Temporal discretization	Fully implicit (backward Euler) method
Linearization	Picard iterative process
Oscillation control	Difficulties originated when advection is the dominant process are controlled by a flux limiting tool, which is specific to this mixed approach.
Iteration convergence criteria	Relative residual norm of edge concentration
Simulation Results	Profiles in time and space: -Concentration [M L^{-3}]. Average approximations by edge and elements. -Advective-dispersive Flux approximation over the elements [M $L^{-2}T^{-1}$]. Components of the vector. -Transport flux over the edges [M $L^{-1}T^{-1}$]. Residence time distribution -E(t) Function [T^{-1}] -Cumulative residence time distribution function F(t) -Mean residence time Maximal convergence errors: -Concentration error computed as the difference of iterative solutions at the end of each time step. Maximum and minimum adimensional numbers calculated (Co, Pe, and Fn)

Section 3.5. Pesticide Degradation

Several models have been proposed to represent the kinetics of biodegradation in soil (Figure 4). An understanding of when to use these models and why they may fail is well explained in Alexander and Scow [1989].

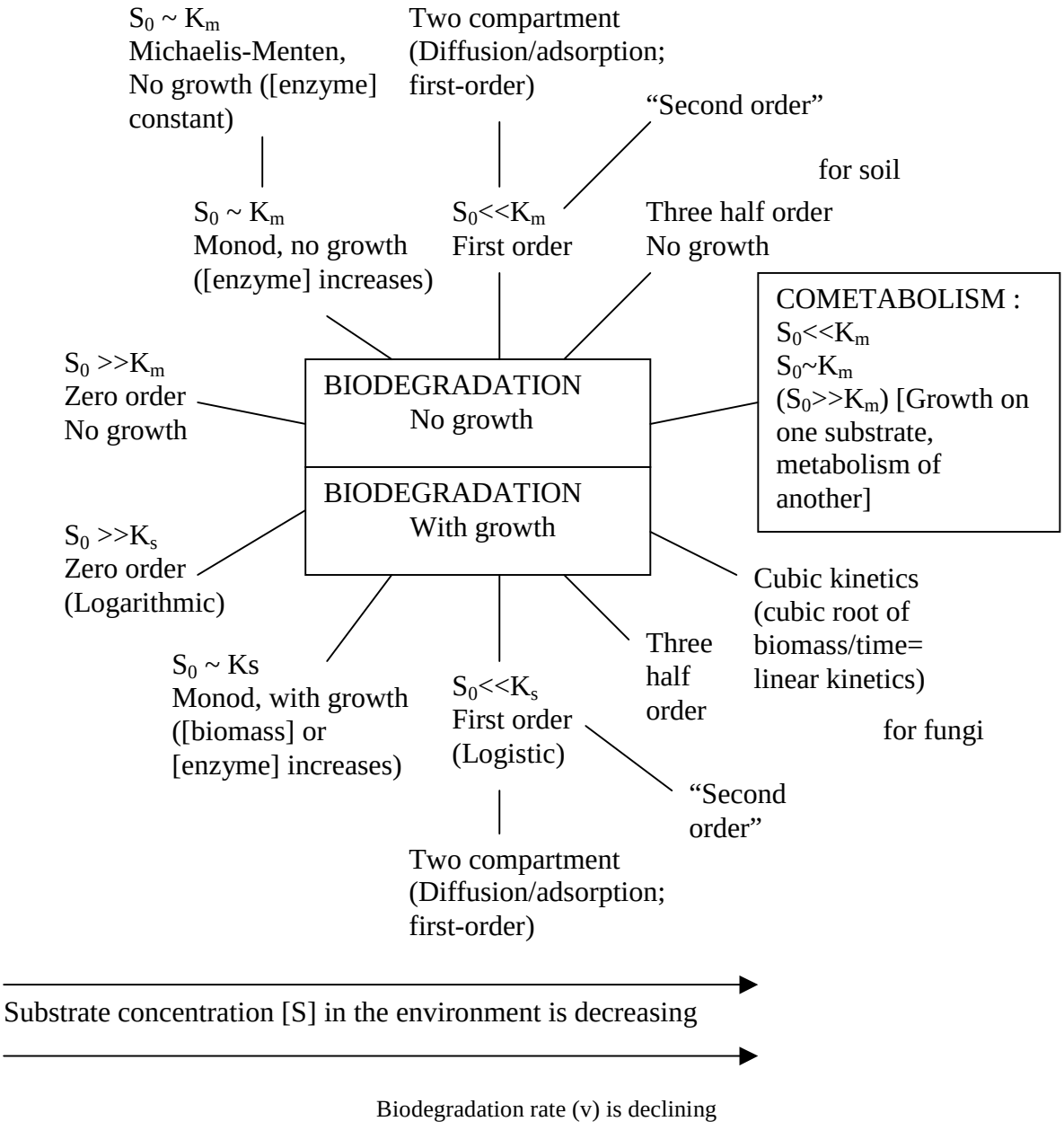

S_0, initial concentration of substrate; K_m, Michaelis constant (substrate concentration at which the rate of enzymatic reaction is half the maximum rate); K_s, Monod constant (substrate concentration at which the rate of growth is half the maximum rate).

Fig. 4. Kinetics analysis of microbial biodegradation/ a variety of models for growing and nongrowing microorganisms [Četkauskaité et al., 1998];

Mathematical formulations have been developed for the kinetics of biodegradation of one organic chemical when the transformations reflect both the metabolisms of that substrate and the simultaneous growth of bacteria on a second organic compound. These formulations are based on coupling of Monod growth kinetics and Michaelis-Menten kinetics. These nine models reflect linear, logistic and exponential growth on one substrate and concentration of the second substrate [Alexander and Scow, 1989]. Shapes of substrate disappearance curves have been proposed only in function of time. Since the 2D mixed hybrid finite element approximation permits observing the spatial variability of pesticides/substrate concentrations and takes into account the different heterogeneities, it is possible to purpose carbon and pesticides disappearance curves according to the soil profile.

Some limitations for modelling chemical kinetics are related to the influence in many transport and transformation process by the presence of other chemicals in a mixture. Modelling chemical interactions in a mixture requires the development of scientific understanding.

Section 3.6. Time Control

The temporal space $]0, Ts[$ is discretized in temporal increments (Δt), which are automatically adjusted at each time level (Figure 5) according to the following rules:

1. There is a minimum and a maximum time step ($\Delta tmin$ and $\Delta tmax$) that are specified by the user. So then, $\Delta tmin \leq \Delta t \leq \Delta tmax$.
2. A maximum temporal increment allowed for the transport equation is estimated by setting as a maximum value 0.5 for the dimensionless Fourier number (Fn), represented by a ratio of the Courant-Friedrichs-Lewy (Co) and Peclet (Pe) numbers.

$$Fn = \frac{Co}{Pe} \leq \frac{1}{2} \tag{6.1}$$

$$Pe = \frac{\sqrt{\left(\frac{Vx}{\Delta x}\right)^2 + \left(\frac{Vz}{\Delta z}\right)^2}}{\frac{Dxx}{\Delta x^2} + \frac{Dzz}{\Delta z^2} - \frac{Dxz}{\Delta x \Delta z}} \tag{6.2}$$

$$Co = \Delta t \sqrt{\left(\frac{Vx}{\Delta x}\right)^2 + \left(\frac{Vz}{\Delta z}\right)^2} \tag{6.3}$$

Where:

Vx, Vz are the pore water velocity in x and z directions, respectively (LT^{-1}),

Δx , Δz are the grid spacing in the x and z direction, respectively (L),

Dxx,

Dzz, are the dispersion coefficients ($L^2\ T^{-1}$).

Dxz

Hereby, for each element G, a maximum temporal increment is given by

$$\Delta t_{\max G\,trans} \le \frac{0.5}{\frac{D_{G,xx}}{(\Delta x)^2}+\frac{D_{G,zz}}{(\Delta z)^2}+\frac{D_{G,xz}}{\Delta x \Delta z}} \tag{6.4}$$

The maximum allowed Δt for the transport ($\Delta t\max_{transport}$) will be the minimum value $\Delta t\max_{G\,trans}$ in the entire spatial domain.

Analogously, a maximum temporal increment allowed for the hydrodynamics ($\Delta t\max_{hydrodynamics}$) is determined using a similar rule by replacing on one hand the dispersion coefficient by a parameter D(h) known as the soil moisture diffusivity, and on the other hand the pore water velocity by the soil moisture velocity v(h). They are given by the functions $D(u)=\frac{K[h(u)]}{C[h(u)]}$, and $v(u)=\frac{1}{C[h(u)]}\frac{dK[h(u)]}{dh}$, where $C(h)=\frac{d\theta}{dh}$ is the soil moisture capacity and u is a variable defined by the Kirchhoff transformation [El-Kadi and Ling, 1993].

If the soil profile is not saturated or it has not reach a specified index of saturation ($\max\left(\frac{\theta_G}{\varphi_G}\right) < tol_{indsat}$), the following approximations for the adimensional numbers will be used:

$$Pe_{hyd} = \frac{\sqrt{\frac{1}{|G|}\left(\frac{1}{C_G}\left.\frac{dK}{dh}\right|_G\right)^2}}{\frac{1}{|G|}\frac{K_G}{C_G}} \tag{6.5}$$

$$Co_{hyd} = \Delta t \sqrt{\frac{1}{|G|}\left(\frac{1}{C_G}\frac{dK}{dh}\bigg|_G\right)^2} \tag{6.6}$$

If the soil profile is saturated or it has reach the specified index of saturation, then Co will be computed using the components of the velocity vector $\vec{v} = \frac{\vec{q}}{n_e}$. The Darcy flux $\vec{q}$ is calculated from the mixed hybrid approximations, and water content might be a good approximation of effective porosity n_e.

$$Co = \Delta t \sqrt{\left(\frac{\vec{q}_{G,x}}{\theta_G \Delta x}\right)^2 + \left(\frac{\vec{q}_{G,z}}{\theta_G \Delta z}\right)^2} \tag{6.7}$$

The maximal temporal increment for the hydrodynamics will be then computed as:

$$\Delta t_{\max G,hyd} = \begin{cases} 0.5|G|\frac{C_G}{K_G} & \text{if} \quad \max\left(\frac{\theta_G}{\varphi_G}\right) < tol_{indsat} \\ \left(\left(\frac{\vec{q}_{G,x}}{\theta_G \Delta x}\right)^2 + \left(\frac{\vec{q}_{G,z}}{\theta_G \Delta z}\right)^2\right)^{-0.5} & \text{if} \quad \max\left(\frac{\theta_G}{\varphi_G}\right) \geq tol_{indsat} \end{cases} \tag{6.8}$$

The maximum allowed Δt for the hydrodynamics ($\Delta t \max_{hydrodynamics}$) will be the minimum value $\Delta t \max_{G\,hyd}$ in the entire spatial domain.

The temporal increment must then not exceed the minimum value between $\Delta t \max_{hydrodynamics}$ and $\Delta t \max_{transport}$.

3. The initial time step Δt will be equal to the minimum value between $\Delta t \max_{hydrodynamics}$ and $\Delta t \max_{transport}$. If this value is larger than the time of simulation T_s, then a smaller default initial value should be used (Δt_{init}). For the next time levels, a heuristic method [Belfort, 2006; Šimůnek et al., 2005] will be used but always respecting the rules 1 and 2.

The rate equations describing the degradation kinetics are integrated over a time step by a fourth order Runge_Kutta method. The key of this method is the use of intermediate time-steps to improve accuracy.

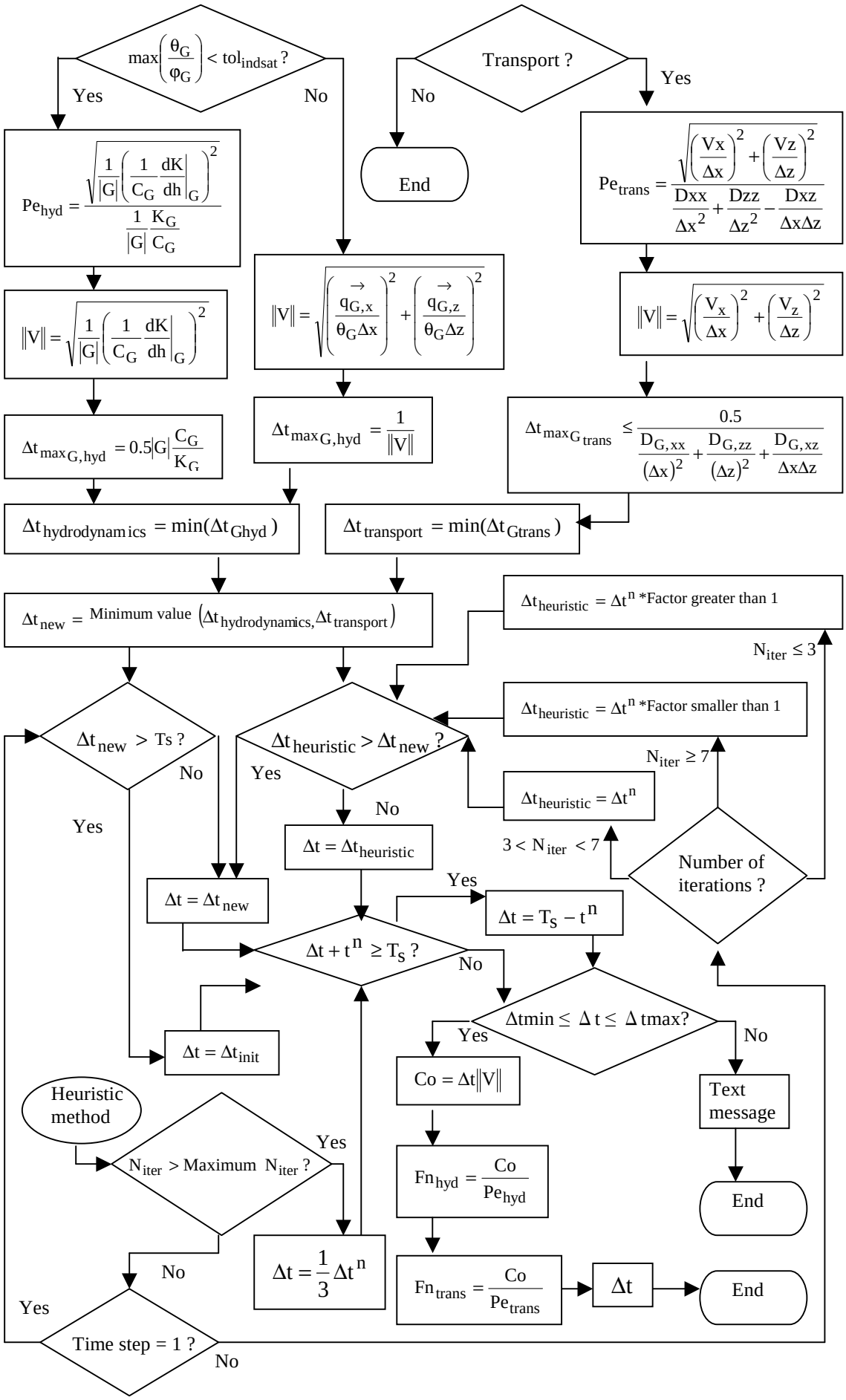

Fig. 5. Adjusted time stepping procedure

Section 3.7. Modelling code, pre- and post processing of results

The modelling code was written using the computer programming language FORTRAN. It makes use of text files for the input of data concerning to the mesh, temporal discretization, and boundary conditions. These files are given by a pre-processor developed specially for the mixed hybrid approximation. Results are printed using text files with a given format for facilitating a visual display using other softwares, such as MATLAB.

Section 3.8. References third chapter

Ackerer, Ph., Younes, A., Mose, R., 1999. Modeling variable density flow and solute transport in porous medium: 1. Numerical model and verification. Transport in Porous Media, 35(3): 345-373.

Alexander, M., Scow, M., 1989. Kinetics of biodegradation in soil. pp. 243-269. In Sawhney BL, Brown K, (ed.). Reactions and movement of organic chemicals in soils, Soil Science Society of America and American Society of Agronomy, SSSA Spec. Publ. 22. SSSA Madison, WI, USA.

Arnold, D.N., Brezzi, F., 1985. Mixed and non conforming finite element methods: Implementation, postprocessing and error estimates. Mathematical modelling and numerical analysis, 19, pp. 7-32.

Bear, J., 1979. Hydraulics of groundwater. Mc Graw-Hill, New York.

Belfort, B., 2006. Modélisation des écoulements en milieux poreux non saturés par la méthode des elements finis mixtes hybrids, Ph. D. thesis, University Louis Pasteur. Strasbourg , France, 2006. 239 pp.

Belfort, B., Lehmann, F., 2005. Comparison of equivalent conductivities for numerical simulation of one-dimensional unsaturated flow. Vadose Zone Journal, 4(4) : 1191-1200.

Bergamaschi, L., Putti, M., 1999. Mixed finite elements and Newton-type linearizations for the solution of Richards' equation. International Journal for Numerical Methods in Engineering, 45(8): 1025-1046.

Binning, P., Celia, M.A., 2002. A forward particle tracking Eulerian-Lagrangian localized adjoint method for solution of the contaminant transport equation in three dimensions. Advances in water resources, 25(2): 147-157.

Brunone, B., Ferrante, M., Romano, N., Santini, A., 2003. Numerical simulations of one-dimensional infiltration into layered soils with the Richards equation using different estimates of the interlayer conductivity. Vadose Zone Journal, 2(2): 193-200.

Carrayrou, J., Mosé, R., Behra, P., 2004. Operator-splitting procedures for reactive transport and comparison of mass balance errors. Journal of Contaminant Hydrology, 68(3-4): 239-268.

Celia, M.A., Bouloutas, E.T., Zarba, R.L., 1990. A general mass-conservative numerical solution for the unsaturated flow equation. Water Resources Research, 26(7): 1483-1496.

Četkauskaité, A., Grigonis, U., Beržinskiené, J., 1998. Biodegradation : Selection of suitable model. Ecotoxicology and Environmental Safety, 40(1): 19-28.

Chavent, G., Jaffre, J., 1986. Mathematical models and finite elements for reservoir simulation, North Holland, Amsterdam, 376 pp.

Chavent, G., Roberts, J.E., 1989. A unified physical presentation of mixed, mixed-hybrid finite elements and usual finite differences for the determination of velocities in waterflow problems. Rapports de Recherche 1107. Programme 7. Calcul Scintifique, Logiciels Numériques et Ingénierie Assistée. Institut National de Recherche en Informatique et en Automatique. 52 pp.

Chavent, G., Roberts, J.E., 1991. A unified physical presentation of mixed, mixed-hybrid finite elements and standard finite difference approximations for the determination of velocities in waterflow problems. Advances in Water Resources 1991, 14(6): 329-348.

Clement, T.P., Wise, W.R., Molz, F.J., 1994. A physically based, two-dimensional, finite-difference algorithm for modeling variably saturated flow. Journal of Hydrology, 161(1-4): 71-90.

Diersch, H.J.G., Perrochet, P., 1999. On the primary variable switching technique for simulating unsaturated-saturated flows. Advances in Water Resources, 23(3): 271-301.

Eisenstat, S.C., 1981. Efficient implementation of a class of preconditioned conjugate gradient methods. SIAMS Journal of Scientific and Statistical Computing 2, 1-4.

El-Kadi, A.I., Ling, G., 1993. The Courant and Peclet number criteria for the numerical solution of the Richards equation. Water Resources Research, 29(10): 3485-3494.

Farthing, M.W., Kees, C.E., Miller, C.T., 2003. Mixed finite element methods and higher order temporal approximations for variably saturated groundwater flow. Advances in Water Resources, 26(4): 373-394.

Fetter, C.W., 1993. Contaminant hydrogeology. MacMillan Publishing Company, New York, 458pp.

Freijer, J.I, Veling, E.J.M., Hassanizadeh, S.M., 1998. Analytical solutions of the convection-dispersion equation applied to transport of pesticides in soil columns. Environmental Modelling and Software, 13(2): 139-149.

Hao, X., Zhang, R., Kravchenko, A., 2005. A mass-conservative switching method for simulating saturated-unsaturated flow. Journal of Hydrology, 311(1-4): 254-265.

Herrera, P. and Valocchi, A., 2006. Positive solution of two-dimensional solute transport in heterogeneous aquifers. Ground water, 44(6): 803-813.

Hillel, D., 1980. Fundamentals of soil physics. Academic Press, New York, 1980. 413 pp.

Hogarth, W.L., Parlange, J.Y., 2000. Application and improvement of a recent approximate analytical solution of Richards' equation. Water research, 36(7): 1965-1968.

Holland, J.F., Martin, J.F, Granata, T., Bouchard, V., Quigley, M., Brown, L. 2004. Effects of wetland depth and flow rate on residence time distribution characteristics. Ecological Engineering 23(3): 189-203.

Hoteit, H., Ackerer, Ph., Mosé, R., Erhel, J., Philippe, B., 2004. New two-dimensional slope limiters for discontinuous Garlerkin methods on arbitrary meshes. International Journal for Numerical Methods in Engineering, 61(14): 2566-2593.

Hoteit, H., Erhel, J., Mosé, R., Philippe, B., Ackerer, Ph., 2002. Numerical reliability for mixed methods applied to flow problems in porous media. Computational Geosciences, 6(2): 161-194.

Huang, K., Mohanty, B.P., van Genuchten, M.Th., 1996. A new convergence criterion for the modified Picard iteration method to solve the variably saturated flow equation. Journal of Hydrology, 178(1-4): 69-91.

Ippisch, O., Vogel, H.J., Bastian, P., 2006 . Validity limits for the van Genuchten-Mualem model and implications for parameter estimation and numerical simulation. Advances in Water Resources, 29(12): 1780-1789.

Ju, S.-H., Kung, K.-J.S., 1997. Mass types, elements orders and solution schemes for the Richards equation. Computers and Geosciences, 23(2): 175-187.

Kavetski, D., Binning, P., Sloan, S.W., 2001. Adaptative time stepping and error control in a mass conservative numerical solution of the mixed form of Richards equation. Advances in Water Resources, 24(6): 595-605.

Kirkland, M.R., Hills, R.G., Wierenga, P.J., 1992. Algorithms for solving Richards' equation for variably saturated soils. Water Resources Research, 28(8): 2049-2058.

Kosugi, K., 2008. Comparison of three methods for discretizing the storage term of the Richards equation. Vadose Zone Journal, 7(3) : 957-965.

Kroes, J.G., Van Dam, J.C., 2003. Reference manual SWAP: Version 3.0.3. Alterra-Report 773. Alterra Green World Res., Wageningen, the Netherlands. 211 pp.

Kumar, A., Jaiswal, D.K., Kumar, N., 2009 Analytical solutions of one-dimensional advection-diffusion equation with variable coefficients in a finite domain. Journal of Earth System Science, 118(5): 539-549.

Kumar, A., Jaiswal, D.K., Kumar, N., 2010 Analytical solutions to one-dimensional advection-diffusion equation with variable coefficients in semi-finite media. Journal of Hydrology, 380(3-4): 330-337.

Leij, F.J., Dane, J.H., 1990. Analytical solutions of the one-dimensional advection equation and two- or threedimensional dispersion equation. Water Resources Research, 26(7): 1475–1482.

Leij, F.J., Skaggs, T.H., van Genuchten, M.Th., 1991. Analytical solutions for solute transport in three-dimensional semi-infinite porous media. Water resources research, 27(10): 2719-2733.

Liu, C., Ball, W.P., Ellis, J.H., 1998. An analytical solution to the one-dimensional solute advection-dispersion equation in multi-layer porous media. Transport in porous media, 30(1): 25-43.

Manzini, G., Ferraris, S., 2004. Mass-conservative finite volume methods on 2-D unstructured grids for the Richards' equation. Advances in Water Resources, 27(12): 1199-1215.

Mazzia, A., Bergamaschi, L., Dawson, C.N., Putti, M., 2002. Godunov mixed methods on triangular grids for advection-dispersion equations. Computational Geosciences, 6(2): 123-139.

Mosé, R., Siegel, P., Ackerer, P., Chavent, G., 1994. Application of the mixed hybrid finite element approximation in a groundwater flow model: Luxury or necessity?. Water Resources Research, 30(11): 3001-3012.

Nayagum, D., 2001. Simulation numérique de la pollution du sous-sol par les produits pétroliers et dérives : Application au cas d'un écoulement diphasique monodimensionnel, PhD Thesis, University Louis Pasteur. Strasbourg, France, 151p.

Ojeda, E., Caldentey, J., Saaltink, M.W., Garcia, J. 2008. Evaluation of relative importance of different microbial reactions on organic matter removal in horizontal subsurface-flow constructed wetlands using a 2D simulation model. Ecological Engineering, 34(1): 65-75.

Oltean, C., Buès, M.A., 2001. Coupled groundwater flow and transport in porous media. A conservative or nonconservative form?. Transport in Porous Media, 44(2): 219-246.

Pan L., Wierenga, P.J., 1995. A transformed pressure head-based approach to solve Richard's equation for variably saturated soils. Water Resources Research, 31(4): 925-931.

Parlange, J.-Y., Hogarth, W.L., Barry, D.A., Parlange, M.B., Haverkamp, R., Ross, P.J., Steenhuis, T.S., DiCarlo, D.A., Katul, G., 1999. Analytical approximation to the solutions of Richards' equation with applitation to infiltration, ponding, and time compression approximation. Advances in Water Resources, 23(2): 189-194.

Prasad, K.S.H., Kumar, M.S.M., Sekhar, M., 2001. Modelling flow through unsaturated zones: Sensitivity to unsaturated soil properties. Sadhana. Academy Proceedings in Engineering Sciences, 26(6): 517-528.

Qi, X.-B., Zhang, X.-X., Pang, H.-B., 2008. An efficient multiple-dimensional finite element solution for water flow in variably saturated soils. Agricultural Sciences in China, 7(2): 200-209.

Raviart, P.A., Thomas, J.M., 1977. A mixed finite method for the second order elliptic problems. pp. 292-315. In Galligani I., Magenes, E., (ed.). Mathematical aspects of the finite element methods, Lecture Notes in Math 606, Springer: New York.

Rees, I., Masters, I., Malan, A.G., Lewis, R.W., 2004. An edge-based finite volume scheme for saturated-unsaturated groundwater flow. Computer Methods in Applied Mechanics and Engineering, 193(42-44): 4741-4759.

Richards, L.A., 1931. Capillary conduction of liquids through porous mediums. Physics, 1(5): 318-333.

Romano, N., Brunone, B., Santini, A., 1998. Numerical analysis of one-dimensional unsaturated flow in layered soils. Advances in Water Resources, 21(4): 315-324.

Ronkanen, A.-K., Kløve, B., 2008. Hydraulics and flow modelling of water treatment wetlands constructed on peatlands in Northern Finland. Water Research, 42(14): 3826-3836.

Salamon, P., Fernàndez-Garcia, D., Gómez-Hernández, J.J., 2006. A review and numerical assessment of the random walk particle tracking method. Journal of Contaminant Hydrology, 87(3-4): 277-305.

Shahraiyni, H.T., Ashtiani, B.A., 2009. Comparison of finite difference schemes for water flow in unsaturated soils. International Journal of Mechanical, Industrial and Aerospace Engineering, 3(1): 10-14.

Siegel, P., Mosé, R., Ackerer, Ph., Jaffre, J., 1997. Solution of the advection-diffusion equation using a combination of discontinuous and mixed finite elements. International Journal for Numerical Methods in Fluids, 24(6): 595-613.

Šimůnek, J., van Genuchten, M.Th., Šejna, M., 2005. The HYDRUS-1D Software package for simulating the movement of water, heat, and multiple solutes in variably saturated media, Version 3.0, HYDRUS Software Series 1, Department of Environmental Sciences, University of California Riverside, Riverside, California, USA. 240 pp.

Stephens, D.B., Hsu, K.-C., Prieksat, M.A., Ankeny, M.D., Blandford, N., Roth, T.L., Kelsey, J.A., Whitworth, J.R., 1998. A comparison of estimated and calculated effective porosity. Hydrologeology Journal, 6(1): 156-165.

Sun, N.-Z., 1999. A finite cell method for simulating the mass transport process in porous media. Water Resources Research, 35(12): 3649-3662.

Tartakovsky, D.M., 2000. An analytical solution for two-dimensional contaminant transport during groundwater extraction. Journal of Contaminant Hydrology, 42(2-4):273-283.

Tocci, M.D., Kelley, C.T., Miller, C.T., 1997. Accurate and economical solution of the pressure-head form of Richards' equation by the method of lines. Advances in Water Resources, 20(1): 1-14.

Tracy, F.T., 1995. 1-D, 2-D and 3-D analytical solutions of unsaturated flow in groundwater. Journal of Hydrology, 170(1-4): 199-214.

Tracy, F.T., 2006. Clean two-and three-dimensional analytical solutions of Richard's equation for testing numerical solvers. Water Resources Research, 42, 11 pp. W08503, doi: 10.1029/2005WR004638

Tracy, F.T., 2007. Three-dimensional analytical solution of Richards' equation for a box-shaped soil sample with piecewise-constant head boundary conditions on the top. Journal of Hydrology, 336(3-4): 391-400.

Van Dam, J.C., Feddes, R.A., 2000. Numerical simulation of infiltration, evaporation and shallow groundwater levels with the Richards equation. Journal of Hydrology, 223(1-4): 72-85.

Van Genuchtan, M. Th., 1980. A closed-form for predicting the hydraulic conductivity of unsaturated soils. Soil Science Society of America Journal, 44(5): 892-898.

Van Genuchten, M. Th., Alves, W.J., 1982. Analytical solutions of the one-dimensional convective-dispersive solute transport equation. Technical Bulletin 1661. Agricultural Research Service, U.S. Department of Agriculture. 151 pp.

Vanderborght, J., Kasteel, R., Herbst, M., Javaux, M., Thiéry, D., Vanclooster, M., Mouvet, C., Vereecken, H., 2005. A set of analytical benchmarks to test numerical models of flow and transport in soils. Vadose Zone Journal, 4(1): 206-221.

Younes, A., Mose, R., Ackerer, P., Chavent, G., 1999. A new formulation of the mixed finite element method for solving elliptic and parabolic PDE with triangular elements. Journal of Computational Physics, 149(1): 148-167.

Younes, 2005. A moving grid Eulerian Lagrangian localizated adjoint method for solving one-dimensional nonlinear advection-diffusion-reaction. Transport in Porous Media, 60(2): 241-250.

Younes, A., Ackerer, P., Lehmann, F., 2006. A new mass lumping scheme for the mixed hybrid finite element method. International Journal for Numerical Methods in Engineering, 67(1): 89-107.

Werner, T.M., Kadlec, R.H., 2000. Wetland residence time distribution modeling. Ecological Engineering 15(1-2): 77-90.

Wexler, E.J., 1992. Analytical solutions for one- two- and three-dimensional solute transport in ground-water systems with uniform flow. Techniques of water-resources investigations, U.S. Geological Survey. Book 3, Chapter B7: 190 pp.

Williams, G.A., Miller, C.T., 1999. An evaluation of temporally adaptive transformation approaches for solving Richards' equation. Advances in Water Resources 22(8): 831-840.

Zheng, C., 1993. Extension of the method of characteristics for simulation of solute transport in three dimensions. Ground water, 31(3): 456-465.

4

Chapter 4 – Verification of the model

This chapter contains the results of several simulations, for one and two-dimensional test cases, performed in order to verificate the model. Comparison of the model results and those from the literature was carried out. Verification was also performed using analytical solutions or other well-known models, such as HYDRUS.

.

Section 4.1. Infiltration – Comparison with HYDRUS 1D

In order to test the ability of the model to handle a flux boundary condition, a one-dimensional example was designed. It consists of infiltration into a homogeneous unsaturated soil column of length L=100 cm. The specific soil parameters used in the modified Mualem-van Genuchten model are reported in Annexe III (material C). Boundary and initial conditions for the hydrodynamics and transport models are shown in Table 2. It was assigned a value of 3 cm to the longitudinal and transversal dispersivities.

Table 2. Initial and boundary conditions for the one-dimensional test case

Condition	Hydrodynamics	Transport
Initial	$h(0 \le z \le 100\text{cm}, t = 0) = -200\text{cm}$	$C(z \ne 0, t = 0) = 0.1\text{g/l}$
Boundary	$q(z = 0, t \ge 0) = 8.64\text{cm/d}$	$C(z = 0, t \ge 0) = 1.0\text{g/l}$

In Figure 6, the hydrodynamics results obtained when time increments are automatically adjusted are compared to those achieved when a constant time step is used. The simulation time was 0.25 d. As it can be seen, there is a good approximation between the curves obtained applying HYDRUS [Šimůnek et al., 2005] with an initial time step 1.1974×10^{-3} d and the MHFEM using adjusted time steps (3116 time steps: 1.1974×10^{-3} d $\ge \Delta t \ge 1.7029 \times 10^{-5}$d). There is also a good agreement of the curves obtained using a constant time step with a length similar to the time range interval used by the adjusted time algorithm (250 time steps: $\Delta t = 1 \times 10^{-3}$d). However, if the time step selection is done out of this range we can observe slight differences in the hydrodynamics approximation (10 time steps: $\Delta t = 2.5 \times 10^{-2}$ d) , see Figure 6a.

The hydrodynamics criterion for the time step selection is predominant for small Peclet number, consequently no effect had been observed in the solute transport approximations by using constant time steps (Figure 6b). As it was expected, the increase of the Peclet number induces a deviation in the curves using constant time step.

Even though the number of time steps and the CPU time of simulation can be large, we decided to use an adjusted time step rather than a constant time step, because an inadequate time step selection may lead to an inaccurate approximation for the hydrodynamics and solute transport calculations (Figure 6).

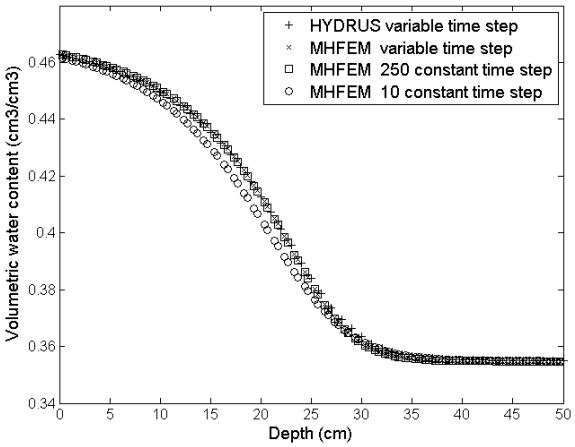

a) Hydrodynamics

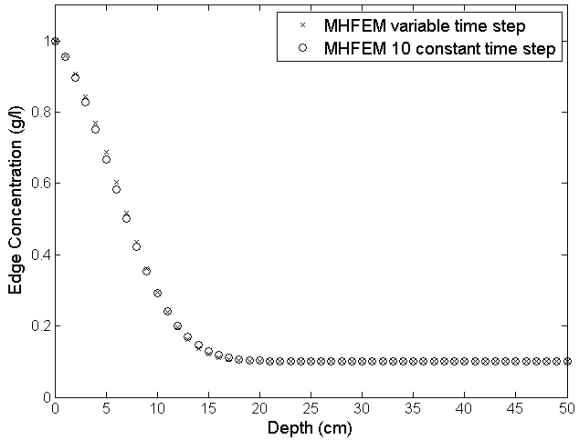

b) Transport Pe=1.22

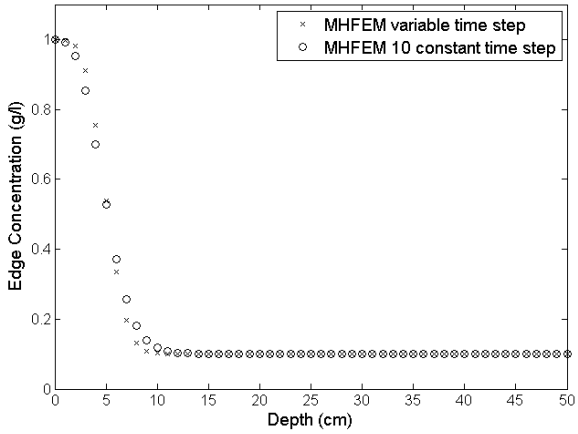

c) Transport Pe=1.22x10^3

Fig. 6. Effect of time step on the hydrodynamics and on the transport

Section 4.2. Transport verification: 1D test case - HYDRUS 1D

A difficulty solving the transport equation is attributed to the change in the nature of the equation from parabolic to almost hyperbolic as the advective transport becomes prominent in relation to the dispersive transport (large Peclet number).

The model was tested using different values of dispersivity ($\alpha_L = \alpha_T$). The requirement of the flux limiter, when advection is the dominant process (high Peclet number), is being confirmed through the Figure 7. For these test cases a value of η=0.5 was considered. The effect of increasing the Peclet number is evident over both, mesh and edge concentrations. In addition, the correction made while using the suggested flux limiter are obvious.

For low Peclet numbers (Figure 7a), the results obtained by the MHFEM in the calculation of mesh or edge concentration show a good agreement to those obtained by HYDRUS. In this case, concentration results are independent of the implementation of the flux limiting tool.

At high Peclet numbers (Figure 7b), oscillations in edge concentration calculations are observed using HYDRUS or MHFEM without flux limiter. Non-precise mesh concentrations are also reached. It is remarkable that there is a strong difference between the value of concentration calculated at the baricenter of the mesh and the edge concentration values surrounding this mesh. This behavior is noticeable at the Dirichlet boundary condition. Moreover for the case $Pe \to \infty$ (Figure 7c), the mesh concentration approximation remains relatively constant and equal to the initial concentration value.

Nevertheless, oscillations were inhibited with the help of the flux limiting tool in all cases. Therefore, the suggested flux limiting tool makes it possible to preserve precision and unconditional stability at low and very high Peclet numbers. A sensitivity analysis has been then performed to evaluate the influence of the parameter η.

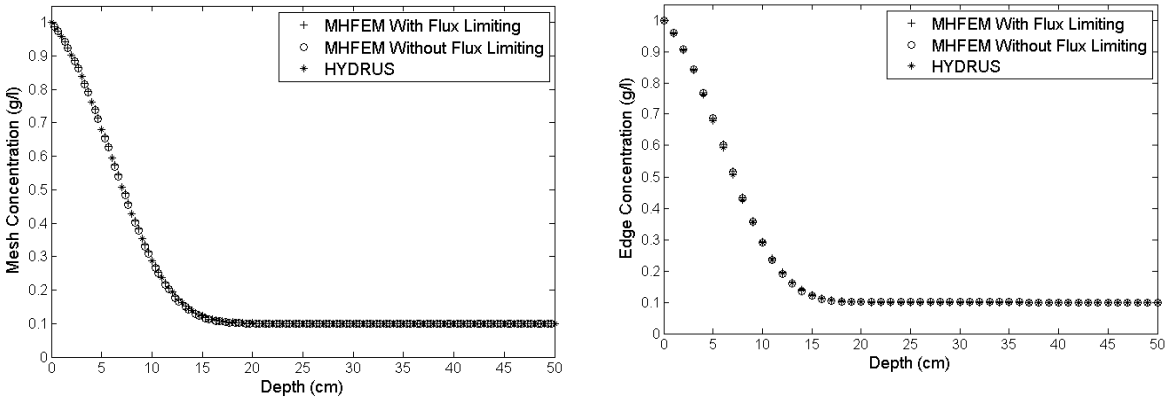

a) Dispersivity 3 cm , max Pe=1.22

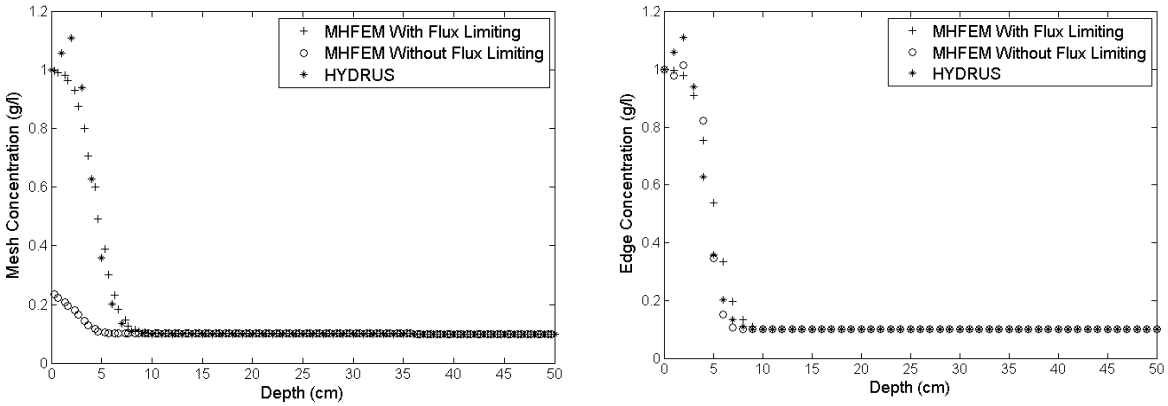

b) Dispersivity $3x10^{-3}$ cm, max Pe=$1.22x10^{3}$

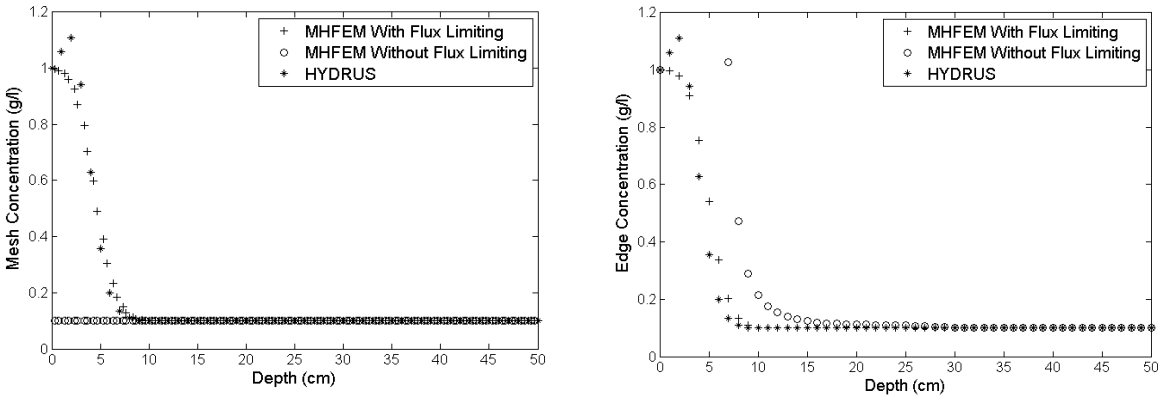

c) Dispersivity $3x10^{-6}$ cm, max Pe=$1.22x10^{6}$

Fig. 7. Flux limiter effect for different Peclet number

4.2.1. Flux Limiter Sensitivity Analysis

η is a ponderation parameter for the advective and dispersive parts of flux through an edge. Therefore, it ranges between 0 and 1. As stated before, at low Peclet numbers concentration results are independent of the flux limiter implementation (Figure 7a). Thus, the effect of the flux limiter application over the edge concentration calculation is also in relation to the Peclet number. Figure 8 shows a comparison among edge concentration results obtained for different values of the parameter η, when max Pe = 12.2, max Pe = 1.22×10^3, and max Pe = 1.22×10^6, respectively.

Edge concentration results remain relatively insensitive to the variation of the ponderation parameter for 0.5 and 1.0 values. Stable and relative identical solutions are then provided. When $\eta = 0$ the diffusion effect highly increase with the Peclet number. In fact, according to equation (4.28), the transport flux at each mesh and its forward edge are pondered by the same weight when $\eta = 0$, otherwise the forward edge have a higher weight than the mesh.

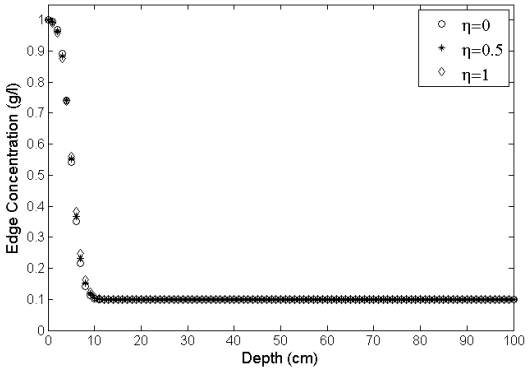

a) max Pe = 1.22

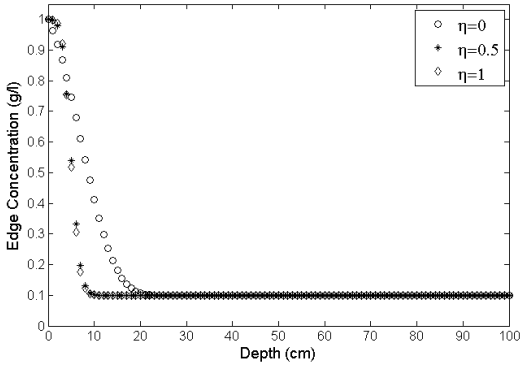

b) max Pe=1.22×10^3

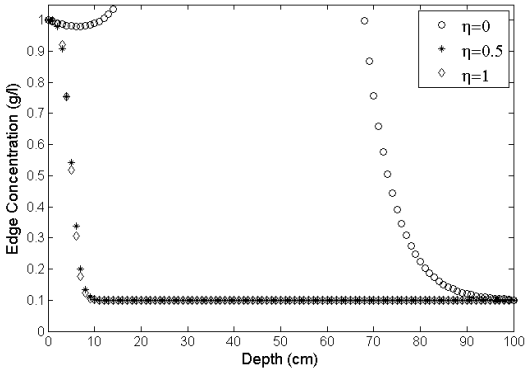

c) max Pe=1.22×10^6

Fig. 8. Ponderation Parameter Sensitivity

Section 4.3. Transport verification: 2D test case –Analytical solution

A two-dimensional test case for the transport in saturated media was carried out. The initial condition is zero initial concentration. The domain discretization and the boundary conditions are presented through the scheme in Figure 9.

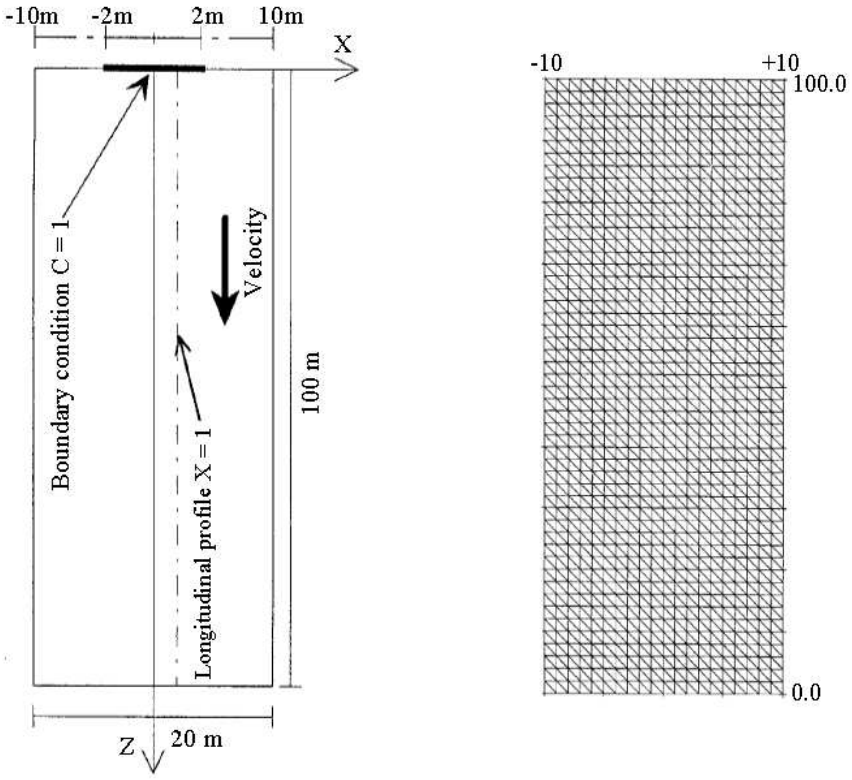

Fig. 9. Two dimensional convection-dispersion problem (left) and regular mesh (right)

With the aim of testing the performance of the model, this problem was solved for various values of the dimensionless Peclet number. The solution was displayed at the simulation time equal to 20 d. The parameters used in the different cases are reported in Table 3. The results are compared to the analytic solution given by Leij Feike and Dane [1990] in Siegel et al. [1997].

Table 3. Parameters used in various cases

Case	Vx ($m\ d^{-1}$)	Vz ($m\ d^{-1}$)	α_L ($m^2\ d^{-1}$)	α_T ($m^2\ d^{-1}$)	Δx (m)	Δz (m)	Pe
1	0.0	1.0	1.0	0.1	1.0	1.0	0.91
2	0.0	1.0	0.1	0.01	0.5	1.0	7.14
3	0.0	1.0	$1x10^{-5}$	$1x10^{-6}$	0.5	1.0	$7.14x10^{4}$

Concentration profiles are numerically approximated on the centre of the meshes for the MHFEM, while analytical solutions are calculated on the nodes. For this reason, iso-concentration lines are presented instead of scattered points, in order to provide a better way of comparison between results.

The first two-dimensional test case considers a small Peclet number (Pe < 2). The iso-concentration lines obtained by the application of the MHFEM without flux limiter are in good agreement with the analytical solution (Figure 10).

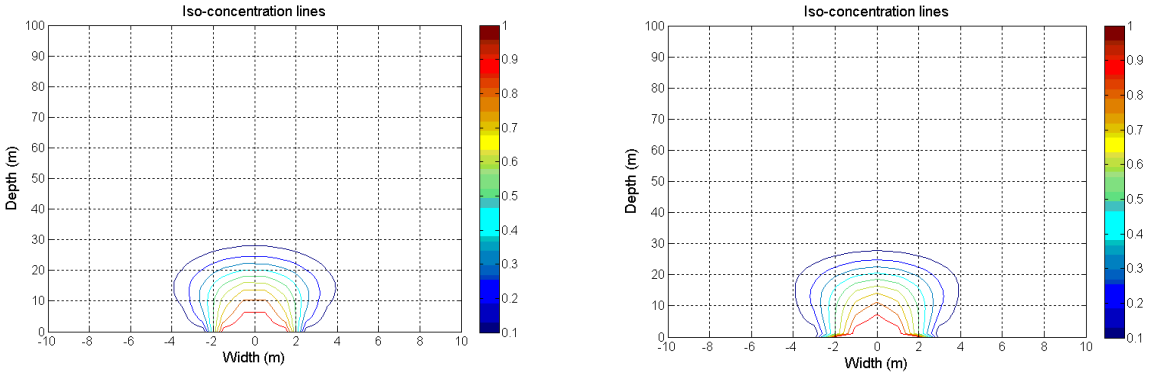

a) MHFE numerical solution b) analytical solution

Fig. 10. Iso-concentration lines: first test case

In the second test case Peclet number was increased (Pe = 7.1). While using the MHFEM without flux limiting, unstable and less accurate results were obtained (Figure 11a). The MHFEM approximation, in comparison to the analytical solution, is visibly improved when applying the flux limiter (Fig 11b).

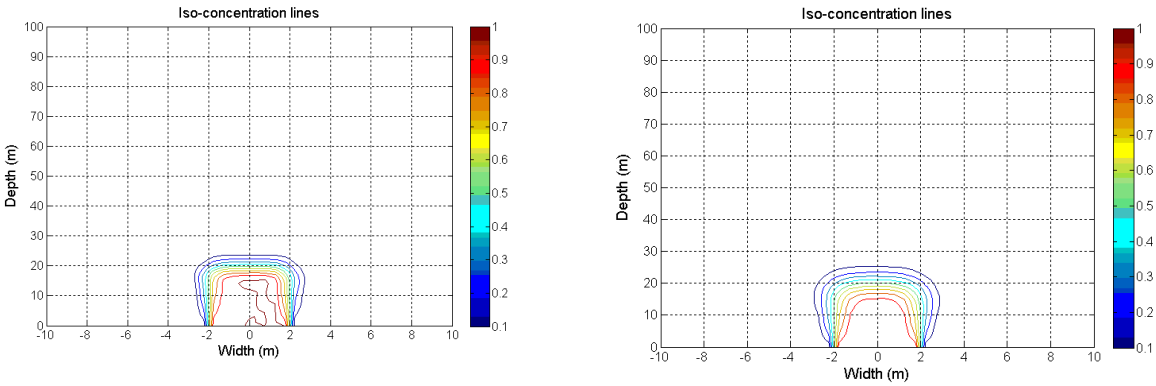

a) MHFE without flux limiting b) MHFE with flux limiting, $\eta = 1$

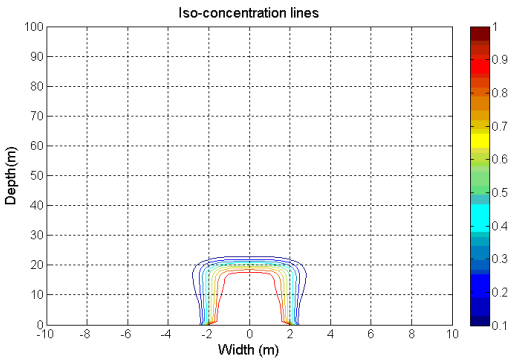

c) Analytical solution

Fig. 11. Iso-concentration lines: second test case

For a very high Peclet number (Pe=7.14x10^4), the results obtained with the application of the flux limiter were stable and matched up well to the analytical solution (Figure 12).

The two-dimensional transport verification has shown that the developed model is a good numerical tool for 2D transport approximation in saturated porous media. In addition, it was observed a satisfactory flux limiter performance.

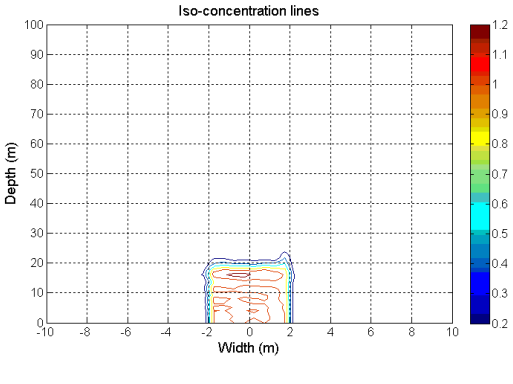

a) MHFE without flux limiting

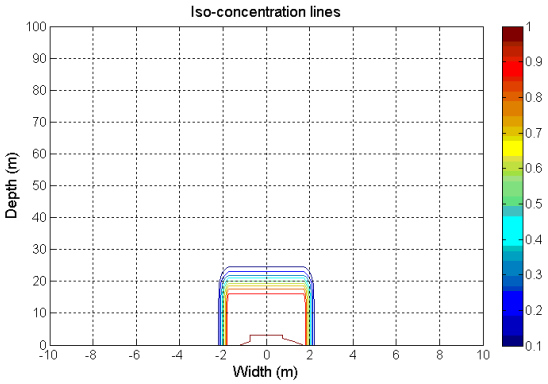

b) MHFE with flux limiting, η = 1

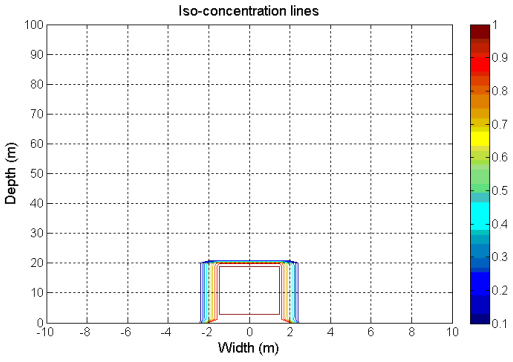

c) Analytical solution

Fig. 12. Iso-concentration lines: third test case

Section 4.4. Variable Transformation 1D [Pan and Wierenga, 1995]

Several one-dimensional cases were simulated using layered or uniform soil profiles (Figure 13). Soil properties listed in Appendix III.

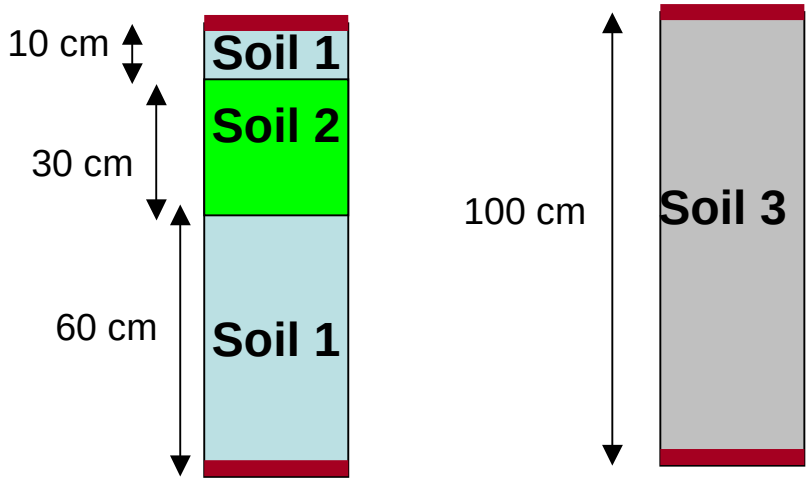

a) Layered soil profile b) Uniform Soil Profile

Fig. 13. Soil profiles for Pan and Wierenga [1995] test cases

Initial pressure and boundary conditions applied in each case are described in Table 4.

Table 4. Initial pressure and boundary conditions

Test case	Initial Pressure, cm	Upper boundary	Lower Boundary	Simulation Time, T_s, s	Profile Type
1-1	-50000	3.4722×10^{-4} cm s^{-1}	0 cm s^{-1}	21600	Layered
1-2	-1000	3.4722×10^{-4} cm s^{-1}	0 cm s^{-1}	1800	Layered
1-3	-200	3.4722×10^{-4} cm s^{-1}	0 cm s^{-1}	13680	Layered
2-1	-50000	8.3333×10^{-5} cm s^{-1}	0 cm s^{-1}	43200	Layered
2-2	-1000	8.3333×10^{-5} cm s^{-1}	0 cm s^{-1}	28800	Layered
2-3	-200	8.3333×10^{-5} cm s^{-1}	0 cm s^{-1}	14400	Layered
3-1	-50000	+ 100 cm	+ 100 cm	180	Uniform
3-2	-1000	+ 100 cm	+ 100 cm	180	Uniform
3-3	-200	+ 100 cm	+ 100 cm	180	Uniform
4-1	-50000	- 75 cm	- 75 cm	18000	Uniform
4-2	-1000	- 75 cm	- 75 cm	18000	Uniform
4-3	-200	- 75 cm	- 75 cm	18000	Uniform

Pressure head and water content distributions were simulated using the parameters shown in Table 5. Calculations were performed using the Richards equation on their h-based form, mixed-form or using a switching method between these two forms. A transformed pressure was introduced as the dependent variable and results were compared to those without using transformation of variable.

Table 5. Simulation parameters

tol_r	tol_a	tol_c	tol_{indsat}	Δt_{init}	Maximum number iterations in a time step	Factor greater than 1	Factor smaller than 1
$1x10^{-5}$	$1x10^{-1}$	$1x10^{-5}$	0.95	$1x10^{-3}$	10	0.9	1.1

4.4.1. Pressure head and water content distributions

Results show that the method is numerically robust for all cases of variably saturated, heterogeneous media, and first or second type boundary conditions. For all test cases the mixed hybrid formulation with mass condensation scheme was applied (using the different forms of the Richard equation, and transforming or not the variable of pressure). Pressure head and water content distributions were in good agreement with Pan and Wierenga [1995] results (Figure 14).

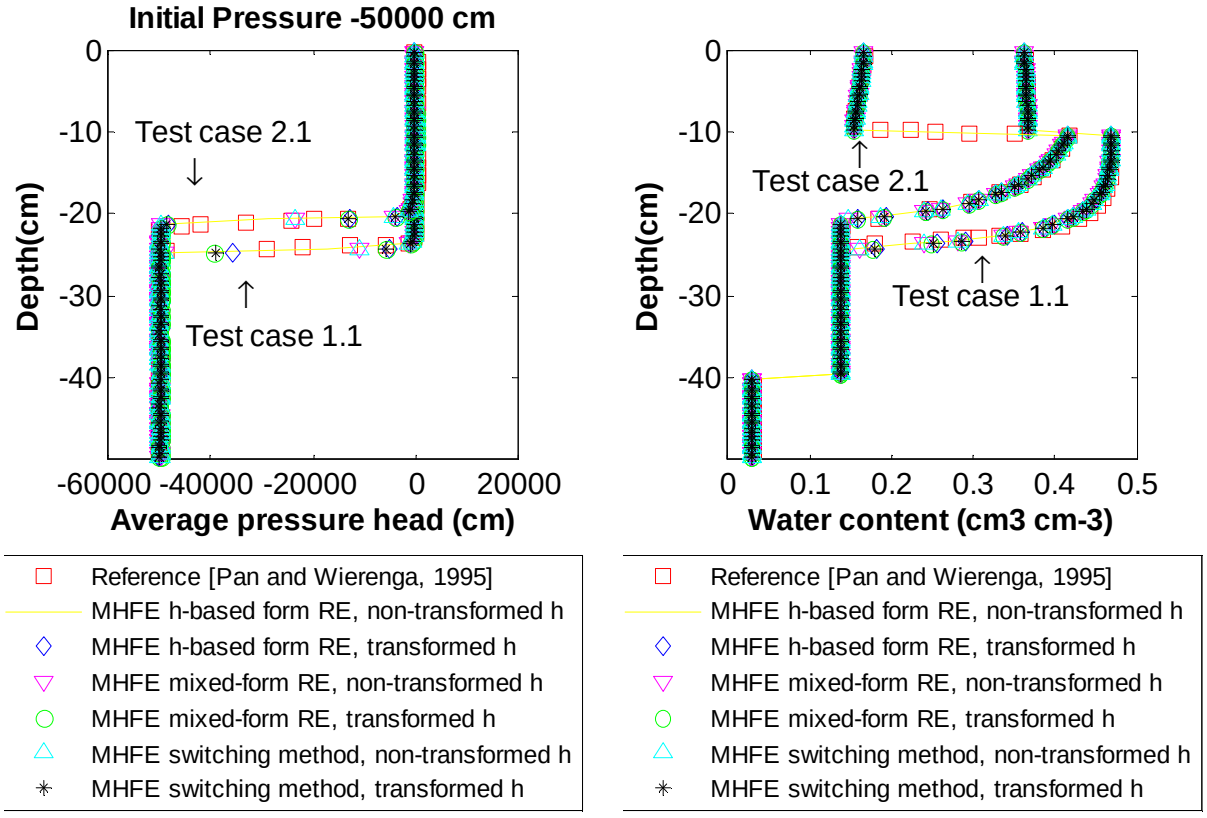

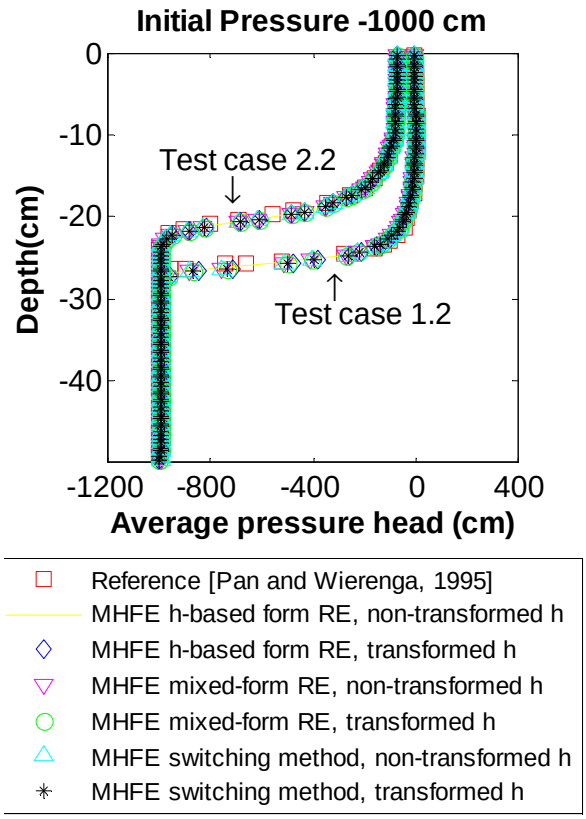
Initial Pressure -1000 cm
Depth(cm)
Average pressure head (cm)
Test case 2.2
Test case 1.2
0
-10
-20
-30
-40
-1200
-800
-400
0
400
Reference [Pan and Wierenga, 1995]
MHFE h-based form RE, non-transformed h
MHFE h-based form RE, transformed h
MHFE mixed-form RE, non-transformed h
MHFE mixed-form RE, transformed h
MHFE switching method, non-transformed h
MHFE switching method, transformed h

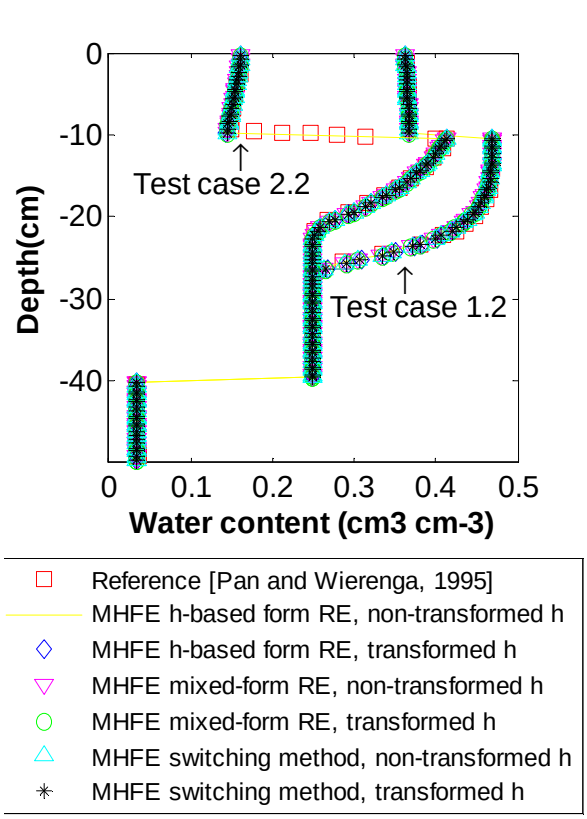
Depth(cm)
Water content (cm3 cm-3)
Test case 2.2
Test case 1.2
0
-10
-20
-30
-40
0
0.1
0.2
0.3
0.4
0.5
Reference [Pan and Wierenga, 1995]
MHFE h-based form RE, non-transformed h
MHFE h-based form RE, transformed h
MHFE mixed-form RE, non-transformed h
MHFE mixed-form RE, transformed h
MHFE switching method, non-transformed h
MHFE switching method, transformed h

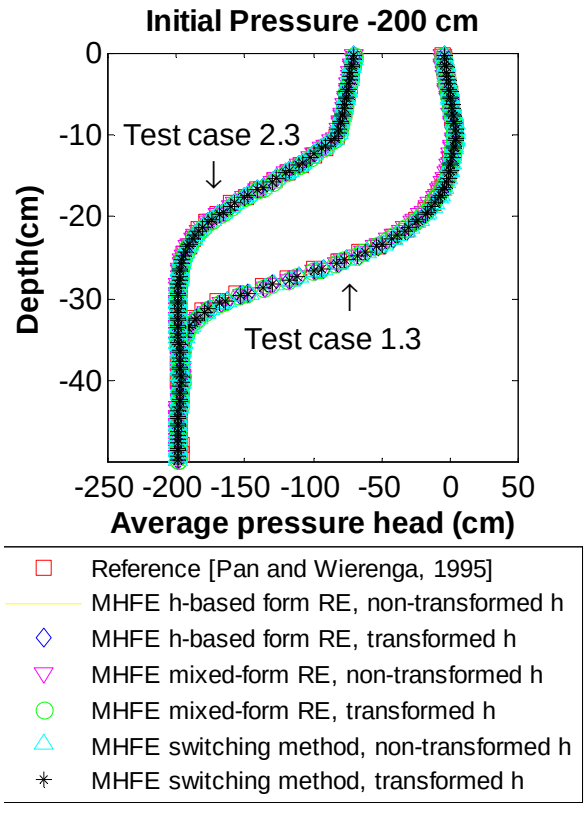
Initial Pressure -200 cm
Depth(cm)
Average pressure head (cm)
Test case 2.3
Test case 1.3
0
-10
-20
-30
-40
-250
-200
-150
-100
-50
0
50
Reference [Pan and Wierenga, 1995]
MHFE h-based form RE, non-transformed h
MHFE h-based form RE, transformed h
MHFE mixed-form RE, non-transformed h
MHFE mixed-form RE, transformed h
MHFE switching method, non-transformed h
MHFE switching method, transformed h

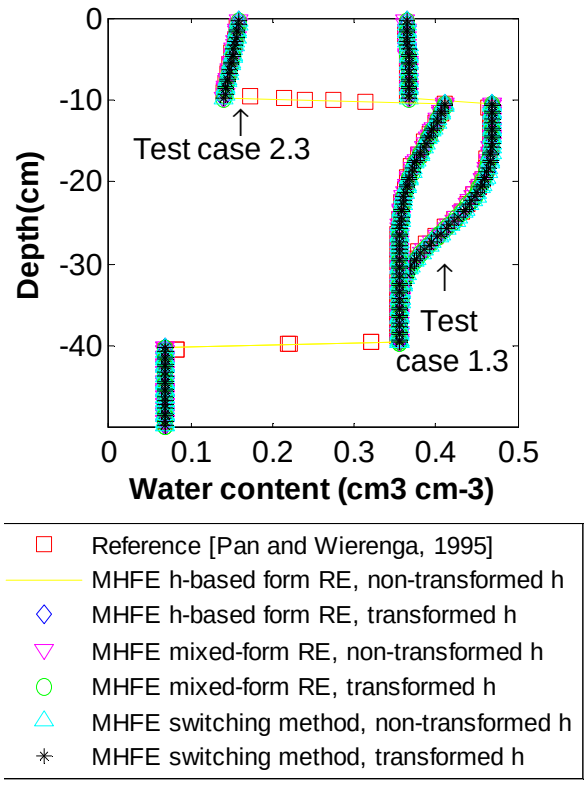
Depth(cm)
Water content (cm3 cm-3)
Test case 2.3
Test
case 1.3
0
-10
-20
-30
-40
0
0.1
0.2
0.3
0.4
0.5
Reference [Pan and Wierenga, 1995]
MHFE h-based form RE, non-transformed h
MHFE h-based form RE, transformed h
MHFE mixed-form RE, non-transformed h
MHFE mixed-form RE, transformed h
MHFE switching method, non-transformed h
MHFE switching method, transformed h

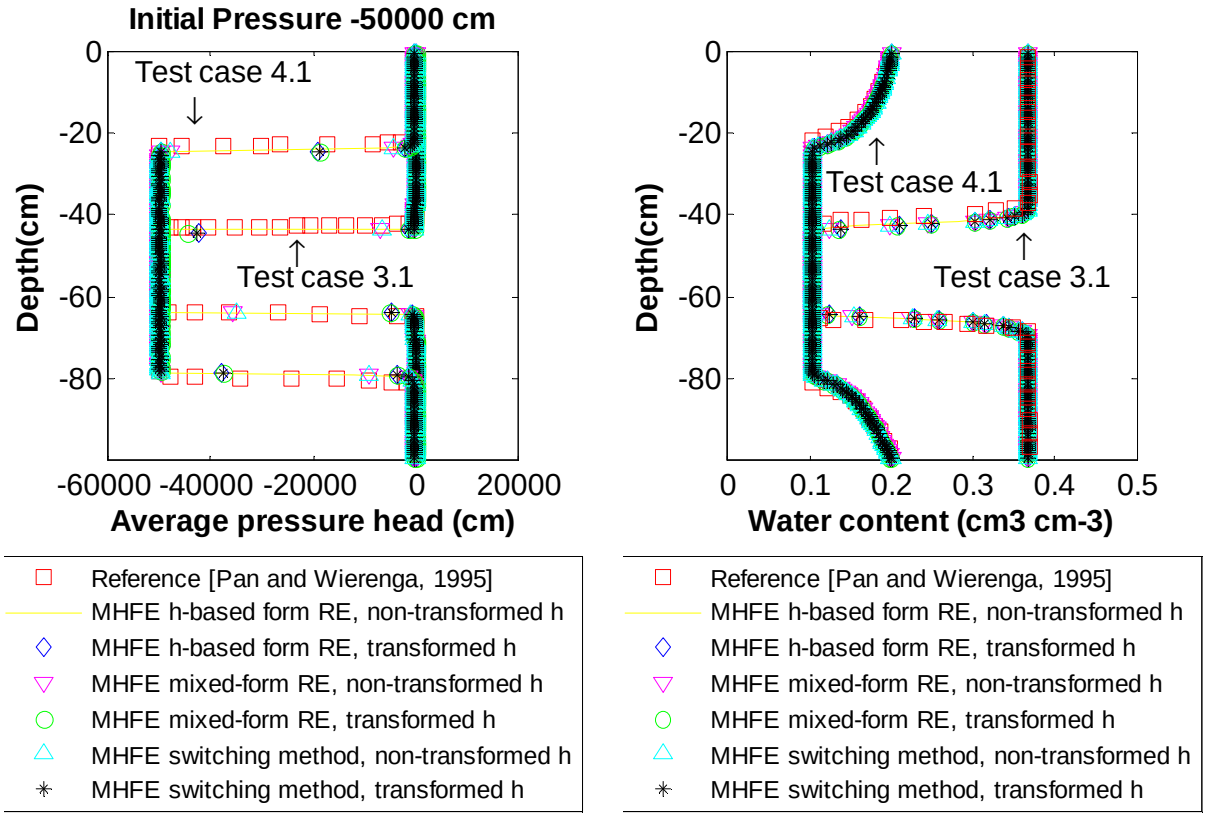
Initial Pressure -50000 cm
Test case 4.1
Test case 3.1
Depth(cm)
Average pressure head (cm)
Water content (cm3 cm-3)
Reference [Pan and Wierenga, 1995]
MHFE h-based form RE, non-transformed h
MHFE h-based form RE, transformed h
MHFE mixed-form RE, non-transformed h
MHFE mixed-form RE, transformed h
MHFE switching method, non-transformed h
MHFE switching method, transformed h

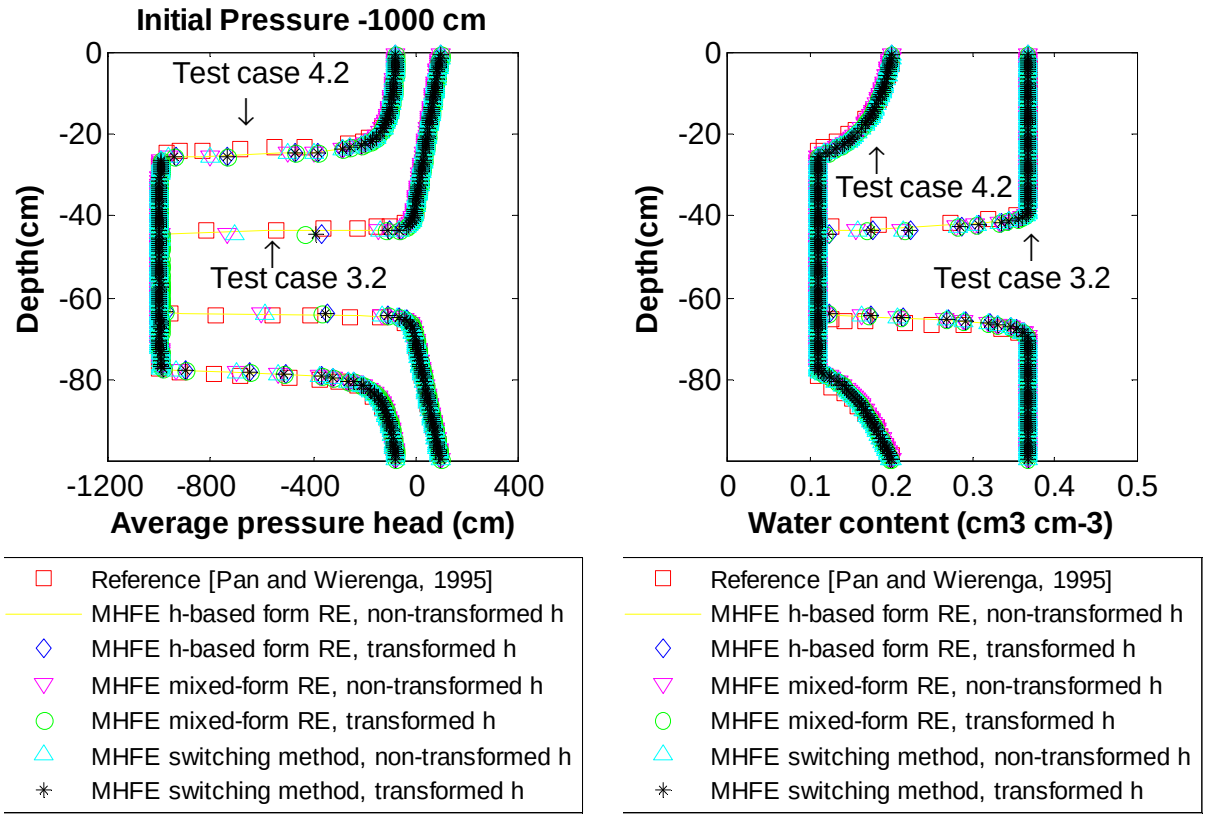
Initial Pressure -1000 cm
Test case 4.2
Test case 3.2
Depth(cm)
Average pressure head (cm)
Water content (cm3 cm-3)
Reference [Pan and Wierenga, 1995]
MHFE h-based form RE, non-transformed h
MHFE h-based form RE, transformed h
MHFE mixed-form RE, non-transformed h
MHFE mixed-form RE, transformed h
MHFE switching method, non-transformed h
MHFE switching method, transformed h

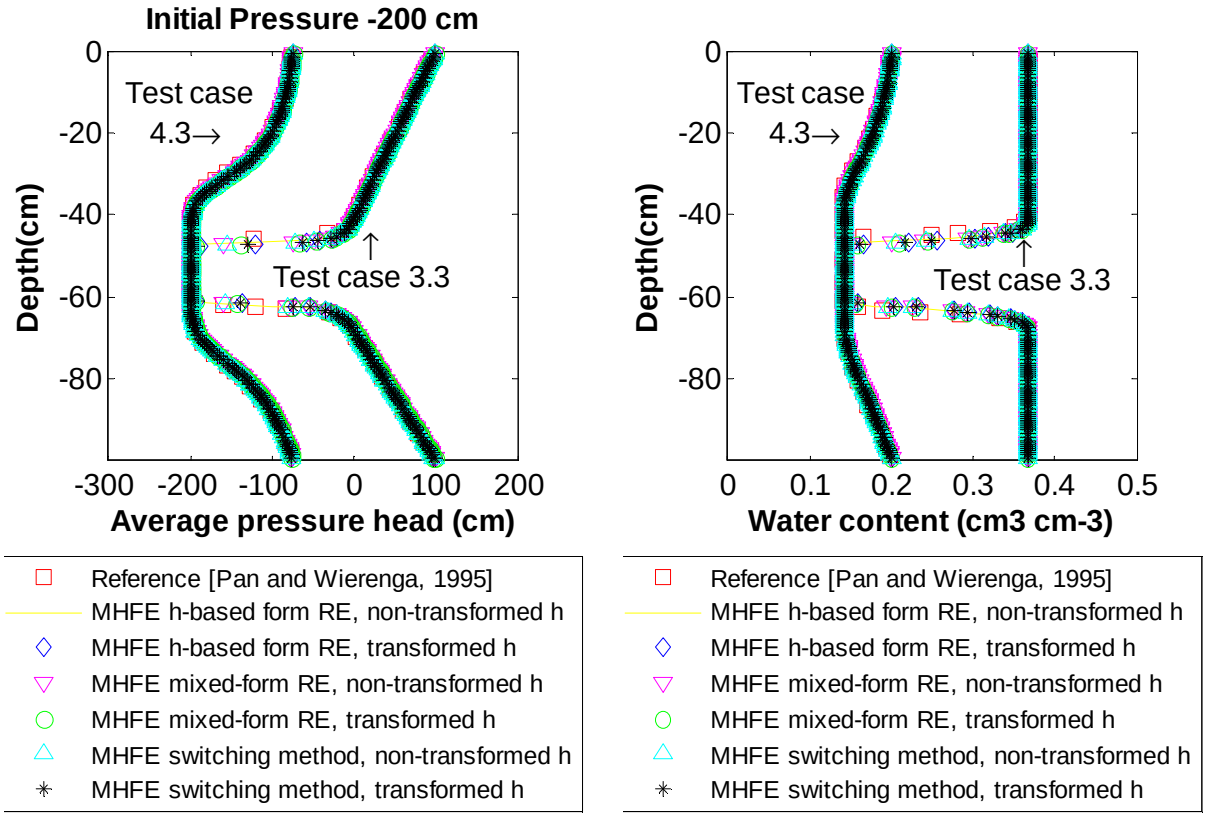

Fig. 14. Pressure head and water content distributions - Pan and Wierenga [1995] test cases.

4.4.2. Indicator parameters definition

Appendix IV presents information about the indicator parameters related to the time stepping size procedure and the computation of errors, when the mixed hybrid formulation with mass condensation scheme is implemented. Table 6 lists these parameters and gives a reference to find the parameter definition within this text document.

Table 6. Parameters description

Discrete information		
Parameter	**Definition**	**Reference**
RE form	Richards Equation form: Standard pressure based form, mixed form, or the primary variable switching technique	Section 3.3.7. –3.3.10
tol_f	Tolerance for the switching procedure	Section 3.3.10
κ (cm^{-1})	constant used in the transformation of the variable pressure head h into a new dependent variable $\hat{h}$	Section 3.3.1. Eq.(3.2)

Time indicator parameters		
Parameter	**Definition**	**Reference**
NI	Total number of iterations during the simulation	
Time steps	Total number of time steps during the simulation	

Δt av	Average time step size	Section 3.6
Δt max	Maximum time step size	Section 3.6
Δt min	Minumum time step size	Section 3.6
Pe max	Maximum value during all the simulation for the Pe_{hyd} number	Section 3.6
Co max	Maximum value for the Courant-Friedrichs-Lewy number	Section 3.6

Error indicator parameters

Parameter	Definition	Reference
ε_{MB}	Global mass balance error	Section 3.3.17 Eq. 3.65
E_{1G} max	Error from the mass balance (difference) computed locally for one element G in a given time step Δt^n using the variable approximations by edge	Eq. 3.67
E_{2G} max	Error from the mass balance (difference) computed locally for one element G in a given time step Δt^n using the variable approximations by element	Eq. 3.68
$\varepsilon_{MB}{}^n$ max	Maximum value for the mass balance error computed at each time step from the mass balance ratio MB^n	Eq. 3.66
$\varepsilon_{MB}{}^n$ min	Minimum for the mass balance error computed at each time step from the mass balance ratio MB^n	Eq. 3.66
Δh max	Maximal convergence error found during all the simulation for average element mean pressure	Eq. 3.69
$\Delta\theta$ max	Maximal convergence error found during all the simulation for water content in the element	Eq. 3.70
Δh_d max	Measure of disagreement or discrepancy between the average pressure calculated in the element and the arithmetic mean of the three edge pressures belonging to this element	Eq. 3.71

4.4.3. Indicator Parameters correlations

In this section, we discuss significant correlations between the indicator parameters. The analysis was performed case by case. Appendix V contains the results from the cross-input correlations. The correlation coefficient, r, is a number between –1 and 1 that measures the degree to which two variables are linearly related. We have chosen to discuss the mathematical relationships between the parameters that have an absolute value of the correlation coefficient $|r| \geq 0.86$.

In the following comments, two groups of parameters are distinguished: parameters that are explicitly indicators of the time, and those that are indicators of the error. We remind the reader that the 12 cases tested differ by the nature of the porous media, the initial and boundary conditions. Indeed, the test cases (1-1, 1-2, 1-3, 2-1, 2-2, 2-3) concern heterogeneous medium and a Neumann boundary condition. While the tests cases (3-1, 3-2, 3-3, 4-1, 4-2, 4-3) concern homogeneous medium and Dirichlet boundary condition.

4.4.3.1. Correlations between time-indicator parameters

As it was expected, for all test cases there is a strong negative correlation between the total number of time steps (Time steps) and the average time step size (Δt av). In the same way, the correlation between the total number of iterations (NI) and the average time step size (Δt av) is also negative, but not for all the cases (r = -0.0337 for test case 4.2). A strong correlation positive between the total number of iterations (NI) and the total number of time steps (Time steps) is also observed, except for test case 4.2 (r = 0.0474).

The correlation coefficient between Pe max and Co max is positive and consistently superior to 0.9 for the test cases simulating a Neumann condition. It is the same for the coefficient of correlation between Co max and Δt max for the test cases simulating Dirichlet conditions (with exception of test case 3.3, where r = 0.126).

4.4.3.2. Correlations between error-indicator parameters

For the test cases simulating a negative pressure imposed as Dirichlet condition:

- the global mass balance error ε_{MB} has on the one hand a strong negative correlation with the local mass balance errors E_{1G} max and E_{2G} max, and on the other hand it has a strong positive correlation with the minimum error calculated at each time step ε_{MB}^{n} min;
- the local mass balance errors have on the one hand a strong positive correlation between them and on the other hand a strong negative correlation with ε_{MB}^{n} min;
- ε_{MB}^{n} max is correlated negatively with the local errors, and positively to the global mass balance error, but the correlation coefficient is not superior to 0.9 for all cases.

Δh max has a positive correlation with $\Delta\theta$ max for all test cases with a Dirichlet condition, but not in all these cases the correlation coefficient is superior to 0.9.

4.4.3.3. Correlations between time-indicator and error-indicator parameters

For the test cases simulating a negative pressure imposed as Dirichlet condition, Δt min is on the one hand correlated negatively to ε_{MB}, and ε_{MB}^{n} min, and on the other hand is positively correlated to the local mass balance errors E_{1G} max and E_{2G} max.

Δh_d max has a positive correlation with the total number of iterations and time steps for the test cases 2-1, 2-2, and 2-3.

After case by case analysis, the following analysis is a global approach merging all cases.

4.4.4. Agglomerative Hierarchical Clustering (AHC)

The Agglomerative Hierarchical Clustering (AHC) procedure is used to make up homogeneous groups of objects (classes) on the basis of their description by a set of variables. AHC was applied here to classify in homogeneous groups on the one hand all the indicator parameters included in Table 6, on the other hand the different numerical methods or choice of models. The statistical analysis was performed with the software XLSTAT, which is compatible with Excel.

4.4.4.1. Advantages and disadvantages of AHC

The AHC classification method has the following advantages:

- The objects are grouped together based on the dissimilarities between them. A type of dissimilarity can be chosen which is suited to the subject studied and the nature of the data.
- As a result, a dendrogram represents the progressive grouping of the data. It is then possible to gain an idea of a suitable number of classes into which the data can be grouped.

The disadvantage of this method is that it is slow. Furthermore, the dendrogram can become unreadable if too much data are used, which is not the case in this study.

4.4.4.2. Principle of AHC

The principle of AHC is simple. The iterative process of classification starts by calculating the dissimilarity between the N objects. Then two objects which when clustered together minimize a given agglomeration criterion, are clustered together thus creating a class comprising these two objects. Then the dissimilarity between this class and the N-2 other objects is calculated using the agglomeration criterion. The two objects or classes of objects whose clustering together minimizes the agglomeration criterion are then clustered together. This process continues until all the objects have been clustered.

These successive clustering operations produce a binary clustering tree (dendrogram), whose root is the class that contains all the observations. This dendrogram represents a hierarchy of partitions. Depending upon either user-defined constraints or more objective criteria, it is possible to choose a partition by truncating the tree at a given level. A detailed description about similarities, dissimilarities and agglomeration methods, is available using the help tool of XLSTAT 2010.

4.4.5. AHC Variables definition

For this statistical analysis, two types of variables were defined:

4.4.5.1. Discrete variables

According to the following definitions (Table 7), discrete variables describing the choice of the model is composed by 5 alphanumeric charaters identifying: the type of boundary condition (N or D), the specified top boundary condition (1, 2, 3 or 4), the initial condition on pressure (A, I, or W), the tolerance used for the switching procedure representing the type of the Richards equation used (H, M or S), and the type of primary variable used (T or P).

Table 7. Discrete variables definition

N	Neumann condition
1	Neumann condition : high flux imposed (1.25 cm/h)
2	Neumann condition : low flux imposed (0.3 cm/h)
D	Dirichlet condition
3	Dirichlet condition : positive pressure imposed (+100 cm)
4	Dirichlet condition : negative pressure imposed (- 75 cm)
A	Arid soil (very dry) : initial pressure –50000 cm
I	Intermediate soil : initial pressure –1000 cm
W	Wet soil : initial pressure -200 cm
H	h-based form of the Richards equation ($tol_f = 0.0$)
M	Mixed form of the Richards equation ($tol_f = 1.0$)
S	Switching technique between h-based and mixed forms ($tol_f = 0.9$)

T Transformed pressure head is used (κ = -0.04 cm^{-1})

P Transformed pressure head is not used (κ = 0.00 cm^{-1})

For example: N1AHT means the simulation results are obtained by setting a Neumann boundary condition (N), with a high flux imposed (1), arid soil (A), the Richards equation was solved using the h-based form (H) and the primary variable used was a transformed pressure head (T). There are in total 72 discrete variables.

4.4.5.1. Continuous variables

Continuous variables carry the quantitative information obtained after simulation. Fifteen continuous variables (time and error indicators) were defined in Appendix IV.

4.4.6. Summary statistics

Table 8 summarize the general statistical analysis of the data:

Table 8. Statistical analysis of the data

Variable	Observations	Minimum	Maximum	Mean	Std. deviation
NI	72	2.09E+03	3.12E+04	1.06E+04	7.83E+03
Time steps	72	9.20E+02	7.59E+03	3.00E+03	1.62E+03
Δt av	72	2.37E-02	1.57E+01	6.84E+00	5.01E+00
Δt max	72	5.34E-02	2.16E+02	2.66E+01	4.19E+01
Δt min	72	3.94E-13	6.95E+00	8.58E-01	1.37E+00
Pe max	72	6.36E-05	5.83E-02	3.91E-02	1.56E-02
Co max	72	5.66E-03	2.42E-01	3.62E-02	4.53E-02
ε_{MB}	72	-8.54E-08	3.69E-07	2.95E-10	5.22E-08
E_{1G} max	72	3.85E-16	6.15E-07	3.69E-08	1.27E-07
E_{2G} max	72	6.85E-16	2.05E-06	5.45E-08	2.55E-07
ε_{MB}^{n} max	72	-1.44E-10	1.00E+00	1.34E-01	2.95E-01
ε_{MB}^{n} min	72	-1.38E+06	-1.11E-12	-3.22E+04	1.68E+05
Δh max	72	4.63E-03	1.11E+01	7.90E-01	2.31E+00
$\Delta\theta$ max	72	1.76E-07	1.03E-03	6.15E-05	1.81E-04
Δh_d max	72	2.92E+00	3.33E+04	5.85E+03	8.62E+03

4.4.7. Clustering results

Data analysis enabled the re-grouping of discrete variables (choice of the model), or continuous variables, in homogeneous groups.

4.4.7.1. Re-grouping of discrete variables

In order to re-group the discrete variables, figure 15 shows the dendrogram representing the hierarchy obtained using an euclidean distance as the dissimilarity metric between points and the Ward Agglomeration method. Three class centroids were distinguished (Table 9).

Table 9. Class centroids

Continuous variables	Class 1	2	3
NI	20008.1667	4570.58333	9837.58333
Time steps	4980.04167	1862.5	2456.33333
Δt av	4.73970669	10.4850808	0.07669958
Δt max	10.3895763	46.2545702	0.20896371
Δt min	0.00050247	1.71656628	0.00014006
Pe max	0.03917482	0.04635188	0.01728739
Co max	0.01916639	0.05240829	0.02144732
ε_{MB}	-5.6503E-11	-1.3807E-08	4.3304E-08
E_{1G} max	2.9632E-08	1.9424E-08	1.037E-07
E_{2G} max	1.7244E-08	7.9371E-09	2.6855E-07
ε_{MB}^{n} max	0.40334453	1.7667E-06	2.1555E-05
ε_{MB}^{n} min	-96505.1929	-6.8357E-07	-2.1985E-07
Δh max	1.07293852	0.07612148	2.36799893
$\Delta\theta$ max	2.8189E-05	7.1564E-06	0.00029123
Δh_d max	17295.0341	95.3805578	229.470986

The highest Total number of iterations during the simulation (NI) was obtained for class 1 follwed by class 3 and class 2. Concerning the local mass balance errors (E_{1G} max and E_{2G} max) the highest value was obtained for class 3 followed by class 1 and class 2, the same order was obtained for Δh max, $\Delta\theta$ max. Hence, class 2 has the minimum NI, E_{1G} max, E_{2G} max, Δh max, $\Delta\theta$ max and also the minimum Δh_d max (Table 9).

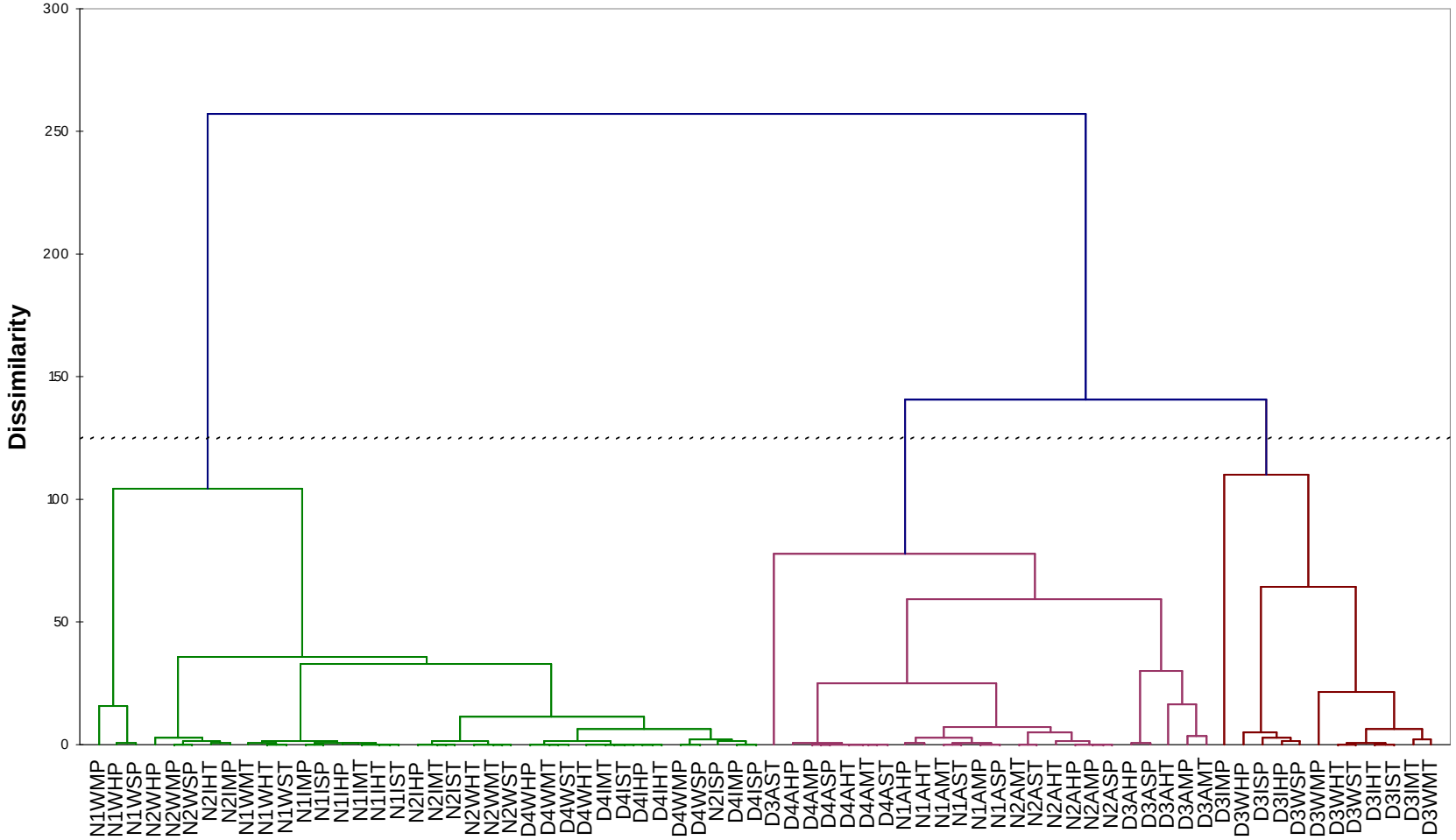

Fig.15. Dendrogram for discrete variables

The central objects for class1, class2 and class3 are representated by discrete variables D3AHT, N1WST and D3WSP, respectively. So that it is possible to make link between the choice of models (discrete variables) and their advantageous characteristics. Distances between the centroids of class 1 to the class 2 and class 3 are in the same order of magnitude ($9.9x10^4$). The distance between the centroids of class 2 and class 3 is shorter ($5.3x10^3$). Table 10 summarize the results by class.

Table 10. AHC Results by class (re-grouping discrete variable)

Class		
1	2	3
N1AHP	N1IHP	D3IHP
N1AHT	N1IHT	D3IHT
N1AMP	N1IMP	D3IMP
N1AMT	N1IMT	D3IMT
N1ASP	N1ISP	D3ISP
N1AST	N1IST	D3IST
N2AHP	N1WHP	D3WHP
N2AHT	N1WHT	D3WHT
N2AMP	N1WMP	D3WMP
N2AMT	N1WMT	D3WMT
N2ASP	N1WSP	D3WSP
N2AST	N1WST	D3WST
D3AHP	N2IHP	
D3AHT	N2IHT	
D3AMP	N2IMP	
D3AMT	N2IMT	
D3ASP	N2ISP	
D3AST	N2IST	
D4AHP	N2WHP	
D4AHT	N2WHT	
D4AMP	N2WMP	
D4AMT	N2WMT	
D4ASP	N2WSP	
D4AST	N2WST	
	D4IHP	
	D4IHT	
	D4IMP	
	D4IMT	
	D4ISP	
	D4IST	
	D4WHP	
	D4WHT	
	D4WMP	
	D4WMT	
	D4WSP	
	D4WST	

From the results above it can be deduced that:

- The first class is distinguished by arid soil initial conditions. All simulations concerning this type of initial pressure condition are in this group, regardless of the boundary conditions that were imposed, the form of the equation to solve, or the primary variable used.
- The third class is characterized by Dirichlet boundary conditions with a positive pressure imposed, except for soil arid initial conditions.
- The second class deals on the one hand with Neumann boundary conditions except for arid soil initial conditions, and on the other hand with Dirichlet boundary conditions with negative pressure imposed, except for arid soils initial conditions.
- The three classes are regardless of the form of the equation to solve and the primary variable used.

4.4.7.2. Re-grouping of continuous variables

In order to re-group the continuous variables, figure 16 shows the dendrogram representing the hierarchy obtained using an euclidean distance as the dissimilarity metric between points and the Ward Agglomeration method. Three class centroids were distinguished. The central objects for class1, class2 and class3 are representated by discrete variables Time steps, Δt min, and E_{1G} max, respectively. Distances between the centroids of class 2 to the class 1 and class 3 are in the same order of magnitude ($2.5x10^5$). The distance between the centroids of class 1 and class 3 is shorter ($3.7x10^4$). Table 11 summarize the results by class.

Table 11. AHC Results by class (re-grouping continuous variables)

Class		
1	2	3
NI	Δt av	ε_{MB}
Time steps	Δt max	E_{1G} max
ε_{MB}^n max	Δt min	E_{2G} max
Δh max	Pe max	
$\Delta\theta$ max	Co max	
Δh_d max	ε_{MB}^n min	

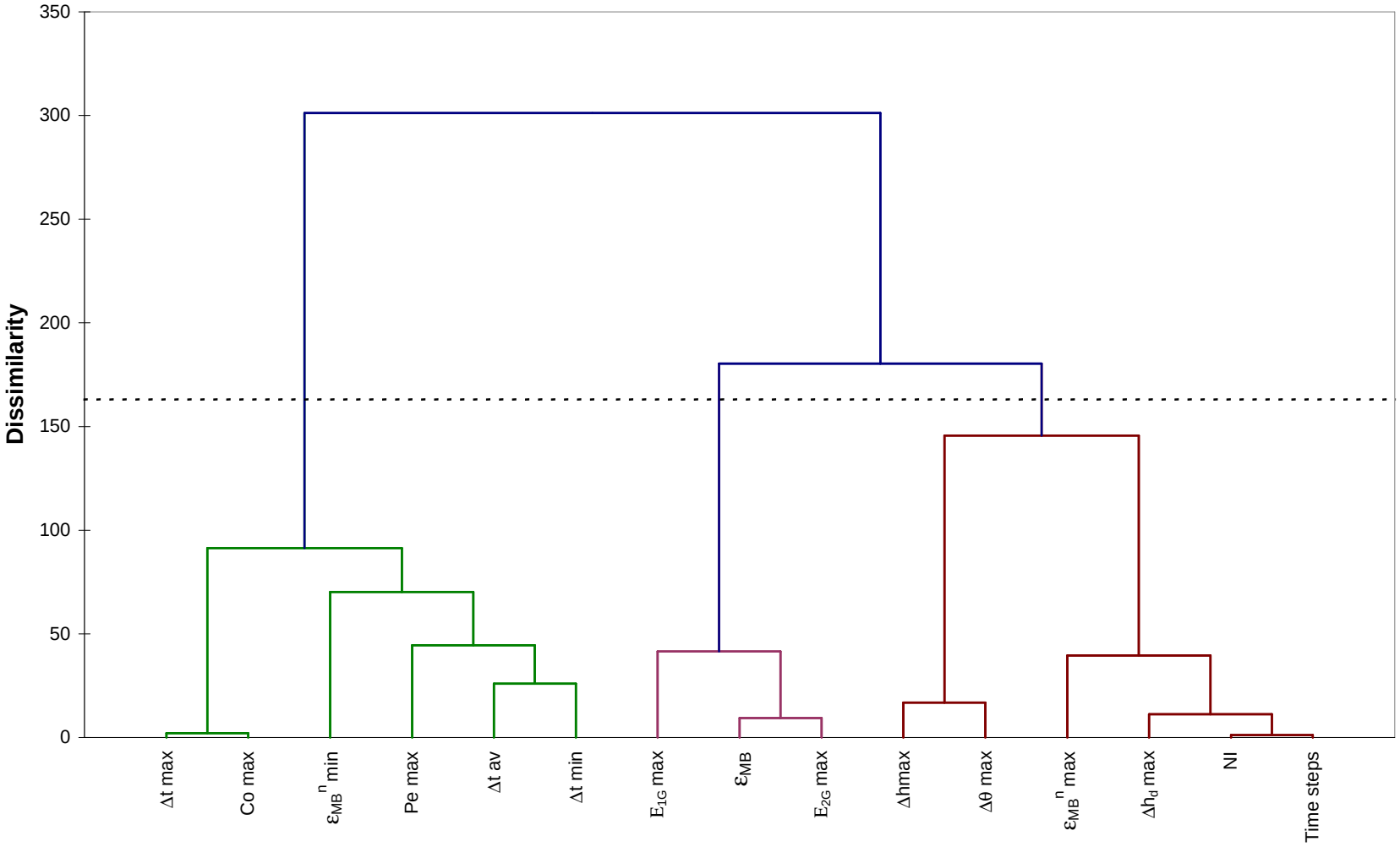

Fig.16. Dendrogram for continuous variables

From the results by class it can be deduced that:

- The third class represents only global and local mass balance errors. Therefore, it can be considered as an indicator of mass conservation.
- Pe max and Co max numbers are numerical parameters involved in the time stepping size procedure. As it was expected, they are directly related with explicit time parameters (Δt_{av}, Δt_{min}, Δt_{max}) , and they were group together in class 2.
- The parameters Δh_{max}, $\Delta \theta_{max}$, and Δh_d max are indicators of precision, which are directly related with the total number of iterations and time steps. They were grouped in class 1.
- The previous comments associated with the fact that the shortest distance between centroids was found between class 1 and class 3, suggest that the global and the local mass balance errors have more proximity to the precision parameters (class 3) than to the time controlling parameters (class 2).

4.4.8. Selection of appropriate models

The re-grouping of the quatitative variables by classes enable to define centers of gravity for each class. In the following paragraphs we propose which simulations are the best suited for each test case.

The choice of the models was performed by sorting in ascending order with a progressive constraint the observation values of the three quantitave variables constituting the centers of gravity of each class (defined in section 4.4.7.2). That is to say, a number of time steps minimum, a Δt min maximum and the smallest E_{1G} max. Thus, for each test case, we propose in Appendix VI, a table that identifies which form of the Richards equation is best suited, the relevance of the switching technique as well as the utility of the transformation of the primary variable.

The test cases 1.1 and 2.1 simulate the infiltration in an arid soil with a Neumann condition, by imposing low and high flux, respectively. The best adapted model proposes the mixed form of the Richards equation with transformation of the variable of pressure. It should be noted in both cases, that the first three most relevant models use the variable transformation technique.

The test cases 1.2 and 2.2 simulate the infiltration in an intermediate soil with a Neumann condition, by imposing low and high flux, respectively. The best adapted model proposes the application of the variable transformation technique for both cases and the application of the switching technique for test case 1.2 and h based form of the Richards equation for test case 2.2.

The test cases 1.3 and 2.3 simulate the infiltration in an wet soil with a Neumann condition, by imposing low and high flux, respectively. The best adapted model proposes for test case 1.3 to not transform the variable of pressure and to apply the switching technique. For test case 2.3, transformation of variable and the h-based form of the Richards equation is proposed.

The test cases 3.1 and 4.1 simulate the infiltration in an arid soil with a Dirichlet boundary condition, by imposing positive and negative pressures, respectively. The best adapted model proposes the transformation of the variable of pressure coupled to the switching technique for test case 3.1 and the non transformation of pressure coupled to the mixed-form of the Richards equation for test case 4.1.

The test cases 3.2 and 4.2 simulate the infiltration in an intermediate soil with a Dirichlet boundary condition, by imposing positive and negative pressures, respectively. The best adapted model proposes the mixed-form of the Richards equation for both cases, the transformation of pressure for test case 3.2, and the non-transformation of the primary variable for testcase 4.2.

The test cases 3.3 and 4.3 simulate the infiltration in a wet soil with a Dirichlet boundary condition, by imposing positive and negative pressures, respectively. The best adapted model proposes the mixed-form of the Richards equation and the transformation of the primary variable for both test cases.

From this analysis, it is deduced that the less indicated models, according to the established criteria of selection, are those applying the non-transformation of the primary variable coupled to the mixed-form or the h-based form of the Richards equation, with two exceptions (N1WMT, D4WHT). In particular, the models coupling the h-based form of the Richards equation and the non-transformation of the primary variable are the less indicated for the problems applying Neumann boundary conditions with a low flux imposed. H-based form of the Richards equation is less indicated for problems applying Dirichlet boundary conditions with a negative pressure imposed, while the non-transformation of the primary variable are the less indicated for problems applying Dirichlet boundary conditions with a positive pressure imposed .

Section 4.5. Standard MHFEM formulation

As mention in section 3.3.13, convergence might be difficult due to non-physical oscillations, when solving the hydrodynamics system of equations using the standard mixed hybrid formulation. Solution for test case 1.3 [Pan and Wierenga, 1995] was obtained using a convergence tolerance criterion $\mathrm{tol_r} = 3\mathrm{x}10^{-2}$. Even if the pressure head distribution at the final time of simulation might have a good agreement with the reference curve (Figure 17), oscillations in the solution are seen at intermediate times, for the top boundary edge pressure (Figure 19). These oscillations have been associated with time-dependent terms. Figure 18 show the time step size as a function of time, it can be seen that the time when disagreement between the pressure curves at the top boundary condition are present (Figure 19), corresponds to the time when the standard MHFEM method uses higher time step sizes than the MHFEM with mass condensation scheme.

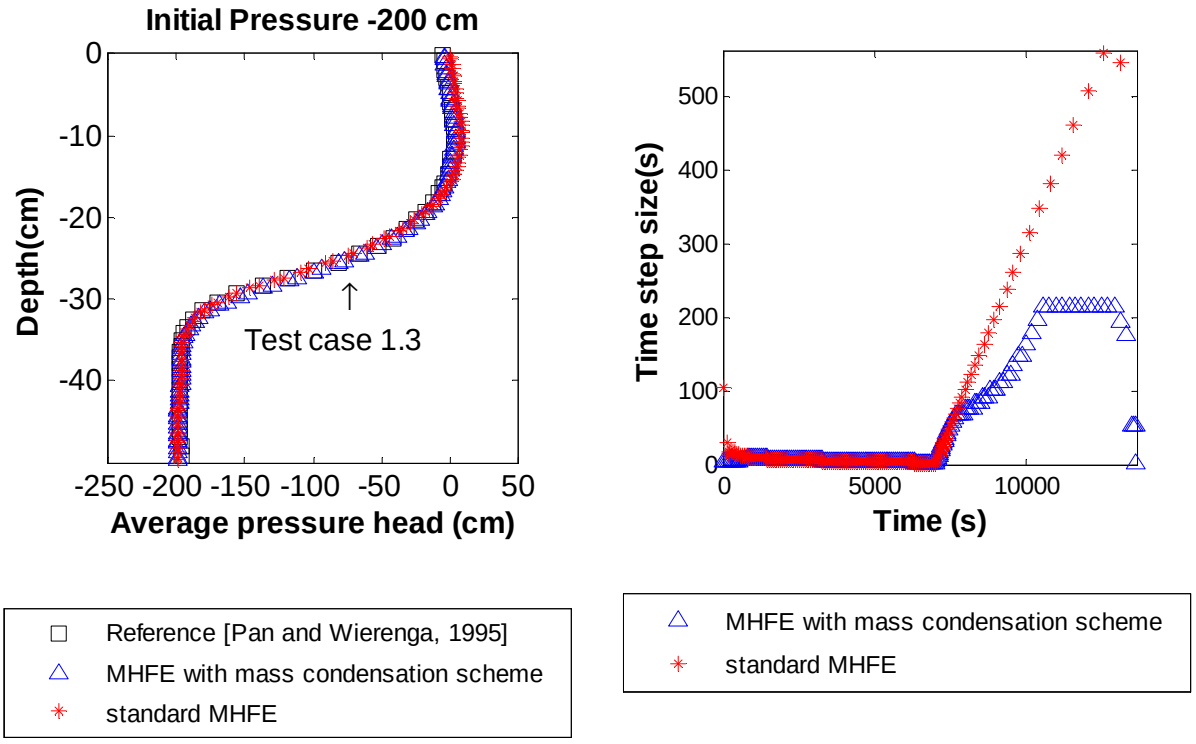

Fig. 17. Pressure distribution when using standard mixed hybrid formulation

Fig. 18. Time step size as a function of time

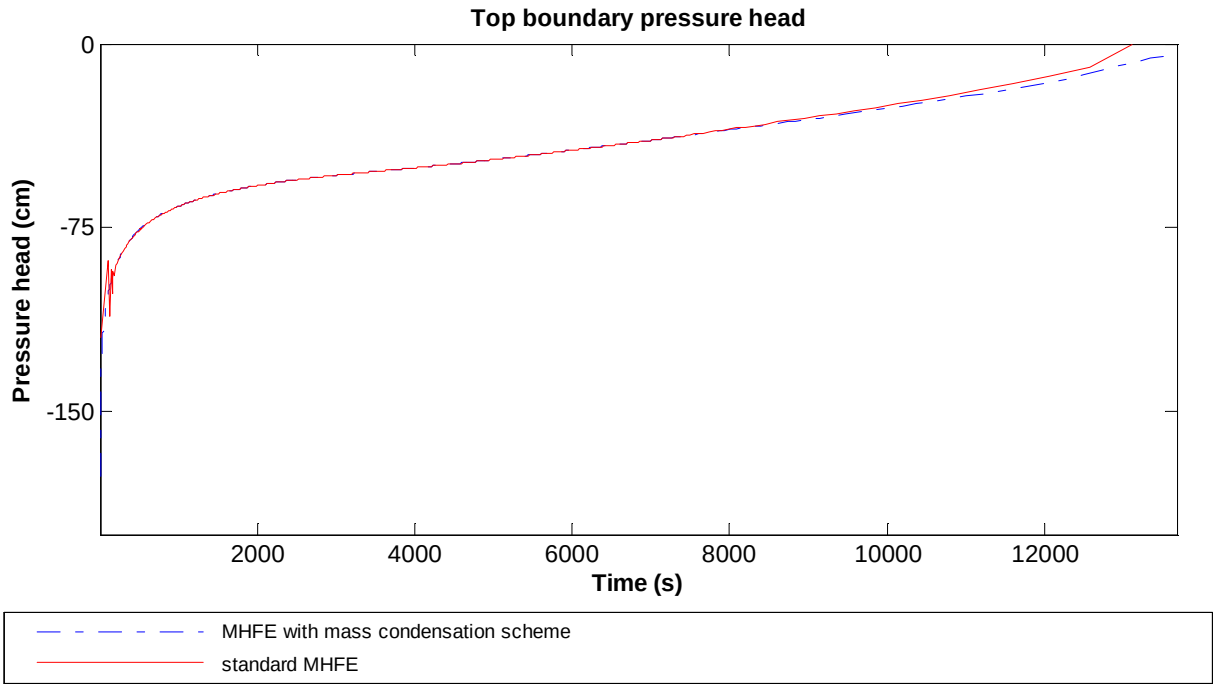

Fig. 19. Top boundary pressure head evolution when using standard mixed hybrid formulation

Section 4.6. Infiltration under Dirichlet condition [Celia et al., 1990]

This test represents an infiltration in a homogeneous porous medium (Material A, Appendix III). The 1D example was presented by Celia et al., [1990] and it was used in other numerical studies [El Kadi and Ling, 1993; Mitchell and Mayer, 1998; Lehmann and Ackerer, 1998; Babajimopoulos, 2000]. Pressure-controlled boundary conditions were applied on the top (-75 cm) and the bottom of the column (-1000cm), with an initial pressure head of –1000 cm along the entire column. Figure 20 shows the results for a time of simulation of 1 day, using a nodal spacing of 0.25 cm, 1.00 cm, 2.5 cm and 5.0 cm compared to the dense grid solution obtained by Celia et al., [1990], which has been adopted as reference solution. Simulations were performed using the absolute and relative pressure tolerances $tol_a = 1x10^{-1}$ cm $tol_r = 1x10^{-4}$, respectively and an absolute water content tolerance criterion $tol_c = 1x10^{-4}$.

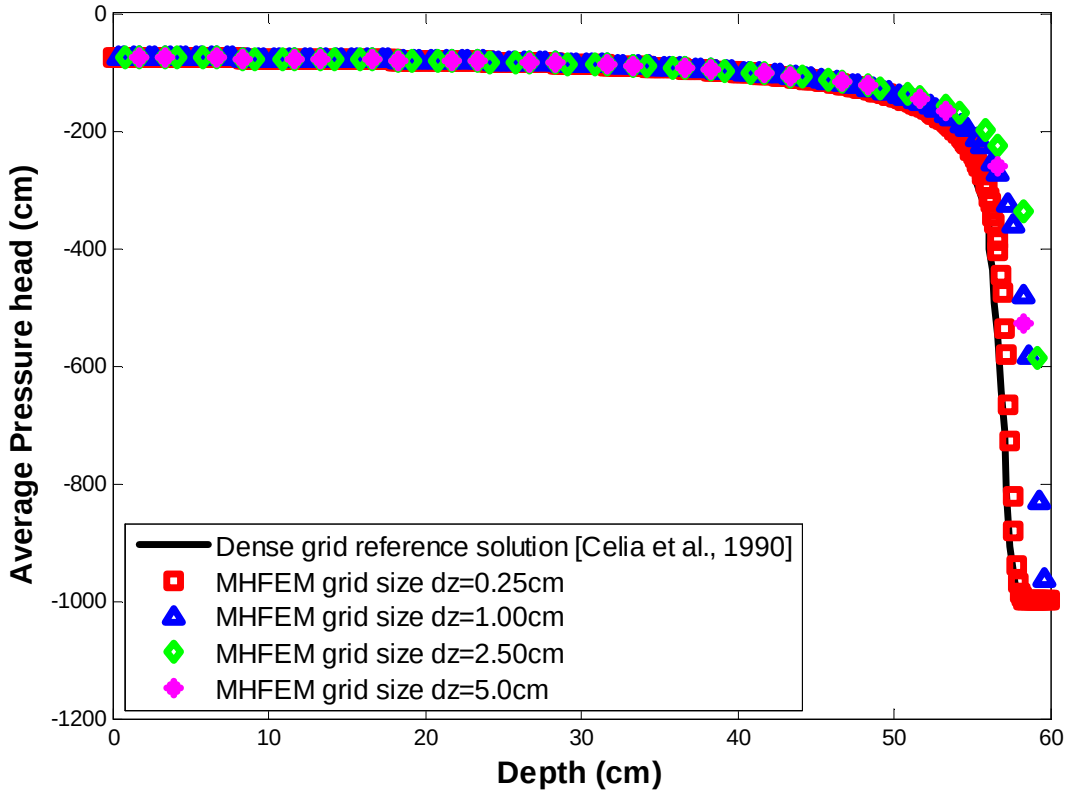

Fig. 20. Pressure head profile as a function of depth after 1 day of simulation. Celia et al. [1990] infiltration test case.

El Kadi and Ling, [1993] concluded in their study that errors in the solutions obtained by Celia et al. [1990] are associated with the mesh sizes and in a greater extent to time step size. In this case, an efficient solution was obtained with a grid size of 0.25 cm and a variable time step. Figure 21 shows the maximum values for the adimensional numbers reached over the entire time of simulation. Figure 22 shows the size of Δt as a function of time.

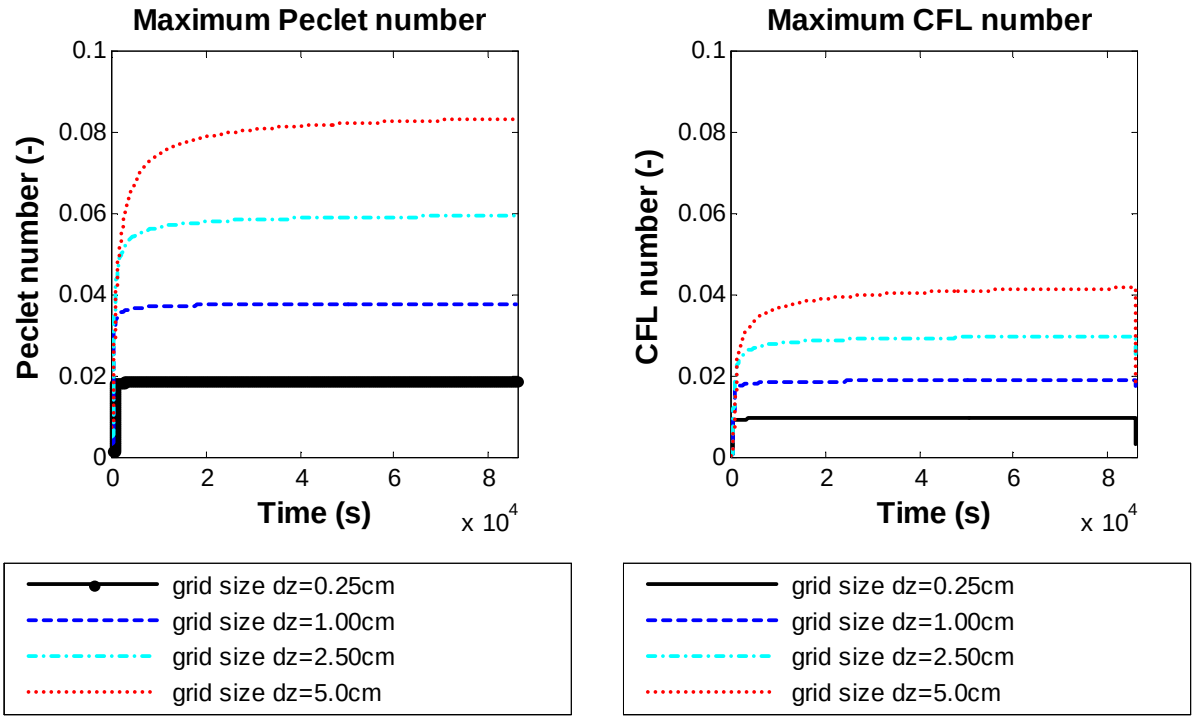

a) Peclet number variation b) CFL number variation

Fig. 21. Peclet and CFL number variation

As it can be seen, the mass conservative scheme reduce the influence of truncation errors. Consequently, the mass balance ratio MB^n as a function of time step is near the unity, except for a grid size 5.0 cm where the effect of the time step size is bigger (Figure 23). Figure 24 shows the maximum value for the local mass balance errors $E_{1G,}$ and E_{2G}, respectively, as a function of time step. Even if the local mass balance errors are so small to be appreciable, global mass balance error might be more important (Figure 25). Moreover, the mass balance error calculated for a single time step $\varepsilon_{MB}{}^n = 1 - MB^n$ might be higher than the global mass balance error, as it is the case for grid size of 5.0 cm (Figure 26) .

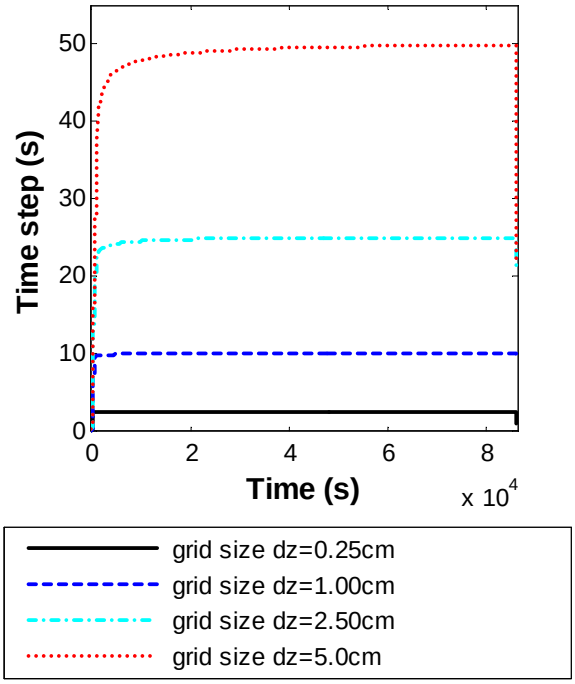

Fig. 22. Time step size as a function of time

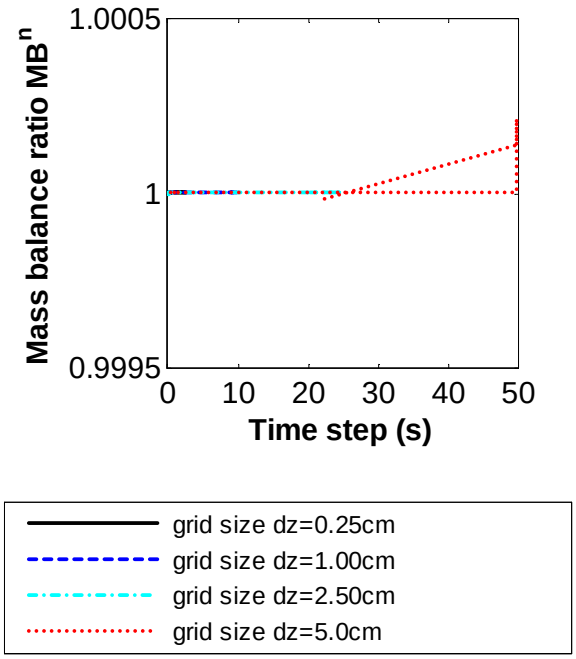

Fig. 23. Mass balance ratio for a single time step (MB^n) as a function of Δt

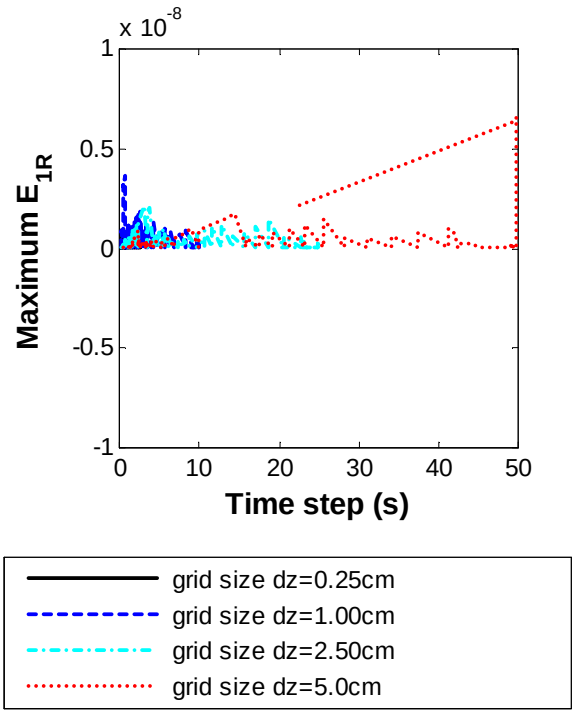

a) Max (E_{1G})

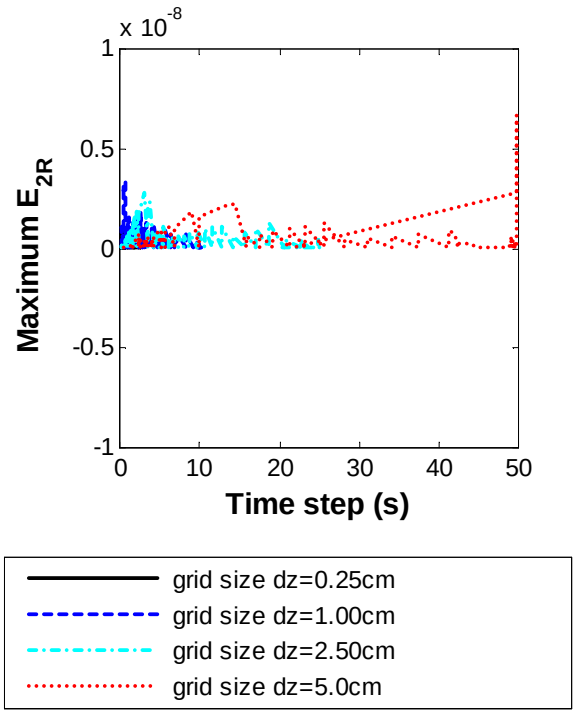

b) Max (E_{2G})

Fig. 24. Local mass balance error

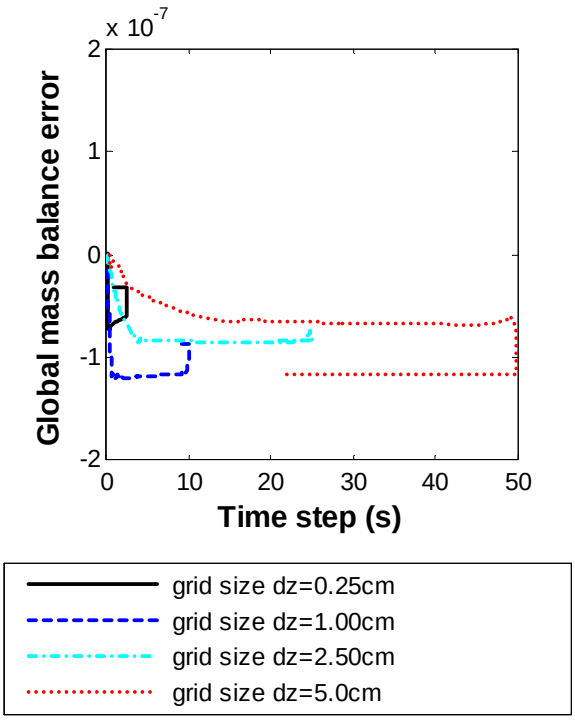

Fig. 25. Global mass balance error (ε_{MB})

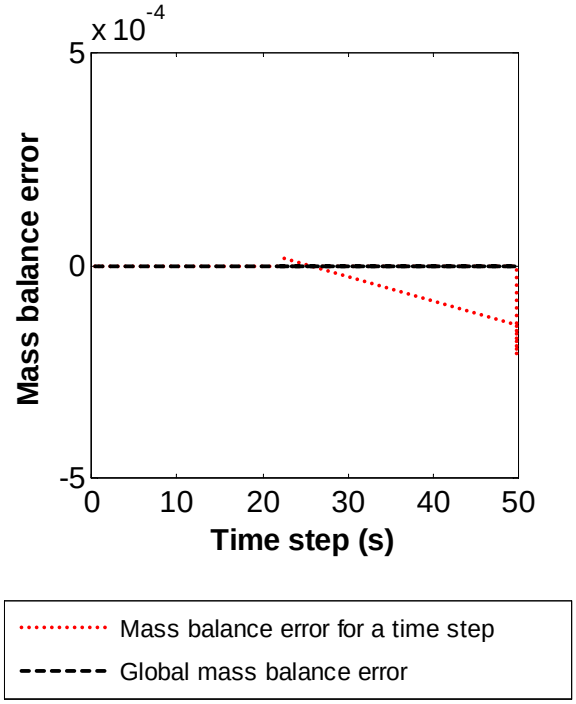

Fig. 26. Mass balance error for a single time step (ε_{MB}^{n}) and global mass error (ε_{MB}) variation

Section 4.7. Top boundary conditions [Van Dam and Feddes, 2000]

The ability of the model to deal with problems related with the top boundary condition was tested for two cases of extremes conditions at sand soil (Material B in Appendix III). Transitions from unsaturated to saturated soil and viceversa were simulated. The performance of the model to calculate cummulative infiltration or evaporation was verified. Results are compared with the refence case denoted R [Van Dam and Feddes, 2000], for a nodal distance Δz_i =0.1 cm and a convergence criterion of $\left|\theta_i^{n+1,m} - \theta_i^{n+1,m-1}\right| < 0.0001$.

4.7.1. Ponded conditions: Infiltration under intensive rain at a dry soil.

The rainfall rate was 1000 mm d^{-1}. The initial conditions on water content were equal to 0.1. At the reference case, the hydraulic head gradient at the soil surface is large enough to absorb the infiltration rate of 1000 mm d^{-1}, until a time of simultation t= 0.008 d. At this moment, the flux boundary condition is replaced by a head condition (h_{sur} = $h_{pondmax}$ = 0.0 mm), and the infiltration rate starts to gradually decrease. The cummulative amount of infiltration obtained in the refence case was 39 mm.

We use the mixed hybrid finite element method to solve the mixed-form of the Richards' equation, with a tolerance criteria $tol_a = 1x10^{-1}$ mm. tol_r and tol_c were set equal to $1x10^{-4}$. The infiltration rate started decreasing at a time of simulation of $9.2x10^{-3}$ d (Figure 27). Table 12 shows the different values calculated as cumulative amount of infiltration and time parameters for each simulation.

Table 12. Cummulative amount of infiltration

Method		κ (cm^{-1})	Total iteration number	Time Step number, Nt	Δt_{av} x10^5	Δt_{max} x10^4	Δt_{min} x10^8	ε_{MB}	Cumulative amount of infiltration
MC	h-based	0.0	7509	2084	4.7	2.6	0.7	$2.14x10^{-13}$	40.2499
MC	h-based	-0.04	6419	1468	6.8	4.5	1.8	$-7.51x10^{-11}$	39.9316
MC	mixed	0.0	7042	1948	5.1	2.3	1.7	$-7.81x10^{-7}$	40.1229
MC	mixed	-0.04	6468	1404	7.1	4.9	2.0	$5.53x10^{-7}$	40.0576
MC	switch	0.0	6669	1818	5.5	2.4	2.8	$-7.59x10^{-7}$	40.1192
MC	switch	-0.4	6336	1405	7.1	4.9	0.3	$3.38x10^{-7}$	40.0487

MC= MHFEM with mass condensation scheme

The number of iterations needed to get the solution decreases when using the method of transformed pressure. Cumulative amount of infiltration is nearly the same for all the methods.

4.7.2. High evaporation at a wet soil

The potential evaporation rate was 5 mm d^{-1}. The initial pressure was –2000 mm. At the reference case, the top flux boundary condition is replaced by a head-controlled condition ($h_{sur} = h_{atm} = -1377$ m) at a time of simulation of 1.1 d (Figure 28). The cummulative actual evaporation obtained in a period of 5 days at the reference case was 11 mm. Table 13 shows the different values calculated as the cumulative amount of evaporation and time parameters for each simulation.

Table 13. Cumulative amount of evaporation

Method		κ (cm^{-1})	Total iteration number	Time step number	Δt_{av} x10^4	Δt_{max} x10^4	Δt_{min} x10^5	ε_{MB}	Cumulative amount of evaporation, mm
MC	h-based	0.0	18675	7477	6.6	6.6	9.6	-5.13×10^{-12}	10.9155
MC	h-based	-0.04	35577	7477	6.6	6.6	9.5	-4.37×10^{-11}	10.2422
MC	mixed	0.0	19156	7477	6.6	6.6	9.6	-3.44×10^{-12}	10.9192
MC	mixed	-0.04	35475	7477	6.6	6.6	9.6	-8.65×10^{-11}	10.2401
MC	switch	0.0	19156	7477	6.6	6.6	9.6	-3.44×10^{-12}	10.9192
MC	switch	-0.04	35475	7477	6.6	6.6	9.6	-8.65×10^{-11}	10.2401

MC= MHFEM with mass condensation scheme

The selection of an appropriate equivalent conductivity when simulating infiltration in dry soil or high evaporation from wet soils is important. Geometric, weighted and integrated formulations produce better solutions than a traditional scheme using a mean conductivity calculated with a mean pressure head [Belfort and Lehmann, 2005]. However, the use of the geometric mean to estimate the hydraulic conductivity underestimates the water fluxes or leads to convergence problems. The method proposed here to estimate the mean hydraulic conductivity for an element consists in assigning the maximum value calculated with the edge pressure heads. As it can be seen, results show agreement with those presented by Van Dam and Feddes [2000]. Smaller estimations of evaporation rate were observed when using transformed pressure heads.

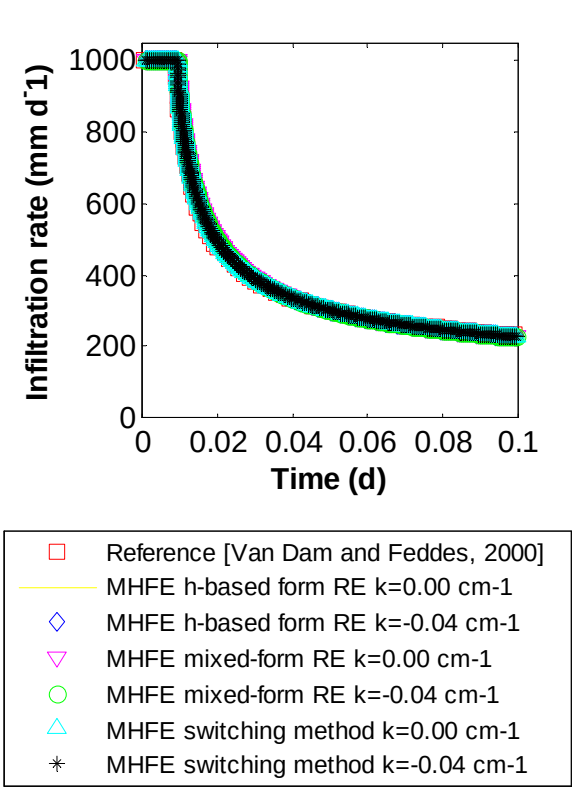

Fig. 27. Infiltration rate

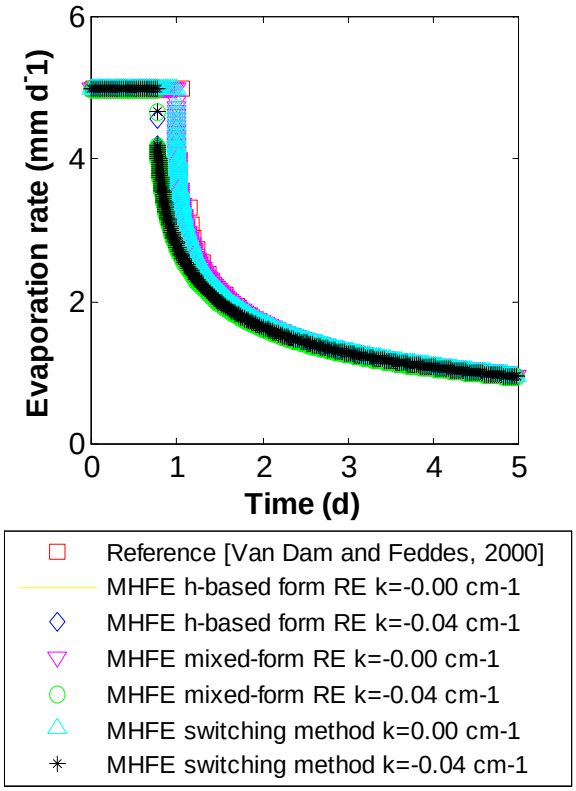

Fig. 28. Evaporation rate

Section 4.8. References fourth chapter

Babajimopoulos, C., 2000. Revisiting the Douglas-Jones method for modelling unsaturated flow in a cultivated soil. Environmental Modelling and Software, 15(3): 303-312.

Belfort, B., Lehmann, F., 2005. Comparison of equivalent conductivities for numerical simulation of one-dimensional unsaturated flow. Vadose Zone Journal, 4(4) : 1191-1200.

Celia, M.A., Bouloutas, E.T., Zarba, R.L., 1990. A general mass-conservative numerical solution for the unsaturated flow equation. Water Resources Research, 26(7): 1483-1496.

El-Kadi, A.I., Ling, G., 1993. The Courant and Peclet number criteria for the numerical solution of the Richards equation. Water Resources Research, 29(10): 3485-3494.

Kirkland, M.R., Hills, R.G., Wierenga, P.J., 1992. Algorithms for solving Richards' equation for variably saturated soils. Water Resour. Res. 28, 2049-2058.

Lehmann, F., Ackerer, Ph., 1998. Comparison of iterative methods for improved solutions of the fluid flow equation in partially saturated porous media. Transport in porous media, 31(3): 276-292.

Leij, F.J., Dane, J.H., 1990. Analytical solutions of the one-dimensional advection equation and two- or three-dimensional dispersion equation. Water Resour. Res. 26, 1475–1482.

Mitchell, R.J., Mayer, A.S., 1998. A numerical model for transient-hysteretic flow and solute transport in unsaturated porous media. Journal of Contaminant Hydrology, 30(3-4): 243-264.

Pan L., Wierenga, P.J., 1995. A transformed pressure head-based approach to solve Richard's equation for variably saturated soils. Water Resources Research, 31(4): 925-931.

Rabe-Hesket, S., Everitt, B. 2004. A handbook of statistical analysis using stata. Third edition. Chapman & Hall/ CRC , Boca Raton, Florida, USA, xiii + 308 pp.

Siegel, P., Mosé, R., Ackerer, Ph., Jaffre, J., 1997. Solution of the advection-diffusion equation using a combination of discontinuous and mixed finite elements. International Journal for Numerical Methods in Fluids, 24(6): 595-613.

Šimůnek, J., van Genuchten, M.Th., Šejna, M., 2005. The HYDRUS-1D Software package for simulating the movement of water, heat, and multiple solutes in variably saturated media, Version 3.0, HYDRUS Software Series 1, Department of Environmental Sciences, University of California Riverside, Riverside, California, USA. 240 pp.

Van Dam, J.C., Feddes, R.A., 2000. Numerical simulation of infiltration, evaporation and shallow groundwater levels with the Richards equation. Journal of Hydrology, 223(1-4): 72-85.

5

Chapter 5 – Application of the model

The model was applied to perform a numerical tracer tests on an experimental site. The residence time distribution of a horizontal-flow constructed wetland (HFCW) was estimated using different boundary conditions. The impact that soil and pollutant properties have on the residence time distribution was analysed for several test cases.

SECTION 5.1. Adsorption distribution impact on preferential transport within Horizontal Flow Constructed Wetland (HFCW)

Adrien wanko[1a] Gabriela Tapia[b] Robert Mosé[a] Caroline Gregoire[b]

[a] *Urban Hydraulic Systems* – IMFS - UdS / CNRS

2 rue Boussingault 67000 STRASBOURG ,

[b] UMR7517/LyGes Laboratoire d'Hydrologie et de Géochimie de Strasbourg – UdS/CNRS

1 rue Blessig 67084 STRASBOURG CEDEX

Abstract

Predicting preferential water flow and solute transport in soils is in the interest of scientists and engineers in the fields of agricultural soil, forest hydrology, soil physics and wastewater treatment by constructed wetland. In artificial wetlands, any preferential pathway induces an insufficient residence time of pollutants in the soil, making an incomplete and unfinished biodegradation processes, a wrong evaluation of the hydraulic residence time of the system which would hinder its management in a complete system with several entities of treatment and a non-homogeneous growth of the biofilm in the solid filter mass. This paper is a contribution in tracer experiment data analysis within a horizontal flow constructed wetland built in a storm water basin. A two dimensional numerical model was used to simulate flow and reactive solute transport. The flow model was successfully calibrated in very dry soil conditions. The adsorption profiles used in the reactive transport modeling are those of five molecules: Metolachlor, Atrazine, Deethylatrazine (DEA), deisopropylatrazine (DIA), and hydroxyatrazine (HA). We show that the adsorption distribution is an internal factor of soil which is responsible to the "preferential" pathway transport in a homogeneous gravel texture. The mean residence time of pollutants within the filter is strongly correlated with the average value of the adsorption coefficient. Moreover we note a lack of significant impact of the heterogeneity of the medium on the statistical moments of breakthrough curve. It appears that a uni-modal breakthrough curve is not significant to the absence of preferential flow in the medium and at least a two-dimensional display can provide sufficient evidence on the presence or absence of preferential pathways. Finally, using a PLS regression, it is possible to perfectly discriminate the number of peaks of concentration and the asymmetry of the breakthrough curve.

Key words : Constructed Wetland; Modeling; Pesticides; Preferential transport; tracer experiment

[1] Corresponding author : awanko@engees.u-strasbg.fr, Tel : 00 (33) 88 24 82 87, Fax : 00 (33) 88 24 82 83

5.1.1. Introduction

Preferential flow is not only a theoretical challenge, but it has a significant importance in enhancing leaching of pollutants from the surface to deeper layers up to groundwater. The contamination danger of groundwater is increased due to this phenomenon [Coppola *et al.*, 2009]. In fact, rapid movement of agricultural chemicals through soil to groundwater via preferential flow pathways is one of the leading causes of water contamination [Jaynes *et al.*, 2001; Lee *et al.*, 2001]. Furthermore, the presence of preferential pathways may cause significant losses of water and nutrients to the plants [Bouma and Dekker, 1978; Kosmas *et al.*, 1991 in Ohrstrom *et al.*, 2004]. According to Mosaddeghi *et al.* [2008], experimental observations indicated that preferential flow is the rule rather than the exception in most structured soils, and continuous pores, which are several times larger than a bacterium allow bacterial transport over significant distances. Their results revealed that soil water and bacterial velocities were higher in the silt loam soil. They attributed the difference to aggregation, structural stability and macropores enhancing preferential flow in the soil with the greater clay content. Scientific literature has taken the measure of this phenomenon through numerous publications on the subject. Major efforts are still necessary to get qualitative but also rigorous description: moreover we need to improve quantitative indicators of preferential flow and transport processes through soils. Coppola [2009] emphasis the fact that local-scale heterogeneities and non-equilibrium type of preferential flow are obviously expected to be highly related, but quantification of this relationship remains a great challenge. Predicting preferential water flow and solute transport in soils is in the interest of scientists and engineers in the fields of agricultural soil, forest hydrology, soil physics and wastewater treatment by constructed wetland. In artificial wetlands, any preferential pathway induces:

1. An insufficient residence time of pollutants in the soil, making an incomplete and unfinished biodegradation process,

2. A wrong evaluation of the hydraulic residence time of the system which would hinder its management in a complete system with several entities of treatment,
3. A non-homogeneous growth of the biofilm in the solid filter mass, leading to a predominating biomass activity located around the preferential pathway. This process would cause a weak effectiveness of the system size.

   In wastewater treatment through a vertical or horizontal sand filter, a well done tracer experiments give information in most cases about the type of flow (plug flow, dispersive or diffusive flow, etc…) as well as the residence time in the artificial wetland. This last parameter has to be at least bigger than the degradation time of the pollutants within the porous structure.

With the aim of better locating the preferential pathways and of identifying the factors influencing it, Malmstrom *et al.,* [2008] show that the existence of preferential flow paths can cause temporally separated concentration peaks in response to a single chemical reaction chain, even in a geochemically homogeneous domain, making the interpretation of the concentration curves non-trivial. Although an unimodal, log-normal distribution in many cases may accurately describe the flow situation, it is clear that preferential flow may be responsible for a large part of the total mass transport [Gupta *et al.,* 1999; Simic and Destouni,1999]. To investigate the potential effect of preferential flow paths, a bimodal distribution, which is the sum of two weighted unimodal distribution (one representing the slower/normal flow paths, and the other representing the faster/preferential flow paths), has been considered [Rosqvist *et al.,* 2000; Malmstrom *et al.,* 2008]. This mathematical decomposition is made possible due to a steady-state mode within the vertical flow filter. Although this approach is not possible in our study because of horizontal flow constructed wetland, we retain the fact that, the presence of bimodal breakthrough curves is a physical interpretation of preferential pathways.

Many authors have used dye patterns in order to reveal and to visualize preferential flows in field experiments [Yasuda *et al.,* 2001; Ohrstrom *et al.,* 2002]. Conservative dyes like Brilliant Blue FCF and Bromide (Br2) have been used as a tracer to determine preferential flows in various experiments [e.g. Smith and Davis, 1974; Hills *et al.,* 1991; Jabro *et al.,* 1991; Reichenberger *et al.,* 2002; Ohrstrom *et al.,* 2003; Suliman et *al.,* 2006]. Ohrstrom *et al.,* [2003] conclude that the solute movement with preferential flow implies that small scale differences in soil texture can not be the only cause of the preferential flow in the studied soil. By studying quantitative indices to characterize the extent of preferential flows in soils, Kamra *et al.* [2005] conclude that the breakthrough curves (BTCs) obtained with the leakage data of individual columns, exhibited different shapes including some with early breakthrough and increased tailing, which qualitatively indicate the presence of preferential flows.

Studies with non-conservative dyes like pesticides and herbicides have also highlighted the preferential flow in soils [Jaynes *et al.,* 2001; Reichenberger *et al*., 2002]. According to Reichenberger *et al.,* [2002], the knowledge concerning the contribution of preferential flows to pesticide leaching under field conditions is still scarce. After working about pesticide displacement along preferential flow pathways, Reichenberger *et al.,* [2002] achieved to very important conclusions summed up in the following. It is, so, not possible to quantitatively determine the portion of total pesticide displacement caused by preferential flows. Nevertheless, beyond the main tracer front at soil tillage depth, transport along preferential flow pathways was obviously responsible of the major part of the total pesticide displacement. This part was about two to five times higher for the nonpolar than for the polar pesticides.

The polar or nonpolar behavior of pesticides in solution is an important factor in the adsorption process in soils. Moreover soil can exhibit different adsorption coefficient at different depths. The big issue of this paper is to observe the impact of an heterogeneous adsorption distribution coefficient within a single texture soil on preferential pathways.

The paper contributes in the tracer experiment data analysis in porous media by highlighting the influence of homogeneous and heterogeneous adsorption coefficient distribution on the HFCW residence time distribution.

Numerical transport experiments are conducted after hydrodynamic calibration within the porous medium. Using a two dimensional numerical model which simulates solute transport in porous media, three numerical test modalities are performed:

- Experiments without adsorption, allowing the hydraulic residence time determination;
- Experiments with an homogeneous distribution of the linear adsorption coefficient;
- And finally experiments with a heterogeneous distribution of the linear adsorption coefficient.

5.1.2. Material and methods

In order to study treatment potentialities to mitigate non-point source pesticide pollution in constructed wetland systems, the European LIFE ENVIRONMENT Project Artwet (LIFE 06 ENV/F/000133) implement mitigation solutions at six demonstration and experimental sites. The project includes a storm water basin located in Alsace, France. This hydraulic structure is placed at the rural/urban interface, and at the bottom of vineyard hills. It concentrates all the contaminated hydrological surface flows, and it allows the accumulation of the sediments that are transported from the parcels. With the objective of increasing the retention capacities of pollutants in storm water basin, an horizontal flow constructed wetland (HFCW) was built inside the storm water basin (see Figure 29 below).

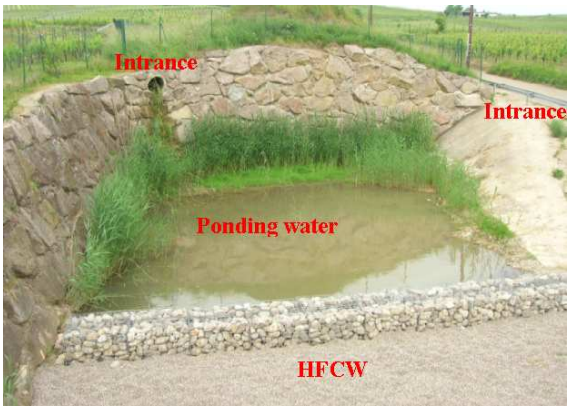

Fig. 29. An HFCW within a storm water basin

To have a better understanding of the hydrodynamics and transport in this experimental site, a two-dimensional numerical model was developed. The use of a two-dimensional model is justified by the need of taking into account the heterogeneities of the medium and the initial conditions, like heterogeneity of water content and high local concentrations on the infiltration surface.

The hydrodynamic system is simulated by the application of the Richards' equation (1). This formulation physically describes the flow in a variably saturated porous medium.

$$C(h)\frac{\partial h}{\partial t} = \nabla[K\nabla(h+z)] + W(x,z,t) \qquad (1)$$

Where: W(x,z,t) is the sink/source terms [T^{-1}],

x and z (depth) are the spatial coordinates [L],

t is time [T],

C(h) is the soil moisture capacity [L^{-1}],

K is the unsaturated hydraulic conductivity [LT^{-1}],

h is the soil water pressure head [L].

The solute transport is described by a classical advection-dispersion equation (2) with the presence of sink/source term which takes into account the pesticide degradation.

$$\frac{\partial(\theta C)}{\partial t}+\frac{\partial(\rho S)}{\partial t}-\nabla(\theta D\nabla C)+\nabla\left(\vec{q}\,C\right)=f(x,z,t) \qquad (2)$$

Where: f(x,z,t) is the sink/source terms [$ML^{-3}T^{-1}$],

C is solution concentration [ML^{-3}],

S is absorbed concentration [ML^{-3}],

ρ is soil bulk density [ML^{-3}],

t is time [T],

$\vec{q}$ is volumetric flux [LT^{-1}],

D is the dispersion tensor [L^2T^{-1}],

and θ is soil volumetric water content [L^3L^{-3}].

The numerical tool used to solve these equations is the mixed hybrid finite element method (MHFEM). This technique is particularly well adapted to the simulation of heterogeneous flow field [Mosé *et al.*, 1994; Younes *et al.*, 1999]. It has been applied in previous works concerning mainly to the flow in heterogeneous saturated porous medium.

The originality here is to simulate both, flow and solute transport, with the application of MHFEM for a variably saturated porous medium.

5.1.2.1. 2D Hydrodynamic modelling

A two-dimensional (2D) flow domain Ω is defined, and is space-discretized into triangular elements *K*. The Darcy flux $\vec{q}=-K\nabla(h+z)$ is approximated over each element by a vector $\vec{q}_K$ belonging to the lowest order Raviart-Thomas space [Raviart and Thomas,

1977]. On each element this vector function has the following properties: $\nabla \vec{q}_K$ is constant over the element *K*, $\vec{q}_K \vec{n}_{K,E_i}$ is constant over the edge E_i of the triangle, $\forall i = 1,2,3$, where $\vec{n}_{K,E_i}$ is the normal unit vector exterior to the edge E_i. $\vec{q}_K$ is perfectly determined by knowing the flux through the edges [Chavent and Roberts, 1991]. Moreover, with the MHFEM, the normal component of $\vec{q}_K$ is continuous from *K* to the adjacent element *K'* and $\vec{q}_K$ is calculated with the help of the vector fields basis $\vec{w}_i$, used as basis functions over each element *K*. These vector fields are defined by $\int_{Ei} \vec{w}_j \cdot \vec{n}_{K,E_i} = \delta_{i,j}$, $\forall i = 1,2,3$. Where δ_{ij} is the Kronecker symbol. So that, these functions correspond to a vector $\vec{q}_K$ having a unitary flux through the edge E_i, and null flux through the other edges:

$$\vec{q}_K = \sum_{j=1}^{3} Q_{K,E_j} \vec{w}_j \qquad (3)$$

with $Q_{K,Ej}$ the water flux over the edge Ej belonging to the element *K*.

The estimation of the conductivity can be represented by the relationship $K_K = k_K\left(K_K^A\right)$. Where, over each element *K*, k_K is the unsaturated hydraulic conductivity function [LT^{-1}] given by the modified Mualem-van Genuchten expression [Ippisch *et al.*, 2006], K_K^A is a dimensionless anisotropy tensor.

5.1.2.2. 2D Transport modelling (a new approach)

For the transport equation, we use an original formulation, $\vec{q}_{advection,dispersion} = -\theta D \nabla C + \vec{q} C$ where $\vec{q}$ is the volumetric flux [LT^{-1}], given by (3). The convective and dispersive flux is approximated over each element by a unique vector

$\vec{q}_{adv-disp\,K}$ belonging to the lowest order Raviart-Thomas space. Therefore, $\nabla \vec{q}_{adv-disp\,K}$ is constant over the element *K*, and $\vec{q}_{adv-disp\,K}\,\vec{n}_{K,E_i}$ is constant over the edge E_i, $\forall i = 1,2,3$. $\vec{q}_{adv-disp\,K}$ can be perfectly determined by knowing the transport flux through the edges (4).

$$\vec{q}_{adv-disp\,K} = \sum_{j=1}^{3} Q_{adv-disp\,K,E_j}\,\vec{w}_j \tag{4}$$

with $Q_{adv\text{-}dispK,Ej}$ the advective-dispersive flux over the edge Ej belonging to the element *K*.

Following a similar procedure to that well described specifically for the hydrodynamics by several authors [Mosé et al., 1994; Nayagum, 2001; Belfort 2006] we developed the below formulation for the advective dispersive flux :

$$Q_{adv-disp\,K,E_i} = -\sum_{j=1}^{3} B^{-1}_{K,i,j}\,TC_{K,E_i} + C_K\left(\sum_{j=1}^{3} B^{-1}_{K,i,j} + Q_{K,E_i}\right) \qquad \forall i = 1,2,3 \tag{5}$$

Where: C_K is the average concentration at the element *K*.

TC_{K,E_j} is the average concentration at the edge E_j.

B_K is a symmetric and invertible 3 x 3 matrix, defined by

$$B_K = \left\lfloor B_{K,i,j} \right\rfloor_{3,3} \quad B_{K,i,j} = \int_k \left(\theta_K{}^{-1} D_K{}^{-1}\,\vec{w}_j\right)\vec{w}_i \tag{6}$$

D_K is the dispersion tensor where its components are given by:

$$\theta D_{i,j} = (\alpha_L - \alpha_T)\frac{q_i q_j}{|q|} + (\theta Dm + \alpha_T |q|)\delta_{i,j} \tag{7}$$

with: Dm the molecular diffusion coefficient [$L^2\,T^{-1}$],

α_L the longitudinal dispersivity of solid matrix [L],

α_T the transversal dispersivity of solid matrix [L],

q_i , q_j the components of Darcy flux q [LT^{-1}],

θ the soil volumetric water content [L^3L^{-3}].

$\delta_{i,j}$ the Kronecker's symbol [-]

5.1.2.2. Numerical Solution

Time discretization was carried out applying the fully implicit (backward Euler) method to the equation (2), and using the approximations over the element K,

$$\left(\frac{\left(\theta_K^{n+1}+k_{d_K}^{n+1}\rho_K^{n+1}\right)C_K^{n+1}-\left(\theta_K^{n}+k_{d_K}^{n}\rho_K^{n}\right)C_K^{n}}{\Delta t}\right)|K|+\nabla\vec{q}_{adv-disp_K}^{\,n+1}|K|-F_K^{n+1}=0 \qquad \forall K\in\Omega \tag{8}$$

with $F_K^{n+1}=\int_K f\left(C_K^{n+1},t^{n+1}\right)$ and $k_{d_K}=\frac{S_K}{C_K}$ the isotherm linear adsorption coefficient.

Then, from the expressions (4) and (5) we can deduce equation (9) below :

$$\nabla\vec{q}_{adv-disp_K}^{\,n+1}=\frac{1}{|K|}\sum_{i=1}^{3}Q_{adv-disp_{K,E_i}}^{n+1}=\frac{1}{|K|}\left[-\sum_{i=1}^{3}\sum_{j=1}^{3}B_{K,i,j}^{-1}TC_{K,E_j}^{n+1}+C_K^{n+1}\sum_{i=1}^{3}\left(\sum_{j=1}^{3}B_{K,i,j}^{-1}+Q_{K,E_i}^{n+1}\right)\right] \tag{9}$$

Substituting (9) in (8) and multiplying the resulting equation by $\frac{\lambda_K}{\gamma_K}$, we get the expression:

$$C_K^{n+1}=\frac{\left(\theta_K^{n}+k_{d_K}^{n}\rho_K^{n}\right)C_K^{n}}{\theta_K^{n+1}+k_{d_K}^{n+1}\rho_K^{n+1}+\lambda_K}+\frac{\lambda_K\sum_{i=1}^{3}\sum_{j=1}^{3}B_{K,i,j}^{-1}TC_{K,E_j}^{n+1}}{\gamma_K\left(\theta_K^{n+1}+k_{d_K}^{n+1}\rho_K^{n+1}+\lambda_K\right)}+\frac{\lambda_K F_K^{n+1}}{\gamma_K\left(\theta_K^{n+1}+k_{d_K}^{n+1}\rho_K^{n+1}+\lambda_K\right)} \tag{10}$$

where: $\gamma_K=\sum_{i=1}^{3}\left(\sum_{j=1}^{3}B_{K,i,j}^{-1}+Q_{K,i}^{n+1}\right)$, and $\lambda_K=\frac{\gamma_K\Delta t}{|K|}$.

Denoting $\beta_K=\frac{\lambda_K}{\theta_K^{n+1}+k_{d_K}^{n+1}\rho_K^{n+1}+\lambda_K}$; then $1-\beta_K=\frac{\theta_K^{n+1}+k_{d_K}^{n+1}\rho_K^{n+1}}{\theta_K^{n+1}+k_{d_K}^{n+1}\rho_K^{n+1}+\lambda_K}$

we obtain an expression to estimate the average concentration in the element K.

$$C_K^{n+1} = \left(\frac{\theta_K^n + k_{d_K}^n \rho_K^n}{\theta_K^{n+1} + k_{d_K}^{n+1} \rho_K^{n+1}} \right) (1-\beta_K) C_K^n + \frac{\beta_K \sum_{i=1}^{3} \sum_{j=1}^{3} B_{K,i,j}^{-1} TC_{K,E_j}^{n+1}}{\gamma_K} + \frac{\beta_K F_K^{n+1}}{\gamma_K} \quad (11)$$

The continuity equation (12) is provided for all the interior edges E_i ($\forall i = 1,2,3$) of the domain Ω . The edge E_i is common to the frontiers of the elements K and K'.

$$Q_{adv-disp\,K,E_i} + Q_{adv-disp\,K',E_i} = 0 \quad (12)$$

Following a similar procedure to that well described specifically for the hydrodynamics by several authors [Mosé *et al.*, 1994; Nayagum, 2001; Belfort, 2006] equations (11) and (12) allow the mixed hybrid formulation for transport equation. The readers are referred in these articles for the matrix transformations.

This method will lead for the hydrodynamics to a system of linear equations, where the unknowns are the water pressure traces (Th). The number of unknowns is equal to the number of edges to which the pressure has not been imposed. Analogously, for the transport the unknowns are traces of concentration. The matrix associated with the hydrodynamics equations system is symmetric and definite positive. Therefore, it can be effectively solved by the conjugate gradient method, preconditioned with an incomplete Cholesky decomposition using the Eisenstat procedure. In contrast, the matrix associated with the transport is nonsymmetric. Thus, the conjugate gradient squared iterative method with the Eisenstat ILU preconditioning procedure will be used to solve this algebraic system.

5.1.2.4. Numerical experiences

With the aim of studying the influence of the adsorption coefficient on the flow in a single texture gravel, 7 numerical tracer experiments are undertaken (see Table 14).

Table 14. Numerical experiences

Experiences	Linear adsorption	Adsorption distribution	pollutants
Case 1	No	--	--
Case 2	Yes	Homogeneous	Atrazine
Case 3	Yes	Heterogeneous	Atrazine
Case 4	Yes	Heterogeneous	DEA
Case 5	Yes	Heterogeneous	DIA
Case 6	Yes	Heterogeneous	HA
Case 7	Yes	Heterogeneous	Metolachlor

The adsorption profiles used are those of the following molecules: metolachlor, atrazine and the conversion products (deethylatrazine (DEA), deisopropylatrazine (DIA), hydroxyatrazine (HA)). These adsorption parameters come from Vryzas *et al.*, [2007], who conduct an experimental study in the soil profile of a river basin. The graph below (Figure 30) showing the adsorption parameter along the soil profile is so obtained thanks to Vryzas *et al.* [2007] experimental data.

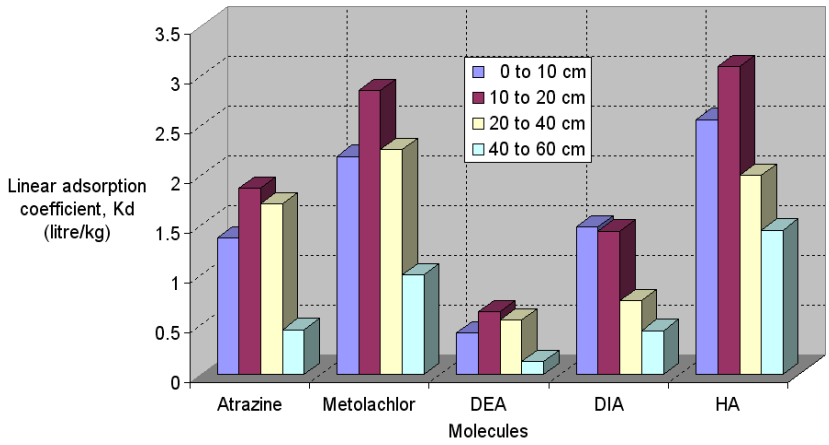

Fig. 30. Adsorption coefficients in soil profile

5.1.2.5. Time moments analysis

Time moments analysis was applied to characterize the shapes of experimental BTCs in term of mean breakthrough time, degree of spreading and asymmetry, which was also used to estimate the transport parameters. A residence time distribution (RTD) can be evaluated by adding a tracer pulse into the system and then getting the tracer concentration at the outlet as a function of time. Then the outlet concentration C(t) was plotted as a function of time, where t is more precisely the elapsed time since the tracer injection. The residence time distribution function, commonly notated by E(t), is given by:

$$E(t) = \frac{C(t)Q(t)}{M} \tag{13}$$

where Q(t) is the flow rate of the system, M is the total mass of tracer injected in the HFCW. The temporal moments around the origin are defined as :

$$\mu_n = \int_0^\infty t^n E(t) \cdot dt \quad n = 0,1,2,3,\ldots \tag{14}$$

where t is, again, the elapsed time since the tracer injection and the subscript n is the order of the moment. The zeroth moment, μ_0, is equal to the mass of solute eluted through the outlet. The first moment, μ_1, characterizes the mean of the BTCs or the mean residence time of the solute in the reactor. In addition to the absolute moments defined above, the central moments, $\mu_n^{'}$, are often used:

$$\mu_n^{'} = \int_0^\infty (t - \mu_1) E(t) \cdot dt \quad n = 0, 1, 2, 3,\ldots \tag{15}$$

In particular, $\mu_2^{'} = \mu_2 - \mu_1^2$ is the variance of the distribution and characterizes its spreading out around the average. $\mu_3^{'}$ characterizes the asymmetry of the distribution and $\mu_4^{'}$ its flatness.

5.1.3. Results and discussions

5.1.3.1. Hydrodynamic verification : The perched water table problem

Kirkland *et al.,* [1992] presented a two-dimensional problem of a developing perched water table surrounded by very dry unsaturated conditions. It is a good test problem to show the variable switching ability in both unsaturated and saturated zones. The problem is described in Figure 31. Water infiltrates with a very large rate into a very dry soil at the initial pressure ψ^0 =-500 m and encounters a clay barrier which allows for the formation of a perched water table. Again this exercise is a very difficult test because of the value of the initial pressure, which induces very sharp pressure gradients. All boundaries are no flow except where the infiltration is imposed. The material properties of the problem are summarized in Table 15 for the Van Genuchten -Mualem parametric model, where K, $\theta_{Sat.}$, $\theta_{Res.}$ are the hydraulic conductivity, the saturated water content, and the residual water content respectively; α and n are the form parameters.

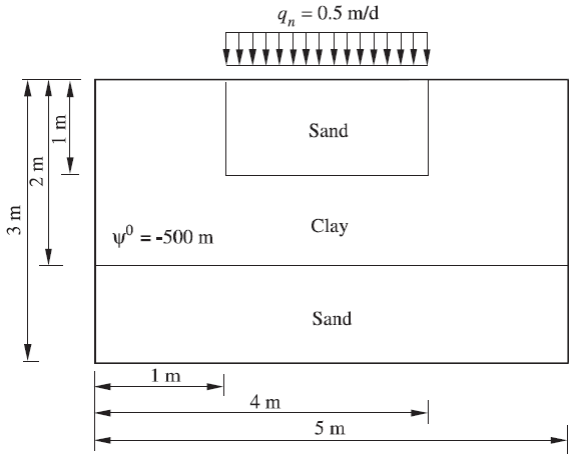

Fig. 31. Perched water table problem

Table 15: Material properties for the perched water problem

Material	K (m/s)	$\theta_{Sat.}$	$\theta_{Res.}$	α(1/m)	n
Sand	$6.26\ 10^{-5}$	0.36	0.08	2.80	2.24
Clay	$1.52\ 10^{-6}$	0.47	0.23	1.04	1.39

A comparison of the model pressure contours (continues lines) at 1-day with Kirkland *et al.*'s results (dispersed marks) reveals a good agreement as displayed in Figure 32 below. All pressure contours agree well. The developed model including the mathematical formulation, the mixed hybrid finite element numerical method and the variable switching technique allows a very good approximation of the hydrodynamic within the porous medium.

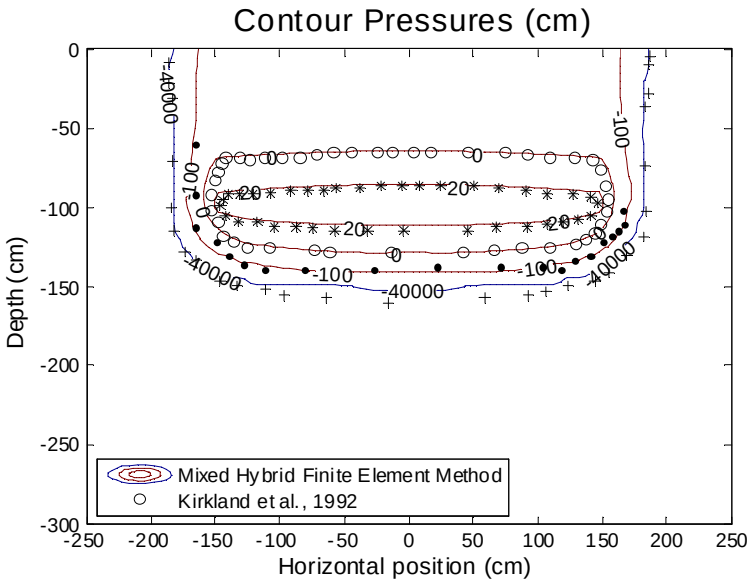

Fig. 32. Simulated pressure contours at t =1 day : pressure head contours in (cm).

5.1.3.2. The steady state condition within the HFCW

Below are presented the studied area (Figure 33) and the domain mesh (Figure 34).

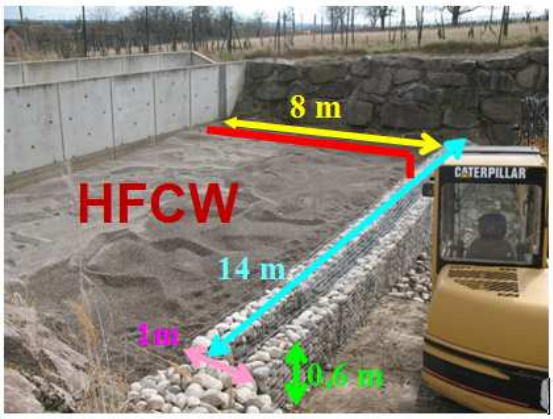

Fig. 33. View of the studied area

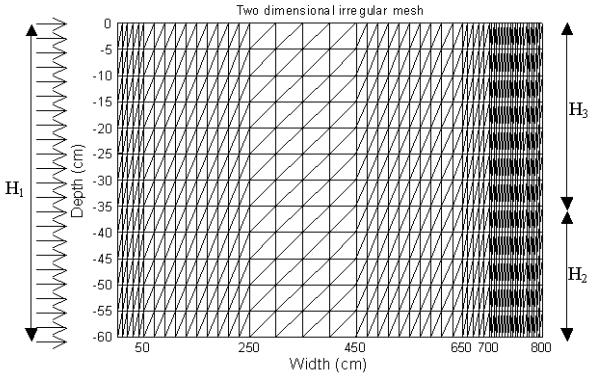

Fig. 34. Domain and boundary conditions.
Inlet : imposed flux (Q = 0.031cm/s);
Outlet : Along H_2, free drainage (if unsaturated condition) then hydrostatic condition (if fully saturated); along H_3, zero flux condition. Initial pressure within all the domain : -60cm

The following Table 16 presents the flow parameters as the analytical expression of the piezometric head and the specific flow rate for the steady state.

Table 16. The analytical expression of the piezometric head and the specific flow rate

H_1 :	height of the inlet-HFCW
H_2 :	height of the outlet-HFCW
S :	HFCW cross section
x :	position along the width
L :	HFCW width
K :	saturated hydraulic conductivity
Q :	specific flow rate : $Q = K.\frac{\left(H_1^2 - H_2^2\right)}{2.L.S}$
H(x) :	piezometric head : $H(x) = \sqrt{H_1^2 - \left(H_1^2 - H_2^2\right).\frac{x}{L}}$

The material properties of the problem are summarized in Table 17 for the Van Genuchten - Mualem parametric model.

Table 17. Material properties for the HFCW media

Material	K (cm/s)	$\theta_{Sat.}$	$\theta_{Res.}$	α(1/cm)	n
gravel	1.0	0.290	0.026	14.10	1.8

Figure 35-a shows the evolution of the saturation within the porous media toward the steady state. At each time, the fully saturated condition are reached in the filter below the 0 cm pressure isoline while the unsaturated condition is present above this isoline. As that can be observed, steady state condition is reached after 5 hours of infiltration. At this time, the numerical simulation reveals a very good agreement with the analytical solution.

The flow direction in the filter for the steady state condition can be observed in figure 35-b. The developed model including the mathematical formulation for fully saturated and unsaturated conditions , and the switching technique between these conditions allows a very good approximation of the hydrodynamic within the porous medium.

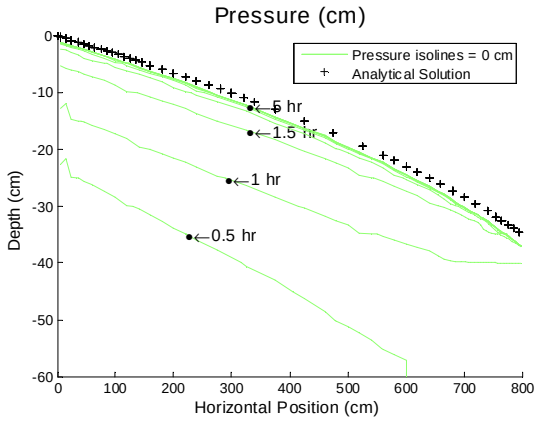

Figure 35-a: Isolines up to the steady state

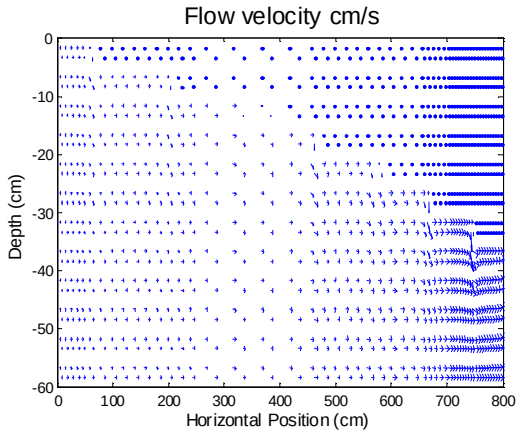

Figure 35-b: Flow velocity for the steady state

Fig. 35. Simulated pressure isolines up to the steady state (a) and flow velocity for the steady state (b)

5.1.3.3. Preferentiel pathway within homogeneous texture

a) Qualitative indicators

- **One dimensional representation of preferential pathways**

Figures 36 below shows the breakthrough curves for each pesticide and for the five cells of the HFCW outlet (boundary H2 in the mesh, see figure 34).

From these curves, three main characteristics could be observed:

- Symmetric and unimodal BTCs when the porous media is considered either without adsorption or with an uniform adsorption distribution. It is seldom the case in field conditions.
- Asymmetric and unimodal BTCs for DIA and HA pesticides.
- Asymmetric and bimodal BTCs for Atrazine, DEA and Metolachlor pesticides.

The non-monotonic behavior (concentrations first increased, then decreased before continuing to increase) common to all chemical solutes represents transport along common preferential flow paths [Jaynes *et al.* 2001]. So that, we are in presence of preferential flow within the HFCW. Preferential flows are due to the heterogeneous adsorption distribution within the porous medium. Moreover, the existence of preferential flow paths can cause temporally separated concentration peaks in response to a single chemical reaction chain, even in a geochemically homogeneous domain, making the interpretation of the concentration curves non-trivial [Mamltrom *et al*., 2008]. Our results are in agreement with Mamltrom *et al* statement. For all the simulated cases, indeed, the HFCW gravel texture is homogeneous. Regarding Cheng *et al.* [2007] results with their experimental tracer tests, the factors affecting

preferential flows include internal and external factors. Internal factors are related to soil characteristics such as soil particle constitution and soil types. External factors include farming methods, irrigation methods and precipitation characteristics. We show in this study the fact that the adsorption distribution is an internal factor which is responsible to the preferential pathway transport in a homogeneous gravel texture.

- **Two dimensional representation of preferential pathways**

For each pesticide the figure 37 below highlights the spatial concentration distribution in the longitudinal section of the horizontal filter. For non-zero adsorption cases, two states are represented: the first state at time t = 2h after the injection and the second state when one concentration peak gets out of the filter.

At time t = 2 hours, at least two spots (peaks) with high concentrations have been formed in the cases where the porous media has a variety of adsorption coefficient. This observation is remarkable even for the case of HA and DIA which present uni-modal breakthrough curves at the output (See Figures 36-e and 36-f and corresponding Figures 37-e and 37-f). Hence, a uni-modal curve is not significant to the absence of preferential flows in the medium. Consequently, two-dimensional display can at least provide sufficient evidence on the presence or absence of preferential pathways.

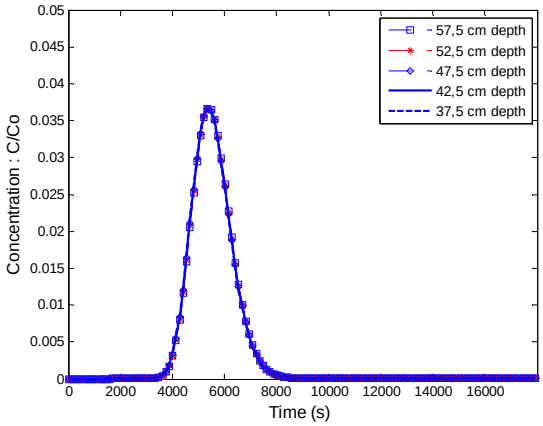

Figure 36-a): No adsorption

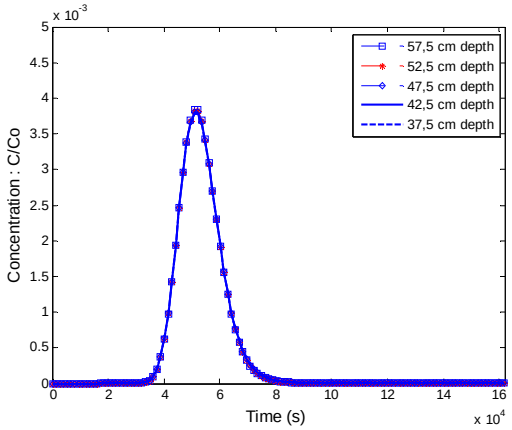

Figure 36-b): Uniform adsorption

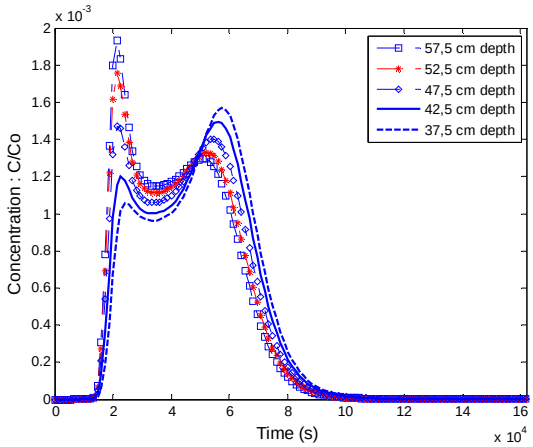

Figure 36-c): Atrazine BTCs

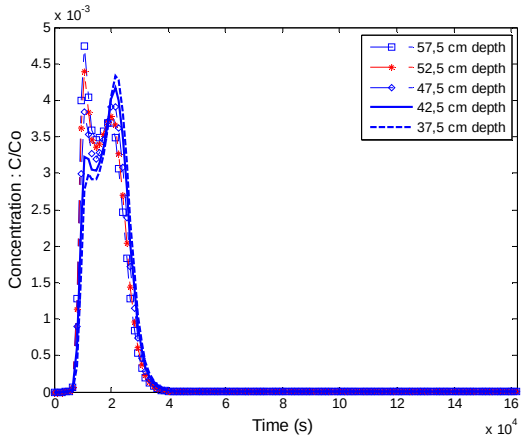

Figure 36-d): DEA BTCs

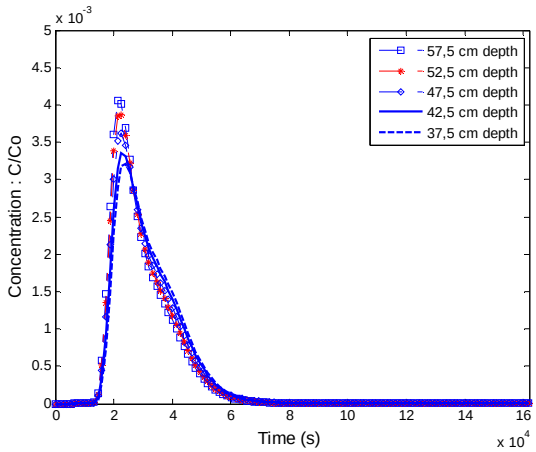

Figure 36-e): DIA BTCs

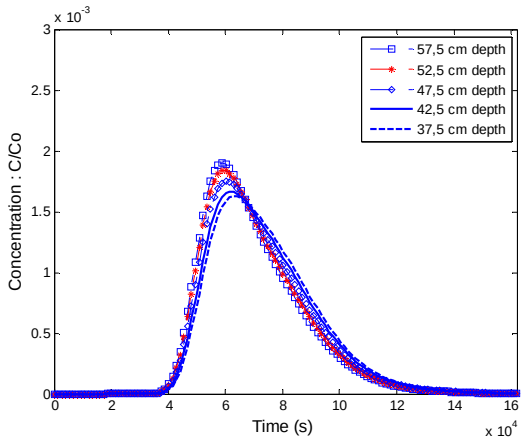

Figure 36-f): HA BTCs

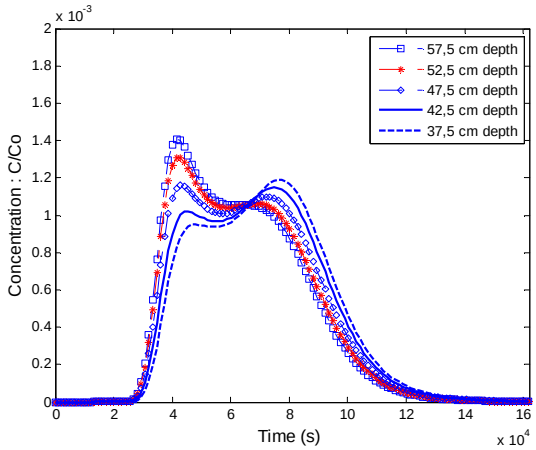

Figure 36-g): Metolachlor BTCs

Fig. 36. The adsorption distribution influence on the Breakthrough Curves (BTCs)

When adsorption is heterogeneous, there is a wide spread of concentration at the bottom of the filter (see figure 37). This fact is caused by a low adsorption in depth, leading to variable mean residence times of pollutant depending on the depth: it is the retardation factor impact on the transport.

The tail of concentration reaches the output with a much more important dilution in the deepest cells (see figures 37). Hence, the second peak of concentration is the weakest at the bottom. This trend is exactly reversed for the first peak. These results are of special importance for horizontal filters instrumentation.

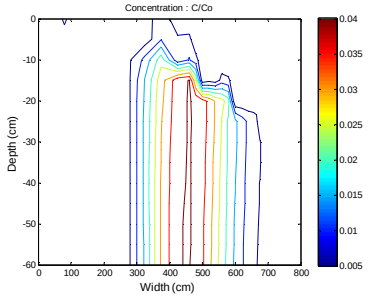

Figure 37-a): No adsorption (2D display)

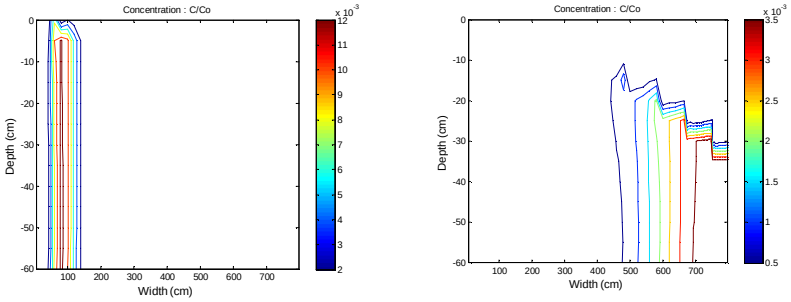

Figure 37-b): Uniform adsorption (2D display)

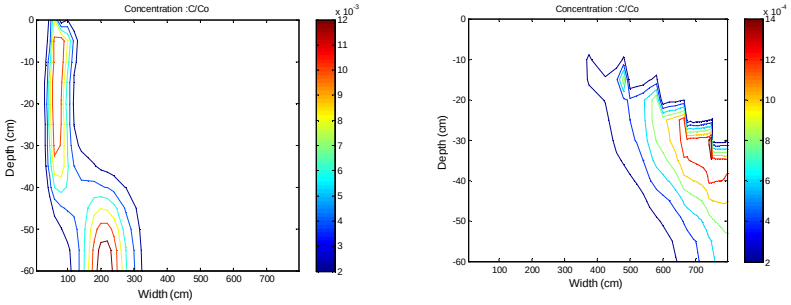

Figure 37-c): Atrazine (2D display)

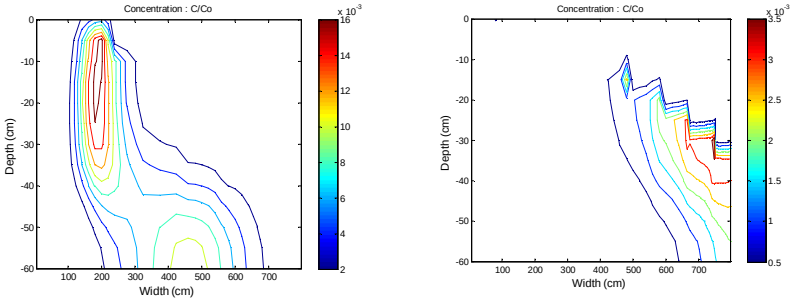

Figure 37-d): DEA (2D display)

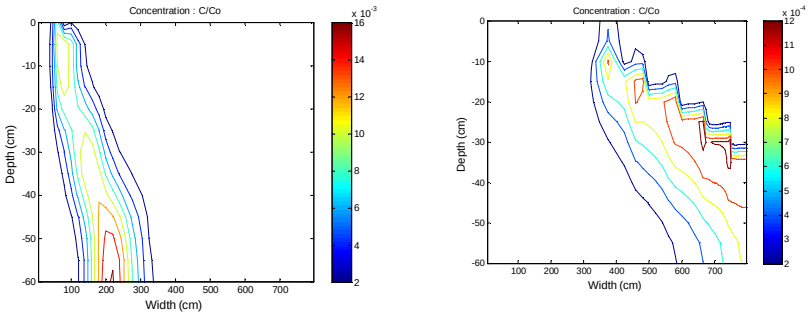

Figure 37-e): DIA (2D display)

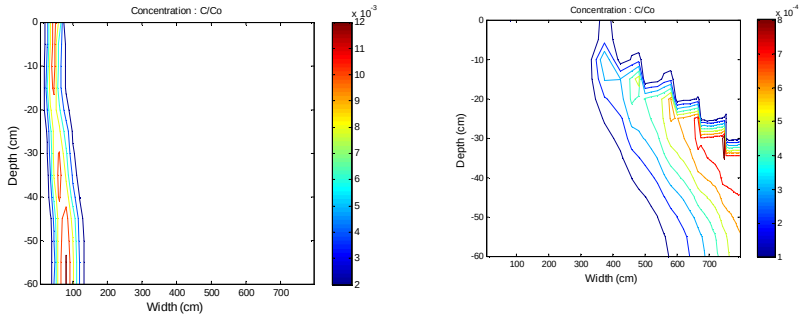

Figure 37-f): HA (2D display)

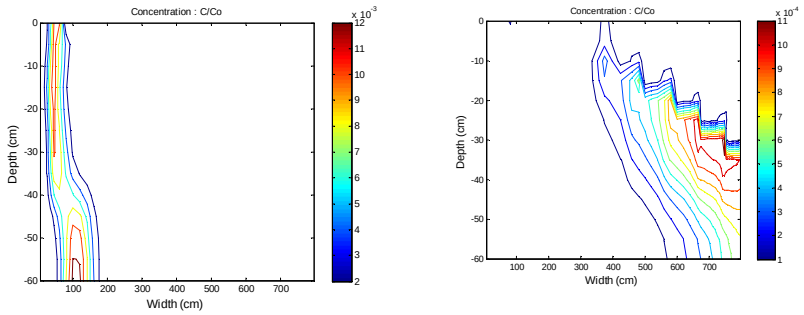

Figure 37-f): Metolachlor (2D display)

Fig. 37. Iso-concentrations - Two dimensional representation of preferential transport left(at time t=2h), right (when the last peak is getting out)

b) Quantitative indices to characterize the extent of preferential flow in soils: the moment analysis

Temporal moments of individual BTC numerical tests were computed to characterize the mean breakthrough time, variance and asymmetry of respective pesticide curves. Preferential pathways are therefore characterized in terms of moments of pesticide BTCs.

The table 18 below shows some physical characteristics related to the adsorption and statistical parameters from the analysis of breakthrough curves.

Table 18. Adsorption parameters and statistical moments

Cases	Mean_Kd	CV	Mean_RT	μ_2'	μ_3'	μ_4'	Peak	Asymmetric[2]
No adsorp.	0	0	5529,6	1	1	1	1	0
Uniform adsorp.	1,37	0	53241	106	2174	20888	1	0
Atrazine	1,26	0,47	46019	508	5440	111046	2	1
DEA	0,4	0,5	18480	70	1471	17962	2	1
DIA	0,88	0,49	30843	190	6014	54846	1	1
HA	2,09	0,28	72056	540	17164	181246	1	1
Metolachlor	1,93	0,36	67265	748	14269	240871	2	1

CV is the variation coefficient reflecting the heterogeneous distribution of adsorption coefficient Kd on the depth of the bed.

[2] 0 for symmetric BTC and 1 for asymmetric BTC

- **Precision of numerical calculation**

The HFCW dimensions, the specific volume (V) of water saturation when the steady state is reached and the feeding rate (Q) allow the theoretical calculation of the hydraulic residence time (T_0).

V = 176.4 cm (specific volume) and T_0 = V/Q is then equal to 1 hour 35 min.

Regarding case 1, the average residence time of water is 5529.6 seconds i.e. 1 hour 32 min, which is indeed very close to the theoretical calculation (with a precision of around 97%).

c) Correlation study : the Partial Least Square (PLS) regression

PLS is a predictive technique which can handle many independent variables, even when there are more predictors than cases and even when predictors display multicollinearity.
The X variables (the predictors) are reduced to principal components, as are the Y variables (the dependents). The components of X are used to predict the scores on the Y components, and the predicted Y component scores are used to predict the actual values of the Y variables. In constructing the principal components of X, the PLS algorithm iteratively maximizes the strength of the relation of successive pairs of X and Y component scores by maximizing the covariance of each X-score with the Y variables.

In the following analysis, the endogenous or dependents variables (Y) are the statistical moments of BTC: Mean_RT, μ_2', μ_3', μ_4'. And the exogenous or the predictors variables (X) are either measured variables or observable variables: CV, Mean_Kd, Mode, asymmetry. The number of factors or axis was determined by the tool PLS selection in Tanagra (a free statistic software: http://eric.univ-lyon2.fr/~ricco/tanagra/fr/tanagra.html) using the Predicted Residual

Sum of Squares and the Residual Sum of Squares. For more information the reader could have a look on (Tenenhaus, 1998)

The coefficients of the table 19 above will assess the contribution of each exogenous variable in explaining the values of the endogenous variable. Hence, if the exogenous for any pesticide are known, the statistic moments of the BTC could be determined.

Table 19. The PLS regression coefficients

X/Y	Mean_RT	μ_2'	μ_3'	μ_4'
Mean_Kd	1.059	0.461	0.176	0.280
CV	0.043	-0.837	-1.552	-1.353
Peak	0.066	0.714	-0.101	0.606
Asymmetric	-0.298	2.054	4.126	3.228
Constant	0.118	-2.488	-2.803	-3.172

However, there is a great difficulty of interpreting the loadings of the exogenous variables because they are based on crossproduct relations with the response variables, which are not based as in conventional factor analysis on correlations among the independent variables.
However, in the first column, we note that the mean residence time is mostly explained by the average value of the adsorption coefficient. It is therefore appropriate to investigate the linear correlation between the mean residence time in the HFCW and predictors (see table 20 below).

Table 20. The determination coefficient between the Mean_RT and the predictors

Mean_RT	Mean_Kd	CV	Peak	Asymmetric
R^2	0.9969	0.0717	0.0755	0.3452

It appears, in particular, a strong correlation between the mean residence time and adsorption coefficient (see figure 38 below). Although this relationship is useful, there is no explanation for the presence of preferential flows. We note the lack of significant impact of the heterogeneity of the medium (CV value) on the statistical moments of BTC.

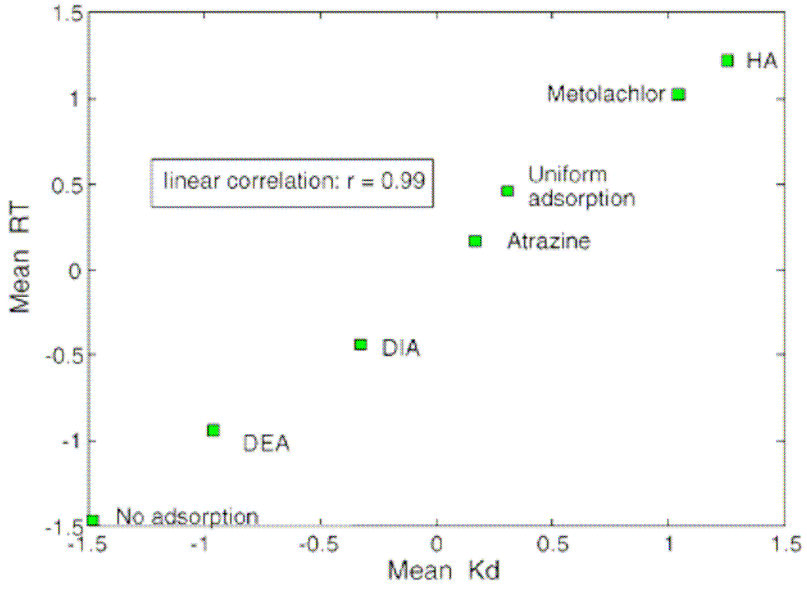

Fig. 38. Linear correlation between the mean RT and the Mean Kd.

The PLS regression also provides orthogonal factorial axes optimized for the explanation of the predicted variables. They are of decreasing signification. The choice of the first 2 axes is relevant and sufficient.

The graph 36 below allows the visualization of the proximities or oppositions between the observable ones and the axes of regression. The table 21 gives the contribution of the exogenous variables in the explanation of the endogenous ones. Hence the importance of the predicted variables (X) in projection are determined.

The variable of adsorption (more precisely the mean Kd value) is very different from the other variables and has an identical contribution on the two factorial axes (see table 21).

Table 21. Variable importance in the projection

Predictors	Axis_1	Axis_2
Mean_Kd	1.6233	1.5137
CV	0.4697	0.7268
Mode	0.4319	0.5634
Asymmetry	0.9786	0.9290

Consequently, the simulated case in absence of adsorption (No adsorption in the figure 39) is opposed to HA and METOLACHLOR molecules, that have the highest coefficient of adsorption.

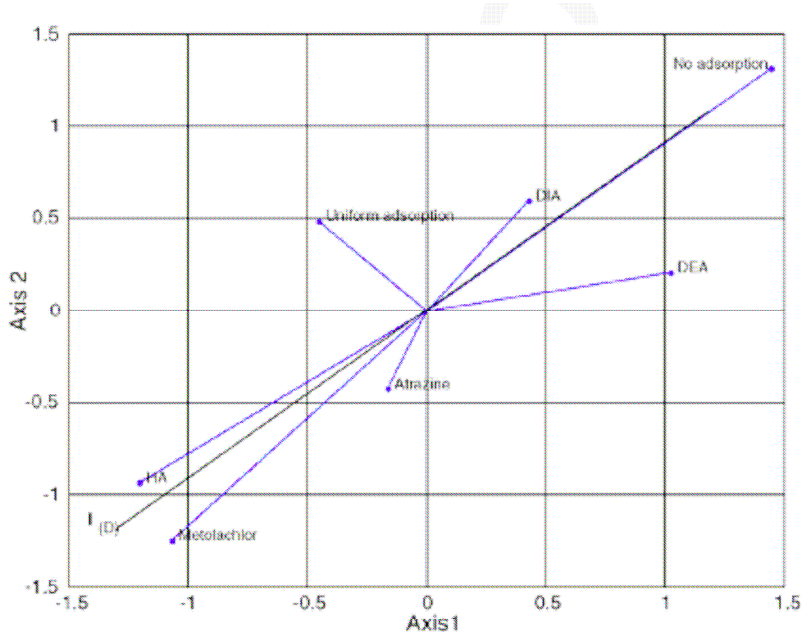

Fig. 39. Biplot for observable distributions on PLS regression axes 1 and 2.

In addition it is notable to note that all the pesticides being located below the (D)-axis induced a bimodal distribution. So that, the study makes possible to perfectly discriminate the number of peaks of concentration, which is related to preferential flows.

5.1.4. Conclusion

Preferential flow is not only a theoretical challenge, but it has a significant importance in enhancing leaching of pollutants from the surface to deeper layers up to groundwater. The danger of groundwater contamination is increased due to this phenomenon. After successful hydrodynamic calibration within the porous medium, numerical transport experiments are conducted in the context of an horizontal flow constructed wetland. Using a two dimensional solute transport in porous media model based on a mixed hybrid finite element approximation, three test modalities are performed:

- Experiment without adsorption, allowing the hydraulic residence time determination (the breakthrough curves are symmetrical with only one mode),
- Experiment with an homogeneous distribution of the linear adsorption coefficient (the breakthrough curves are almost symmetrical with only one mode),
- Experiments with heterogeneous distribution of the linear adsorption coefficient (the breakthrough curves are asymmetrical with either one or two modes according to the rate of the adsorption coefficient dispersion).

The adsorption profiles used are those of five pesticides : Metolachlor, Atrazine and the conversion products (deethylatrazine (DEA), deisopropylatrazine (DIA), hydroxyatrazine (HA)).

The numerical model used to simulate the solute transport was successfully calibrated in a very dry soil. The developed model including the mathematical formulation for fully saturated and unsaturated conditions and the switching technique between these conditions allows a very good approximation of hydrodynamic within the porous medium. These numerical experiments allow us to obtain the following main results. First, the adsorption distribution is a soil internal factor, which is responsible to the preferential pathway transport even in a

homogeneous sand texture. Secondly, a uni-modal BTC curve is not significant to the absence of preferential flow in the medium. Solely, the two-dimensional display can provide very precisely evidence on the presence of preferential pathways. Third, it appears a strong correlation between the mean residence time and the mean value of the adsorption coefficient and it is remarkable that the variation coefficient has not a bigger influence on the transport pathway. Finally, the PLS regression allows to discriminate the number of peaks of concentration of the distribution and confirms that the mean value of Kd is the most influent parameter in this transport problem. The next step will be to confront the results of our analyses with the data collected with the rain events at the Rouffach storm water basin.

5.1.5. References Section 5.1.

Belfort, B., 2006. Modélisation des écoulements en milieux poreux non saturés par la méthode des éléments finis mixtes hybrides. Th. Doct. Univ. Louis Pasteur. Strasbourg, 220pp.

Bouma, J and Dekker, L.W., 1978. A case study on infiltration into dry clay soil. 1. Morphological observations. Geoderma 20, pp. 27–40.

Chavent, G. and Roberts, J.E., 1991. A unified physical presentation of mixed, mixed-hybrid finite elements and standard finite difference approximations for the determination of velocities in waterflow problems. *Adv. Water Resour*., 14, pp. 329-348.

Cheng, J., Zhang, H., Zhang, Y. Shi, Y., He, F., Qi, S and Sun, Y., 2006. Affecting factors of preferential flow in the forest of the three gorges area, yangtze river, journal of soil and water conservation, 20**,** pp. 28–33

Coppola, A., Kutílek, M and Frind, E.O., 2009. Transport in preferential flow domains of the soil porous system: Measurement, interpretation, modelling, and upscaling, Journal of Contaminant Hydrology 104, pp.1-3

Gupta, A., Destouni, G and Jensen, M.B., 1999. Modelling tritium and phosphorous transport by preferential flow in structured soil. J. Contam. Hydrol. 35, pp. 389–407.

Hills, R.G., Wierenga, P.J., Hudson, D.B and Kirkland, M.R.,1991. The second Las Cruces trench experiment: experimental results and two-dimensional flow predictions, Water Resour. Res. 27, pp. 2707–2718

Ippisch, O., Vogel, H.J and Bastian, P., 2006. Validity limits for the van Genuchten-Mualem model and implications for parameter estimation and numerical simulation. *Adv. Water Resour.,* 29, pp. 1780-1789.

Jabro, J.D., Lotse, E.G., Simmons, K.E and Baker, D.E, 1991. A field study of macropore flow under saturated conditions using a bromide tracer. J. Soil Water Conserv. 46, pp. 376–380.

Jaynes, D.B. Ahmed, S.I., Kung, K.-J. S. and Kanwar**,** R. S., 2001. Temporal Dynamics of Preferential Flow to a Subsurface Drain, Soil Sci. Soc. Am. J. 65 , pp.1368–1376.

Kamra, S.K and Lennartz, B., 2005. Quantitative indices to characterize the extent of preferential flow in soils, Environmental Modelling & Software 20, pp. 903-915

Kirkland, M.R., Hills, R.G and Wierenga, P.J., 1992. Algorithms for solving Richards equation for variably saturated soils. *Water Resources Research* 28, pp. 2049-2058.

Kosmas, C., Moustakas, N., Kallianou C and Yassoglou, N., 1991. Cracking patterns, bypass flow and nitrate leaching in Greek irrigated soils. Geoderma 49, pp. 139–152.

Lee, J., Horton, R., Noborio, K and Jaynes, D.B., 2001. Characterization of preferential flow in undisturbed, structured soil columns using a vertical TDR probe, Journal of Contaminant Hydrology 51, pp. 131–144

Malmstrom, M. E., Berglund, S and Jarsjo, J., 2008. Combined effects of spatially variable flow and mineralogy on the attenuation of acid mine drainage in groundwater, Applied Geochemistry 23, pp. 1419–1436.

Mosaddeghi, M.R., Mahboubi, A.A., Zandsalimi, S and Unc. A., 2008. Influence of organic waste type and soil structure on the bacterial filtration rates in unsaturated intact soil columns, Journal of Environmental Management, doi:10.1016/j.jenvman.2008.01.009.

Mosé, R., Siegel, P., Ackerer, P and Chavent, G., 1994. Application of the mixed hybrid finite element approximation in a groundwater flow model: Luxury or necessity?. *Water Resour. Res.,* 30, pp. 3001-3012.

Nayagum, D., 2001. Simulation numérique de la pollution du sous-sol par les produits pétroliers et dérives : Application au cas d'un écoulement diphasique monodimensionnel, Th. Doct. Univ. Louis Pasteur. Strasbourg, 151 pp.

Ohrstrom, P., Hamed, Y., Persson, M. and Berndtsson, R., 2004. Characterizing unsaturated solute transport by simultaneous use of dye and bromide, Journal of Hydrology 289, pp. 23–35

Raviart, P.A and Thomas, J.M., 1977. A mixed finite method for the second order elliptic problems., pp. 292-315 In Galligani I., Magenes, E., (ed.). Mathematical aspects of the finite element methods, Lecture Notes in Math 606, Springer: New York.

Reichenberger, S., Amelung, W., Laabs, V., Pinto, A., Totsche, K.U and Zech, W., 2002 Pesticide displacement along preferential flow pathways in a Brazilian Oxisol, Geoderma 110, pp. 63– 86

Rosqvist, H and Destouni, G., 2000. Solute transport through preferential pathways in municipal solid waste, J.Contam. Hydrol. 46, pp. 39–60

Simic, E and Destouni, G., 1999. Water and solute residence times in a catchment: stochastic–mechanistic model interpretation of 18O transport. Water Resour. Res. 35, pp. 2109–2119.

Smith, S.J and Davis, R.J., 1974. Relative movement of bromide and nitrate through soils. J. Environ. Qual. 3, pp. 152–155.

Suliman, F., French, H.K., Haugen, L.E., Sovik, A.K., 2006. Change in flow and transport patterns in horizontal subsurface flow constructed wetlands as a result of biological growth, ecological engineering 2 7, pp. 124–133

Tenenhaus, M., 1998. PLS regression - Theory and application *Editions Technip, Paris,* 254 *pp*. 320 F. *ISBN* 2-7108-0735-1

Vryzas, Z., Vassiliou, G., Alexoudis, C and Papadopoulou-Mourkidou, E., 2007. Kinetics and adsorption of metolachlor and atrazine and the conversion products (deethylatrazine, deisopropylatrazine, hydroxyatrazine) in the soil profile of a river basin, European Journal of Soil Science, 58, pp. 1186 – 1199.

Yasuda, H., Berndtsson, Persson, R.H., Bahri, A and Takuma, K., 2001. Characterizing preferential transport during flood irrigation of a heavy clay soil using the dye Vitasyn Blau. Geoderma 100, pp. 49–66.

Younes, A., Mose, R., Ackerer, P and Chavent, G., 1999. A new formulation of the mixed finite element method for solving elliptic and parabolic PDE with triangular elements, *J. Comput. Phys.,* 149, pp. 148-167.

Section 5.2. A new empirical law to accurately predict solute retention capacity within horizontal flow constructed wetlands (HFCW)

Adrien wanko[3a] Gabriela Tapia[b] Robert Mosé[a] Caroline Gregoire[b]

[a] *Urban Hydraulic Systems* – IMFS - UdS / CNRS

2 rue Boussingault 67000 STRASBOURG ,

[b] UMR7517/LyGes Laboratoire d'Hydrologie et de Géochimie de Strasbourg – UdS/CNRS
1 rue Blessig 67084 STRASBOURG CEDEX

Abstract

Constructed wetlands are being considered as a sustainable and promising option, whose performance, cost and resources utilization can complement or replace conventional water treatment. The literature reported the fact that an insufficient residence time of pollutants in soils induces an incomplete and unfinished biodegradation process. In this work, engineering solutions are proposed with the objective of significantly increasing the solute retention capacity in the horizontal flow constructed wetland (HFCW). Using several numerical tracers experiments with different operating scenarios, such as the HFCW physical configuration, the flow rate, the boundary conditions, the adsorption layer thickness, practical methods and a new empirical law are suggested in order to substantially increase the adsorption ability in the HFCW, and hence the pollutant removal. Furthermore, it appears that there is no impact of the adsorbent layer thickness on the solute mean residence time with high values of adsorption coefficient (K_d). For smaller K_d values, the deeper the adsorption layer thickness, the higher the retention time.

Key words : Adsorption layer; Constructed wetland; Empirical law; Modeling; Pollutant; Tracer experiment

5.2.1. Introduction

Over the last decades, interest in the optimization of the biological, physical, and chemical processes that occur in natural wetland systems as an option for wastewater treatment has significantly increased [Mitsch, 1995; Bavor et al., 1995; Mitchell et al., 1995; Gopal and Mitsch, 1995; Shutes, 2001]. Constructed wetlands (CWs) are engineered systems that have been designed and constructed to utilize the natural processes involving wetland vegetation, soils, and the associated microbial assemblages to assist in treating wastewaters [Vymazal *et.al.*, 2006]. Constructed wetlands are being considered a sustainable and promising option, whose performance, cost and resources utilization can complement or replace conventional water treatment [Tack et al., 2007; Arias and Brown, 2009; Zhang et al.,

[3] Corresponding author : awanko@engees.u-strasbg.fr, Tel : 00 (33) 88 24 82 87, Fax : 00 (33) 88 24 82 83

2009]. Vymazal and Kröpfelová [2008] presented a list of examples of the use of constructed wetlands for the treatment of different types of pollution. The abilities of constructed wetlands to improve water quality are widely recognized, and their efficiency reducing suspended solids, biological oxygen demand, nitrogen, phosphorus, trace metal, toxic organic compounds, pathogens and other pollutants has been reported in several studies [Jing et al., 2001; Ye et al., 2001; Lim et al., 2003; Karathanasis et al., 2003; Huett et al., 2005; Vymazal, 2007; Vymazal and Kröpfelová, 2009, Khan et al., 2009, Kröpfelová et al., 2009; Tang et al., 2009].

As plant and microorganism efficiency is inconsistent through the seasons, residence time within constructed wetland is sometimes too short to achieve organic compounds breakdown by micro-organisms or metal uptake by plants [Huguenot et al., 2010]. Hence, most of the time, pollutants are not properly retained in constructed wetland because the adsorption kinetic is usually to slow compared to the hydraulic retention time. An insufficient residence time of pollutants in soils induces an incomplete and unfinished biodegradation process [Wanko et al., 2009]. To alleviate this phenomenon, a potentially relevant method related to the addition of sorbing materials [Alkan and Dogan, 2001; Shen and Duvnjak, 2005; Altundogan et al., 2007; Veli and Alyuz, 2007; Ahmaruzzaman, 2008, in Huguenot et al. 2010] could be used. The sorbing material should increase the solute retention capacity on the top of the constructed wetland, hence promoting the pollutant transfer from the liquid to the solid phase, thus avoiding the discharge of polluted water. Increased pesticide residence time in constructed wetland is then expected to be suitable for biological treatment. An optimal residence time distribution will allow pollutants fixation in the soil, so their concentration could be reduced according to various degradation processes. Therefore, an hydraulic management of the constructed wetland can be suggested in relation with the time of pollutant degradation.

The aim of this paper, in order to optimize the solute retention capacity in CWs, particularly in horizontal flow constructed wetlands (HFCWs), is to identify key performance parameters and provide engineering solutions. Using the model, numerical tracer tests to simulate several HFCW operation scenarios were performed. After working on the adsorption distribution impact on preferential flow in HFCWs [Wanko et al., 2009], practical methods and a new empirical law are suggested in order to significantly increase the solute retention capacity in HFCWs.

5.2.2. Material and methods

5.2.2.1. Description of the study area

In order to study treatment potentialities to mitigate non-point source pesticide pollution in constructed wetland systems, the European LIFE ENVIRONMENT Project Artwet (LIFE 06 ENV/F/000133) implement mitigation solutions at six demonstration and experimental sites. The project includes a storm water basin located in Alsace, France. This hydraulic structure is placed at the rural/urban interface, and at the bottom of vineyard hills. It concentrates all the contaminated hydrological surface flows, and it allows the accumulation of the sediments that are transported from the parcels. Initially the stormwater basin was used for regulation flow proposes. In order to optimizate the pesticides mitigation processes, an HFCW was constructed inside the stormwater basin (see figure 40).

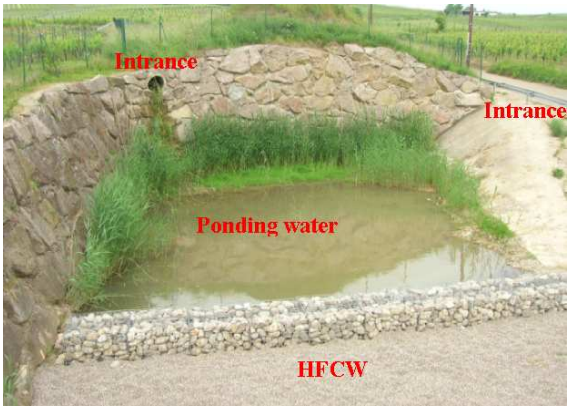

Fig. 40. An HFCW within a storm water basin

Pesticide mitigation has already been observed, but effectiveness still has to be demonstrated for weakly and moderately sorbing compounds [Reichenberger et al., 2007]. Hence pesticides are frequently detected at storm basins outlet.

Pesticide sorption on storm basin sediments was already demonstrated with atrazine [Tao and Tang, 2004]. Low cost mineral and organic sorbents for metals [Bailey et al., 1999; Kurniawan et al., 2006] and organic compounds [Ahmaruzzaman, 2008] are required for such rustic treatment plants. Recently, attention has been paid to agricultural waste materials [Swami and Buddhi, 2006; Sud et al., 2008]. Several studies have been carried out on copper [Kurniawan et al., 2006], fewer on herbicides such as glyphosate [Akhtar et al., 2007] diuron [Fernandez-Bayo et al., 2008].

5.2.2.2. The governing equations

To have a better understanding of the hydrodynamics and transport in this experimental site, a 2D numerical model was developed. The use of a two-dimensional model is justified by the need to take into account the heterogeneities of the medium and the initial conditions, like heterogeneity of water content and high local concentrations on the infiltration surface.

The hydrodynamic system is simulated by the application of Richards' equation (1). This formulation physically describes the flow in a variably saturated porous medium.

$$C(h)\frac{\partial h}{\partial t} = \nabla[K\nabla(h+z)] + W(x,z,t) \quad (1)$$

Where: W(x,z,t) is the sink/source terms [T^{-1}],
x and z (depth) are the spatial coordinates [L],
t is time [T],
C(h) is the soil moisture capacity [L^{-1}],
K is the unsaturated hydraulic conductivity [LT^{-1}],
h is the soil water pressure head [L].

The solute transport is described by a classical advection-dispersion equation (2) with the presence of sink/source term, which takes into account the pesticide degradation.

$$\frac{\partial(\theta C)}{\partial t} + \frac{\partial(\rho S)}{\partial t} - \nabla(\theta D\nabla C) + \nabla\left(\vec{q}\,C\right) = f(x,z,t) \quad (2)$$

Where: f(x,z,t) is the sink/source terms [$ML^{-3}T^{-1}$],
C is solution concentration [ML^{-3}],
S is absorbed concentration [MM^{-1}],
ρ is soil bulk density [ML^{-3}],
t is time [T],
$\vec{q}$ is volumetric flux [LT^{-1}],
D is the dispersion tensor [L^2T^{-1}],
and θ is soil volumetric water content [L^3L^{-3}].

The numerical tool used to solve these equations is the mixed hybrid finite element method (MHFEM). The readers who are interested by the 2D model development and verification, the mixed hybrid finite element used as numerical method and the time moment analysis should read the previous article Wanko *et al.* [2009].

5.2.3. Results and discussion

5.2.3.1. The steady state condition within the HFCW

a)- Hydrodynamic verification: 2D heterogeneous (nine block) and dry soil

Model verification was performed by comparing the reference results with those computed for two-dimensional flow cases in variably saturated porous media. The test region was 500 cm wide by 30 cm deep, and it was divided into nine alternating blocks of clay and sand (Materials C and D). A constant flux of 5 cm day^{-1} was applied to the top center 100 cm of the domain and a non-flux boundary condition was applied elsewhere (Figure 41). Figure 42 shows a comparison between the reference [Kirkland, 1992] and calculated results for an infiltration problem in heterogeneous (nine blocks) and very drying soil (Initial pressure: -500 m).

The good match obtained not only confirms the validity of the numerical method applied, but it also shows the robustness of the method to give a solution for heterogeneous soils with abruptly changing wetness conditions.

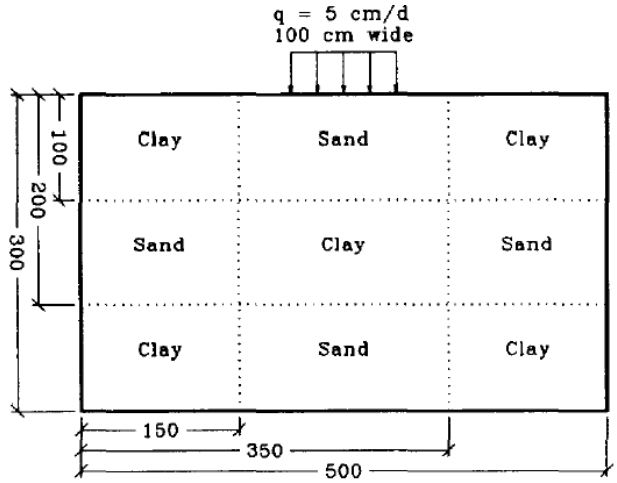

Fig. 41. Boundary conditions: 9 blocks problem.
Unsaturated soil. Zero flux boundary conditions except as noted. All dimensions are in centimeters.

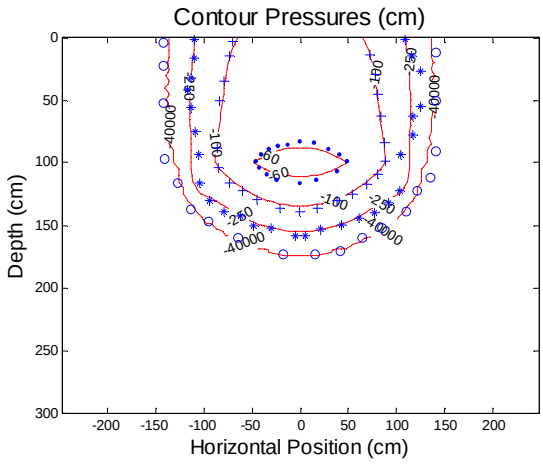

Fig. 42. Contour pressures 9 blocks problem.
12.5-day simulation, -50 000 cm initial pressure, continuous lines (MHFEM) and mark (Kirkland et al.'s results, 1992)

b)- Study cases: Initial and boundaries conditions

The hydraulic load is added to the system as a Neumann boundary condition on all left side edges. The output of the system is located in the base-right side edges. Zero flux condition is considered in all the rest of boundary edges. Below are presented the studied area (Figure 43) and the domain mesh (Figure 44). For all cases, hydrodynamic simulation was performed until the system reaches the steady state.

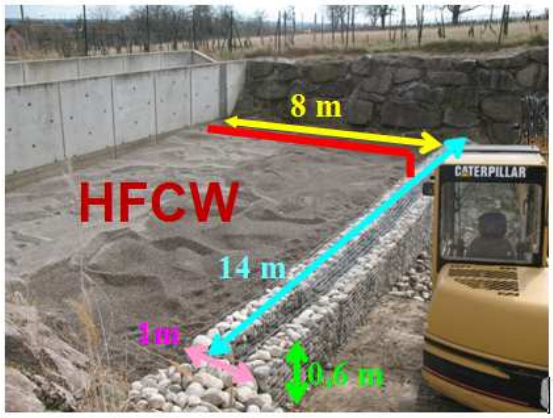

Fig. 43. View of the studied area

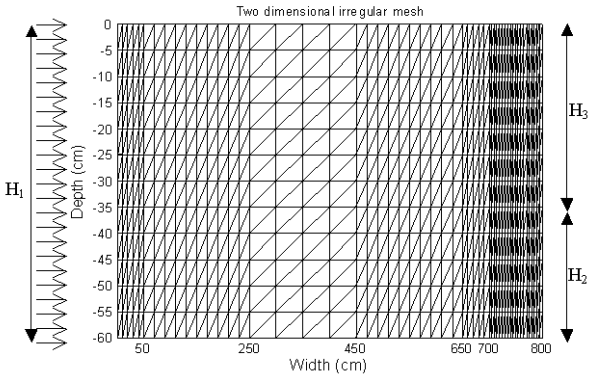

Fig. 44. Domain and boundary conditions

Inlet : imposed flux (Q);

Outlet : Along H_2, free drainage (if unsaturated condition) then hydrostatic condition (if fully saturated); along H_3, zero flux condition. Initial pressure within all the domain : -60cm

Table 22 presents the flow parameters as the analytical expression of the piezometric head and the specific flow rate for the steady state.

Table 22. The analytical expression of the piezometric head and the specific flow rate

H_1 :	Height of the inlet-HFCW
H_2 :	Height of the outlet-HFCW
S :	HFCW cross section
x :	Position along the width

L :	HFCW width
K :	saturated hydraulic conductivity
Q :	specific flow rate : $Q = K.\frac{\left(H_1^2 - H_2^2\right)}{2.L.S}$
H(x) :	piezometric head : $H(x) = \sqrt{H_1^2 - \left(H_1^2 - H_2^2\right).\frac{x}{L}}$

The material properties of the problem are summarized in Table 23 for the Van Genuchten - Mualem parametric model. Where K, θ_{Sat}, θ_{Res}, are the hydraulic conductivity, the saturated water content, and the residual water content, respectively; α and n are the form parameters.

Table 23. Material properties for the HFCW media

Material	K (cm/s)	$\theta_{Sat.}$	$\theta_{Res.}$	α(1/cm)	n
gravel	1.0	0.290	0.026	14.10	1.8

c)- Steady state conditions for different hydraulic conditions

Hydrodynamic simulations were performed using different hydraulic loads in order to achieve steady state for output length of 25, 15 and 5 cm. These different heights correspond to different opening possibilities at the outlet of the experimental site (see figure 44). Figure 45 shows the hydrodynamic evolution through time until steady state is reached. For each case, the fully saturated condition are reached in the filter below the 0 cm pressure isoline while the unsaturated condition is present above this isoline. In general, for all the cases, the steady state condition is reached after 5 hours of infiltration. At this time, the numerical simulation reveals a very good agreement with the analytical solution. The developed model including the mathematical formulation for fully saturated and unsaturated conditions, and the switching technique between these conditions allows a very good approximation of the hydrodynamic within the porous medium.

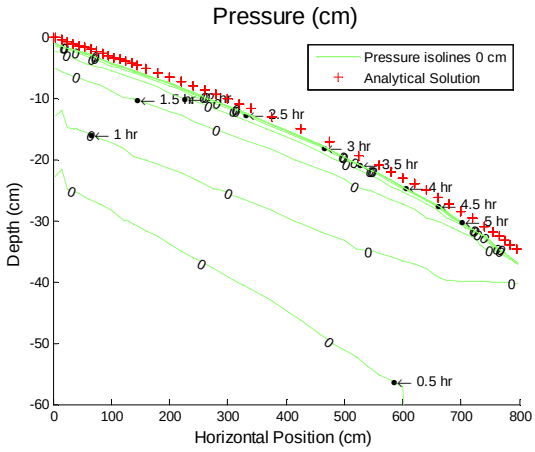

a) Output H_2 = 25 cm; Q = 0.031 cm/s

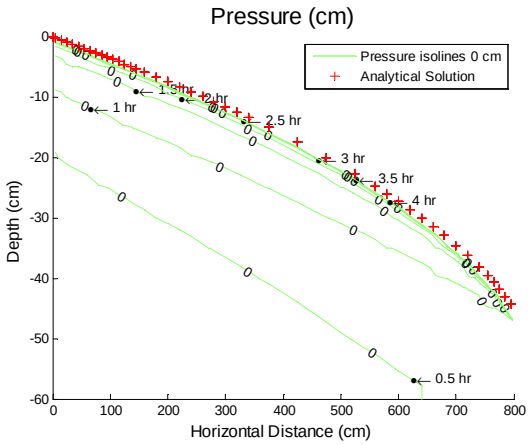

b) Output H_2 = 15 cm; Q = 0.035 cm/s

Fig. 45. Simulated pressure isolines up to the steady state for different hydraulic conditions

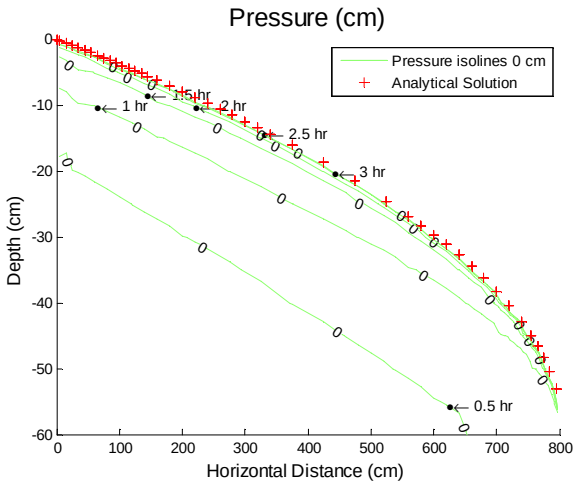

c) Output H_2 = 5 cm; Q = 0.037 cm/s

5.2.3.2. Choosing a suitable operation conditions for the HFCW

Once that hydrodynamic steady state conditions are reached in the system, several constructed wetland operation scenarios were simulated using numerical conservative tracer experiments. The residence time distribution is the system response to an instantaneous injection of a concentrated inert tracer. To reproduce this condition in the model, simulations of the solute transport were performed considering a zero initial concentration. The tracer is injected during the first 10 time steps of simulation as a Neumann boundary condition in all left boundary edges. Wanko et al [2009] presents the equations allow the time moment analysis calculations.

Table 24 compares mean residence times calculated for different cases with the same tracer mass input at different flow rates and output height hence pressure profiles. These cases consider no adsorption in soil.

Table 24. Mean Residence time for different cases considering no adsorption

Output height	Flow rate Q	Mean Residence Time
25 cm	0.031 cm/s	5512 sec
15 cm	0.035 cm/s	4586 sec
15 cm	0.031 cm/s	4924 sec
5 cm	0.037 cm/s	4198 sec
5 cm	0.031 cm/s	4199 sec

a)- Fixed flow rate for different output height

In the cases where the same flow rate (0.031 cm/s) and tracer mass input were used for different output height (25cm, 15cm, 5cm), we observed that contrary to what would be expected, the mean residence time is larger when the output height is bigger not when it is smaller. When the output height is the smallest, the effective flow volume below the zero isoline pressure is the smallest (see figure 45), hence the solute is less diluted, giving as result a smaller mean residence time.

b)- Fixed output height for different flow rates

In the cases with same output height but different hydraulic load a shorter mean residence time distribution was observed when increasing the hydraulic load as it was expected. However, the output height becomes a limiting factor when it is small and hydraulic load has no more effect in the mean residence time (see case of 5 cm).

Optimal operation conditions for the artificial wetland are those that allow a mean residence time of the pollutant higher than its half live. The higher mean residence time for the test cases was obtained when the output height is 25 cm and the hydraulic load (flow rate) is 0.031 cm/s. If the residence time is not sufficient, suitable additional materials could be added in HFCW in order to increase it. Thus, it would be interesting to test for the chosen hydraulic condition (figure 45 a), what would be the impact on the residence time due to the localization of an adsorption layer.

5.2.3.3. Improving solute storage capacities within HFCWs – the adsorption layer location

A sensibility analysis was performed in order to determinate the feasibility to locate a vertical or horizontal adsorption layer (Figure 46).

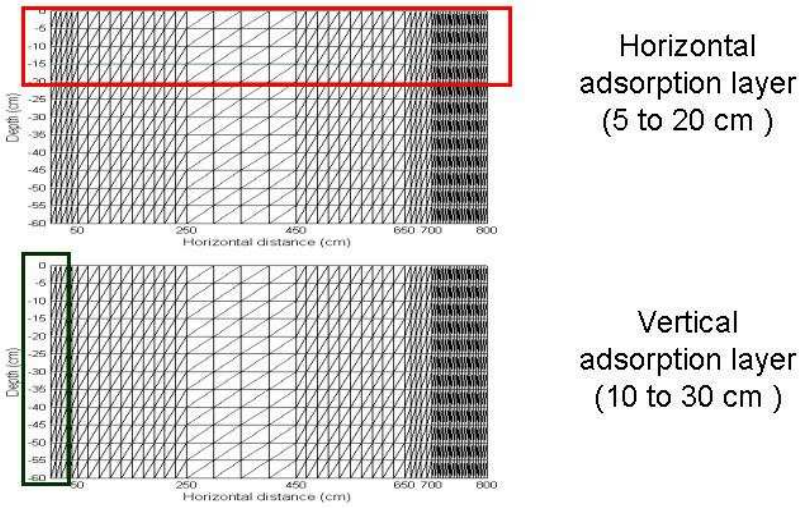

Fig. 46. Adsorption layer localization

The parameter observed to determine the impact of the adsorption layer was the percentage of retention given by the following equation:

$$\%\ \text{retention} = \frac{\text{Input tracer mass} - Q_{output} \cdot C_{output}}{\text{Input tracer mass}} \times 100 \qquad (3)$$

where Q_{output} and C_{output} are the flow rate and the solute concentration at the output respectively.

Table 25. Feasibility in the localization of an adsorption layer

Localization	Adsorption layer thickness	% Mass retention	Mean Residence Time (s)
Horizontal	10 cm	4	10853
	20 cm	27	12964
Vertical	10 cm	0.0	8620
	20 cm	0.0	11698
	30 cm	0.0	14777

Results shown in Table 25 above were calculated using an adsorption coefficient (K_d=S/C) equal to 5.3 L kg^{-1} and a soil bulk density ρ_s equal to 1.80 g cm^{-3}. According to these results the mean residence time increases logically when increasing the adsorption layer thickness. However, for a vertical adsorption layer the percentage of retention remains constant and equal to zero, in contrast to the adsorption layer located horizontally. Indeed, for vertical layer, almost all the adsorbent layer is located below the hydrostatic water level (0 pressure iso-line see figure 45) in the gravel filter. In this case, as K_d is associated a reversible adsorption, there is no retention for the cases. This layer will simply introduce a retardation in the mass transfer. For the horizontal layer, the situation is different because in this case, the sorbent layer is partly located in the vadose zone, associated with very low velocities and hence contributes to the creation of retention. Due to no retention for the vertical sorbent layers, we will in the following consider the horizontal sorbent layer cases.

5.2.3.4. A Law for solute retention capacity

Using the model, forty numerical tracer experiments have been performed in order to propose a new law for solute retention capacities within HFCW. For the same flow rate and output height, four different adsorption layers depth (20cm, 15cm, 10cm, 5cm) were tested. For each adsorption layer, ten different adsorption coefficient (K_d) values were used (0.0 to 810 L/kg, the high values of K_d allow to obtain the trend).

a)- The adsorption layer thickness effect on the residence time

First of all, it is important to explain the fact that in general the residence time is defined for conservative tracers, that means for zero solute retention within the constructed wetland. In this numerical study, non conservative tracers were used, hence the residence time distribution was considered only for the solute that flow out the filter. The figure 47 shows the mean residence time depending on both the adsorption layer thickness and the K_d values.

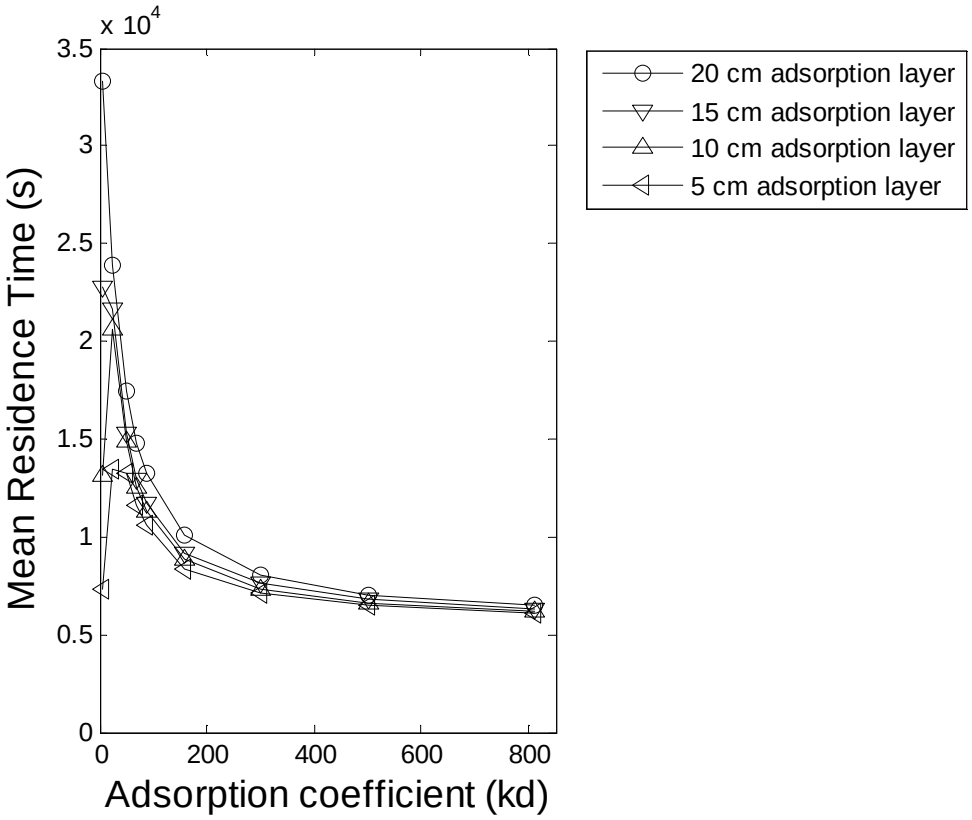

Fig. 47. Mean Residence Time distribution in an horizontal adsorption layer

Three important behaviors could be highlighted from these tested cases:

- For the different adsorption layer tested, the mean residence times are similar when the K_d values are very high. Hence, there is no impact of the adsorption layer thickness with high K_d values. Indeed, higher the K_d value is, the more readily the species are sorbed to the soil surface. A high K_d value provides an estimate of the maximum concentration of a solute sorbed to the soil. Due to the saturated water content θ_{Sat}, the solute sorbed mass is limited. Hence the mean residence time will become constant for high K_d value.
- For smaller K_d values, we observe that the deeper the adsorption layers' thickness is, the higher the retention time is. This is physically understandable; in fact the adsorption site will increase with the thickness. It is noticeable that the retention times growth with the K_d values, reach their maximum and then decrease. These behaviors are present for 5 cm and 10 cm adsorption layer thickness. In fact smaller K_d values assume that the soil has little or no ability to slow solute movement. Consequently, the solute would travel in the direction and at the rate of the water. The zero K_d value

corresponds to the most conservative solute, hence the minimum mean residence time distribution.

- For 15 cm and 20 cm adsorption layer thickness, the mean retention times appear to be strictly decreasing on the figure for the chosen K_d values. In fact there is also a maximum, which is in this case obtained for very close to zero K_d values.

When performing the treatment of wastewater inside the HFCW, there is a significant interaction effect between the different adsorption layer thicknesses and the retention time. Moreover there is no significant impact of the thickness for high K_d values.

b)- Solute retention capacities (SRC) and adsorption layer thickness

Figure 48 shows the trend of the retention capacities when Kd varies for each adsorption layer thickness. The simulations were obtained with an output height of 25 cm. The empirical law constructed below was derived using only the data from this case.

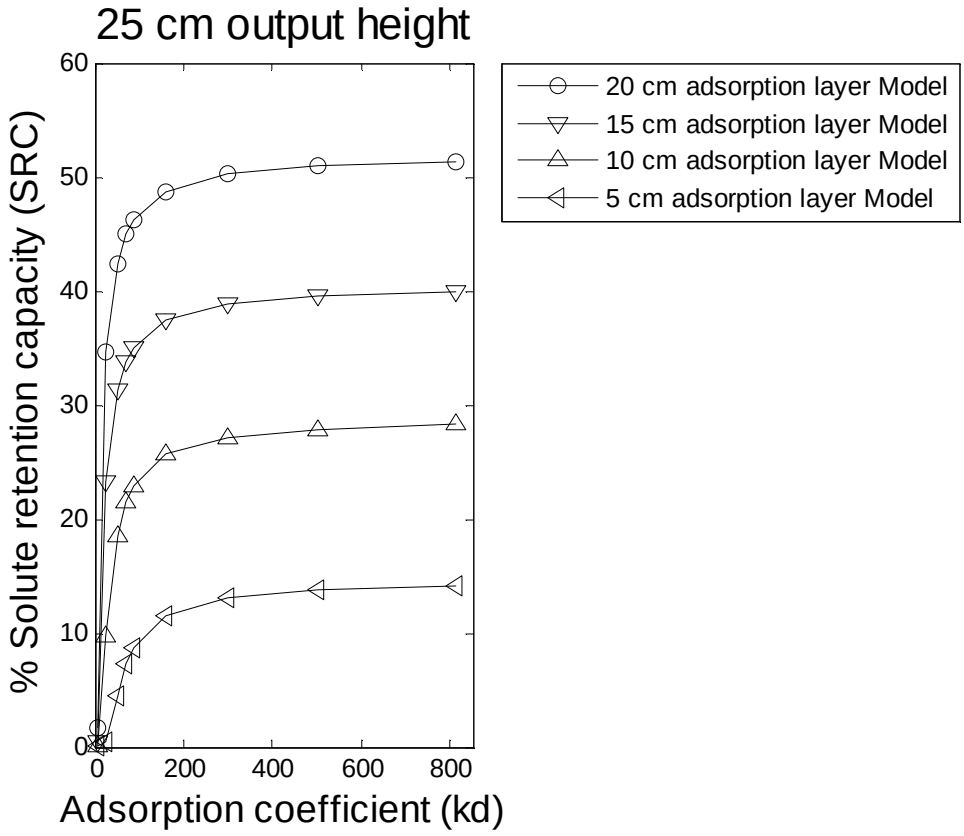

Fig. 48. Solute retention capacity – 25cm output height

We observe an exponential growth of the retention capacity with a maximum reached for each thickness. As it was expected, the higher the adsorption layer thickness is, the higher the maximum retention capacity value gets. Hence we are able to propose a new empirical law for retention capacities within HFCW that takes into account the flow rate, the output height, the adsorption layer thickness, and the saturated water volume inside the wetland. The solute retention capacity curves for each of the different adsorption layer thickness have a similar profile that can be obtained using the following equation using an exponential decay fitting:

$$SRC = A_i + B_i \cdot \exp(-K_d/C_j) \tag{4}$$

Where Ai, Bi are constants related with the layer thickness L_i [L] and Cj [-] is a constant related to the fixed hydraulic conditions (the flow rate Q_j [L^2T^{-1}] and the outlet height h_j [L]). This empirical equation allow the calculation of the solute retention capacity within an HFCW, for a given layer thickness L_i, fixed hydraulic conditions (Q_j ,h_j) and any adsorption coefficient K_d.

Using a statistical analysis with the above constants and the simulation data, equation (4) is rewritten as follow:

$$SRC = 156{,}67 \cdot \left(\frac{L_i}{H}\right) \cdot \left[1 - \exp(-K_d/C_j)\right] \tag{5}$$

where :

L_i The thickness of the adsorption layer [L],

H The total height of the HFCW [L],

$1/C_j$ Coefficient strongly correlated with the total water content (V_j) under the water table level (zero pressure line) within the HFCW;

Vj
$$V_j = \theta_{Sat} \cdot \int_0^{W=8m} H_j(x) \cdot dx \tag{6}$$

$$\frac{1}{C_j} = 52{,}49 \cdot \ln(V_j) + 7{,}64 \tag{7}$$

where $H_j(x)$ is the water table level (zero pressure isoline) associated to the fixed hydraulic conditions (Q_j, h_j). W [L] is the width of the domain. V_j [L^2]

depends on the hydraulic conditions (Qj, hj). Different (Qj, hj) couples allow to fit Eq. (7) with a determination coefficient $R^2 = 0.99$

c)- Empirical law interpretation

Knowing the thickness of the adsorption layer, and the physical and hydraulic parameter of the HFCW, the purpose mathematical relation makes possible the calculation of the solute retention capacity (SRC) for any adsorption coefficient. This empirical law should have a great importance for waste water treatment. In fact, the treatment capacity inside the HFCW will always be smaller than the solute retention capacity.

5.2.3.5. Empirical law verification and validation

Using numerical tracers experiments with different hydraulic conditions (flow rate and outlet height), the solute retention capacities are calculated using Eq. (3) and the results are compared with those obtained by the proposed empirical law (Fig. 49).

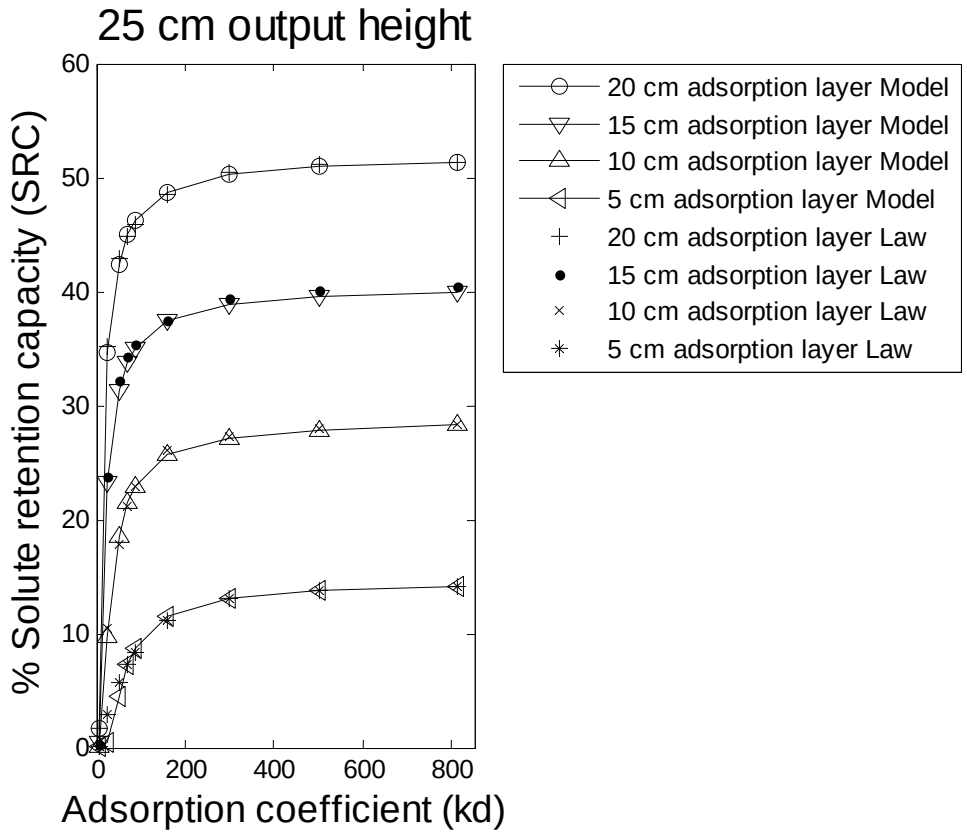

Figure a): empirical law validation – 25 cm output height

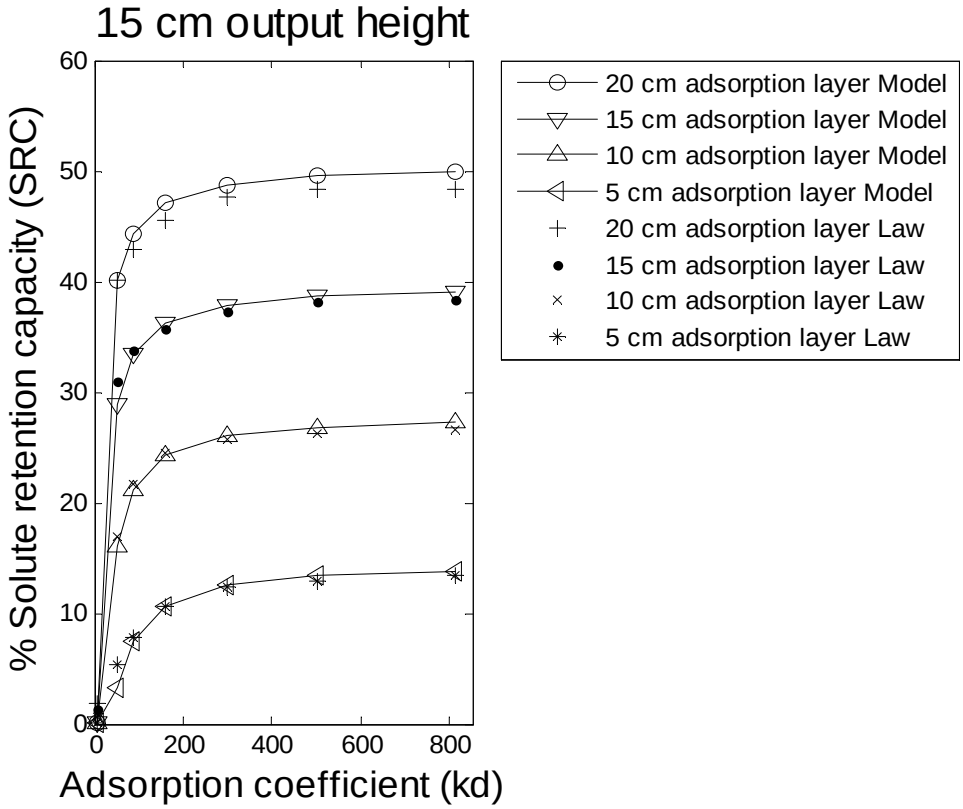

Figure b): empirical law validation – 15 cm output height

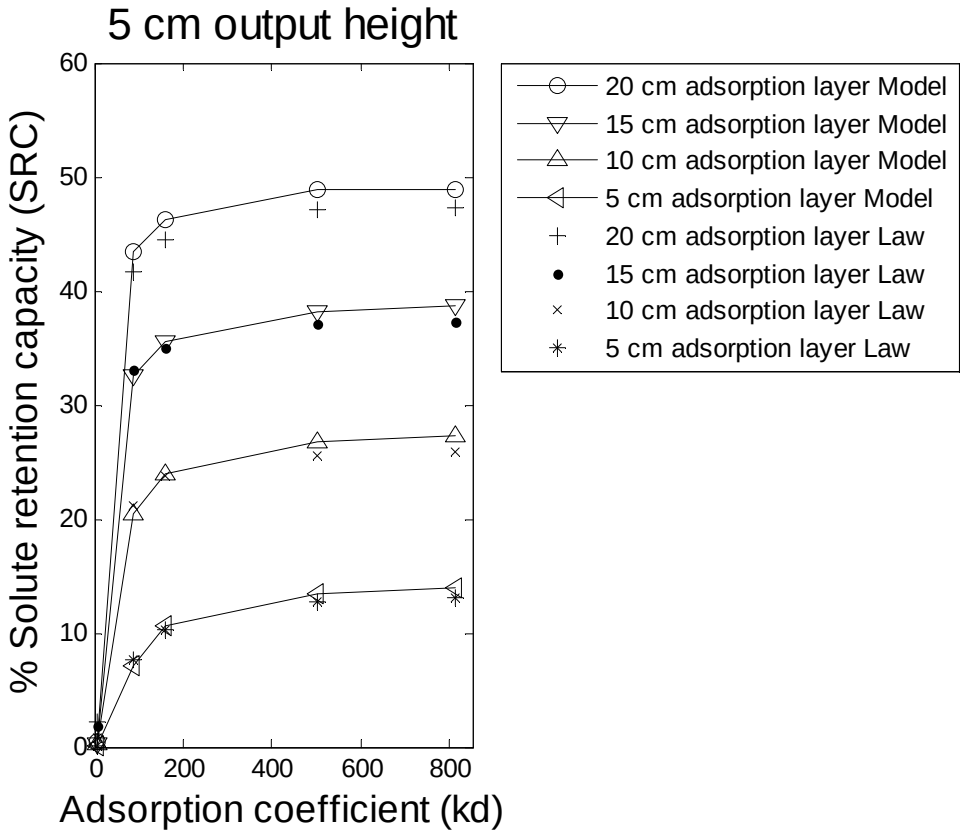

Figure c): empirical law validation – 5 cm output height

Fig. 49. Solute retention capacity – empirical law validation

Outputs heights of 15 cm and 5cm, respectively Figure 49 b and c have been tested. This law met the expectd values computed by the model. Therefore, it is possible to estimate the solute retention capacity within the HFCW for different conditions using this empirical law.

This empirical law allows to well configure HFCW by estimating the pollutant retention capacity. This is possible if the hydraulic conditions are well known and the order of magnitude of the adsorption coefficient well estimated. The fact that the remediation capacity is smaller than the retention capacity is clear, so that the purpose of this empirical relation is to design the filter in order to achieve high level of pollutant retention and hence pollutant remediation.

However, the choice of a sorbing material for adsorption layer needs to be seriously investigated. Low cost mineral and organic sorbents for metals [Bailey et al., 1999; Kurniawan et al., 2006] and organic compounds [Ahmaruzzaman, 2008] are required for such rustic treatment plants. Several studies have been carried out on this subject. Recently, Huguenot *et al.* [2010] have tested experimentally different sorbents to study their ability to sorb copper and herbicides in liquid and sediments. The sorbents were perlite (0.6mm up to 6mm in diameter), vermiculite (diameter less than 5mm), sediment (collected in a vineyard storm basin), dried sugar beet pulp (from sugar refinery) and corncob upplied by local farmers. All sorbents were used without pre-treatment.

The major result of their study is that several sorbents requiring no preliminary treatment, i.e., sugar beet pulp for Cu and sand for diuron and 3,4-DCA, were able to sorb more than 50% of the corresponding pollutant at the studied concentration.

Moreover, natural substrates such as grass, dead leaves, decaying vegetation, straw and sediments could be used as adsorbent layer. Studying the influence of hydrodynamics on the transfer of pesticides in agricultural ditches, Boutron [2000] used the hemp fibres as a simplified model of natural substrates. He also proposed some criteria for the selection of adsorbent layer. The use of adsorbent materials in constructed wetland associated with the proposed empirical law for the filter design would enhance the effectiveness of retention.

5.2.4. Conclusion

Constructed wetlands are being considered a sustainable and promising option, whose performance, cost and resources utilization can complement or replace conventional water treatment. This technology for wastewater treatment is rustic and the design always needs some improvements in order to enhance the pollutant removal performances. In this study, we test horizontal and vertical adsorbent layer configuration. Due to no retention for the vertical adsorbent layer configurations, we study only the horizontal one. Hence by using these horizontal adsorbent layers, we propose methods and a new empirical law in order to significantly increase the solute retention capacity in HFCW. Testing the impact of these horizontal adsorbent layers on the solute residence time distribution**,** three important behaviors have been highlighted:

- For the different adsorption layers tested, the mean residence times are similar when the K_d values are very high. There is no impact of the adsorption layer thickness with high adsorption coefficient (Kd) values.
- For smaller K_d values, we observe that the deeper the adsorption layers' thickness is, the higher the retention time is.
- For 15 cm and 20 cm adsorption layer thickness, the mean retention times appear to be strictly decreasing with K_d values.

Knowing the thickness of the adsorption layer, and the physical and hydraulic parameters of the HFCW, the purposed mathematical relation makes possible the calculation of the solute retention capacity (SRC) for any adsorption coefficient. Using the different experimental tests related to sorbing materials in the literature and the purpose empirical law, the experimentally constructed wetland has to be performed for verification and validation.

5.2.5. References Section 5.2.

Ahmaruzzaman, M., 2008. Adsorption of phenolic compounds on low-cost adsorbents: a review, Advances in Colloid Interface Science, 143(1-2): 48–67.

Akhtar, M., Hasany, S.M., Bhanger, M.I., Iqbal, S., 2007. Low cost sorbents for the removal of methyl parathion pesticide from aqueous solutions. Chemosphere, 66(10): 1829–1838.

Alkan, M., Dogan, M., 2001. Adsorption of Copper(II) onto perlite, Journal of Colloid and Interface Science, 243(2): 280–291.

Altundogan, H.S., Arslan, N.E., Tumen, F., 2007 Copper removal from aqueous solutions by sugar beet pulp treated by NaOH and citric acid. Journal of Hazardous Materials, 149(2): 432–439.

Arias, M.E., Brown, M.T., 2009. Feasibility of using constructed treatment wetlands for municipal wastewater treatment in the Bogotá Savannah, Colombia. Ecological Engineering, 35(7): 1070-1078.

Bailey, S.E., Olin, T.J., Bricka, R.M., Adrian, D.D., 1999. A review of potentially low-cost sorbents for heavy metals, Water Research, 33(11): 2469–2479.

Bavor, H.J., Roser, D.J., Adcock, P.W., 1995. Challenges for the development of advanced constructed wetlands technology. Water Science and Technology, 32(3): 13-20.

Fernández-Bayo, J.D., Romero, E., Schnitzler, F., Burauel, P., 2008. Assessment of pesticide availability in soil fractions after the incorporation of winery-distillery vermicomposts, Environmental Pollution. 154(2): 330–337.

Gopal, B., Mitsch, W.J., 1995. The role of vegetation in creating and restoring wetlands – An international perspective. Ecological Engineering, 5(1): 1-3.

Huett, D.O., Morris, S.G., Smith, G., Hunt, N., 2005. Nitrogen and phosphorus removal from plant nursery runoff in vegetated and unvegetated subsurface flow wetlands. Water Research, 39(14): 3259-3272.

Huguenot, D., Bois, P., Jézéquel, K., Cornu, J.Y., Lebeau, T., 2010. Selection of low cost materials for the sorption of copper and herbicides as single or mixed compounds in increasing complexity matrices. Journal of Hazardous Materials 182 (1-3): 18–26

Jing, S.-R., Lin, Y.-F., Lee, D.-Y., Wang, T.-W., 2001. Nutrient removal from polluted river water by using constructed wetlands. Bioresource Technology, 76(2): 131-135.

Karathanasis, A.D., Potter, C.L., Coyne, M.S., 2003. Vegetation effects on fecal bacteria, BOD, and suspended solid removal in constructed wetlands treating domestic wastewater. Ecological Engineering, 20(2): 157-169.

Khan, S., Ahmad, I., Shah, M.T., Rehman, S., Khaliq, A., 2009. Use of constructed wetland for the removal of heavy metals from industrial wastewater. Journal of Environmental Management, 90(11): 3451-3457.

Kirkland, M.R., Hills, R.G., Wierenga, P.J., 1992. Algorithms for solving Richards' equation for variably saturated soils. Water Resources Research, 28(8): 2049-2058.

Kröpfelová, L., Vymazal, J., Švehla, J., Štíchová, J., 2009. Removal of trace elements in three horizontal sub-surface flow constructed wetlands in the Czech Republic. Environmental Pollution, 157(4): 1186-1194.

Kurniawan, T.A., Chan, G.Y.S., Lo, W.H., Babel, S., 2006. Comparisons of low-cost adsorbents for treating wastewaters laden with heavy metals, Science of the Total Environment, 366(2-3): 409–426.

Lim, P.E., Tay, M.G., Mak, K.Y., Mohamed, N., 2003. The effect of heavy metals on nitrogen and oxygen demand removal in constructed wetlands. The Science of the Total Environment, 301(1-3): 13-21.

Mitchell, D.S., Chick, A.J., Raisin, G.W., 1995. The use of wetlands for water pollution control in Australia: an ecological perspective. Water Science and Technology, 32(3): 365-373.

Mitsch, W.J., 1995. Restoration and creation of wetlands –providing the science and engineering basis and measuring success. Ecological Engineering, 4(2): 61-64.

Reichenberger, S., Bach, M., Skitschak, A., Frede, H.G. 2007. Mitigation strategies to reduce pesticide inputs into ground- and surface water and their effectiveness; A review. Science of the total environment, 384(1-3): 1-35.

Shen, J. Duvnjak, Z., 2005. Adsorption kinetics of cupric and cadmium ions on corncob particles, Process Biochemestry, 40 (11): 3446–3454.

Shutes, R.B.E., 2001. Artificial wetlands and water quality improvement. Environment International, 26(5-6): 441-447.

Sud, D., Mahajan, G., Kaur, M.P., 2008. Agricultural waste material as potential adsorbent for sequestering heavy metal ions from aqueous solutions – a review. Bioresource Technolology, 99(14): 6017–6027.

Swami, D. Buddhi, D., 2006. Removal of contaminants from industrial wastewater through various non-conventional technologies: a review, International Journal of Environment and Pollution, 27(4): 324–346.

Tack, F.M.G., De Pauw, N., Du Laing, G. Rousseau, D., 2007. Contaminants in natural and constructed wetlands : Pollutant dynamics and control. Science of the Total Environment, 380(1-3): 1-2.

Tang, X., Eke, P.E., Scholz, M., Huang, S., 2009. Processes impacting on benzene removal in vertical-flow constructed wetlands. Bioresource Technology, 100(1): 227-234.

Tao, Q.H. and Tang, H.X., 2004. Effect of dye compounds on the adsorption of atrazine by natural sediment. Chemosphere 56(1): 31–38.

Veli, S., Alyüz, B., 2007. Adsorption of copper and zinc from aqueous solutions by using natural clay, Journal of Hazardous Materials, 149(1): 226–233.

Vymazal, J. 2007. Removal of nutrients in various types of constructed wetlands. Science of the Total Environment, 380(1-3): 48-65.

Vymazal, J., Greenway, M., Tonderski, K., Brix, H., Mander, Ü., 2006. Constructed Wetlands for Wastewater Treatment. Ecological Studies,Vol. 190 J.T.A.Verhoeven,B.Beltman,R.Bobbink,and D.F.Whigham (Eds.) Wetlands and Natural Resource Management © Springer-Verlag Berlin Heidelberg 2006

Vymazal, J., Kröpfelová, L., 2008. Wastewater treatment in constructed wetlands with horizontal sub-surface flow. Serie Environmental Pollution 14. Springer, Dordrecht, The Netherlands. 566 pp.

Vymazal, J., Kröpfelová, L., 2009. Removal of organics in constructed wetlands with horizontal sub-surface flow: A review of the field experience. Science of the Total Environment, 407(13): 3911-3922.

Wanko, A., Tapia, G., Mosé, R., Gregoire, C., 2009. Adsorption distribution impact on preferential transport within horizontal flow constructed wetland (HFCW). Ecological Modelling, 220(23): 3342–3352.

Ye, Z.H., Whiting, S.N., Qian, J.H., Lytle, C.M., Lin, Z.-Q., Terry, N., 2001. Trace element removal from coal ash leachate by a 10-year-old constructed wetland. Journal of Environmental Quality, 30(5): 1710-1719.

Zhang, D., Gersgberg, R.M., Tan Soon Keat, 2009. Constructed wetlands in China. Ecological Engineering, 35(10): 1367-1378

6

Chapter 6 – Conclusions and perspectives

Concern is increasing about the effects of pesticides on the environment and human health. Several methods are being considered for pesticide risk reduction. These methods are approached from the point of view of management and development of remediation techniques. One of these techniques, considered as a promising option, are constructed wetlands. Constructed wetlands have been widely used in water treatment. Recently, their use in the treatment of pesticide non-point source pollution has aroused intense interest. Their potentialities to mitigate agricultural non-point source pesticide pollution are currently being studied. The different processes that ocurrs in constructed wetlands includes: hydrodynamics, transport and fate of pesticides. A model to simulate pesticide dynamics in a soil profile must be then included for the study of these processes. Therefore, the present thesis work has a primary interest in developping a numerical model to simulate the hydrodynamics, transport and fate of pesticides.

Firstly, the mixed hybrid finite element was used to obtain a new formulation in a global approach to simulate water flow and solute transport in variably saturated porous medium. This formulation is based on Raviart-Thomas' space properties. The two-dimensional flow domain was divided into rectangular triangles. Different techniques were used in the hydrodynamic modelling, such as the transformation of the primary variable of pressure. For a better convergence behavior, a technique that switches between the mixed-form and the pressure-head based form of the Richard's equation was applied. Special attention was given to the top boundary conditions dealing with ponding or evaporation problems. In order to avoid non-physical oscillation problems, a mass condensation scheme was implemented in the model.

For solving the transport equation, a new global approach was presented. This method uses a MHFEM approximation for both advection and dispersion terms. It includes a flux limting tool to control oscillation originated when convection is the dominant process. Different models for the kinectis of biodegradation in soil were also implemented. Time discretization plays an important role during the simulation. Thus, time discretization was made in variable time steps. An inadequate time step selection may lead to an inaccurate approximation for the hydrodynamics and solute transport calculations.

Later, after the development of all the equations of the model and the implementation in the programming code, using Fortran Language, the model was validated by performing several simulations and the comparision of the numerical approximations obtained with reference results found in the literature. Validation was also carried out by comparison of results with analytical solutions, or the application of the well-known commercial model (HYDRUS) for one-dimensional test cases within unsaturated porous media. In all cases, good agreement of results was obtained.

Once the validation of the model was performed, the interpretation of results became important. For the hydrodynamics a set of test cases were simulated by using differents model options (depending upon the primary variable used, the form of the equation to solve, and the initial and boundary conditions applied). As simulation result, a group of time and error indicator parameters was defined. Observations of these parameters were analysed statistically, and re-grouped according to their dissimilarities. The interpretation of the correlation between parameters and their re-grouping according to dissimilarities gave as result information that could be very useful for the selection of the most suitable option-model to apply, depending on the initial and boundary conditions to simulate. For the transport model, the help of the flux limiter made it possible to get accuracy and unconditional stability in the results for low and very high Peclet numbers.

After the model validation, the model was applied to perform numerical tracer tests on an experimental site. Literature has reported the fact that insufficient residence time of pollutants in soils induces an incomplete and unfinished biodegradation process. Therefore, with the objective to increase the solute retention capacity in horizontal flow constructed wetlands (HFCW), several operations scenarios were simulated, in order to propose engineering solutions that permit the optimization of the HFCW. The influence of homogeneous and heterogeneous adsorption coefficient distribution on the HFCW residence time distribution was studied. It was shown that the adsorption distribution is an internal factor of soil, which is responsible to the preferential pathway transport in a homogeneous

gravel texture. Additionally, other optimization parameters related to the boundary conditions, flow rate, physical configuration, and adsorbent layer thickness were studied. Moreover, a new empirical law was developped in order to increase the adsorption ability in the HFCW. An important conclusion from this optimization study was that no impact was observed when changing the adsorbent layer thickness when high values of adsorption coefficient values were applied. For smaller K_d values, we observe that the deeper the adsorbent layer thickness is, the higher is the retention time is. A strong correlation between the mean residence time and the mean value of the adsorption coefficient was numerically confirmed for the experimental case. The mean value of K_d was also found as the most influent parameter in this transport problem.

Further work, will be the analysis with data collected from the experimental site. Degradation kinetics models were already implemented in the simulation programming code, however their validation and experimental application will be the objective of future studies.

Appendixes

Appendix I. Reference Transformation

1. Transformation from an element of reference to an element in the physical space

$$F_{2D} : \hat{G} \rightarrow G$$

$$\hat{M}\begin{pmatrix} u \\ v \end{pmatrix} \rightarrow M\begin{pmatrix} x(u,v) \\ z(u,v) \end{pmatrix}$$

Reference Element $\hat{G}$ **Element** G **in the physical space**

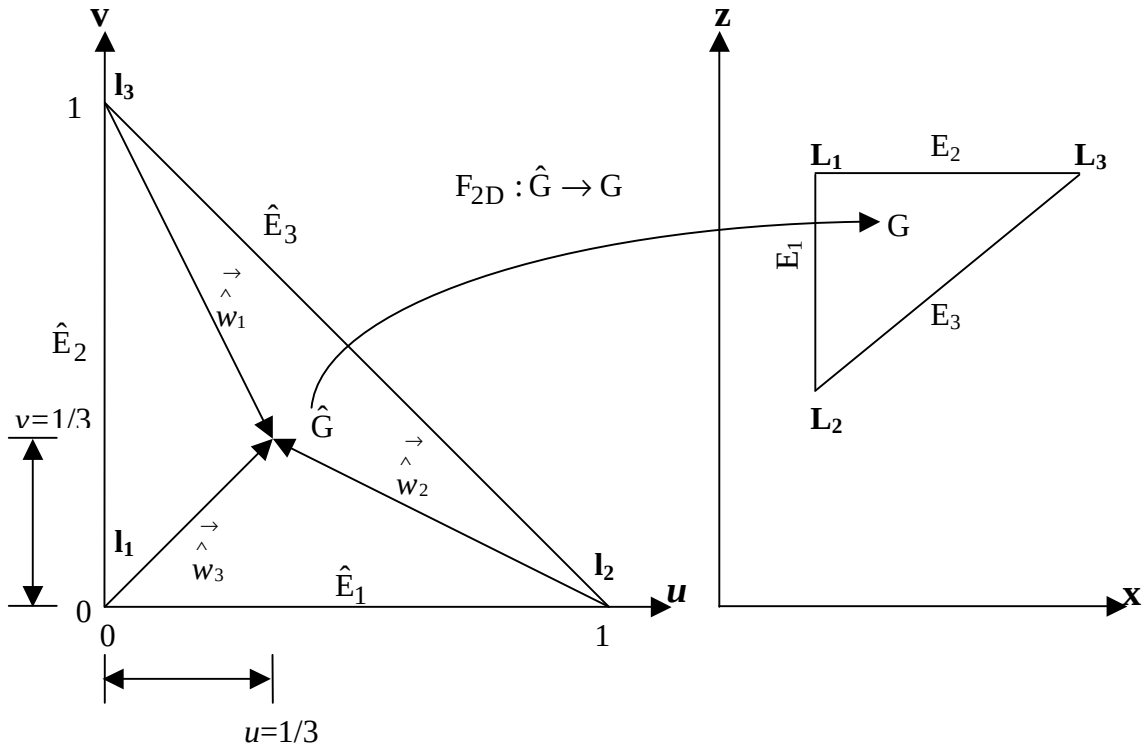

The system represents a function $F_{2D,}$ that maps a point (u,v) in an uv-coordinate system into a point (x,y) in a xy-coordinate system.

$$l_1(0,0) \xrightarrow{F_{2D}} L_1(x_{L_1}, z_{L_1})$$
$$l_2(1,0) \xrightarrow{F_{2D}} L_2(x_{L_2}, z_{L_2})$$
$$l_3(0,1) \xrightarrow{F_{2D}} L_3(x_{L_3}, z_{L_3})$$

The analytic expressions of $x(u,v)$ and $z(u,v)$ are:

$$x(u,v)=\left(N_{l_1},N_{l_2},N_{l_3}\right)\begin{bmatrix}x_{L_1}\\x_{L_2}\\x_{L_3}\end{bmatrix} \qquad z(u,v)=\left(N_{l_1},N_{l_2},N_{l_3}\right)\begin{bmatrix}z_{L_1}\\z_{L_2}\\z_{L_3}\end{bmatrix}$$

Where the base functions of interpolation are equal to the geometric transformation functions:

$$N_{l_1}=m_{\hat{G},l_1}=1-u-v \qquad N_{l_2}=m_{\hat{G},l_2}=u \qquad N_{l_3}=m_{\hat{G},l_3}=v$$

So then the nodal coordinates $x(u,v)$ and $z(u,v)$ can be expressed as:

$$x(u,v)=(1-u-v)x_{L_1}+(u)x_{L_2}+(v)x_{L_3}=x_{L_1}+ua+vb$$

$$z(u,v)=(1-u-v)z_{L_1}+(u)z_{L_2}+(v)z_{L_3}=z_{L_1}+uc+vd$$

where : $a=x_{L_2}-x_{L_1}$, $b=x_{L_3}-x_{L_1}$,

$c=z_{L_2}-z_{L_1}$, $d=z_{L_3}-z_{L_1}$

A vector transformation can be written as:

$$\vec{w}_i(x,z)=\frac{J\,\hat{\vec{w}}_i(u,v)}{\det J}$$

The Jacobian matrix J associated with the transformation F_{2D} is defined by:

$$J_{2D}=\begin{bmatrix}\frac{\partial x}{\partial u} & \frac{\partial x}{\partial v}\\ \frac{\partial z}{\partial u} & \frac{\partial z}{\partial v}\end{bmatrix} = \begin{bmatrix}x_{L_2}-x_{L_1} & x_{L_3}-x_{L_1}\\ z_{L_2}-z_{L_1} & z_{L_3}-z_{L_1}\end{bmatrix} =\begin{bmatrix}a & b\\ c & d\end{bmatrix}$$

And its determinant, denoted as $\det J=ad-bc$

The base functions associated with the edges E_i are defined over $\hat{G}$:

$$\hat{\vec{w}}_1=\begin{bmatrix}u\\v-1\end{bmatrix} \qquad \hat{\vec{w}}_2=\begin{bmatrix}u-1\\v\end{bmatrix} \qquad \hat{\vec{w}}_3=\begin{bmatrix}u\\v\end{bmatrix}$$

Therefore, the vector transformation can be written as:

$$\vec{w}_i(x,z)=\begin{pmatrix} \dfrac{J_{11}\hat{w}_{iu}+J_{12}\hat{w}_{iv}}{\det J} \\ \dfrac{J_{21}\hat{w}_{iu}+J_{22}\hat{w}_{iv}}{\det J} \end{pmatrix}$$

where J_{ij} is the ij component of the Jacobian matrix J

$$\vec{w}_1=\begin{bmatrix} \dfrac{\hat{w}_{1u}J_{11}+\hat{w}_{1v}J_{1,2}}{\det J} \\ \dfrac{\hat{w}_{1u}J_{21}+\hat{w}_{1v}J_{2,2}}{\det J} \end{bmatrix} = \begin{bmatrix} \dfrac{ua+bv-b}{ad-bc} \\ \dfrac{uc+vd-d}{ad-bc} \end{bmatrix}$$

$$\vec{w}_2=\begin{bmatrix} \dfrac{\hat{w}_{2u}J_{11}+\hat{w}_{2v}J_{1,2}}{\det J} \\ \dfrac{\hat{w}_{2u}J_{21}+\hat{w}_{2v}J_{2,2}}{\det J} \end{bmatrix} = \begin{bmatrix} \dfrac{(u-1)a+bv}{ad-bc} \\ \dfrac{(u-1)c+vd}{ad-bc} \end{bmatrix}$$

$$\vec{w}_3=\begin{bmatrix} \dfrac{\hat{w}_{3u}J_{11}+\hat{w}_{3v}J_{1,2}}{\det J} \\ \dfrac{\hat{w}_{3u}J_{21}+\hat{w}_{3v}J_{2,2}}{\det J} \end{bmatrix} = \begin{bmatrix} \dfrac{ua+bv}{ad-bc} \\ \dfrac{uc+vd}{ad-bc} \end{bmatrix}$$

2. Transformation from an element in the physical space to an element of reference

The transformation from an element in the physical space to an element of reference by an integral of a scalar function can be expressed as

$$\int_G f(x,z)dxdz = \int_{\hat{G}} f(x(u,v),z(u,v))\det J dvdu$$

Thus, the components of the matrix B_G can be calculated as

$$B_{ij} = \int_G \left(\frac{w_{ix}}{L_{xx}} w_{jx} + \frac{w_{iz}}{L_{zz}} w_{jz} \right) dxdz$$

$$= \int_{\hat{G}} \left(\left(\frac{J_{11} \hat{w}_{iu} + J_{12} \hat{w}_{iv}}{L_{xx} \det J} \right) \left(\frac{J_{11} \hat{w}_{ju} + J_{12} \hat{w}_{jv}}{\det J} \right) + \left(\frac{J_{21} \hat{w}_{iu} + J_{22} \hat{w}_{iv}}{L_{zz} \det J} \right) \left(\frac{J_{21} \hat{w}_{ju} + J_{22} \hat{w}_{jv}}{\det J} \right) \right) \det J dvdu$$

$$= \int_{u=0}^{1} \int_{v=0}^{1-u} \left(\left(\frac{w_{ix}}{kx} \right) w_{jx} + \left(\frac{w_{iz}}{kz} \right) w_{jz} \right) \det J dvdu$$

$$B_{11} = \int_{u=0}^{1} \int_{v=0}^{1-u} \left(\left(\frac{w_{1x}}{kx} \right) w_{1x} + \left(\frac{w_{1z}}{kz} \right) w_{1z} \right) \det J dvdu$$

$$B_{11} = \frac{1}{12} \frac{3b^2 k_z + 3d^2 k_x - 3abk_z - 3cdk_x + a^2 k_z + c^2 k_x}{k_z k_x (ad - bc)}$$

$$B_{12} = \int_{u=0}^{1} \int_{v=0}^{1-u} \left(\left(\frac{w_{1x}}{kx} \right) w_{2x} + \left(\frac{w_{1z}}{kz} \right) w_{2z} \right) \det J dvdu$$

$$B_{12} = -\frac{1}{12} \frac{b^2 k_z + d^2 k_x - 3abk_z - 3cdk_x + a^2 k_z + c^2 k_x}{k_z k_x (ad - cb)}$$

$$B_{13} = \int_{u=0}^{1} \int_{v=0}^{1-u} \left(\left(\frac{w_{1x}}{kx} \right) w_{3x} + \left(\frac{w_{1z}}{kz} \right) w_{3z} \right) \det J dvdu$$

$$B_{13} = -\frac{1}{12} \frac{b^2 k_z + d^2 k_x + abk_z + cdk_x - a^2 k_z - c^2 k_x}{k_z k_x (ad - cb)}$$

$$B_{21} = \int_{u=0}^{1} \int_{v=0}^{1-u} \left(\left(\frac{w_{2x}}{kx} \right) w_{1x} + \left(\frac{w_{2z}}{kz} \right) w_{1z} \right) \det J dvdu$$

$$B_{21} = -\frac{1}{12} \frac{b^2 k_z + d^2 k_x - 3abk_z - 3cdk_x + a^2 k_z + c^2 k_x}{k_z k_x (ad - cb)}$$

$$B_{22} = \int_{u=0}^{1} \int_{v=0}^{1-u} \left(\left(\frac{w_{2x}}{kx} \right) w_{2x} + \left(\frac{w_{2z}}{kz} \right) w_{2z} \right) \det J dvdu$$

$$B_{22} = \frac{1}{12} \frac{b^2 k_z + d^2 k_x - 3abk_z - 3cdk_x + 3a^2 k_z + 3c^2 k_x}{k_z k_x (ad - cb)}$$

$$B_{23} = \int_{u=0}^{1}\int_{v=0}^{1-u}\left(\left(\frac{w_{2x}}{kx}\right)w_{3x} + \left(\frac{w_{2z}}{kz}\right)w_{3z}\right)\det J dv du$$

$$B_{23} = \frac{1}{12}\frac{b^2k_z + d^2k_x - abk_z - cdk_x - a^2k_z - c^2k_x}{k_z k_x (ad - cb)}$$

$$B_{31} = \int_{u=0}^{1}\int_{v=0}^{1-u}\left(\left(\frac{w_{3x}}{kx}\right)w_{1x} + \left(\frac{w_{3z}}{kz}\right)w_{1z}\right)\det J dv du$$

$$B_{31} = -\frac{1}{12}\frac{b^2k_z + d^2k_x + abk_z + cdk_x - a^2k_z - c^2k_x}{k_z k_x (ad - cb)}$$

$$B_{32} = \int_{u=0}^{1}\int_{v=0}^{1-u}\left(\left(\frac{w_{3x}}{kx}\right)w_{2x} + \left(\frac{w_{3z}}{kz}\right)w_{2z}\right)\det J dv du$$

$$B_{32} = \frac{1}{12}\frac{b^2k_z + d^2k_x - abk_z - cdk_x - a^2k_z - c^2k_x}{k_z k_x (ad - cb)}$$

$$B_{33} = \int_{u=0}^{1}\int_{v=0}^{1-u}\left(\left(\frac{w_{3x}}{kx}\right)w_{3x} + \left(\frac{w_{3z}}{kz}\right)w_{3z}\right)\det J dv du$$

$$B_{3,3} = \frac{1}{12}\frac{b^2k_z + d^2k_x + abk_z + cdk_x + a^2k_z + c^2k_x}{k_z k_x (ad - cb)}$$

And the matrix inverse B_G^{-1}

$$deno = \left(a^2k_z - abk_z + d^2k_x - cdk_x + b^2k_z + c^2k_x\right)(ad - bc)$$

$$B_{K11}^{-1} = 2\begin{pmatrix} -a^3bk_z^2 + c^2d^2k_x^2 - c^3dk_x^2 + a^2b^2k_z^2 + 3b^2c^2k_xk_z + 3a^2d^2k_xk_z \\ +2a^2c^2k_xk_z + a^4k_z^2 + c^4k_x^2 - 4abcdk_xk_z - abc^2k_xk_z - a^2cdk_xk_z \end{pmatrix} / deno$$

$$B_{K12}^{-1} = -2\begin{pmatrix} 2a^3bk_z^2 - c^2d^2k_x^2 + c^3dk_x^2 - a^2b^2k_z^2 + ab^3k_z^2 + cd^3k_x^2 - 2b^2c^2k_xk_z \\ -2a^2d^2k_xk_z + b^2cdk_xk_z + abd^2k_xk_z + 2abcdk_xk_z + abc^2k_xk_z + a^2cdk_xk_z \end{pmatrix} / deno$$

$$B_{K13}^{-1} = -2\begin{pmatrix} -2a^3bk_z^2 + 2c^2d^2k_x^2 - 2c^3dk_x^2 + 2a^2b^2k_z^2 - ab^3k_z^2 - cd^3k_x^2 \\ -b^2c^2k_xk_z - a^2d^2k_xk_z + 2a^2c^2k_xk_z + a^4k_z^2 + c^4k_x^2 - b^2cdk_xk_z \\ -abd^2k_xk_z + 6abcdk_xk_z - 2abc^2k_xk_z - 2a^2cdk_xk_z \end{pmatrix} / deno$$

$$B_{K21}^{-1} = -2\begin{pmatrix} a^3bk_z^2 - c^2d^2k_x^2 + c^3dk_x^2 - a^2b^2k_z^2 + ab^3k_z^2 + cd^3k_x^2 \\ -2b^2c^2k_xk_z - 2a^2d^2k_xk_z + b^2cdk_xk_z + abd^2k_xk_z \\ +2abcdk_xk_z + abc^2k_xk_z + a^2cdk_x \end{pmatrix} / \text{deno}$$

$$B_{K22}^{-1} = 2\begin{pmatrix} c^2d^2k_x^2 + a^2b^2k_z^2 - ab^3k_z^2 - cd^3k_x^2 + 2b^2d^2k_xk_z + 3b^2c^2k_xk_z \\ +3a^2d^2k_xk_z + b^4k_z^2 + d^4k_x^2 - b^2cdk_xk_z - abd^2k_xk_z - 4abcdk_xk_z \end{pmatrix} / deno$$

$$B_{K23}^{-1} = 2\begin{pmatrix} a^3bk_z^2 - 2c^2d^2k_x^2 + c^3dk_x^2 - 2a^2b^2k_z^2 + 2ab^3k_z^2 + 2cd^3k_x^2 \\ -2b^2d^2kxk_z + c^2b^2k_xk_z + a^2d^2k_xk_z - b^4k_z^2 - d^4k_x^2 + 2b^2cdk_xk_z \\ +2abd^2k_xk_z - 6abcdk_xk_z + abc^2k_xk_z + a^2cdk_xk_z \end{pmatrix} / deno$$

$$B_{K31}^{-1} = -2\begin{pmatrix} -2a^3bk_z^2 + 2c^2d^2k_x^2 - 2c^3dk_x^2 + 2a^2b^2k_z^2 - ab^3k_z^2 - cd^3k_x^2 \\ -b^2c^2k_xk_z - a^2d^2k_xk_z + 2a^2c^2k_xk_z + a^4k_z^2 + c^4k_x^2 - b^2cdk_xk_z \\ -abd^2k_xk_z + 6abcdk_xk_z - 2abc^2k_xk_z - 2a^2cdk_xk_z \end{pmatrix} / den$$

$$B_{K32}^{-1} = 2\begin{pmatrix} a^3bk_z^2 - 2c^2d^2k_x^2 + c^3dk_x^2 - 2a^2b^2k_z^2 + 2ab^3k_z^2 + 2cd^3k_x^2 \\ -2b^2d^2kxk_z + c^2b^2k_xk_z + a^2d^2k_xk_z - b^4k_z^2 - d^4k_x^2 + 2b^2cdk_xk_z \\ +2abd^2k_xk_z - 6abcdk_xk_z + abc^2k_xk_z + a^2cdk_xk_z \end{pmatrix} / deno$$

$$B_{K33}^{-1} = 2\begin{pmatrix} -3a^3bk_z^2 + 4c^2d^2k_x^2 - 3c^3dk_x^2 + 4a^2b^2k_z^2 - 3\,\&\,b^3k_z^2 - 3cd^3k_x^2 \\ +2b^2d^2k_xk_z + 4b^2c^2k_xk_z + 4a^2d^2k_xk_z + 2a^2c^2k_zk_x + b^4k_z^2 + d^4k_x^2 \\ +c^4k_x^2 - 3b^2cdk_xk_z - 3abd^2k_xk_z - 3abc^2k_xk_z - 3a^2cdk_xk_z \end{pmatrix} / deno$$

Appendix II. Vector components of the Darcy flux approximation

$$\vec{q}_G = \sum_{j=1}^{3} Q_{G,E_j} \vec{w}_j$$

The vector $\vec{w}_j$ is computed using the coordinates at the centroid of the reference element ($u = 1/3$, and $v = 1/3$). See Appendix I for more detailed information about the transformation vector.

$$\vec{w}_1 = \begin{bmatrix} \dfrac{ua + bv - b}{ad - bc} \\ \dfrac{uc + vd - d}{ad - bc} \end{bmatrix} = \begin{bmatrix} \dfrac{(1/3)a - (2/3)b}{ad - bc} \\ \dfrac{(1/3)c - (2/3)d}{ad - bc} \end{bmatrix}$$

$$\vec{w}_2 = \begin{bmatrix} \dfrac{(u-1)a + bv}{ad - bc} \\ \dfrac{(u-1)c + vd}{ad - bc} \end{bmatrix} = \begin{bmatrix} \dfrac{(1/3)b - (2/3)a}{ad - bc} \\ \dfrac{(1/3)d - (2/3)c}{ad - bc} \end{bmatrix}$$

$$\vec{w}_3 = \begin{bmatrix} \dfrac{ua + bv}{ad - bc} \\ \dfrac{uc + vd}{ad - bc} \end{bmatrix} = \begin{bmatrix} \dfrac{(1/3)a + (1/3)b}{ad - bc} \\ \dfrac{(1/3)c + (1/3)d}{ad - bc} \end{bmatrix}$$

Therefore, the components of the vector function $\vec{q}_G$ belonging to the lowest order Raviart-Thomas space are computed as:

$$\vec{q}_{G_x} = \frac{(1/3)a - (2/3)b}{ad - bc} Q_{G,E_1} + \frac{(1/3)b - (2/3)a}{ad - bc} Q_{G,E_2} + \frac{(1/3)a + (1/3)b}{ad - bc} Q_{G,E_3}$$

$$\vec{q}_{G_z} = \frac{(1/3)c - (2/3)d}{ad - bc} Q_{G,E_1} + \frac{(1/3)d - (2/3)c}{ad - bc} Q_{G,E_2} + \frac{(1/3)c + (1/3)d}{ad - bc} Q_{G,E_3}$$

Or expressed in terms of $Q_{Total} = Q_{G,E_1} + Q_{G,E_2} + Q_{G,E3}$

$$\vec{q}_{G_x} = \frac{(1/3)aQ_{Total} + (1/3)bQ_{Total} - bQ_{G,E_1} - aQ_{G,E_2}}{ad - bc}$$

$$\vec{q}_{G_z} = \frac{(1/3)cQ_{Total} + (1/3)dQ_{Total} - dQ_{G,E_1} - cQ_{G,E_2}}{ad - bc}$$

Appendix III. Soil parameters used in the modified Mualem-van Genuchten model

	Material	K_s ($cm\ s^{-1}$)	θ_s	θ_r	α (cm^{-1})	n	τ	h_e (cm)	Reference
	Soil 1	0.006262	0.3658	0.0286	0.0280	2.2390	0.5	0	[Pan and Wierenga, 1995]
	Soil 2	0.0001516	0.4686	0.1060	0.0104	1.3954	0.5	0	[Pan and Wierenga, 1995]
	Soil 3	0.00922	0.3680	0.1020	0.0335	2.0000	0.5	0	[Pan and Wierenga, 1995]
A		$0.922x10^{-2}$	0.368	0.102	0.0335	2	0.5	0	Celia et al., 2000
B	Sand	$2.025x10^{-4}$	0.43	0.01	0.0249	1.507	-0.140	0	[Van Dam and Feddes, 2000]
C	Glendale clay loam	$1.516x10^{-4}$	0.4686	0.1060	0.0104	1.3954	0.5	0	[Kirkland et al., 1992]
D	Berino loamy fine sand	$6.262x10^{-3}$	0.3658	0.0286	0.0280	2.2390	0.5	0	[Kirkland et al., 1992]

Appendix IV. Test case results

Test case	RE form	tol_f	κ (cm^{-1})	NI	Time steps	Δt av	Δt max	Δt min	Pe max $x10^2$	Co max $x10^2$	ε_{MB}	E_{1G} max	E_{2G} max	ε_{MB}^n max	ε_{MB}^n min	Δh max	$\Delta\theta$ max	Δh_d max
1.1	h-based	0	0.00	21278	5465	3.952	7.161	$1x10^{-3}$	5.8	2.8	$1.1x10^{-12}$	$6.9x10^{-15}$	$1.0x10^{-14}$	0.89	-19.4	0.481	$8.3x10^{-6}$	15801
1.1	h-based	0	-0.04	17069	4580	4.716	14.08	$1x10^{-3}$	5.8	2.8	$-1.3x10^{-10}$	$1.5x10^{-14}$	$2.1x10^{-14}$	0.97	-41835.0	0.258	$9.5x10^{-6}$	15419
1.1	Mixed	1	0.00	18390	4910	4.399	12.69	$1x10^{-3}$	5.8	2.8	$2.7x10^{-9}$	$9.8x10^{-8}$	$3.6x10^{-8}$	0.57	-1.3	0.198	$7.0x10^{-6}$	15793
1.1	Mixed	1	-0.04	16705	4448	4.856	24.94	$1x10^{-3}$	5.8	2.8	$1.4x10^{-10}$	$2.0x10^{-9}$	$2.0x10^{-9}$	0.42	-52114.3	0.192	$3.2x10^{-6}$	15417
1.1	Switch	0.9	0.00	18390	4910	4.399	12.69	$1x10^{-3}$	5.8	2.8	$-6.4x10^{-10}$	$5.9x10^{-10}$	$3.6x10^{-10}$	0.57	-1.3	0.198	$9.4x10^{-6}$	15793
1.1	Switch	0.9	-0.04	16723	4452	4.851	24.94	$1x10^{-3}$	5.8	2.8	$-1.8x10^{-10}$	$3.8x10^{-11}$	$3.5x10^{-11}$	0.42	-52114.3	0.192	$4.9x10^{-6}$	15417
2.1	h-based	0	0.00	17835	4647	9.296	13.79	$1x10^{-3}$	4.4	2.2	$2.1x10^{-12}$	$4.6x10^{-16}$	$7.2x10^{-16}$	0.71	-94.6	0.286	$7.2x10^{-7}$	15618
2.1	h-based	0	-0.04	15114	4266	10.12	18.03	$1x10^{-3}$	4.4	2.2	$-1.1x10^{-9}$	$3.5x10^{-15}$	$1.1x10^{-14}$	0.82	-200319.8	0.686	$2.9x10^{-7}$	15191
2.1	Mixed	1	0.00	15716	4405	9.807	15.55	$1x10^{-3}$	4.4	2.2	$-4.5x10^{-10}$	$1.6x10^{-10}$	$1.0x10^{-10}$	0.79	-397.0	0.191	$9.7x10^{-7}$	15609
2.1	Mixed	1	-0.04	15197	4244	10.17	15.15	$1x10^{-3}$	4.4	2.2	$-1.0x10^{-9}$	$1.1x10^{-11}$	$2.3x10^{-13}$	0.33	-250445.4	0.184	$1.7x10^{-7}$	15816
2.1	Switch	0.9	0.00	15716	4405	9.807	15.55	$1x10^{-3}$	4.4	2.2	$-4.5x10^{-10}$	$1.6x10^{-10}$	$1.0x10^{-10}$	0.79	-397.0	0.191	$9.7x10^{-7}$	15609
2.1	Switch	0.9	-0.04	15197	4244	10.17	15.15	$1x10^{-3}$	4.4	2.2	$-1.0x10^{-9}$	$1.1x10^{-11}$	$2.3x10^{-13}$	0.33	-250445.4	0.184	$1.7x10^{-7}$	15186

Test case	RE form	tol_f	κ (cm^{-1})	NI	Time steps	Δt av	Δt max	Δt min	Pe max $x10^2$	Co max $x10^2$	ε_{MB}	E_{1G} max	E_{2G} max	ε_{MB}^n max	ε_{MB}^n min	Δh max	$\Delta\theta$ max	Δh_d max
1.2	h-based	0	0.00	6893	2662	6.761	65.83	0.475	5.8	8.5	$-5.7x10^{-15}$	$5.0x10^{-14}$	$7.8x10^{-14}$	$2.2x10^{-10}$	$-1.6x10^{-10}$	0.092	$9.8x10^{-6}$	189.5
1.2	h-based	0	-0.04	6544	2519	7.145	66.25	1.426	5.8	8.1	$-5.7x10^{-15}$	$5.7x10^{-14}$	$9.9x10^{-14}$	$6.5x10^{-12}$	$-5.6x10^{-11}$	0.115	$9.5x10^{-6}$	161.6
1.2	Mixed	1	0.00	6565	2587	6.957	65.81	1.759	5.8	8.5	$-3.2x10^{-8}$	$2.6x10^{-8}$	$3.0x10^{-8}$	$2.0x10^{-6}$	$-2.9x10^{-6}$	0.174	$9.7x10^{-6}$	182.2
1.2	Mixed	1	-0.04	6513	2515	7.157	72.89	1.585	5.8	8.1	$7.0x10^{-9}$	$1.2x10^{-8}$	$1.2x10^{-8}$	$3.3x10^{-6}$	$-4.1x10^{-8}$	0.124	$9.7x10^{-6}$	161.5
1.2	Switch	0.9	0.00	6459	2551	7.056	65.83	1.760	5.8	8.5	$-3.6x10^{-8}$	$9.5x10^{-10}$	$6.4x10^{-10}$	$3.0x10^{-12}$	$-4.6x10^{-7}$	0.158	$9.1x10^{-6}$	173.0
1.2	Switch	0.9	-0.04	6516	2515	7.157	60.23	1.585	5.8	8.1	$1.5x10^{-9}$	$1.5x10^{-10}$	$1.4x10^{-10}$	$6.8x10^{-8}$	$-4.1x10^{-8}$	0.124	$7.0x10^{-6}$	161.5
2.2	h-based	0	0.00	5288	2138	13.47	27.66	1.585	4.3	2.1	$1.1x10^{-16}$	$4.0x10^{-16}$	$7.9x10^{-16}$	$1.8x10^{-9}$	$-1.2x10^{-12}$	0.086	$5.2x10^{-6}$	162.6
2.2	h-based	0	-0.04	4866	2026	14.21	31.99	4.557	4.3	2.1	$4.0x10^{-14}$	$1.6x10^{-15}$	$2.5x10^{-15}$	$3.3x10^{-11}$	$-3.1x10^{-11}$	0.104	$3.3x10^{-6}$	135.0
2.2	Mixed	1	0.00	5084	2092	13.76	28.86	5.284	4.3	2.1	$-3.8x10^{-8}$	$1.0x10^{-9}$	$4.7x10^{-10}$	$-1.4x10^{-10}$	$-4.3x10^{-6}$	0.138	$6.7x10^{-6}$	155.6
2.2	Mixed	1	-0.04	4850	2026	14.21	31.99	2.005	4.3	2.1	$3.2x10^{-9}$	$1.7x10^{-10}$	$4.2x10^{-11}$	$3.7x10^{-8}$	$-6.3x10^{-8}$	0.127	$2.8x10^{-6}$	135.0
2.2	Switch	0.9	0.00	5001	2064	13.95	28.79	0.252	4.3	2.1	$-4.2x10^{-8}$	$1.2x10^{-9}$	$4.7x10^{-10}$	$-1.3x10^{-10}$	$-1.0x10^{-5}$	0.127	$6.7x10^{-6}$	144.8
2.2	Switch	0.9	-0.04	4850	2026	14.21	31.99	2.005	4.3	2.1	$3.2x10^{-9}$	$1.7x10^{-10}$	$4.2x10^{-11}$	$3.7x10^{-8}$	$-6.3x10^{-8}$	0.127	$2.8x10^{-6}$	135.0

Test case	RE form	tol_f	κ (cm^{-1})	NI	Time steps	Δt av	Δt max	Δt min	Pe max $x10^2$	Co max $x10^2$	ε_{MB}	E_{1G} max	E_{2G} max	ε_{MB}^n max	ε_{MB}^n min	Δh max	$\Delta\theta$ max	Δh_d max
1.3	h-based	0	0.00	4436	1764	7.755	215.7	0.972	5.8	24	$-1.0x10^{-14}$	$1.5x10^{-13}$	$1.8x10^{-13}$	$3.2x10^{-12}$	$-5.0x10^{-12}$	0.029	$9.1x10^{-6}$	9.091
1.3	h-based	0	-0.04	4431	1773	7.715	57.02	1.844	5.7	7.7	$-2.8x10^{-14}$	$6.6x10^{-14}$	$7.6x10^{-14}$	$6.4x10^{-12}$	$-5.3x10^{-12}$	0.021	$7.0x10^{-6}$	6.610
1.3	Mixed	1	0.00	4376	1749	7.821	195.9	1.836	5.8	21	$2.2x10^{-9}$	$6.1x10^{-7}$	$5.0x10^{-8}$	$1.5x10^{-5}$	$-7.4x10^{-8}$	0.034	$9.4x10^{-6}$	7.354
1.3	Mixed	1	-0.04	4484	1789	7.646	51.83	1.844	5.8	7.0	$2.4x10^{-8}$	$3.1x10^{-8}$	$1.8x10^{-7}$	$1.0x10^{-5}$	$-2.7x10^{-8}$	0.020	$7.8x10^{-6}$	6.612
1.3	Switch	0.9	0.00	4381	1749	7.821	195.9	1.836	5.8	22	$6.9x10^{-9}$	$5.9x10^{-10}$	$4.3x10^{-10}$	$-3.7x10^{-13}$	$-7.5x10^{-8}$	0.027	$9.9x10^{-6}$	7.354
1.3	Switch	0.9	-0.04	4491	1788	7.651	51.82	1.844	5.8	7.0	$7.0x10^{-10}$	$2.4x10^{-10}$	$9.3x10^{-11}$	$5.2x10^{-8}$	$-2.7x10^{-8}$	0.076	$6.8x10^{-6}$	6.612
2.3	h-based	0	0.00	2352	970	14.84	27.10	6.947	4.3	2.1	$-2.0x10^{-14}$	$3.8x10^{-16}$	$6.8x10^{-16}$	$1.1x10^{-12}$	$-1.1x10^{-12}$	0.004	$4.8x10^{-6}$	4.375
2.3	h-based	0	-0.04	2094	920	15.65	34.49	2.018	4.3	2.1	$2.3x10^{-14}$	$1.4x10^{-15}$	$2.4x10^{-15}$	$4.7x10^{-12}$	$-4.7x10^{-12}$	0.004	$4.9x10^{-6}$	2.936
2.3	Mixed	1	0.00	2210	931	15.46	34.49	3.759	4.3	2.1	$-1.9x10^{-8}$	$6.4x10^{-10}$	$1.8x10^{-10}$	$-1.4x10^{-10}$	$-1.5x10^{-7}$	0.005	$4.8x10^{-6}$	3.532
2.3	Mixed	1	-0.04	2092	921	15.63	34.49	1.391	4.3	2.1	$1.6x10^{-8}$	$2.2x10^{-10}$	$2.2x10^{-10}$	$1.6x10^{-5}$	$-2.6x10^{-8}$	0.011	$7.4x10^{-6}$	2.920
2.3	Switch	0.9	0.00	2210	931	15.46	34.49	3.759	4.3	2.1	$-1.9x10^{-8}$	$6.4x10^{-10}$	$1.8x10^{-10}$	$-1.4x10^{-10}$	$-1.5x10^{-7}$	0.005	$4.8x10^{-6}$	3.532
2.3	Switch	0.9	-0.04	2092	921	15.63	34.49	1.391	4.3	2.1	$1.6x10^{-8}$	$2.2x10^{-10}$	$2.2x10^{-10}$	$1.6x10^{-5}$	$-2.6x10^{-8}$	0.011	$7.4x10^{-6}$	2.920

Test case	RE form	tol_f	κ (cm^{-1})	NI	Time steps	Δt av	Δt max	Δt min	Pe max $x10^2$	Co max $x10^2$	ε_{MB}	E_{1G} max	E_{2G} max	ε_{MB}^n max	ε_{MB}^n min	Δh max	$\Delta\theta$ max	Δh_d max
3.1	h-based	0	0.00	30017	6443	0.027	0.069	$7x10^{-9}$	2.4	0.6	$-1.4x10^{-13}$	$4.5x10^{-16}$	$1.7x10^{-15}$	$1.4x10^{-12}$	$-1.5x10^{-12}$	9.367	$1.4x10^{-4}$	16443
3.1	h-based	0	-0.04	29236	6588	0.027	0.071	$8x10^{-8}$	0.006	0.7	$-2.7x10^{-11}$	$6.9x10^{-16}$	$1.8x10^{-15}$	$1.0x10^{+0}$	$-9.1x10^{+4}$	0.191	$6.1x10^{-5}$	33254
3.1	Mixed	1	0.00	31239	7590	0.023	0.053	$8x10^{-8}$	2.4	0.5	$1.1x10^{-9}$	$4.5x10^{-7}$	$5.5x10^{-8}$	$9.4x10^{-6}$	$-1.8x10^{-7}$	0.183	$2.9x10^{-5}$	16443
3.1	Mixed	1	-0.04	28507	6283	0.028	0.077	$3x10^{-13}$	2.3	0.7	$5.4x10^{-12}$	$1.5x10^{-7}$	$3.1x10^{-7}$	$5.1x10^{-5}$	$-9.0x10^{-10}$	0.184	$2.7x10^{-5}$	16435
3.1	Switch	0.9	0.00	31076	7549	0.023	0.053	$8x10^{-8}$	2.4	0.6	$-6.5x10^{-10}$	$4.7x10^{-10}$	$6.9x10^{-10}$	$5.1x10^{-8}$	$-2.5x10^{-7}$	11.10	$2.9x10^{-4}$	16443
3.1	Switch	0.9	-0.04	27127	5917	0.030	0.080	$8x10^{-8}$	0.006	0.8	$2.8x10^{-10}$	$1.2x10^{-10}$	$3.2x10^{-10}$	$1.0x10^{+0}$	$-1.3x10^{+6}$	0.196	$6.0x10^{-5}$	33254
4.1	h-based	0	0.00	19600	4784	3.762	9.675	$2x10^{-6}$	3.7	1.8	$-8.7x10^{-14}$	$4.7x10^{-16}$	$7.2x10^{-16}$	$1.8x10^{-12}$	$-1.7x10^{-12}$	0.343	$1.0x10^{-6}$	16172
4.1	h-based	0	-0.04	16640	4037	4.458	9.897	$3x10^{-9}$	3.7	1.8	$2.8x10^{-10}$	$1.1x10^{-15}$	$2.0x10^{-15}$	$1.9x10^{-9}$	$-1.2x10^{-9}$	0.192	$7.6x10^{-7}$	16081
4.1	Mixed	1	0.00	15144	3656	4.923	9.897	$2x10^{-5}$	3.7	1.8	$-3.3x10^{-10}$	$3.1x10^{-11}$	$3.8x10^{-11}$	$1.1x10^{-12}$	$-4.7x10^{-8}$	0.178	$8.0x10^{-7}$	16171
4.1	Mixed	1	-0.04	16568	4021	4.476	9.897	$3x10^{-9}$	3.7	1.8	$2.4x10^{-10}$	$1.3x10^{-12}$	$1.2x10^{-12}$	$2.2x10^{-9}$	$-1.3x10^{-9}$	0.190	$7.5x10^{-7}$	16081
4.1	Switch	0.9	0.00	15144	3656	4.923	9.897	$2x10^{-5}$	3.7	1.8	$-3.3x10^{-10}$	$3.1x10^{-11}$	$3.8x10^{-11}$	$1.1x10^{-12}$	$-4.7x10^{-8}$	0.178	$8.0x10^{-7}$	16171
4.1	Switch	0.9	-0.04	16568	4021	4.476	9.897	$3x10^{-9}$	3.7	1.8	$2.4x10^{-10}$	$1.3x10^{-12}$	$1.2x10^{-12}$	$2.2x10^{-9}$	$-1.3x10^{-9}$	0.190	$7.5x10^{-7}$	16081

Test case	RE form	tol_f	κ (cm^{-1})	NI	Time steps	Δt av	Δt max	Δt min	Pe max $x10^2$	Co max $x10^2$	ε_{MB}	E_{1G} max	E_{2G} max	ε_{MB}^n max	ε_{MB}^n min	Δh max	$\Delta\theta$ max	Δh_d max
3.2	h-based	0	0.00	13573	3401	0.052	0.139	$2x10^{-5}$	2.2	1.2	$-3.0x10^{-14}$	$8.4x10^{-16}$	$2.9x10^{-15}$	$1.4x10^{-12}$	$-1.4x10^{-12}$	5.013	$8.6x10^{-4}$	291.3
3.2	h-based	0	-0.04	8667	2158	0.083	0.208	$1x10^{-4}$	0.3	1.9	$3.2x10^{-13}$	$1.3x10^{-15}$	$4.7x10^{-15}$	$1.2x10^{-5}$	$-7.0x10^{-8}$	0.163	$5.9x10^{-5}$	598.3
3.2	Mixed	1	0.00	12538	3153	0.057	0.160	$1x10^{-4}$	2.2	1.5	$3.6x10^{-7}$	$4.9x10^{-7}$	$2.0x10^{-6}$	$1.2x10^{-4}$	$-4.8x10^{-7}$	0.165	$3.4x10^{-5}$	291.0
3.2	Mixed	1	-0.04	8592	2149	0.083	0.214	$8x10^{-8}$	2.4	1.9	$-1.8x10^{-8}$	$8.1x10^{-8}$	$4.4x10^{-7}$	$4.2x10^{-5}$	$-4.5x10^{-8}$	0.154	$6.0x10^{-5}$	292.7
3.2	Switch	0.9	0.00	11930	2987	0.060	0.155	$2x10^{-4}$	2.2	1.5	$-2.0x10^{-8}$	$1.1x10^{-9}$	$1.6x10^{-9}$	$4.0x10^{-8}$	$-8.4x10^{-7}$	8.564	$5.1x10^{-4}$	291.0
3.2	Switch	0.9	-0.04	8707	2171	0.082	0.204	$2x10^{-4}$	0.3	2.0	$3.8x10^{-9}$	$2.8x10^{-10}$	$7.2x10^{-9}$	$1.2x10^{-5}$	$-6.5x10^{-8}$	0.140	$7.5x10^{-5}$	598.1
4.2	h-based	0	0.00	5650	2052	8.771	9.902	$1x10^{-2}$	3.7	1.8	$-1.2x10^{-14}$	$5.4x10^{-16}$	$8.3x10^{-16}$	$1.7x10^{-12}$	$-1.6x10^{-12}$	0.116	$6.5x10^{-6}$	231.5
4.2	h-based	0	-0.04	5248	2005	8.977	9.903	$7x10^{-4}$	3.7	1.8	$1.5x10^{-13}$	$1.4x10^{-15}$	$2.1x10^{-15}$	$1.2x10^{-11}$	$-1.4x10^{-11}$	0.140	$4.2x10^{-6}$	228.5
4.2	Mixed	1	0.00	5580	1974	9.118	9.902	$7x10^{-2}$	3.7	1.8	$-8.5x10^{-8}$	$1.9x10^{-9}$	$2.0x10^{-9}$	$-5.9x10^{-15}$	$-9.9x10^{-7}$	0.139	$8.1x10^{-6}$	230.6
4.2	Mixed	1	-0.04	5248	2004	8.982	9.903	$7x10^{-4}$	3.7	1.8	$-1.0x10^{-8}$	$4.2x10^{-11}$	$4.1x10^{-11}$	$1.9x10^{-12}$	$-3.7x10^{-8}$	0.125	$4.0x10^{-6}$	228.5
4.2	Switch	0.9	0.00	5580	1974	9.118	9.902	$7x10^{-2}$	3.7	1.8	$-8.5x10^{-8}$	$1.9x10^{-9}$	$2.0x10^{-9}$	$-5.9x10^{-15}$	$-9.9x10^{-7}$	0.139	$8.1x10^{-6}$	230.6
4.2	Switch	0.9	-0.04	5248	2004	8.982	9.903	$7x10^{-4}$	3.7	1.8	$-1.0x10^{-8}$	$4.2x10^{-11}$	$4.1x10^{-11}$	$1.9x10^{-12}$	$-3.7x10^{-8}$	0.125	$4.0x10^{-6}$	228.5

Test case	RE form	tol_f	κ (cm^{-1})	NI	Time steps	Δt av	Δt max	Δt min	Pe max $x10^2$	Co max $x10^2$	ε_{MB}	E_{1G} max	E_{2G} max	ε_{MB}^n max	ε_{MB}^n min	Δh max	$\Delta\theta$ max	Δh_d max
3.3	h-based	0	0.00	10694	2667	0.067	0.196	$2x10^{-4}$	2.2	1.7	$3.3x10^{-14}$	$1.1x10^{-15}$	$4.4x10^{-15}$	$1.3x10^{-12}$	$-2.7x10^{-12}$	9.679	$1.0x10^{-3}$	69.09
3.3	h-based	0	-0.04	7430	1843	0.097	0.272	$1x10^{-4}$	1.5	2.6	$4.6x10^{-14}$	$2.4x10^{-15}$	$6.7x10^{-15}$	$4.7x10^{-11}$	$-3.9x10^{-11}$	9.643	$7.0x10^{-5}$	86.32
3.3	Mixed	1	0.00	10979	2745	0.065	0.199	$6x10^{-5}$	1.5	2.9	$1.0x10^{-7}$	$6.1x10^{-7}$	$2.7x10^{-7}$	$2.9x10^{-5}$	$-4.1x10^{-7}$	8.885	$4.2x10^{-5}$	46.28
3.3	Mixed	1	-0.04	7166	1784	0.100	0.285	$1x10^{-5}$	2.2	2.5	$9.3x10^{-8}$	$5.6x10^{-8}$	$4.4x10^{-7}$	$3.5x10^{-5}$	$-7.7x10^{-8}$	7.965	$5.7x10^{-5}$	57.60
3.3	Switch	0.9	0.00	10451	2606	0.069	0.195	$2x10^{-4}$	1.5	2.8	$-1.0x10^{-8}$	$8.5x10^{-10}$	$1.2x10^{-9}$	$1.5x10^{-8}$	$-5.0x10^{-7}$	4.181	$6.0x10^{-4}$	46.28
3.3	Switch	0.9	-0.04	7324	1812	0.099	0.275	$2x10^{-4}$	1.5	2.6	$-5.0x10^{-10}$	$2.9x10^{-10}$	$2.3x10^{-10}$	$1.7x10^{-8}$	$-1.2x10^{-7}$	0.088	$8.0x10^{-5}$	85.45
4.3	h-based	0	0.00	3856	1857	9.693	9.927	1.222	3.7	1.8	$-5.5x10^{-15}$	$5.7x10^{-16}$	$8.4x10^{-16}$	$2.6x10^{-12}$	$-2.0x10^{-12}$	0.026	$7.6x10^{-6}$	15.71
4.3	h-based	0	-0.04	3823	1857	9.693	9.928	0.511	3.7	1.8	$4.4x10^{-16}$	$1.2x10^{-15}$	$2.3x10^{-15}$	$1.0x10^{-11}$	$-1.0x10^{-11}$	0.034	$9.8x10^{-6}$	17.27
4.3	Mixed	1	0.00	3827	1852	9.719	9.927	1.704	3.7	1.8	$-8.5x10^{-8}$	$1.6x10^{-9}$	$1.6x10^{-9}$	$-3.0x10^{-11}$	$-1.7x10^{-6}$	0.032	$9.1x10^{-6}$	15.39
4.3	Mixed	1	-0.04	3788	1846	9.750	9.928	1.380	3.7	1.8	$-6.6x10^{-9}$	$1.5x10^{-10}$	$1.6x10^{-10}$	$-8.1x10^{-12}$	$-1.2x10^{-7}$	0.035	$9.3x10^{-6}$	14.93
4.3	Switch	0.9	0.00	3827	1852	9.719	9.927	1.704	3.7	1.8	$-8.5x10^{-8}$	$1.6x10^{-9}$	$1.6x10^{-9}$	$-3.0x10^{-11}$	$-1.7x10^{-6}$	0.032	$9.1x10^{-6}$	15.39
4.3	Switch	0.9	-0.04	3788	1846	9.750	9.928	1.380	3.7	1.8	$-6.6x10^{-9}$	$1.5x10^{-10}$	$1.6x10^{-10}$	$-8.1x10^{-12}$	$-1.2x10^{-7}$	0.035	$9.3x10^{-6}$	14.93

Appendix V. Linear correlations

Y	X	Correlation coefficient r											
		1-1	**1-2**	**1-3**	**2-1**	**2-2**	**2-3**	**3-1**	**3-2**	**3-3**	**4-1**	**4-2**	**4-3**
NI	Time steps	0.99	0.88	0.98	0.97	1.00	0.95	0.93	1.00	1.00	1.00	0.05	0.89
NI	Δt av	-0.98	-0.87	-0.98	-0.96	-1.00	-0.95	-0.94	-1.00	-1.00	-1.00	-0.03	-0.89
NI	Δt max	-0.84	-0.04	-0.76	-0.67	-0.93	-0.83	-0.95	-0.99	-0.99	-0.90	-1.00	-0.77
NI	Δt min	0.00	-0.96	-0.02	0.00	-0.09	0.99	0.15	-0.23	0.14	-0.65	0.76	-0.08
NI	Pe max	0.82	0.39	-0.82	-0.94	-0.40	-0.44	0.67	0.62	0.00	-0.58	-0.75	-0.82
NI	Co max	0.83	0.32	-0.76	-0.95	-0.43	-0.51	-0.96	-0.99	-0.12	-0.90	-0.98	-0.80
NI	ε_{MB}	0.08	0.30	0.58	0.89	-0.26	-0.49	0.04	0.40	0.04	0.41	-0.55	-0.20
NI	E_{1G} max	0.08	-0.17	-0.55	-0.09	0.13	0.05	0.42	0.34	0.48	-0.71	0.60	0.19
NI	E_{2G} max	0.06	-0.15	0.35	-0.06	0.19	-0.44	-0.23	0.31	-0.15	-0.71	0.60	0.18
NI	ε_{MB}^{n} max	0.49	-0.24	-0.19	0.30	-0.59	-0.62	-0.66	0.18	-0.04	-0.01	-0.55	0.05
NI	ε_{MB}^{n} min	0.79	0.12	0.62	0.65	-0.14	-0.16	0.76	-0.42	-0.59	0.71	-0.59	-0.20
NI	Δh max	0.86	-0.62	0.41	-0.13	-0.49	-0.61	0.52	0.61	0.60	0.94	-0.05	-0.88
NI	$\Delta\theta$ max	0.47	0.35	-0.79	0.45	0.66	-0.62	0.47	0.72	0.61	0.82	0.91	-0.69
NI	Δh_d max	0.80	0.73	-0.31	0.67	0.98	1.00	-0.66	-0.68	-0.66	0.02	0.99	0.43
Time steps	Δt av	-1.00	-1.00	-1.00	-1.00	-1.00	-1.00	-1.00	-1.00	-1.00	-1.00	-1.00	-1.00
Time steps	Δt max	-0.88	-0.07	-0.87	-0.60	-0.94	-0.96	-0.99	-0.99	-0.99	-0.90	-0.06	-0.44
Time steps	Δt min	0.00	-0.75	0.14	0.00	-0.07	0.96	0.41	-0.23	0.13	-0.65	-0.61	-0.49
Time steps	Pe max	0.87	0.78	-0.91	-0.83	-0.36	-0.67	0.54	0.62	0.01	-0.58	-0.68	-0.54
Time steps	Co max	0.88	0.73	-0.87	-0.84	-0.39	-0.73	-0.95	-0.99	-0.12	-0.90	-0.24	-0.47
Time steps	ε_{MB}	0.12	-0.19	0.63	0.97	-0.29	-0.21	0.09	0.41	0.05	0.41	0.80	0.02
Time steps	E_{1G} max	0.14	0.07	-0.51	0.14	0.17	-0.24	0.51	0.35	0.48	-0.72	-0.77	-0.03
Time steps	E_{2G} max	0.12	0.09	0.41	0.18	0.22	-0.55	-0.21	0.32	-0.14	-0.71	-0.77	-0.04
Time steps	ε_{MB}^{n} max	0.50	-0.21	-0.13	0.49	-0.58	-0.46	-0.54	0.19	-0.03	-0.01	0.19	0.34
Time steps	ε_{MB}^{n} min	0.85	-0.23	0.61	0.82	-0.15	0.15	0.59	-0.42	-0.59	0.72	0.78	0.01
Time steps	Δh max	0.81	-0.20	0.34	-0.15	-0.43	-0.46	0.35	0.60	0.60	0.94	-0.83	-0.65
Time steps	$\Delta\theta$ max	0.53	0.45	-0.86	0.66	0.68	-0.46	0.44	0.72	0.60	0.81	-0.37	-0.38
Time steps	Δh_d max	0.85	0.97	-0.47	0.83	0.99	0.96	-0.53	-0.68	-0.66	0.02	0.17	0.79
Δt av	Δt max	0.90	0.07	0.87	0.59	0.94	0.96	0.99	0.99	0.99	0.85	0.05	0.44
Δt av	Δt min	0.00	0.74	-0.13	0.00	0.06	-0.96	-0.38	0.19	-0.16	0.72	0.63	0.48
Δt av	Pe max	-0.89	-0.79	0.91	0.81	0.35	0.66	-0.55	-0.63	0.00	0.50	0.67	0.54
Δt av	Co max	-0.90	-0.74	0.87	0.83	0.38	0.72	0.96	0.99	0.12	0.85	0.23	0.47
Δt av	ε_{MB}	-0.15	0.20	-0.62	-0.97	0.31	0.22	-0.07	-0.42	-0.01	-0.50	-0.81	-0.02
Δt av	E_{1G} max	-0.17	-0.08	0.52	-0.17	-0.18	0.23	-0.49	-0.36	-0.46	0.78	0.78	0.03
Δt av	E_{2G} max	-0.16	-0.10	-0.41	-0.21	-0.24	0.54	0.20	-0.34	0.17	0.77	0.78	0.03
Δt av	ε_{MB}^{n} max	-0.50	0.21	0.14	-0.50	0.59	0.46	0.54	-0.21	0.06	-0.08	-0.20	-0.34
Δt av	ε_{MB}^{n} min	-0.88	0.24	-0.61	-0.84	0.17	-0.13	-0.64	0.49	0.59	-0.78	-0.78	-0.01
Δt av	Δh max	-0.78	0.18	-0.34	0.15	0.42	0.47	-0.36	-0.62	-0.61	-0.90	0.83	0.65

Y	X	Correlation coefficient r											
		1-1	**1-2**	**1-3**	**2-1**	**2-2**	**2-3**	**3-1**	**3-2**	**3-3**	**4-1**	**4-2**	**4-3**
Δt av	Δθ max	-0.57	-0.45	0.86	-0.68	-0.69	0.47	-0.44	-0.70	-0.62	-0.76	0.38	0.38
Δt av	Δh_d max	-0.88	-0.97	0.47	-0.85	-0.99	-0.97	0.54	0.69	0.65	0.07	-0.16	-0.79
Δt max	Δt min	0.00	0.02	-0.53	0.00	0.19	-0.86	-0.40	0.11	-0.24	0.25	-0.75	-0.57
Δt max	Pe max	-0.79	-0.10	0.97	0.75	0.08	0.83	-0.56	-0.56	0.02	0.88	0.76	0.74
Δt max	Co max	-0.79	-0.08	1.00	0.75	0.11	0.87	0.96	0.99	0.13	1.00	0.98	1.00
Δt max	ε_{MB}	-0.16	0.16	-0.51	-0.65	0.57	-0.03	-0.07	-0.30	0.08	0.03	0.54	0.66
Δt max	E_{1G} max	-0.22	0.34	0.39	-0.01	-0.46	0.49	-0.45	-0.22	-0.38	0.33	-0.59	-0.66
Δt max	E_{2G} max	-0.20	0.29	-0.35	0.01	-0.50	0.62	0.31	-0.19	0.25	0.33	-0.59	-0.65
Δt max	ε_{MB}^n max	-0.73	0.74	0.08	0.35	0.68	0.32	0.55	-0.05	0.15	0.45	0.53	0.56
Δt max	ε_{MB}^n min	-0.86	0.05	-0.43	-0.34	0.49	-0.40	-0.56	0.47	0.59	-0.33	0.58	0.66
Δt max	Δh max	-0.66	-0.03	-0.25	0.78	0.24	0.33	-0.45	-0.71	-0.65	-1.00	0.05	0.74
Δt max	Δθ max	-0.83	0.76	0.93	-0.23	-0.87	0.32	-0.51	-0.78	-0.67	-0.99	-0.90	0.66
Δt max	Δh_d max	-0.80	-0.08	0.81	-0.45	-0.94	-0.86	0.55	0.62	0.62	-0.46	-0.99	0.15
Δt min	Pe max	0.00	-0.21	-0.31	0.00	0.12	-0.52	-0.49	-0.64	-0.22	-0.24	-0.15	-0.16
Δt min	Co max	0.00	-0.14	-0.54	0.00	0.13	-0.58	-0.34	0.25	-0.27	0.25	-0.62	-0.53
Δt min	ε_{MB}	0.00	-0.46	0.16	0.00	-0.02	-0.48	0.16	-0.06	-0.92	-0.96	-0.96	-0.72
Δt min	E_{1G} max	0.00	0.41	0.21	0.00	-0.06	-0.04	0.08	-0.19	-0.55	1.00	0.98	0.72
Δt min	E_{2G} max	0.00	0.40	0.26	0.00	0.04	-0.54	-0.63	-0.22	-0.93	1.00	0.98	0.73
Δt min	ε_{MB}^n max	0.00	0.34	0.31	0.00	-0.26	-0.66	0.50	-0.23	-0.94	-0.75	-0.55	-0.90
Δt min	ε_{MB}^n min	0.00	-0.40	-0.49	0.00	0.31	-0.09	-0.34	-0.45	0.05	-1.00	-0.97	-0.72
Δt min	Δh max	0.00	0.80	0.14	0.00	0.14	-0.66	-0.15	0.15	0.51	-0.34	0.50	-0.07
Δt min	Δθ max	0.00	-0.28	-0.29	0.00	-0.03	-0.67	0.14	-0.23	0.56	-0.09	0.96	-0.22
Δt min	Δh_d max	0.00	-0.55	-0.93	0.00	0.03	1.00	0.50	0.61	0.43	0.75	0.67	-0.84
Pe max	Co max	1.00	1.00	0.96	1.00	1.00	1.00	-0.55	-0.63	-0.82	0.88	0.87	0.79
Pe max	ε_{MB}	0.32	-0.75	-0.50	-0.72	-0.76	-0.34	-0.02	0.24	0.20	0.50	-0.13	-0.02
Pe max	E_{1G} max	0.42	0.27	0.49	0.36	0.84	0.88	0.43	0.36	-0.27	-0.15	0.07	0.02
Pe max	E_{2G} max	0.41	0.30	-0.29	0.34	0.82	0.83	0.36	0.38	0.37	-0.16	0.07	0.03
Pe max	ε_{MB}^n max	0.17	-0.17	0.19	0.01	-0.05	0.19	-1.00	0.31	0.28	0.82	0.17	-0.07
Pe max	ε_{MB}^n min	0.99	-0.54	-0.65	-0.38	-0.73	-0.80	0.68	-0.39	0.53	0.15	-0.08	-0.01
Pe max	Δh max	0.42	0.40	-0.17	0.17	0.90	0.23	0.51	0.44	0.54	-0.83	0.50	0.99
Pe max	Δθ max	0.49	0.40	0.96	-0.15	0.40	0.18	0.33	0.41	0.47	-0.95	-0.42	0.98
Pe max	Δh_d max	1.00	0.90	0.64	-0.42	-0.26	-0.47	-1.00	-1.00	-0.07	-0.82	-0.83	0.05
Co max	ε_{MB}	0.32	-0.80	-0.51	-0.74	-0.74	-0.27	-0.27	-0.30	0.26	0.03	0.38	0.60
Co max	E_{1G} max	0.41	0.29	0.38	0.35	0.83	0.83	-0.58	-0.25	0.41	0.33	-0.43	-0.59
Co max	E_{2G} max	0.39	0.32	-0.35	0.33	0.80	0.84	0.30	-0.22	0.18	0.33	-0.43	-0.59
Co max	ε_{MB}^n max	0.17	-0.15	0.07	0.00	-0.02	0.25	0.54	-0.09	0.24	0.45	0.45	0.49
Co max	ε_{MB}^n min	0.98	-0.56	-0.42	-0.39	-0.71	-0.74	-0.61	0.40	-0.67	-0.33	0.42	0.60

Y	X	Correlation coefficient r											
		1-1	**1-2**	**1-3**	**2-1**	**2-2**	**2-3**	**3-1**	**3-2**	**3-3**	**4-1**	**4-2**	**4-3**
Co max	Δh max	0.44	0.46	-0.25	0.18	0.91	0.29	-0.33	-0.66	-0.78	-0.99	0.18	0.79
Co max	$\Delta\theta$ max	0.49	0.39	0.92	-0.17	0.36	0.24	-0.32	-0.79	-0.71	-0.99	-0.81	0.72
Co max	Δh_d max	1.00	0.87	0.81	-0.44	-0.29	-0.54	0.54	0.69	-0.29	-0.46	-1.00	0.14
ε_{MB}	E_{1G} max	0.98	-0.38	0.00	0.36	-0.98	-0.68	0.81	0.98	0.74	-0.93	-1.00	-1.00
ε_{MB}	E_{2G} max	0.98	-0.41	0.96	0.39	-0.99	0.13	0.05	0.97	0.94	-0.93	-1.00	-1.00
ε_{MB}	ε_{MB}^n max	-0.13	0.10	0.56	0.48	0.58	0.84	0.01	0.94	0.98	0.90	0.55	0.93
ε_{MB}	ε_{MB}^n min	0.33	0.68	0.19	0.91	0.92	0.80	-0.14	-0.30	-0.18	0.93	1.00	1.00
ε_{MB}	Δh max	-0.17	-0.85	-0.23	-0.34	-0.52	0.81	-0.64	-0.33	-0.45	0.07	-0.61	-0.02
ε_{MB}	$\Delta\theta$ max	-0.14	-0.15	-0.31	0.79	-0.89	0.85	-0.74	-0.33	-0.51	-0.19	-0.84	-0.09
ε_{MB}	Δh_d max	0.34	-0.42	-0.33	0.93	-0.37	-0.46	0.01	-0.27	-0.52	-0.90	-0.44	0.25
E_{1G} max	E_{2G} max	1.00	1.00	0.13	1.00	0.99	0.64	0.32	1.00	0.47	1.00	1.00	1.00
E_{1G} max	ε_{MB}^n max	-0.16	0.76	0.81	0.50	-0.39	-0.17	-0.43	0.98	0.62	-0.69	-0.50	-0.94
E_{1G} max	ε_{MB}^n min	0.44	-0.88	-0.59	0.67	-0.93	-0.98	0.29	-0.30	-0.50	-1.00	-1.00	-1.00
E_{1G} max	Δh max	-0.24	0.66	-0.02	-0.41	0.66	-0.12	-0.43	-0.35	-0.31	-0.43	0.63	0.03
E_{1G} max	$\Delta\theta$ max	-0.03	0.37	0.40	0.83	0.81	-0.18	-0.48	-0.39	-0.36	-0.18	0.88	0.10
E_{1G} max	Δh_d max	0.44	0.24	0.02	0.67	0.25	0.01	-0.43	-0.38	-0.54	0.68	0.49	-0.26
E_{2G} max	ε_{MB}^n max	-0.18	0.71	0.69	0.55	-0.45	0.64	-0.38	0.99	0.98	-0.69	-0.50	-0.94
E_{2G} max	ε_{MB}^n min	0.42	-0.90	-0.08	0.70	-0.90	-0.49	0.26	-0.28	-0.07	-1.00	-1.00	-1.00
E_{2G} max	Δh max	-0.26	0.67	-0.34	-0.37	0.64	0.68	-0.38	-0.37	-0.43	-0.42	0.63	0.03
E_{2G} max	$\Delta\theta$ max	-0.05	0.35	-0.07	0.85	0.84	0.64	-0.43	-0.41	-0.47	-0.17	0.88	0.10
E_{2G} max	Δh_d max	0.42	0.27	-0.33	0.70	0.31	-0.46	-0.38	-0.39	-0.49	0.69	0.49	-0.26
ε_{MB}^n max	ε_{MB}^n min	0.28	-0.35	-0.48	0.74	0.46	0.35	-0.68	-0.20	-0.16	0.69	0.51	0.93
ε_{MB}^n max	Δh max	0.69	0.29	-0.21	0.45	0.32	1.00	-0.50	-0.49	-0.45	-0.36	0.30	-0.12
ε_{MB}^n max	$\Delta\theta$ max	0.75	0.38	0.25	0.74	-0.74	1.00	-0.32	-0.52	-0.49	-0.59	-0.56	-0.08
ε_{MB}^n max	Δh_d max	0.18	-0.15	-0.18	0.64	-0.60	-0.60	1.00	-0.32	-0.54	-1.00	-0.52	0.57
ε_{MB}^n min	Δh max	0.40	-0.79	-0.05	-0.22	-0.45	0.30	0.34	-0.61	0.12	0.43	-0.63	-0.02
ε_{MB}^n min	$\Delta\theta$ max	0.61	-0.24	-0.63	0.97	-0.79	0.36	0.22	-0.10	0.04	0.18	-0.87	-0.09
ε_{MB}^n min	Δh_d max	0.99	-0.44	0.15	0.99	-0.19	-0.12	-0.68	0.42	0.78	-0.68	-0.49	0.24
Δh max	$\Delta\theta$ max	0.37	0.01	-0.40	-0.28	0.15	1.00	0.92	0.80	0.99	0.97	0.32	0.95
Δh max	Δh_d max	0.39	0.06	-0.20	-0.34	-0.33	-0.60	-0.50	-0.48	-0.11	0.37	-0.16	-0.08
$\Delta\theta$ max	Δh_d max	0.51	0.46	0.61	0.96	0.73	-0.61	-0.32	-0.45	-0.15	0.60	0.85	0.20

Appendix VI. Variable sorting for the selection of the appropiate model

Test case 1.1

Models	Time steps	Δt min	E_{1G} max
N1AMT	4448	0.0010	2.0674E-09
N1AST	4452	0.0010	3.8268E-11
N1AHT	4580	0.0010	1.5123E-14
N1ASP	4910	0.0010	5.9674E-10
N1AMP	4910	0.0010	9.8502E-08
N1AHP	5465	0.0010	6.9864E-15

Test case 2.1

Models	Time steps	Δt min	E_{1G} max
N2AMT	4244	0.0010	1.1361E-11
N2AST	4244	0.0010	1.1361E-11
N2AHT	4266	0.0010	3.5812E-15
N2AMP	4405	0.0010	1.6821E-10
N2ASP	4405	0.0010	1.6821E-10
N2AHP	4647	0.0010	4.6788E-16

Test case 1.2

Models	Time steps	Δt min	E_{1G} max
N1IST	2515	1.5855	1.5964E-10
N1IMT	2515	1.5855	1.2341E-08
N1IHT	2519	1.4269	5.7136E-14
N1ISP	2551	1.7601	9.5124E-10
N1IMP	2587	1.7596	2.6254E-08
N1IHP	2662	0.4756	5.0304E-14

Test case 2.2

Models	Time steps	Δt min	E_{1G} max
N2IHT	2026	4.5575	1.6474E-15
N2IMT	2026	2.0056	1.7584E-10
N2IST	2026	2.0056	1.7584E-10
N2ISP	2064	0.2525	1.2221E-09
N2IMP	2092	5.2849	1.0521E-09
N2IHP	2138	1.5855	4.0731E-16

Test case 1.3

Models	Time steps	Δt min	E_{1G} max
N1WMP	1749	1.8366	6.1468E-07
N1WSP	1749	1.8365	5.9060E-10
N1WHP	1764	0.9729	1.5227E-13
N1WHT	1773	1.8446	6.6138E-14
N1WST	1788	1.8440	2.4116E-10
N1WMT	1789	1.8443	3.1986E-08

Test case 2.3

Models	Time steps	Δt min	E_{1G} max
N2WHT	920	2.0188	1.4045E-15
N2WMT	921	1.3913	2.2682E-10
N2WST	921	1.3913	2.2682E-10
N2WMP	931	3.7591	6.4892E-10
N2WSP	931	3.7591	6.4892E-10
N2WHP	970	6.9479	3.8489E-16

Test case 3.1

Models	Time steps	Δt min	E_{1G} max
D3AST	5917	8.6120E-08	1.2738E-10
D3AMT	6283	3.9378E-13	1.5880E-07
D3AHP	6443	7.7508E-09	4.5190E-16
D3AHT	6588	8.6120E-08	6.9689E-16
D3ASP	7549	8.6120E-08	4.7937E-10
D3AMP	7590	8.6120E-08	4.5015E-07

Test case 4.1

Models	Time steps	Δt min	E_{1G} max
D4AMP	3656	2.8183E-05	3.1267E-11
D4ASP	3656	2.8183E-05	3.1267E-11
D4AMT	4021	3.1315E-09	1.3367E-12
D4AST	4021	3.1315E-09	1.3367E-12
D4AHT	4037	3.1315E-09	1.1568E-15
D4AHP	4784	2.5365E-06	4.7762E-16

Test case 3.2

Models	Time steps	Δt min	E_{1G} max
D3IMT	2149	8.8483E-08	8.1613E-08
D3IHT	2158	1.8681E-04	1.3560E-15
D3IST	2171	2.1501E-04	2.8800E-10
D3ISP	2987	2.1497E-04	1.1051E-09
D3IMP	3153	1.0976E-04	4.9167E-07
D3IHP	3401	2.3890E-05	8.4976E-16

Test case 4.2

Models	Time steps	Δt min	E_{1G} max
D4IMP	1974	7.0364E-02	1.9907E-09
D4ISP	1974	7.0364E-02	1.9907E-09
D4IMT	2004	7.8182E-04	4.2816E-11
D4IST	2004	7.8182E-04	4.2816E-11
D4IHT	2005	7.8182E-04	1.4254E-15
D4IHP	2052	1.8998E-02	5.4635E-16

Test case 3.3

Models	Time steps	Δt min	E_{1G} max
D3WMT	1784	1.9287E-05	5.7000E-08
D3WST	1812	2.4908E-04	2.9426E-10
D3WHT	1843	1.5233E-04	2.4157E-15
D3WSP	2606	2.2080E-04	8.5402E-10
D3WHP	2667	2.2756E-04	1.1216E-15
D3WMP	2745	6.1126E-05	6.1152E-07

Test case 4.3

Models	Time steps	Δt min	E_{1G} max
D4WMT	1846	1.38039	1.5213E-10
D4WST	1846	1.38039	1.5213E-10
D4WMP	1852	1.70419	1.6635E-09
D4WSP	1852	1.70419	1.6635E-09
D4WHP	1857	1.22243	5.7262E-16
D4WHT	1857	0.51126	1.2706E-15

Appendix VII. Publications et communications

Publications :

Wanko, A., **Tapia, G.,** Mosé, R., Gregoire, C., 2011. A new empirical law to accurately predict solute retention capacity within horizontal flow constructed wetlands (HFCW). Ecological Engineering, 37(4): 636-643.

Gregoire, C., Elsaesser, D., Huguenot, D., Lange, J., Lebeau, T., Merli, A., Mose, R., Passeport, E., Payraudeau, S., Schütz, T., Schulz, R., **Tapia-Padilla, G**., Tournebize, J., Trevisan, Marco, Wanko, A. 2009. Mitigation of agricultural nonpoint-source pesticide pollution in artificial wetland ecosystems. Environmental chemistry letters, 7(3): 205-231.

Wanko, A, **Tapia-Padilla, G.,** Mose, R., Gregoire, C. 2009. Transport modelling by mixed hybrid finite element method – a flux limiter development. Journal of Water Sciences, 22(4): 507-522.

Wanko, A., **Tapia, G.,** Mosé, R., Gregoire, C., 2009. Adsorption distribution impact on preferential transport within horizontal flow constructed wetland (HFCW). Ecological Modelling, 220 (23): 3342-3352.

Communications :

Tapia-Padilla, G. Wanko, A., Mosé, R., Gregoire, C. Artificial Wetland modelling for pesticides fate and transport using a 2D Mixed Hybrid Finite Element approximation. 2nd International Symposium on Wetland Pollutant Dynamics and Control WETPOL 2007. University of Tartu, Estonia 16th to 20th September, 2007

Tapia-Padilla, G. Wanko, A., Mosé, R., Gregoire, C. Modelling and optimization of pesticide mitigation processes in artificial wetlands. Journée des doctorants. Ecole Doctorale Science de la Terre, de l'Univers et de l'Environnement Strasbourg. 14 Novembre 2008